CONVECTIVE INSTABILITIES IN A SPARSELY PACKED POROUS MEDIUM WITH THE EFFECT OF ROTATION AND MAGNETIC FIELD

A THESIS SUBMITTED TO
NATIONAL INSTITUTE OF TECHNOLOGY WARANGAL
FOR THE AWARD OF THE DEGREE OF
DOCTOR OF PHILOSOPHY
IN
MATHEMATICS

BY
NILAM VENKATA KOTESWARARAO
(Roll No. 715080)

UNDER THE SUPERVISION OF
Dr. A. BENERJI BABU

DEPARTMENT OF MATHEMATICS
NATIONAL INSTITUTE OF TECHNOLOGY WARANGAL
TELANGANA STATE, INDIA

JULY 2019

NATIONAL INSTITUTE OF TECHNOLOGY WARANGAL
DEPARTMENT OF MATHEMATICS

CERTIFICATE

This is to certify that the thesis entitled "**Convective Instabilities in a Sparsely Packed Porous Medium with the Effect of Rotation and Magnetic Field** " submitted to National Institute of Technology Warangal, for the award of the degree of ***Doctor of Philosophy***, is bonafide research work done by **Mr. NILAM VENKATA KOTESWARA RAO** under my supervision. The contents of this thesis have not been submitted elsewhere for the award of any degree.

Dr. A. BENERJI BABU
Associate Professor
Department of Mathematics
National Institute of Technology
Warangal
Telangana State, INDIA

.

DECLARATION

This is to certify that the work presented in the thesis entitled **"Convective Instabilities in a Sparsely Packed Porous Medium with the Effect of Rotation and Magnetic Field"**, is a record of bonafide work done by me under the supervision of **Dr. A. BENERJI BABU** and has not been submitted elsewhere for the award of any degree.

I declare that this written submission represents my ideas in my own words and where others' ideas or words have been included, I have adequately cited and referenced the original sources. I also declare that I have adhered to all principles of academic honesty and integrity and have not misrepresented or fabricated or falsified any idea / data / fact /source in my submission. I understand that any violation of the above will be a cause for disciplinary action by the Institute and can also evoke penal action from the sources which have thus not been properly cited or from whom proper permission has not been taken when needed.

Nilam Venkata Koteswararao

Roll No. **715080**

Date:____________

ACKNOWLEDGEMENTS

It is a rare privilege and boon that I could associate myself for pursuing my research work with **Dr. A. Benerji Babu**, Associate Professor of Mathematics, National Institute of Technology, Warangal, India. I sincerely record my gratitude for his invaluable guidance and constant encouragement throughout the preparation of this thesis and his involvement and meticulous supervision while my work was in progress. With his inimitable qualities as a good teacher, he chiselled my path towards perfection. Ever since I met him, he has been a perpetual source of motivation, inspiration, encouragement and enlightenment. He is responsible for making the period of my research work an educative and enjoyable learning experience. The thesis would not have seen the light of the day without his unrelenting support and cooperation. I deem it a privilege to have worked under his amiable guidance. My vocabulary is inadequate to express my gratitude.

It is a pleasure to express my thanks to **Prof. D. Srinivasacharya**, Head, Department of Mathematics.

I owe sincere and earnest thanks to **Prof. Y. N. Reddy** for his encouragement and affectionate throughout the period of my research work. I thank the members of the Doctoral Scrutiny Committee, **Prof. Y.N.Reddy, Dr. H.P.Rani**, Department of Mathematics and **Prof.A.Neelakanteswara Rao**, Department of Mechanical Engineering for their valuable suggestions, moral support and encouragement while my work was in progress.

Fellowship provided by **MHRD, India** during the course of my research is gratefully acknowledged.

It is a pleasure to express my thanks to **Prof. K. N. S. Kasi Viswanadham, Prof. J.V.Ramana Murthy, Prof. D. Dutta, Dr. P. Muthu, Dr. H. P. Rani, Dr. R. S. Selvaraj, Dr. T. Kurmayya, Dr. D. Bhargavi, Dr. J. Pranitha, Dr. Ch. Ram Reddy, Dr. E. Satyanarayana, Dr. Y. Sreenivasa Rao** and others faculty members of the Department of Mathematics. I also thank **Dr. M.Raja Vishwanathan** Department of Humanities and Social Sciences for his diligent proof reading of this thesis.

I also express my thanks to my co-research scholars **Mr. G. Shiva Kumar Reddy, Dr. Vayunandha Kishore, Mr. Sharth kumar Reddy, Mr. M. Pavan Kumar Reddy, Dr. Nitish Kumar** and other scholars for their suggestions, technical help and encouragement during my research. I also express my thanks to my best friends **Mr. K.Ramesh Babu, Mr.P. Mallaiah, Dr. J. Soma shaker, Dr. C.S.K.Raju, Mr. Rajavardhan Reddy** and all other friends for their continuous support and encouragement to do this research work.

My most important and deepest gratitude go to my parents **Nilam Koteswararao - Koteswaramma** and **Pasam Venkaiah - Lakshmi**, better half **Swathi Lakshmi**, daughter **Ekta Kiranya**, brothers **Mr. Pasam Srinu, Mr. Pasam Venu, Mr. Pasam Gopi, Mr. Pasam Venkata Rao, Mr. Pasam Anil, Mr. Pasam Venkatesh**, uncle and aunt **Srineevasulu and Ankamma** and other family members for their continuous support and constant encouragement over the years. Their love and affection has been the motivating force behind what I am today.

I am always thankful to **my mathematics teachers**.

. Nilam Venkata Koteswara Rao

A B S T R A C T

The study of linear and nonlinear stability analyis of Rayleigh Benard convection and thermohaline convection in a SPPM (sparsely packed porous medium) with the effects of rotation and magnetic field interest in the natural environment, and important in geophysics, meteorology, oceanography, physics and applied mathematics as well as engineering. The aim of present thesis is to study, Convective instabilities in the presence of horizontal magnetoconvection and vertical rotating convection due to a sparsely packed porous medium. The thesis consists of seven chapters. Chapter 1 deals with general introduction, Chapter 2 explains the linear and nonlinear horizontal magnetoconvection in a sparsely packed porous medium in two parts, Chapter 3 consists of linear and nonlinear horizontal magneto rotating convection in a sparsely packed porous medium, Chapter 4 deals thermohaline convection in a sparsely packed porous medium due to horizontal magnetic field, Chapter 5 consists thermohaline convection in a SPPM due to rotating fluid, Chapter 6 deals stability of thermohaline horizontal magneto convection in a rotating SPPM, Chapter 7 consists of conclusions and scope of the future work. In this thesis Stress-free boundary conditions are used in all chapters. Rayleigh-Benard convection with Magnetoconvection, Rotating convection, Thermohaline convection are multiple diffusive systems. These diffusive system show both stationary convection and oscillatory convection.

Chapter 2 - Chapter 6, we studied the linear stability analysis using normal mode method. We derived critical Rayleigh number at the onset of stationary and oscillatory convection. Takens-Bogdanov bifurcation points and co-dimension two bifurcation points obtained by plotting graphs of neutral curves. The instabilities occurs at Pitchfork bifurcation (stationary convection) and Hopf bifurcation (oscillatory convection) in the parameter regime.

In nonlinear stability analysis using Newell and Whitehead method deriving a nonlinear two-dimensional LG (Landau-Ginzburg) equation at the supercritical Pitchfork bifurcation, discussed about Nusselt number and occurrence of secondary instabilities (Eckhaus and Zigzag instabilities). We derived coupled LG equations at supercritical Hopf bifurcation, discussed about travelling waves and standing wave. Conclusions and Scope of future work are presented in Chapter 7.

NOMENCLATURE

Non-Dimensional Variables

A	Complex amplitude
A_{1L}	Amplitude of left travelling waves
A_{1R}	Amplitude of right travelling waves
Da	Darcy number
L	Lewis number
M	Heat capacity
Nu	Nusselt number
Pr	Prandtl number
Pr_1	Thermal Prandtl number
Pr_2	Magnetic Prandtl number
q	Wave number
Q	Chandrasekhar number
R	Rayleigh number
R_1	Thermal Rayleigh number
R_2	Magnetic Rayleigh number
R_s	Stationary Rayleigh number
R_o	oscillatory Rayleigh number
R_{sc}	Critical stationary Rayleigh number
R_{oc}	Critical oscillatory Rayleigh number

Dimensional Variables

C	Concentration mol/m^3
d	Depth of the layer m
g	Acceleration due gravity m/s^2
H	Magnetic field wb/m^2
H_x	Magnetic field along x-axis wb/m^2
H_y	Magnetic field along y-axis wb/m^2
H_z	Magnetic field along z-axis wb/m^2
K	Permeability H/m
k_T	Thermal diffusivity m^2/s
k_S	Saline diffusivity m^2/s
P	Pressure Pa
ΔS	Salinity difference g/kg
ΔT	Temperature difference k
u	Velocity along x-axis m/s
v	Velocity along y-axis m/s
w	Velocity along z-axis m/s
V	Mean fluid velocity m/s

Greek Symbols

Non-Dimensional Variables

α	Thermal expansion coefficient
β	Solute expansion coefficient
Λ	Brinkmann number
ω	Vorticity

Dimensional Variables

η	Magnetic diffusivity m^2/s
μ	Fluid viscosity $Kg.m^{-1}.s^{-1}$
μ_e	Effective fluid Viscosity $Kg.m^{-1}.s^{-1}$
μ_m	Magnetic Permeability w
ρ	Fluid density kr/m^3
ν	Kinematic viscosity $Kg.m^{-1}.s^{-1}$
θ	Temperature k

Operators

∇	del operator
∇^2	3-D Laplacian operator
∇_h^2	2-D Laplacian operator

Contents

Chapter 1

Introduction and Literature Review

1.1 Introduction

Hydrodynamic stability is an important subject of fluid mechanics, which is concerned with the stability and instability of motion of fluids as well as the problem of transition from laminar to turbulent flows. The instability of flows and their transition to turbulence are a widespread phenomena in various science and engineering applications such as astrophysics, oceanography, geophysics, magnetohydrodynamics, meteorology, etc. The essential hydrodynamic stability problems were recognized and formulated by Helmholtz [42], Kelvin [42], Rayleigh [59] and Reynolds [35]. The instability of flow of fluids and transition to turbulence is investigated experimentally, numerically and through simulation models. The study of mathematical theories in hydrodynamics stability such as bifurcation theory and nonlinear theory becomes very difficult, so computational fluid dynamics plays an important role where Navier-Stokes equations are integrated more accurately. The method of linear stability analysis determines whether the flow is stable or unstable for an infinitely small disturbance; in this method, the governing equations are linearized. Nonlinear governing equations allow disturbances of different wavelengths to interact with each other. The qualitative theory of bifurcation and chaos theory focus on the behaviour of nonlinear dynamical systems, when a small change in the parameters of the system effects a qualitative change in its behaviour or the system behaves completely differently. Some important applications of hydrodynamic stability are KelvinHelmholtz instability [42], Rayleigh-Taylor instability [59] and Rayleigh Benard instabilities [35]. Kelvin-Helmholtz instability occurs when there is velocity difference across the interface between two fluids. Rayleigh-Taylor instability occurs at the interface between two fluids of different densities. Rayleigh-Benard instability occurs when a plane horizontal layer of fluid is heated from below. The study of the stability of fluid is important to understand simplistic systems.

1.2 Rayleigh-Benard Convection

Rayleigh-Benard convection is a natural convection phenomenon that causes instability in a plane horizontal layer of a fluid heated from below to produce a fixed temperature gradient. The warmer fluid moves upwards from the layer heated below, when the density at the layer below becomes lighter than at the top. The buoyancy force and viscosity differences are responsible for the appearance of convection cells. These regular patterns of convection cells are known as Benard cells. In 1900, Benard [18], first made an experiment by heating a layer of fluid from below and observed hexagonal cells, when the convection developed. Motivated by Benard experiments, Lord Rayleigh [91] first derived theoretical conditions for convective motion in a layer of fluid with two free surfaces. The instability of a layer of fluid heated from below depends on the non-dimensional Rayleigh number (R), defined as

$$R = \frac{g\alpha \Delta T d^3}{k\mu}, \tag{1.1}$$

where g is acceleration due to gravity, α is thermal expansion coefficient, ΔT is temperature difference between the upper and lower layers, d is distance between two layer, μ is kinematic viscosity and k is thermal diffusivity. The Rayleigh number characterizes the laminar to turbulence transition flow of a free convection boundary layer. Rayleigh showed that instability sets in when R exceeds a certain critical value R_c and that when R just exceeds R_c a stationary pattern of motions must come to prevail, then there are two possibilities,

1. $R < R_c$: there is no convection, only conduction and steady rolls can't be observed. Besides, the evolution of temperature is linear.
2. $R > R_c$: the exchange is made by conduction and convection and rolls appear. The evolution of temperature becomes non-linear.

Figure 1.1 illustrates the marginal stability curve stability of the neutral curve. Benard Marangoni convection mechanism coexists with Rayleigh mechanism but dominates thin layer. The instabilities driven by surface tension decreases as the

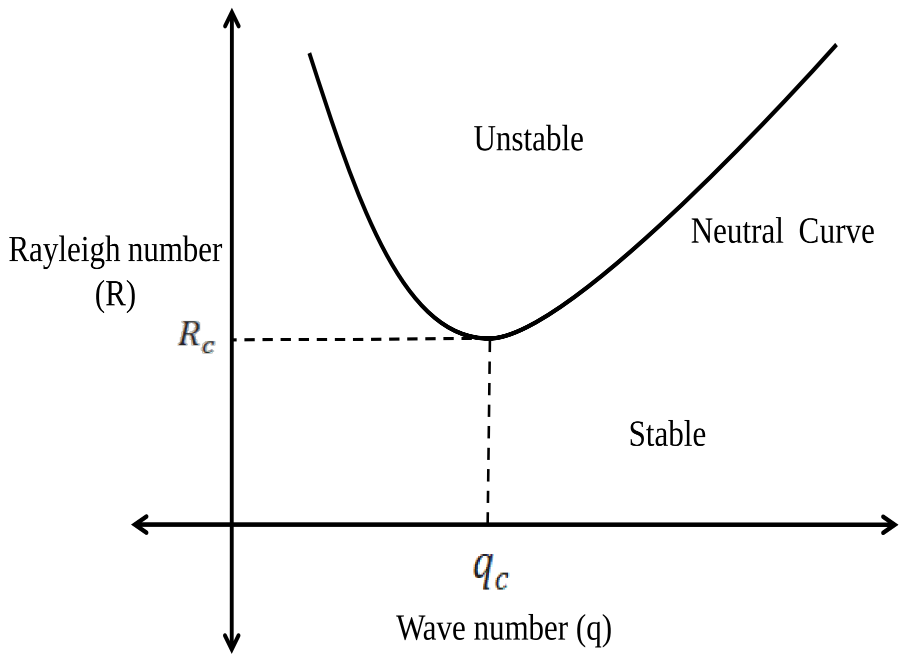

Figure 1.1: Marginal stability curve, Rayleigh number (R) verses Wave number (q).

layer becomes thicker. Thermal convection leads to convective cells of many form such as rolls, square and hexagons.

1.3 Boundary conditions

The fluid is confined between the planes $z = 0$ and $z = 1$. The temperature for perfectly conducting boundaries and normal component of the velocity vanishes, i.e.

$$\theta = w = 0 \quad \text{at} \quad z = 0, 1. \tag{1.2}$$

Since these planes are maintained at constant temperature, the normal component of velocity must vanish on these planes.

Rigid surfaces : When the flow takes place over a rigid plate, the velocity component vanishes at the boundaries i.e. no slip conditions hold. Hence $u = v = 0$, in addition to $w = 0$. This along with equation of continuity implies that

$$\frac{\partial w}{\partial z} = 0. \tag{1.3}$$

Free surfaces: When there is flow over a free surface, the vertical component of velocity vanishes and there is no surface tension at a horizontal free surface. i.e.

$$\tau_{xz} = \mu \left(\frac{\partial u}{\partial z} + \frac{\partial w}{\partial x} \right) = 0, \quad \tau_{yz} = \mu \left(\frac{\partial v}{\partial z} + \frac{\partial w}{\partial y} \right) = 0, \tag{1.4}$$

where μ is the dynamic viscosity and it implies that

$$\frac{\partial u}{\partial z} = \frac{\partial v}{\partial z} = 0. \tag{1.5}$$

This with equation of continuity implies that

$$\frac{\partial^2 w}{\partial z^2} = 0. \tag{1.6}$$

Thus the conditions for free surface are $w = D^2 w = D^4 w = \cdots = 0$ at $z = 0, 1$. Table 1.1 shows critical Rayleigh number corresponding to critical wave number for each set of boundary conditions.

Boundaries	R_c	q_c
Rigid-Rigid	1707.8	3.117
Rigid-Free	1100.7	2.682
Free-Free	657.5	2.221

Table 1.1: Critical Rayleigh number at different boundaries, taken from Chandrasekhar [35]

1.4 Porous medium

A porous medium is a solid containing voids which are either connected or disconnected. The voids are usually filled with a liquid or gas. A porous medium is characterized by porosity. The porous media model is applied in many areas like filtration, mechanics, engineering, geosciences, biophysics and material science. Heat transfer through the porous medium consists of predicting the heat transfer between the medium and the fluid flow. Darcy number (Da) is used to study heat transfer through porous medium and momentum transfer in porous medium.

$$Da = \frac{K}{d^2},$$

where K is the permeability of the medium and d is the characteristic length. Several models have been proposed to explain mathematical and physical aspects of porous media.

Darcy model

Darcy [38] has proposed the fluid motion in a porous medium in 1856 for the first time. It tells us the balance among pressure gradient, viscous force, and gravitational force. The mathematical form Darcy model can be given as

$$\overline{q} = -\frac{K}{\mu}\left(\nabla p - \rho g\right),$$

Where $\overline{q}$ is Darcian velocity, μ is the coefficient of viscosity whereas K represents the permeability of the medium. It was observed that there is an excellent matching of experimental results with Darcy model for a one-dimensional flow at low porosity.

Darcy Brinkman Model

It is assumed that the flow through an anisotropic porous medium with high permeability must reduce to viscous flow in a limit. In viewing this, to to balance the pressure gradient, Brinkman added a significant term $\mu\nabla^2 V$ and reached the need to account for flowing fluids viscous force on a dense pack of spherical particles of a porous mass. Here μ is the effective viscosity. The validity of the Brinkman model is restricted to high porosity medium and its governing equation is given by

$$-\left(\nabla p - \rho g\right) = \frac{\mu}{K}\overline{q} - \mu \nabla^2 \overline{q}. \tag{1.7}$$

Darcy Forchheimer Model

In 1901, Forchheimer conducted experiments and proposed that inertial effects can be accounted for by the addition of the square of velocity in the momentum equation. The modification to Darcy's equation is

$$\left(\mu + \rho c \sqrt{K}|\overline{q}|\right)\overline{q} = -K\left(\nabla p - \rho g\right), \tag{1.8}$$

where c is the dimensionless form drag coefficient and it varies with the nature of the porous medium. The coefficients of Darcy and Forchheimer terms contain both fluid properties and the microstructure of the porous medium. Several other models are available in the literature on porous media, Neild and Bejan [80] only could gave a satisfied discussion on validation and limitations of all the models.

Darcy Lapwood Brinkman Model

When the Laplace of the velocity is small in the porous medium, Darcy Brinkman and Darcy Forchheimer models neglected the shearing action of viscous fluids and fluid inertia was taken into account. As the presence of solid wall near the velocity gradient is high, both fluid inertia and viscous shearing action should be considered. Darcy Brinkman model takes into account both fluid inertia and viscous shearing action.

1.5 Rotation

A fluid motion is characterized by translation, rotation and continuous deformatons. In uniform motion, fluid elements are simply translated without and rotational deformations. Variations in the velocity components with space coordinated causes the rotation and deformations. The rate of change in length per unit original length of a linear fluid element determines the Linear strain or deformation whereas the rate of change of angle between two linear elements which are perpendicular to each other initially, determines the rate of angular deformation. Rotation can be defined as the arithmetic mean of two angular velocities which perpendicular linear segments at a point. The absence of deformation in the fluid rotation is known to be rigid body rotation or pure body rotation. When the rotational components at all points in a flow are observed to be zero, the flow is said to be irrotational.

1.6 Magnetohydrodynamics

The motion of an electrically conducting fluid in the presence of a magnetic field is described by Magneto-hydrodynamics. Because of the motion of conducting fluids across the lines of force of magnetic field, a potential difference would be created which in turn causes a flow of electric currents. The magnetic file produced by the electric currents modifies the magnetic field which has created them and there would be a flow of electric currents across these magnetic fields associated with a body force which is known as Lorentz force. Magnetohydrodynamic and heat transfer for a viscous incompressible fluid over a plate have immense applications in variety of industrial and engineering problems like petroleum industries, plasma studies and geophysics and so on.

1.7 Thermohaline Convection

The study of convective motions when there is more than one diffusing component with different molecular diffusivities, is of recent development in the field of convection. When the diffusing components have opposing effects on the vertical density distribution, a number of interesting phenomena could happen. This phenomenon was first studied with an application to oceans in mind because heat and salinity are contest in oceans related and the process is termed thermohaline or thermosolutal convection. The importance of thermohaline convection study was recognized in many fields such as astrophysics, geophysics, chemistry and limnology. Thermohaline convection has two requirements for it to occurs,

1. The fluid should contain two or more diffusing components with different molecular diffusivities.

2. The components must make opposing contributions to the vertical density gradient. Overstability is a characteristic feature of thermohaline convection, in which temperature and solute concentration are provide two diffusivities. Temperature and salinity act as opposite function on the vertical density gradient of this system. In thermohaline convection, the stable solute gradient is destabilized by raising the temperature of the lower boundary. The stability problems in the thermohaline convection focuses on the stability of periodic solution.

1.8 Chandrasekhar number Q

The Chandrasekhar number is a dimensionless quantity used in magnetic convection to represent ratio of the Lorentz force to the viscosity. It is named after the Indian astrophysicist Subrahmanyan Chandrasekhar. The main function function of Chandrasekhar number is measure of the magnetic field, being proportional to the square of a characteristic magnetic field in a system. The Chandrasekhar number is defined as

$$Q = \frac{H_o^2 d^2}{\mu_o \rho \nu \lambda} \tag{1.9}$$

where μ_o is the magnetic permeability, ρ is the density of the fluid, ν is the kinematic and λ is the magnetic diffusivity. H_o and d are a characteristic magnetic and a length scale of the system respectively.

1.9 Magnetic Permeability

Magnetic permeability, relative increase or decrease in the resultant magnetic field inside a material compared with the magnetizing field in which the given material is located; or the property of a material that is equal to the magnetic flux density B established within the material by a magnetizing field divided by the magnetic field strength H of the magnetizing field. Magnetic permeability μ is defined as $\mu = \frac{B}{H}$. Magnetic flux density B is a measure of the actual magnetic field within a material considered as a concentration of magnetic field lines, or flux, per unit cross-sectional area. Magnetic field strength H is a measure of the magnetizing field produced by electric current flow. The magnetic permeability is defined as the property of the material to allow the magnetic line of force to pass through it. The magnetic line of force is directly proportional to the conductivity of the material. SI unit is Henry per meter (H/M or Hm^2).The magnetic permeability is equal to the ratio of the field intensity to the flux density. It is expressed as, μ_m,

$$\mu_m = \frac{B}{H} \tag{1.10}$$

where B is magnetic flux density and H is magnetic field intensity.

1.10 Magnetic Diffusivity

The magnetic diffusivity is a parameter in plasma physics which appears in the magnetic Reynolds number. It has SI units of m^2/s and is defined as

$$\eta = \frac{1}{\mu_o \rho_o} \tag{1.11}$$

where μ_0 is the permeability of free space, and ρ_0 is the electrical conductivity. A measure of the tendency of a magnetic field to diffuse through a conducting medium at rest; it is equal to the partial derivative of the magnetic field strength with respect to time divided by the Laplacian of the magnetic field, or to the reciprocal of $4\pi\mu\rho$, where μ is the magnetic permeability and ρ is the conductivity in electromagnetic units.

1.11 Long wave instabilities (secondary instabilities)

The two dimensional Landau-Ginzburg equation in fast variables x, y, t and $A(X, Y, T) = \frac{A(x,y,t)}{\epsilon}$, as

$$\lambda_0 \frac{\partial A}{\partial T} - \lambda_1 \left(\frac{\partial}{\partial X} - \frac{i}{2q} \frac{\partial^2}{\partial Y^2} \right)^2 A - \lambda_2 A + \lambda_3 |A|^2 A = 0, \tag{1.12}$$

Newell and Whitehead [77] derived envelope equations, In order to study the properties of a structure with a given phase winding number δq, we write equation (1.12) in fast variables x, y, t and $A(X, Y, T) = \frac{A(x,y,t)}{\epsilon}$, as

$$\begin{aligned} &\frac{\partial A_1}{\partial t} - \Big(\epsilon^2 \frac{\lambda_2}{\lambda_0} - \frac{\lambda_1}{\lambda_0}\delta q^2\Big) A_1 + 2i\delta q \frac{\lambda_1}{\lambda_0}\Big(\frac{\partial}{\partial x} - \frac{i}{2q_{sc}}\frac{\partial^2}{\partial y^2}\Big) A_1 + \\ &\frac{\lambda_1}{\lambda_0}\Big(\frac{\partial}{\partial x} - \frac{i}{2q_{sc}}\frac{\partial^2}{\partial y^2}\Big)^2 A_1 - \frac{\lambda_3}{\lambda_0}|A_1|^2 A_1 = 0, \end{aligned} \tag{1.13}$$

$$A_1 = \left[\frac{\epsilon^2 \lambda_2 - \lambda_1 \delta q^2}{\lambda_3} \right]^{\frac{1}{2}}. \tag{1.14}$$

Let $\tilde{u} + i\tilde{v}$ be an infinitesimal perturbation of steady state solution A_1 given by equation (3.59). Substitute

$$A_1 = \tilde{u} + i\tilde{v} + [\left(\epsilon^2 \lambda_2 - \lambda_1 \delta q^2\right) \lambda_3^{-1}]^{\frac{1}{2}}, \tag{1.15}$$

into equation (1.13) and equate the real and imaginary parts, we obtain

$$\frac{\partial \tilde{u}}{\partial t} = -2\left(\epsilon^2 \frac{\lambda_2}{\lambda_0} - \frac{\lambda_1}{\lambda_0}\delta q^2\right)\tilde{u} + \frac{\lambda_1}{\lambda_0}\tilde{u} - \frac{\lambda_1}{\lambda_2}\partial_2 \frac{\partial \tilde{v}}{\partial x}, \tag{1.16a}$$

$$\frac{\partial \tilde{v}}{\partial t} = \frac{\lambda_1}{\lambda_0}\partial_2 \frac{\partial \tilde{u}}{\partial x} + \frac{\lambda_1}{\lambda_0}\partial_1 \tilde{v}. \tag{1.16b}$$

where $\partial_1 = \frac{\partial^2}{\partial x^2} + \frac{\delta q}{q_{sc}}\frac{\partial^2}{\partial y^2} - \frac{1}{4q_{sc}^2}\frac{\partial^4}{\partial y^4}$ and $\partial_2 = 2\delta q - \frac{1}{q_{sc}}\frac{\partial^2}{\partial y^2}$ We analyse equations (1.16a) and (1.16b) by using normal modes form

$$\tilde{u} = U\cos(q_x x)\cos(q_y y)e^{St}, \qquad \tilde{v} = V\sin(q_x x)\cos(q_y y)e^{St}. \tag{1.17}$$

Substituting equation (1.17) in equations (1.16a) and (1.16b) weget,

$$\Big[2(\epsilon^2\lambda_2 - \lambda_1\delta k^2) + \lambda_0 S + \chi_1\Big]U + \lambda_1\chi_2 q_x V = 0 \tag{1.18a}$$

$$\lambda_1 q_x \chi_2 U + (\chi_1 + \lambda_0 S)V = 0. \tag{1.18b}$$

Here $\chi_1 = \lambda_1\Big(q_x^2 + \frac{q_y^2\delta k}{q_{sc}} + \frac{q_y^4}{4q_{sc}^2}\Big)$ and $\chi_2 = (2\delta k + \frac{q_y^2}{q_{sc}})$. On solving equations (1.18a) and (1.18b), we get

$$S^2 + \frac{2S}{\lambda_0}\Big[2\Big(\epsilon^2\lambda_2 - \lambda_1(\delta k)^2\Big) + \chi_1\Big] + \Big[2\Big(\frac{\epsilon^2\lambda_2}{\lambda_0^2} - \frac{\lambda_1\delta k^2}{\lambda_0^2}\Big) + \chi_1\Big]\psi_1 - q_x^2\chi_2\frac{\lambda_1}{\lambda_0^2} = 0, \tag{1.19}$$

whose real roots are $(S\pm)$,

$$(S\pm) = -\frac{1}{\lambda_0^2}\left\{\Big[2\lambda_0(\epsilon^2\lambda_2 - \lambda_1\delta k q^2) + \lambda_0\chi_1\Big] \pm \Big[2\lambda_0(\epsilon^2\lambda_2 - \lambda_1\delta q^2)^2 + \lambda_1^2 q_x^2\chi_2^2\Big]^{\frac{1}{2}}\right\}. \tag{1.20}$$

The equivalent mode is stable if $S(-)$ is negative and unstable if $S(+)$ is positive. Symmetry significance helps to confine the field of $S(+)$ to $q_x \geq 0, q_y \geq 0$.

Eckhaus Instability

Putting $q_y = 0$ into equation (1.20), we get

$$S^2 + \frac{2S}{\lambda_0}\Big[2(\epsilon^2\lambda_2 - \lambda_1\delta q^2) + \lambda_1 q_x^2\Big] + \frac{\lambda_1 q_x^2}{\lambda_0^2}\Big[2(\epsilon^2\lambda_2 - 3\lambda_1\delta q^2) + q_x^2\Big] = 0, \qquad (1.21)$$

The roots are real numbers and their sum is negative number and the product of roots is positive number, the pattern is stable and if the product of roots is negative number then the pattern becomes unstable. Eckhaus instability defines $q_x^2 \leq 2\Big(3\lambda_1\delta q^2 - \epsilon^2\lambda_2\Big)$ for $|\delta q| \geq \sqrt{\frac{\epsilon^2\lambda_2}{3\lambda_1}}$ and unstable wave tends to zero when $|\delta q| \rightarrow \sqrt{\frac{\epsilon^2\lambda_2}{3\lambda_1}}$.

Zigzag Instability

putting $q_x = 0$ into equation (1.21), we get

$$\lambda_0^2 S^2 + 2S(2\lambda_0\chi_{11} + \lambda_0\chi_{12}) + (2\chi_{11} + \chi_{12})\chi_{12} = 0, \qquad (1.22)$$

where $\chi_{11} = \epsilon^2\lambda_2 - \lambda_1\delta q^2$ and $\chi_{12} = \lambda_1\left(\frac{q_y^2\delta q}{q_s c} + \frac{q_y^4}{4q_{sc}^2}\right)$, the two eigen conditions are unrelated and amplified when $S(-) = -2(\epsilon^2\lambda_2 - \lambda_1\delta q^2) - \frac{\lambda_1}{q_{sc}}q_y^2\delta q - \frac{\lambda_1}{4q_{sc}^2}q_y^2 < 0$ and $S(+) = -\lambda_1 q_y^2\Big(\delta q + \frac{q_y^2}{4q_{sc}}\Big) > 0$. These conditions define the domain of Zigzag Instability when $\delta q_s < 0$.

1.12 Literature Survey

1.12.1 Rayleigh Benard Convection in a Porous Medium with the Effect of Rotation and Magnetic Field.

Rayleigh Benard Convection with the Effect of Rotation

Rayleigh Benard convection with the effect of rotation is an interesting application in hydrodynamic system which combines thermal buoyancy with rotation induced centrifugal and coriolis forces. Chandrasekhar [35], Busse *et al.* [29, 30] and Buell and Ivan [27] investigated the effect of rotation in atmospheric and oceanic flow. A Taylor number (Ta) characterizes the centrifugal forces due to the rotation of a fluid about the vertical axis, relative to viscous forces. Chandrasekhar [35] derived Rayleigh number (R) as a function of Taylor number (Ta). Davies and Oilman [39] found that for a large Ta, the Rayleigh number for steady convection is less and the system is more constrained. Chandrasekhar [35], Tagare *et al.* [119] and Benerji *et al.* [8] studied linear and nonlinear instabilities of Rayleigh Benard convection in rotating fluid between stress-free boundaries and observed the rotation effect on the onset thermal instability.

Rayleigh Benard Convection with Effect of the Magnetic Field

The Rayleigh-Benard convection with an imposed magnetic field has significant importance in astrophysical applications and observation of sunspots. The theory of sunspots was studied by Thompson and Weiss [122]. In outer layers of the sun and other late type stars, thermal convection is affected by the presence of magnetic fields. Thermal stability of magnetoconvection was first carried out by Thomson [124] who observed that the Rayleigh number increases linearly with Chandrasekhar number Q. Chandrasekhar [35], Kloosterziel and Carnevale [56] who observed the onset of stationary convection, predicted that magnetic prandtl number Pr_2would be less than the thermal Prandtl number Pr_1. Nakagawa [74] and Jirlow [54] investigated magnetoconvection experimentally, found that vertical magnetic fields delay the thermal convection and the marginal stability boundary is determined. Bhatia and Steiner [22] found that a magnetic field has a stabilizing effect on thermal convection. In the magnetoconvection, the magnetic field strongly affects all kinds of convective flows by varying the direction and density. The presence of a vertical magnetic field leads the boundary of monotonous instability and increases the stability of the conductive state. The presence of a horizontal magnetic field breaks the symmetry and convection occurs in the form of rolls with axes parallel to them. A strong horizontal magnetic field leads to time-dependent convection and purely geometrical effects cause oscillations. Chandrasekhar [35], Knobloch *et al.* [58], Busse *et al.* [30] , Clever *et al.* [36] and Basak *et al.* [15] investigated a uniform vertical magnetic field that suppresses the onset of convection, reduces convective heat transport across the fluid layer and affects the primary and secondary instabilities. Gotoh and Yamada [48] discussed thermal convection in a horizontal layer of magnetic fluid. Bajaj and Malik [12, 13] studied the Rayleigh Benard convection in magnetic fluids and examined the stability of various flow patterns. Burr and Muller [126] studied RayleighBnard convection in liquid metal layers under the influence of a horizontal magnetic field. The linear and nonlinear stability of magnetoconvection was studied by Kloosterziel and Carnevale [56], Thompson *et al.* [123] and Bhatta [23]. A broad review of magnetoconvection was given by Weiss and Proctor [131]. Their study concerned nonlinear models of the geomagnetic field and interactions of magnetic fields and they combined analytical and computational approach to provide a model for the study of a wide range of problems. Magneto-convection has multi-faceted applications in astrophysics, geophysics, aerodynamics, nuclear reactors, growth of large-diameter semiconductor crystals, meteorology, biomedical problems, engineering and industry. Chandrasekhar [35] identified that if magnetic field is imposed in a purely horizontal field and electromagnetic forces are strong compared to inertial ones, then the flow undergoes a two-dimensional convective rolls which is considerably less than Joule dissipation.

Rayleigh Benard Convection in a Porous Medium

Rayleigh-Benard convection in a porous medium has considerable interest in geophysical fluid dynamics and the phenomenon occurs within the Earth's outer core. Convection in a layer of viscous fluid was first studied by Rayleigh [91]. According to

Darcys law, which states the fluid flowing with velocity V through a porous medium experiences a resistance $\frac{gV}{K}$ per unit mass, where K is the coefficient of permeability and g is gravitational acceleration. Horton and Rogers [53] and Lapwood [61] analyzed the critical Rayleigh number, which determines the onset of natural convection in horizontal isotropic porous layer heated from below and cooled from above assuming Darcy's law. They found that the critical Rayleigh number is $4\pi^2$ corresponding to critical wave number π. This discrepancy between theory and experiments were sought to be removed by Rogers and Morrison [94] and Rogers *et al.* [95] by allowing for temperature dependence of fluid properties and columnar (rather than cellular) form of convection. Lapwood's problem was greatly extended by Wooding [132–134] at different states experimentally and theoretically. Palm *et al.* [82] pointed out that convection in a porous media may provide a convenient means of experimentally demonstrating nonlinear effects in convection such as the preferred cell pattern or hysteresis. Beck [16] was the first who investigated the selection of these roll patterns in rectangular porous boxes according to linear theory. The formulation and derivation of the basic equations using Boussinesq approximation was given in a treatise by Joseph [55]. The linear stability problem for the onset of convection and various nonlinear instability phenomena in porous media have been reviewed by Rees *et al.* [92, 93]. In Benard convection, it is necessary to use extremely thin fluid layers to detect these phenomena, but in porous media the friction force is much larger, so the depth of the fluid layer can be greatly increased. An alternative to Darcys equation is Brinkman equation which is valid for a sparsely packed porous medium.

Rayleigh Benard Convection with the Effect of Rotation and Magnetic Field

Both effects inhibit the onset of instability and elongate the cells which appear at marginal stability. Nakagawa [75] experiments the thermal instability in the presence of magnetic field and rotation successfully. The critical Rayleigh number for the onset of instability, for a constant speed of rotation and strength of magnetic field, was determined by measuring the steady temperature gradients which are established for various rates of heating. The onset of overstability could always be distinguished by the nearly pure sinusoidal oscillations exhibited by the temperature records. The thermal instability with the effect of rotation and magnetic field was theoretically studied by Chandrasekhar [34] and Eltayeb [43]. Gupta *et al.* [49] studied Rayleigh-Benard convection problem under the simultaneous action of a uniform vertical rotation and magnetic field for the validity of principle of exchange of stabilities. Mulone and Rionero [69] studied the nonlinear stability of the magnetic Benard problem with rotation through Lyapunov direct method, in stressfree case and for vanishing stress at the boundaries, the nonlinear critical Rayleigh number has the same behaviour as in the linear case. Friedrich *et al.* [44] experimentally studied the effects of a rotating magnetic field on fluid flow in an electrically conducting melt kept in a cylindrical container heated from below; experimental data were compared to three-dimensional, time-dependent numerical calculations. Volz and Muzuruk [128,129] observed the rotating magnetic field increases the critical Rayleigh number and not affect the onset of instability for axisymmetric. Aurnou and Olson [6] studied thermal convection subject to a uniform rotation and a vertical magnetic field of liquid gallium layer experimentally, measured heat transfer at a low Prandtl number and observed the critical Rayleigh number increases with magnetic energy density and the convective heat transfer is inhibited by rotation. Varshney *et al.* [127] numerically studied the effect of a vertical magnetic field on rotating convection of low Prandtl number liquid metal in a cubical cavity; they found that the magnetic field generates a strong damping effect on flow velocities and heat transfer at low rotation rates. Podvigina [87] studied the onset of rotating convection with an imposed vertical magnetic field, identified the region of parameter values for which rolls emerge at the onset of convection. Ghosh and Pal [45] investigated instabilities and chaos near the onset of convection with free-slip boundaries in the presence of vertical rotation and horizontal magnetic field without Prandtl-number, using Direct numerical simulations.

Rayleigh Benard Convection in a Porous Medium with the Effect of Magnetic Field

Convection in a porous medium with magnetic field is of considerable interest in geophysical fluid dynamics problems, for example, earth's interior and the mushy layer of earth's outer core. Patil and Rudraiah [84] investigated the stability thermal convection in a porous medium of a conducting viscous fluid using normal mode technique and the energy method of stability theories. Rudraiah [98] studied linear theory for stationary and oscillatory modes using the normal modes and simple and Hopf-bifurcations, studied linear and steady nonlinear magnetoconvection in a sparsely packed porous medium using Brinkman model, and considered the effective viscosity μ_e was the same as fluid viscosity μ. Gilver and Altobelli [46] who investigated the phenomenon found that effective fluid viscosity μ_e to fluid viscosity μ takes a value ranging from 0.5 to 10.9. Sekar and Vaidyanathan [106,107] , Borglin *et al.* [26] and Desaive *et al.* [40] studied instability of saturating a porous medium with the effect of rotation in a magnetized ferrofluid. Alchaar *et al.* [3,4] who investigated the phenomena using the Brinkman model obtained closed form solutions based on a parallel flow assumption. Bian *et al.* [24,25] studied convection in a shallow horizontal porous layer, which a transverse magnetic field is applied. Saravanan and Yamaguchi [101] are studied the onset convection in a porous layer with magnetic fluid. The critical Rayleigh number, critical wave number, and the eigenfunctions were calculated using a combination of analytical and numerical methods. Benerji *et al.* [7] investigated the problem of magnetoconvection in a sparsely packed porous medium also studied linear and weakly nonlinear hydrodynamic stability, bifurcations and instabilities.

1.12.2 Thermohaline Convection in a Porous Medium with the Effects of Rotation and Magnetic Field.

Thermohaline Convection with the Effect of Rotation

Thermohaline convection with the effect of rotation has fundamental importance in geophysical problems involving water in oceans, Helium in Hydrogen and sulphur in molten from with iron in earth's outer core. Rotation brings in a new phenomena leading to the distortion of convection cells as well as causing in overstable oscillations. This analysis reveals that for infinitesimal interference in the form of rolls. The marginal state will be oscillatory and the critical Rayleigh number increases with increase in rotation parameter. Further it is found that for disturbances of finite amplitude, subcritical instability is possible, which means that the system becomes unstable to steady finite amplitude disturbances before it becomes unstable to infinitesimal disturbances. The rotating thermohaline convection is consequently expected to show a line of secondary bifurcation which culminates in tertiary bifurcation. For large Prandtl number, there exists only one secondary bifurcation point, not a line of secondary bifurcation points, which culminates in tertiary bifurcation point. The onset of instabilities in rotating thermohaline convection was studied by Subha Sengupta *et al.* [108], Pearlstein [86], Benerji [8], Tagare [118–120].

Thermohaline Convection with the Effect of Magnetic Field

The Thermohaline magneto convection provides a lot of information about the dynamics dealt with by astrophysicists, geophysicists, oceanographers and engineers on a varity of problems. The dynamo theory, which is a significant part of cosmic magneto hydrodynamics, explains the generation mechanism and origin of these magnetic fields and their spatial and temporal evolution and changes. Lortz [62] was the first to study double-diffusive convection with the effect of magnetic field. Malkus and Veronis [66] clarified some of the mathematical aspects of stability criterion. Rudhraiah *et al.* [98, 99] investigated and studied the linear and nonlinear theory of the thermohaline convection in the presence of a magnetic field. The effect of magnetic field and salinity gradient are to suppress the steady convective motions depending on the strength of the magnetic field and under certain conditions where the system is unstable. Banerjee *et al.* [14] and Mohan [68] studied a characterization theorem in magnetothermohaline convection; the total kinetic energy associated with a disturbance is greater than the sum of its total magnetic and concentration energies. Abdullah [1] studied thermosolutal convection in a nonlinear magnetic fluid when the fluid is heated from above and soluted from below. Narayana *et al.* [76] studied magneto thermohaline convection for viscoelastic fluids, Harfash *et al.* [51] in a reacting fluid and Bhadauria and Kiran [19] studied the weakly nonlinear double diffusive magneto convection in Newtonian fluids.

Thermohaline Convection in the Porous Medium

In geothermal areas, the ground water usually contains salts in solution, and hence it is of interest to consider the onset of convection in porous medium when both thermal expansion and solute concentration variations can produce variations in density. The onset of thermohaline convection in a porous medium was first studied by Nield [78] who analysed the effect of a stable salinity gradient of a saturated porous medium using Darcy model. Patil and Rudraiah [84] and Rubin [96, 97] studied the effect of stable and unstable temperature and salinity gradients on the stability of conducting single component and two component fluids in a porous medium using Brinkman model. Patil *et al.* [85] studied various cases of stabilising and destabilising concentrations and temperature gradients for both Brinkman and Darcy models for two component fluids. Poulikakos [88] used Brinkman extension of the Darcy model to study the effect of sparsely packed porous medium on double diffusive convection. Murray and Chen [71] experimentally examined the double-diffusive convection in a porous medium. Parthiban *et al.* [83] studied the effect of inclined gradients on thermohaline convection in a porous medium, Murty *et al.* [72] studied numerically the stability of thermohaline convection in a rectangular box containing a porous medium and Curtis *et al.* [81] studied plume separation by transient thermohaline convection in porous media. Mulone and Straughan [70] used change of variable in an energy method and discussed the coincidence of the critical linear and nonlinear stability parameters. Musuuza *et al.* [73] studied a thermohaline system in which the density gradients arise from salinity and temperature difference. Benerji *et al.* [10] studied the thermohaline convection between stress-free boundaries in a sparsely packed porous medium, using the DLB model. Sekar *et al.* studied [103,104] stability analysis of thermohaline convection in Ferrofluids and dusty ferrofluids in a sparsely packed porous medium.

Thermohaline Convection with the Effect of Rotation and Magnetic Field

The effects of rotation about vertical axis and magnetic field about vertical direction have often been emphasized in the literature by Chandrasekhar [35]. Convection under rotation or magnetic field is interesting because each can stabilize conduction state independently. Similarly oscillatory convection and subcritical steady finite amplitude convection can both occur in presence of a magnetic field and during rotation. Gupta *et al.* [50] and Dhiman [41] analysed the governing equations of thermohaline convection with a uniform vertical rotation and magnetic field. Sekar *et al.* [105] interested to find out the effect of rotation on two component ferrofluids for both sparsely and densely packed porous medium using Brinkman and Darcy models. The thermohaline convection was analysed for both the stationary and oscillatory modes. Mahinder and Pradeep [113] are studied the thermosolutal convection in a couple-stress fluid in a porous medium in the presence of rotation and vertical magnetic field, using normal mode analysis. Chand *et al.* [33] theoretically investigated the effect of rotation with internal angular momentum in a magnetized ferrofluid, soluted and heated from below, and subjected to a transverse uniform magnetic field.

Thermohaline Convection in a Porous Medium with the Effect of Magnetic Field

Thermohaline magneto convction in a porous medium is an example of triple diffusive mechanism, and exercises a huge influence on many science and engineering applications. Marked improvement in theoretical investigation of the planetary and stellar magnetism has come into being, especially in recent years. Sharma *et al.* [109] studied thermohaline convection in a porous medium subject to magnetic field in a layer of fluid subject to a stable salinity gradient. Rayleigh value increased with increase in stable salinity gradient as well as magnetic field. Sunil *et al.* [116, 117] studied convection of saturated porous medium on the effects of rotation and magnetic fields in a ferromagnetic fluid using linear stability analysis. Bhadauria and Srivastava [21] studied thermohaline magneto convection in the porous medium, characterized by BrinkmanDarcy model. Sekar *et al.* studied [102] studied stability analysis of thermohaline convection in ferromagnetic fluids in a densely packed porous medium. Benerji *et al.* [10] used DLB model to study stability analysis of thermohaline magneto convection in a sparsely packed porous medium and obtained the conditions for the occurrence of various types of bifurcations and derived Landau-Ginzburg equations to study the instabilities. Prakesh *et al.* [89] studied linear stability analysis of thermohaline convection in porous medium in the presence of a uniform vertical magnetic field, characterization theorem was proved for magnetothermohaline convection of the Stern type.

1.13 Objective of the Present Work

The objective of the present study is to explore the linear and nonlinear convection in a porous medium with the effects of rotation due to vertical and horizontal magnetic field for single diffusive, double diffusive and triple diffusive systems. Rayleigh Benard convection in a sparsely packed porous medium with magnetic field and rotation and thermohaline convection is an example of double diffusive system. Thermohaline convection in a sparsely packed porous medium with magnetic field and rotation is example of triple diffusive system. In linear and nonlinear analysis, we write analytical conditions for varies bifurcation points and instabilities. Graphically, reprsented the stability regions of Eckhaus and Zigzag instabilities at the onset of Pitchfork bifurcation. At the onset of nonstationary mode we identified travelling wave and standing wave regions for various parameters.

1.14 Outline of the Thesis

This thesis consists of seven chapters. Chapter 1 consists of introduction to the study and is general in it provides rationale for investigations carried out in the thesis. Chapter 2 discusses the linear and nonlinear instabilities of Rayleigh Benard convection in a sparsely porous medium due to horizontal magnetic field. Chapter 3 looks at the instabilities of Rayleigh Benard convection in a sparsely packed porous medium with the effect of rotation and horizontal magnetic field. Chapter 4 investigates linear and nonlinear instabilities of thermohaline convection in a sparsely porous medium due to horizontal magnetic field. Chapter 5 discusses thermohaline convection in a sparsely porous medium with the effect of rotation. Chapter 6 looks at the problem of thermohaline convection in a porous medium with the effect of rotation and horizontal magnetic field. Chapter 7 deals with conclusions and scope of future work.

List of papers published/accepted

1. Babu, A. Benerji, N. Venkata Koteswararao, and G. Shivakumar Reddy. "Instability Conditions in a Porous Medium Due to Horizontal Magnetic Field." *Numerical Heat Transfer and Fluid Flow*, 621-628, 2019.

2. Babu, A. Benerji, N. Venkata Koteswararao,"Nonlinear Instabilities of Horizontal magnetoconvection in a Sparsely Packed Porous Medium", accepted in *Special Topics and Reviews in Porous Media - An International Journal*, 2019.

3. A.Benerji Babu , N.Venkata Koteswara Rao , S. G. Tagare , "Instabilities of Horizontal Magnetoconvection with Rotating Fluid in a Sparsely Packed Porous Media", *Heat Transfer - Asian Research*, 48, 3055-3078, 2019.

List of papers communicated

4. A.Benerji Babu, N.Venkata Koteswara Rao, G.Shiva Kumar Reddy, Weakly Nonlinear Thermohaline Rotating Convection in a Sparsely Packed Porous Medium due to Horizontal Magnetic Field, *Geophysical Journal International*.

5. A.Benerji Babu, N.Venkata Koteswara Rao , S. G. Tagare , Weakly Nonlinear Thermohaline Rotating Convection in a Sparsely Packed Porous Medium, *Earth Interactions*.

6. A.Benerji Babu, N.Venkata Koteswara Rao , S. G. Tagare , Weakly Nonlinear Thermohaline Convection in a Sparsely Packed Porous Medium due to Horizontal Magnetic Field, *Computers and Fluids*.

Chapter 2

(i). Linear Instabilities of Rayleigh Benard Convection in a Sparsely Packed Porous medium due to Horizontal Magnetic Field

(ii). Nonlinear Instabilities of Rayleigh Benard Convection in a Sparsely Packed Porous medium due to Horizontal Magnetic Field

2.1 Introduction

Convection in a plane horizontal fluid heated from below and cooled from above is a conventional problem in hydrodynamic stability. The rolls with axes parallel to the horizontal magnetic field were arises on the set of convection. Magnetoconvection is the study of thermal convection of electrically conducting fluid in the presence of magnetic field. Thompson [125] and Chandrashekar [35] were studied the effect of vertical magnetic field on the onset of convection. The frontier of monotones instability is unnatural only by the vertical component of the magnetic field. However,the property of isotropy, are kept in the case of a purely vertical magnetic field and Busse [28] and Proctor [90] also studied. In the magnetoconvection, the magnetic field strongly affects all kinds of convective flows by varying direction and density. The presence of a vertical magnetic field leads the boundary of monotonous instability and increases the stability of the conductive state. The presence of a horizontal magnetic field breaks the symmetry and arise the convection in the form of rolls with axes parallel to them. The horizontal magnetic field not change the primary instability and affects for secondary instability. A strong horizontal magnetic field lead to time-dependent convection and purely geometrical effects cause oscillations. However Horizontal magnetoconvection in a porous medium has not conventional any attention in-spite of its geophysical application. The linear and nonlinear stability of magnetoconvection was studied by Kloosterziel [56], Thompson [123] and Bhatta [23]. A broad review about magnetoconvection given by Broad Weiss and Proctor [131], concerned nonlinear models of the geomagnetic field and interactions of magnetic fields. Magnetoconvection has multi-faceted applications in astrophysics, geophysics, aerodynamics, nuclear reactors, the growth of large-diameter semiconductor crystals, meteorology, biomedical problems, engineering and industry.

A study of convection in porous medium broadly given by Nield and Bejan [80]. Magnetoconvection in a porous medium by using Darcy's law studied by Anwar [17] and Srivastava [114]. Magnetoconvection in a sparsely packed porous medium studied by Benerji [7] and Shivakumara [112]. Magnetoconvection in a porous medium has important relevance in the study of the Earth's core in geophysics, efficiency of petroleum reservoir and engineering applications.

In this chapter, we studied primary and secondary instabilities and bifurcation of the magnetoconvection in a sparsely packed porous medium due to horizontal magnetic field by deriving Ginzburg Landau equations. At the supercritical pitchfork bifurcation we evolved two-dimensional LG equation derived at the supercritical Hopf bifurcation we evolved one dimensional LG equations at the onset of oscillatory convection and identified secondary instabilities and region of travelling and standing waves. Tagare *et al.* [119, 120], Benerji *et al.* [10] derived one dimensional and two dimensional Ginzburg Landau equations at the onset of stationary and oscillatory convection.

The basic equations for weakly nonlinear magnetoconvection in a sparsely porous medium are derived. Normal mode technique is used to study the linear stability analysis. Two dimensional Ginzburg Landau equation derived and study the transport of heat by convection and occurrence of secondary instabilities. The system of nonlinear one dimensional Ginzburg Landau equations are derived and obtained the stability regions of steady state, standing and travelling waves.

2.2 Basic equations

We considered the thermally and electrically conducting fluid in an unbounded horizontal layer of a thinly packed porous medium with an magnetic field H_o of depth d in the horizontal x-direction. Upper and lower force free bounding surfaces of the layer heated from below is valid Bousssinesq approximation. The temperature variation across the free-free boundaries is $\Delta T'$. The flow in the thinly packed porous medium is governed by the DLB model. The dimensionless equations for horizontal magneto convection in a porous medium are

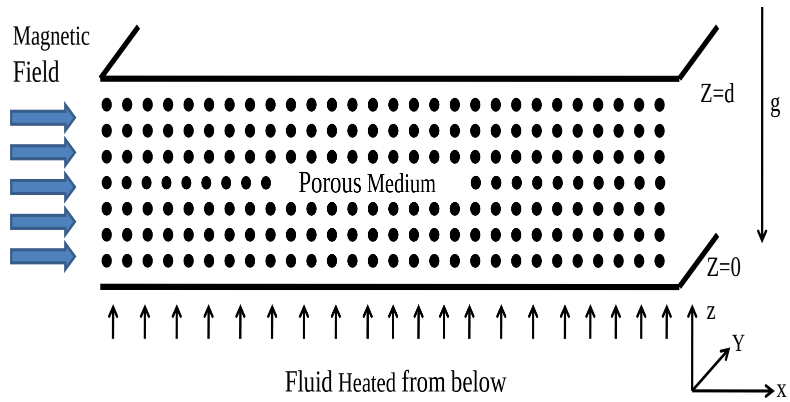

Figure 2.1: Physical Configuration

$$\nabla'.\overline{V}' = 0, \quad \text{and} \quad \nabla'.\overline{H}' = 0, \tag{2.1}$$

$$\rho'_o\left[\frac{1}{\phi}\frac{\partial \overline{V}'}{\partial t'} + \frac{1}{\phi^2}(\overline{V}'.\nabla')\overline{V}'\right] - \frac{\mu_m}{4\pi}\left[H'_o\frac{\partial \overline{H}'}{\partial x'} + (\overline{H}'.\nabla')\overline{H}'\right] =$$
$$-\nabla\left(P' + \frac{\mu_m}{8\pi}|H'|^2 + \frac{\mu_m H_0}{4\pi^2}H'_y\right) + \rho'\overline{g} - \frac{\mu}{K}\overline{V}' + \mu_e\nabla'^2\overline{V}', \tag{2.2}$$

$$M\frac{\partial T'}{\partial t'} + (\overline{V}'.\nabla')T' = \kappa\nabla'^2 T', \tag{2.3}$$

$$\phi\frac{\partial \overline{H}'}{\partial t'} = \nabla' \times (\overline{V}' \times H'_o\hat{e}_y) + \nabla' \times (\overline{V}' \times \overline{H}') + \eta\nabla'^2\overline{H}'. \tag{2.4}$$

The fluid density ρ' is described as

$$\rho' = \rho'_0\left[1 - \alpha(T' - T'_b)\right], \tag{2.5}$$

where ρ'_0 - fluid density, $\alpha = \frac{1}{-\rho'_0}(\frac{\partial\rho'}{\partial T'})$ is thermal expansion coefficient, $\overline{V}'$ - fluid velocity, P' - pressure, $\overline{H}'$ - magnetic field, T' - temperature, g - acceleration due to gravity, ϕ - porosity and $0.8 < \phi < 1$ for DLB model, μ_e - coefficient of effective fluid viscosity, K - permeability of porous medium, μ_m - magnetic permeability, κ - thermal diffusivity and η - magnetic diffusivity. $\Lambda = \mu_e/\mu$ varies from 0.5 to 10.9. The dimensionless quantity M represents the dimensionless Heat capacity.

The conduction state is characterized by

$$\overline{V}'_s = 0, \quad T'_s = T'_0 - (\Delta T'/d)z', \tag{2.6}$$

and we take the temperature perturbation as $\theta' = T' - T'_s$. We use the scaling

$$\begin{array}{llll} x = \dfrac{x'}{d} & u = \dfrac{u'}{\kappa/Md} & t = \dfrac{t'}{Md^2/\kappa} & \overline{H} = \dfrac{\overline{H}'}{\kappa H_o/\eta} \\ y = \dfrac{y'}{d} & v = \dfrac{v'}{\kappa/Md} & \theta = \dfrac{\theta'}{\Delta T'} & P = \dfrac{P'}{\rho'_o M^{-2}\kappa^2 d^{-2}} \\ z = \dfrac{z'}{d} & w = \dfrac{w'}{\kappa/Md} & & \end{array}$$

The basic dimensionless equations are

$$\nabla.\overline{V} = 0, \quad \text{and} \quad \nabla.\overline{H} = 0, \tag{2.7}$$

$$\begin{aligned} \frac{1}{M^2\phi Pr_1}\left[\frac{\partial \overline{V}}{\partial t} + \frac{1}{\phi}(\overline{V}.\nabla)\overline{V}\right] - Q\frac{\partial \overline{H}}{\partial y} - Q\frac{Pr_2}{Pr_1}(\overline{H}.\nabla)\overline{H} = \\ -\nabla\left(\frac{P}{MPr_1} + \frac{Q}{2}\frac{Pr_2}{Pr_1}|\overline{H}|^2 + QH_y\right) - \frac{1}{MD_a}\overline{V} + \frac{\Lambda}{M}\nabla^2\overline{V} + R\theta\hat{e_z}, \end{aligned} \tag{2.8}$$

$$\frac{\partial \theta}{\partial t} + \frac{1}{M}(\overline{V}.\nabla)\theta = \frac{w}{M} + \nabla^2\theta, \tag{2.9}$$

$$\phi\frac{Pr_2}{Pr_1}\frac{\partial \overline{H}}{\partial t} - M\nabla^2\overline{H} = \nabla \times (\overline{V} \times \hat{e}_y) + \frac{Pr_2}{Pr_1}\nabla \times (\overline{V} \times \overline{H}). \tag{2.10}$$

The non dimensional numbers are defined as

$$\begin{array}{lll} R = \dfrac{g\alpha\Delta T d^3}{\kappa\nu} & Pr_1 = \dfrac{\nu}{\kappa} & Pr_2 = \dfrac{\nu}{\eta} \\ Q = \dfrac{\mu_m H_0^2 d^2}{4\pi\rho_0\nu\eta} & Da = \dfrac{K}{d^2} & \end{array} \tag{2.11}$$

Now taking the scalar product of curl of curl of equation (2.8) and equation (2.10) with $\hat{e}_z$. we get,

$$\left(\frac{1}{M^2\phi Pr_1}\frac{\partial}{\partial t}+\frac{1}{MD_a}-\frac{\Lambda}{M}\nabla^2\right)\nabla^2 w+Q\frac{Pr_2}{Pr_1}\hat{e}_z\left\{\nabla\times\left[(\overline{H}.\nabla)\overline{J}-(\overline{J}.\nabla)\overline{H}\right]\right\}$$
$$=\frac{1}{M^2\phi^2 Pr_1}\hat{e}_z\left\{\nabla\times\left[(\overline{V}.\nabla)\overline{W}-(\overline{W}\nabla)\overline{V}\right]\right\}+R\nabla_h^2\theta+Q\frac{\partial}{\partial y}(\nabla^2 H_z), \qquad (2.12)$$

$$\left(\phi\frac{Pr_2}{Pr_1}\frac{\partial}{\partial t}-M\nabla^2\right)H_z-\frac{\partial w}{\partial z}=\frac{Pr_2}{Pr_1}\left[\nabla\times(\overline{V}\times\overline{H})\right]\cdot\hat{e}_z, \qquad (2.13)$$

using equations (2.9), (2.12) and (2.13) can be brought to a form given as

$$\mathcal{L}w=\mathcal{N}, \qquad (2.14)$$

where

$$\mathcal{L}=\mathcal{D}_\phi\mathcal{D}_{Pr_1}\left[\mathcal{D}\nabla^2-Q\partial_y^2\mathcal{D}\nabla^2\right]-\frac{R}{M}\nabla_h^2\mathcal{D}_\phi, \qquad (2.15)$$
$$\mathcal{N}=Q\mathcal{D}\nabla^2\frac{Pr_2}{Pr_1}\partial_y\left[(\overline{H}.\nabla)w-(\overline{V}.\nabla)H_z\right]+\frac{1}{M^2\phi^2 Pr_1}\mathcal{D}\mathcal{D}_\phi\hat{e_z}s_1$$
$$-Q\frac{Pr_2}{Pr_1}\mathcal{D}\mathcal{D}_\phi\hat{e_z}\left\{\nabla\times\left[(\overline{H}.\nabla)\overline{J}-(\overline{J}.\nabla)\overline{H}\right]\right\}-\frac{R}{M}\nabla_h^2\mathcal{D}_\phi(\overline{V}.\nabla)\theta, \qquad (2.16)$$

where $\mathcal{D}=\left(\frac{\partial}{\partial t}-\nabla^2\right)$, $\mathcal{D}_\phi=\left(\phi\frac{Pr_2}{Pr_1}\frac{\partial}{\partial t}-M\nabla^2\right)$, $\mathcal{D}_{Pr_1}=\left(\frac{1}{M^2\phi Pr_1}\frac{\partial}{\partial t}+\frac{1}{MD_a}-\frac{\Lambda}{M}\nabla^2\right)$, $\nabla_h^2=(\frac{\partial^2}{\partial x^2}+\frac{\partial^2}{\partial y^2})$ and $\nabla^2=(\frac{\partial^2}{\partial x^2}+\frac{\partial^2}{\partial y^2}+\frac{\partial^2}{\partial z^2})$.

2.2.1 Boundary Conditions

Let us assume the fluid is contained between $z=0$ and $z=1$, For perfectly conducting boundary with temperature, we have

$$\theta=0 \quad \text{and} \quad H_z=0 \quad \text{on} \quad z=0,z=1 \quad \text{for all} \quad x,y.$$

The tangential stresses on surfaces vanish and stress-free conditions are considered on the surface and vanishing of temperature fluctuations.

$$\tau_{xz} = \mu\left(\frac{\partial u}{\partial z} + \frac{\partial w}{\partial x}\right) = 0, \quad \tau_{yz} = \mu\left(\frac{\partial v}{\partial z} + \frac{\partial w}{\partial y}\right) = 0, \tag{2.17}$$

where μ is the dynamic viscosity, thus equation of continuity implies that $w = D^2w = D^4w = 0$ at $z = 0, 1$.

2.3 (i). Linear Instabilities of Rayleigh Benard Convection in a Sparsely Packed Porous medium due to Horizontal Magnetic Field

Linear stability analysis approach to studying stability of a flow is to analyse how the system responds to small disturbance. The solution of linearised system $\mathcal{L}w = 0$, assumes the periodic disturbances with period $2\pi/l$ along x-direction, periodic disturbances with period $2\pi/m$ along y-direction with growth rate p of the form

$$w = W(z)e^{i(lx+my)+pt}, \tag{2.18}$$

we perform a linear stability analysis of the problem by substituting w into $\mathcal{L}w = 0$, we get

$$\Big\{D_qD_{qp}M_\phi\Big[\frac{\Lambda}{M}D_q - \frac{1}{MD_a} - \frac{p}{M^2\phi Pr_1}\Big] + \frac{Rq^2}{M}M_\phi + Qm^2D_qD_{qp}\Big\}W(z) = 0. \tag{2.19}$$

where $D_q = D^2 - q^2$, $D_{qp} = D^2 - q^2 - p$ and $M_\phi = MD_q - \phi\frac{Pr_2}{Pr_1}p$

2.3.1 Determination of Marginal Stability when Rayleigh number R is a Dependent Variable

Substituting $W(z) = \sin \pi z$ and $p = i\omega$ into equation (2.19), we get

$$R = \frac{M}{q^2} D_1 \left[A_1 + i\omega(B_1\omega^2 + C_1) \right], \tag{2.20}$$

where

$$A_1 = M \left[\left(\Lambda\delta^2 + \frac{1}{Da} \right) \delta^2 + Qm^2 \right] \delta^4 + \left[\frac{\phi^2 Pr_2^2}{MPr_1^2} \left(\Lambda\delta^2 + \frac{1}{Da} \right) \delta^2 + \frac{\phi^2 Pr_2}{Pr_1} Qm^2 \right] \omega^2$$
$$- \frac{\phi Pr_2^2}{M^2 Pr_1^3} \omega^4, \tag{2.21}$$

$$B_1 = \frac{\phi Pr_2^2}{MPr_1^2} \left(\phi\Lambda + \frac{1}{MPr_1} \right) \delta^2 + \frac{\phi^2 Pr_2^2}{DaMPr_1^2}, \tag{2.22}$$

$$C_1 = \left(M\Lambda + \frac{1}{\phi Pr_1} \right) \delta^4 + \frac{M}{Da}\delta^2 + \left(M - \frac{\phi Pr_2}{Pr_1} \right) Qm^2, \tag{2.23}$$

$$D_1 = \frac{\delta^2}{M^4\delta^4 + \phi^2 \frac{Pr_2^2}{Pr_1^2}\omega^2}, \ \delta^2 = \pi^2 + q^2 \text{ and } q^2 = l^2 + m^2. \tag{2.24}$$

Stationary Convection ($\omega = 0$):

Substituting $\omega = 0$ in equation (2.20), we get the stationary Rayleigh number R_s,

$$R_s = \frac{\delta^2}{q^2} \left[Qm^2 + \delta^2 \left(\frac{1}{Da} + \delta^2\Lambda \right) \right], \tag{2.25}$$

The critical stationary Rayleigh number R_{sc} for critical wave numbers l_{sc} and m_{sc} is

$$R_{sc} = \frac{\delta_{sc}^2}{q_{sc}^2} \left[Qm_{sc}^2 + \delta_{sc}^2 \left(\frac{1}{Da} + \delta_{sc}^2\Lambda \right) \right], \tag{2.26}$$

where $\delta_{sc}^2 = \pi^2 + q_{sc}^2$ and $q_{sc}^2 = l_{sc}^2 + m_{sc}^2$. which is convectively stable when $R_s < R_{sc}$, unstable when $R_s > R_{sc}$ and marginal stable when $R_s = R_{sc}$. If the temperatures at stress-free boundaries are fixed and at nonporous medium, $\phi = M = \Lambda = 1$, the value of critical stationary Rayleigh number $R_{sc} = 27\pi^4/4$ for critical wave number

$q_{sc} = \pi/\sqrt{2}$. If there is no periodic disturbance along x-direction and periodic disturbance along y-direction with growth rate p, then the stationary Rayleigh number R_{sy} is,

$$R_{sy} = (m^2+\pi^2)Q + (m^2+\pi^2)^2\left[\frac{1}{Da} + (m^2+\pi^2)\Lambda\right]. \tag{2.27}$$

If there are periodic disturbances along x-direction and no periodic disturbance along y-direction with growth rate p, then stationary Rayleigh number R_{sx} is,

$$R_{sx} = \frac{(l^2+\pi^2)^2}{l^2}\left[\frac{1}{Da} + (l^2+\pi^2)\Lambda\right]. \tag{2.28}$$

Oscillatory Convection ($\omega^2 > 0$):

From equation (2.20), R represents imaginary number but Rayleigh number is always real so equating imaginary part of equation (2.20) to zero. i.e.,

$$B_1\omega^2 + C_1 = 0, \tag{2.29}$$

where B_1 and C_1 are given by equations (2.22) and (2.23). For oscillatory convection $\omega^2 = -\frac{C_1}{B_1} > 0$ since $B_1 > 0$, for oscillatory convection $C_1 < 0$. For oscillatory convection, from the equation (2.29)

$$\omega^2 = \frac{-M^2\phi^2 Pr_1^2\left[M\phi Pr_1(Dam^2Q + \delta^2 + Da\delta^4\Lambda) + Da(\delta^4 - m^2QPr_2)\right]}{\phi^2 Pr_2^2\left(Da\delta^2 + M(1+Da\delta^2\Lambda)\phi Pr_1\right)}, \tag{2.30}$$

A necessary condition for $\omega^2 > 0$ is $Q > \frac{\frac{M\delta_o^2}{Da} + \delta_o^2\left(M\Lambda + \frac{1}{\phi Pr_1}\right)}{m^2\left(\phi\frac{Pr_2}{Pr_1} - M\right)}$ and $\frac{Pr_2}{Pr_1} > \frac{1}{\phi}$. Substituting ω^2 into real part of equation (2.20), we get oscillatory Rayleigh number R_0,

$$R_o = \frac{\delta^2 x_1\left[\frac{M}{Da}\left(x_1\delta^2 + x_2\phi\right) + \delta^4\frac{Pr_2}{Pr_1}\right]}{x_3 q^2\phi^3(Pr_2/Pr_1)^2}, \tag{2.31}$$

where

$$x_1 = Da\delta^2 + (1 + Da\delta^2\Lambda)\phi^2 Pr_2,$$
$$x_2 = Dam^2Q + \delta^2 + Da\delta^4\Lambda,$$
$$x_3 = Da\delta^2 + M(1 + Da\delta^2\Lambda)\phi Pr_1).$$

The following figures 2.2 to 2.4 which are plotted in (q, R)-plane, calculate the Rayleigh value based on the effect of physical parameters Q, Pr_1 and Pr_2. Stationary Rayleigh number is independent of Pr_1 and Pr_2. In figure 2.2, by increasing Chandrasekhar number Q and fixed remaining parameters stationary and oscillatory convection increases. In figure 2.2, at $Q = 5000$, there exists a codimension with two bifurcation points. In figure2.3, there exists a codimension two-bifurcation point occurs for an oscillatory marginal curve at $Pr_1 = 1.2$ while the remaining intersecting points are Takens-Bogdanov (T-B) bifurcation points. In figure 2.4, there exists a co-dimension two-bifurcation point that occurs for an oscillatory marginal curve at $Pr_2 = 1.25$ and the remaining intersecting points are Takens-Bogdanov (T-B) bifurcation points. This co-dimension two bifurcation point moves downwards when Pr_1 increases while co-dimension two bifurcation point moves upwards when Pr_2 decreases. Solid lines represent Rayleigh value at stationary convection R_s and dotted lines represent Rayleigh value at oscillatory convection R_o

2.3.2 Determination of Marginal Stability when Rayleigh number R is an Independent Variable

Substituting $W = \sin \pi z$, in to equation (2.19) we get a third order polynomial in p of the following form:

$$p^3 + Bp^2 + Cp + D = 0, \tag{2.32}$$

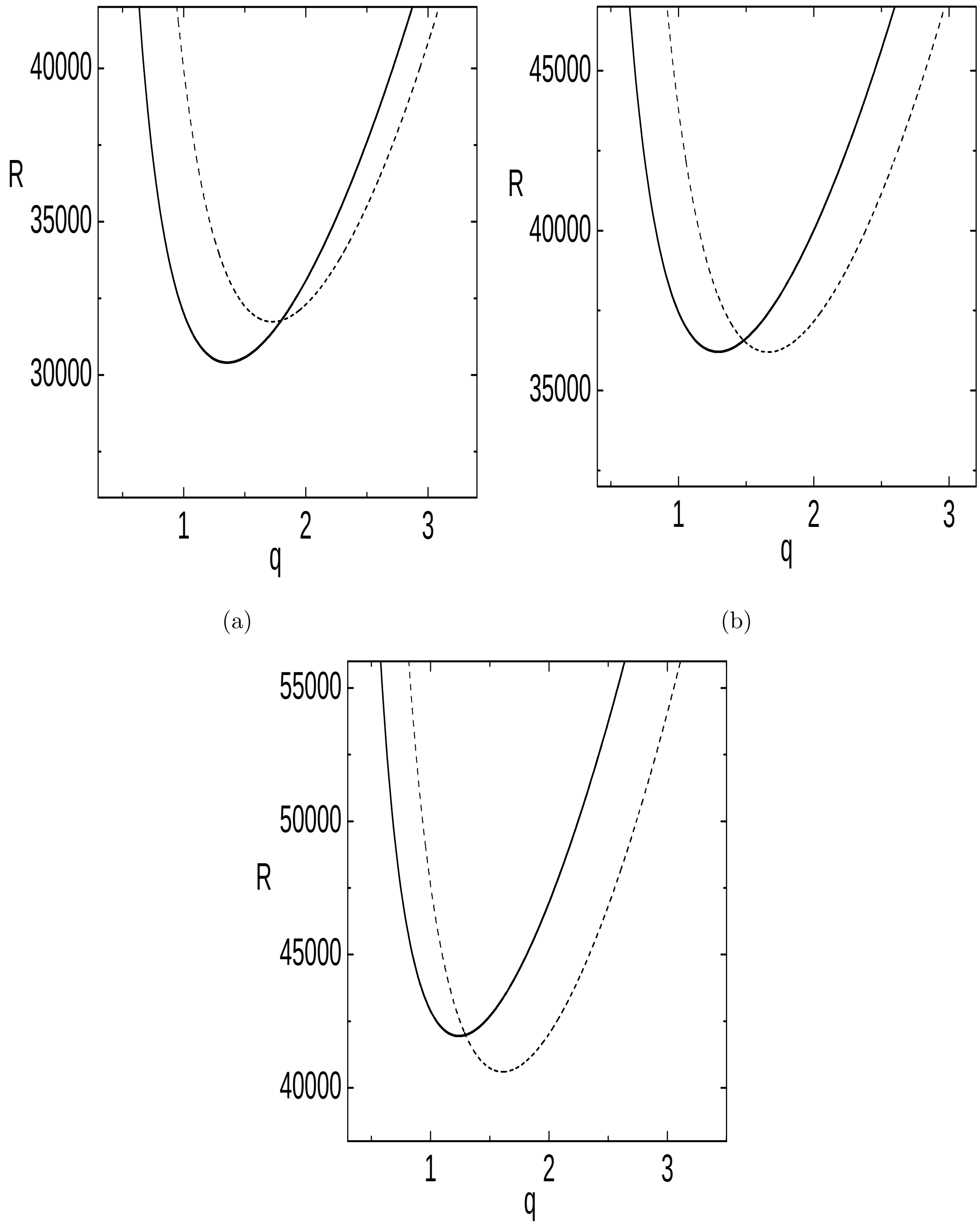

(a) (b) (c)

Figure 2.2: Neutral curves are plotted for $Da = 1500$, $\Lambda = 2$, $M = 0.9$, $\phi = 0.85$, $Pr_1 = 1$, $Pr_2 = 1.65$, (a) $Q = 4000$, (b) $Q = 5000$, (c) $Q = 6000$.

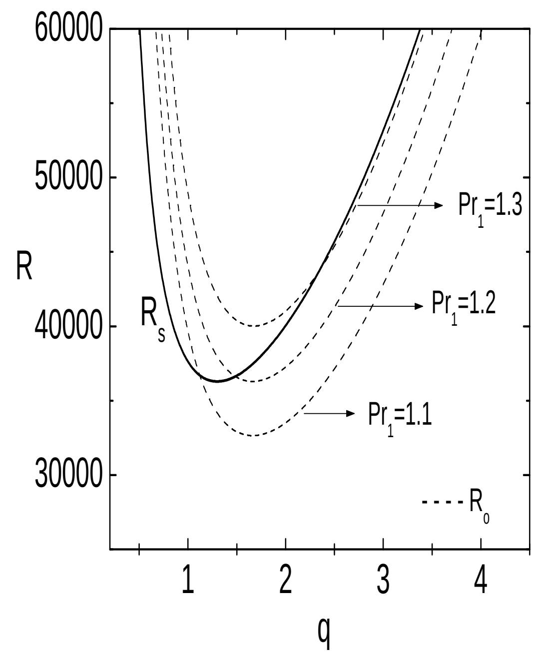

Figure 2.3: Neutral curves are plotted for $Da = 1500$, $\Lambda = 8$, $M = 0.9$, $\phi = 0.85$, $Q = 5000$, $Pr_2 = 1.5$, $Pr_1 = 1.1,\ 1.2,\ 1.3$.

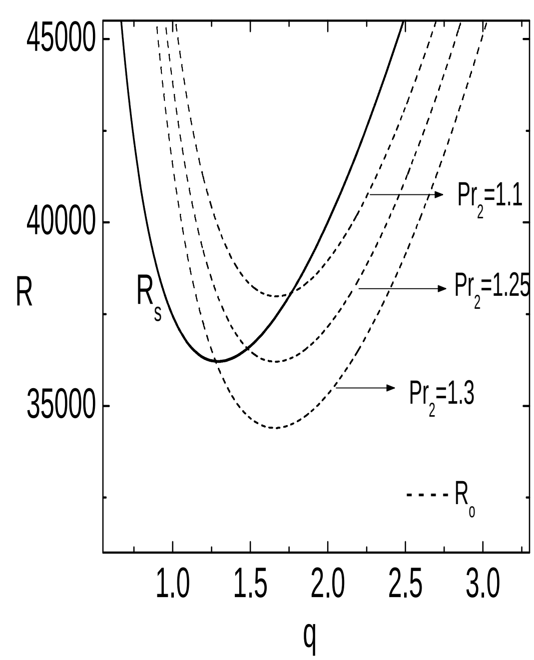

Figure 2.4: Neutral curves are plotted for $Da = 1500$, $\Lambda = 8$, $M = 0.9$, $\phi = 0.85$, $Pr_1 = 1$, $Q = 5000$, $Pr_2 = 1.1,\ 1.25,\ 1.3$.

where

$$B = \delta^2 + Pr_1 \left[\left(\frac{1}{Da} + \delta^2 \Lambda \right) M\phi + \frac{M\delta^2}{\phi Pr_2} \right], \tag{2.33}$$

$$C = \frac{1}{DaM\phi Pr_1} \Big[\left(Da\delta^6 + M\delta^2 Dam^2 Q + \delta^2 + Da\delta^4 \Lambda \right) \phi Pr_1 + \left(-Daq^2 R + \delta^4 + Da\delta^6 \Lambda \right) \phi^2 Pr_2 \Big], \tag{2.34}$$

$$D = M^2 \frac{Pr_1^2}{\delta^2 Pr_2} \left(-q^2 R\delta^2 + m^2 Q\delta^4 + \delta^6 Da + \delta^8 \Lambda \right). \tag{2.35}$$

If cubic polynomial equation (2.32), B is positive. The classification of stability modes of the system are the roots of equation (2.32). Unstable means there exists at least one root of equation (2.32) with $Re(p) > 0$, stable means all roots of equation (2.32) with $Re(p) < 0$. We get pitchfork bifurcaation when $D = 0$ and $BC - D > 0$. We get the Hopf bifurcation when $D > 0$ and $BC - D = 0$. With the root of each cubic equation there is an associated combination of flow field and temperature distribution.

Stationary Convection($w = 0$)

When $p = 0$,the cubic equation becomes $D = 0$

$$\frac{Rq^2}{\delta^2} = Qm^2 + \delta^2 (\frac{1}{Da} + \delta^2 \Lambda). \tag{2.36}$$

If the periodic disturbance only along y-direction,

$$Rm^2 = Qm^2(m^2 + \pi^2) + (m^2 + \pi^2)^2 \left[\frac{1}{Da} + (m^2 + \pi^2)\Lambda \right], \tag{2.37}$$

differentiating equation (2.37) w.r.t m, we get

$$R = Q(\pi^2 + 2m^2)m^2 + \frac{2}{Da}(\pi^2 + m^2) + 3\Lambda(\pi^2 + m^2)^2, \tag{2.38}$$

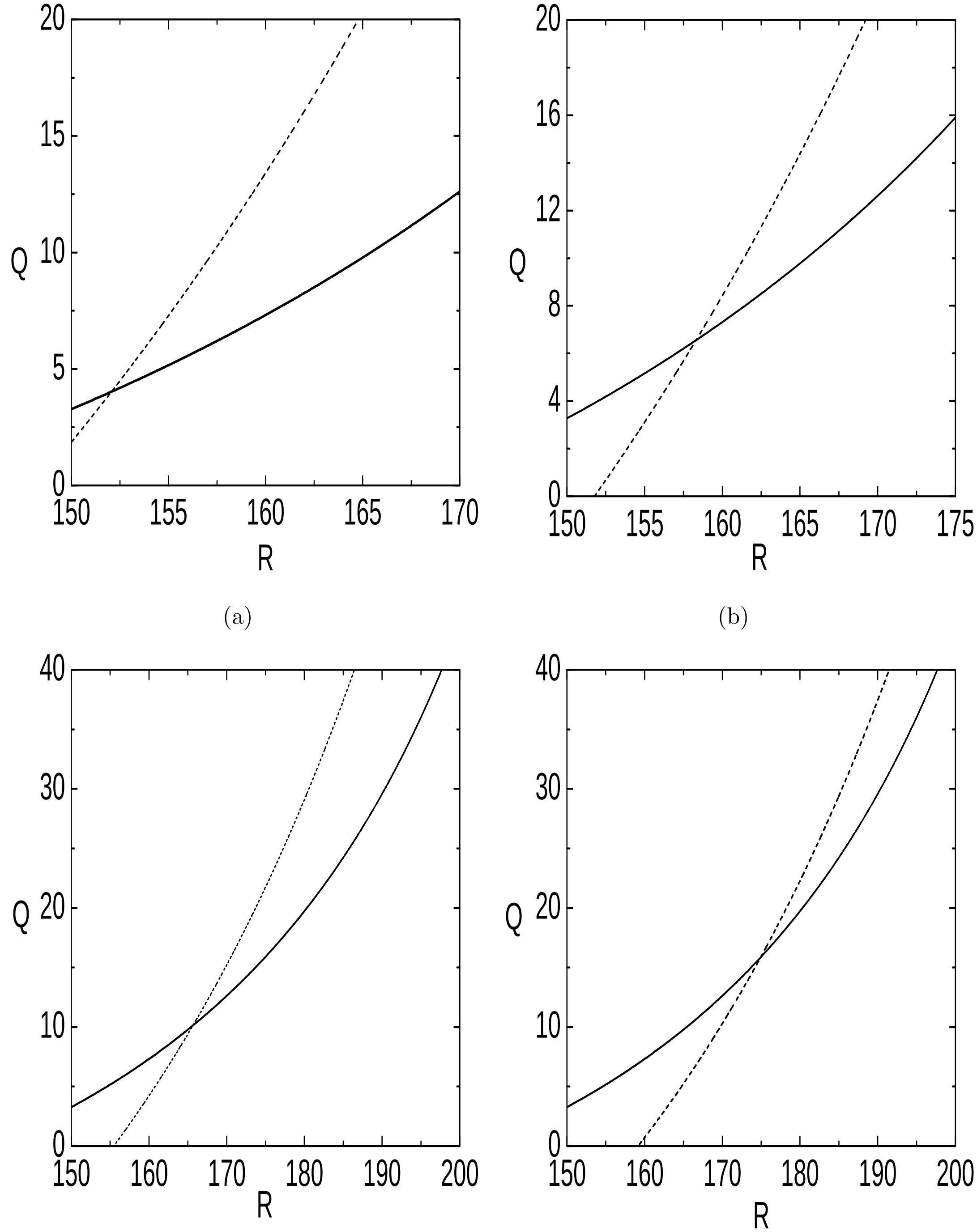

Figure 2.5: Stationary and oscillatory curves in (R, Q)- plane for $Da = 1500$, $\Lambda = 0.85$, $M = 1$, $\phi = 0.9$, $Pr_2 = 4$ at (a) $Pr_1 = 1.85$, (b) $Pr_1 = 1.9$, (c) $Pr_1 = 1.95$, $d)Pr_1 = 2$.

by eliminating R from equations (2.36) and (2.37), we get the stationary Chandrasekhar number Q_s

$$Q_{sc} = \frac{\Lambda(\pi^2+m^2)^3 - 3\Lambda(\pi^2+m^2)^2 m^2 + \frac{1}{Da}(\pi^4 - m^4)}{m^4}, \tag{2.39}$$

from equation (2.37),

$$m^2 = \left(\sqrt{\frac{R}{3\Lambda}} - \pi^2\right)^{\frac{1}{2}}, \tag{2.40}$$

substitute this value in equation (2.39), Then $Q_{sc}(R)$ is the critical stationary Chandrasekhar number.

Oscillatory Convection($w^2 > 0$)

By eliminating R from $w^2 = C$ and $w^2 = \frac{D}{B}$, we get oscillatory chandrasekhar number Q_oc as

$$Q_{oc} = \frac{(\pi^2+m^2)\left[(\pi^2+m^2) + M\Lambda\phi Pr_1(\pi^2+m^2) + \frac{1}{Da}M\phi Pr_1)\right]}{m^2\phi(\phi Pr_2 - MPr_1)}, \tag{2.41}$$

$BC - D = 0$ gives

$$m^2 = \sqrt[3]{\frac{o_1 R}{o_2}}, \tag{2.42}$$

where $o_1 = -\frac{M^2 Pr_2^2}{Pr_2}$ and $o_2 = \frac{1}{M\phi Pr_1} + \frac{1}{\phi^2 Pr_2} - \Lambda^2\phi^2 Pr_2 - \frac{\Lambda\phi Pr_2}{MPr_1}$. Substitute m^2 from equation (2.42) in to equation (2.41), we get critical oscillatory Chandrasekhar number Q_{oc} in terms of R. In Figure 2.5, by increasing the thermal prandtl value the intersection of stationary and oscillatory Rayleigh number and chandrasekhar number increases.

2.4 (ii). Nonlinear Instabilities of Rayleigh Benard Convection in a Sparsely Packed Porous medium due to Horizontal Magnetic Field

2.4.1 Two-dimensional nonlinear LG equation at the onset of stationary convection

According to Newell and Whitehead [77] multiple scale analysis , a small scale convection cell is disturbed on the vital flow. If the scale range is $O(\epsilon)$ then the the collaboration of the cell with itself forces a second harmonic and a standard state of rectification of range $O(\epsilon^2)$ and these in turn impel an $O(\epsilon^3)$ rectification to the structural module of the imposed roll. Let us assume the solution of equations (2.8)-(2.10) in series ϵ have the form

$$f(u, v, w, \theta, H_x, H_y, H_z) = f = \epsilon f_0 + \epsilon^2 f_1 + \epsilon^3 f_2 + \cdots . \tag{2.43}$$

The zeroth order calculations of the linearised problem given by approximation are identified by the eigenvectors

$$\begin{aligned}
u_0 =& \frac{i\pi}{l_{sc}} \left[A e^{i(l_{sc}x + m_{sc}y)} \cos \pi z - c \cdot c \cdot \right], \\
v_0 =& 0, \\
w_0 =& A e^{i(l_{sc}x + m_{sc}y)} \sin \pi z + c \cdot c \cdot, \\
\theta_0 =& \frac{1}{M\delta_{sc}^2} \left[A e^{i(l_{sc}x + m_{sc}y)} \sin \pi z + c \cdot c \cdot \right], \\
H_{x_0} =& \frac{-m\pi}{M l_{sc} \delta_{sc}^2} \left[A e^{i(l_{sc}x + m_{sc}y)} \cos \pi z + c \cdot c \cdot \right], \\
H_{y_0} =& 0, \\
H_{z_0} =& \frac{im}{M\delta_{sc}^2} \left[A e^{i(l_{sc}x + m_{sc}y)} \sin \pi z - c \cdot c \cdot \right],
\end{aligned} \tag{2.44}$$

where $A = A(X, Y, T)$ is the complex scale on the gradual variables X, Y and T and the complex conjugate is represented as c.c. The analytical mode for the linear problem at $R_{1s} = R_{1sc}$ is $e^{iqx}\sin\pi z$. The variables x, y, z and t are scaled by

$$X = \epsilon x, \quad Y = \epsilon^{\frac{1}{2}} y, \quad Z = z \quad T = \epsilon^2 t, \tag{2.45}$$

and are suitably scattered as fast and slow dependent variables in f. The derivative operators can be formulated as

$$\frac{\partial}{\partial x} \to \frac{\partial}{\partial x} + \epsilon\frac{\partial}{\partial X}, \quad \frac{\partial}{\partial y} \to \frac{\partial}{\partial y} + \epsilon^{\frac{1}{2}}\frac{\partial}{\partial Y}, \quad \frac{\partial}{\partial z} \to \frac{\partial}{\partial Z}, \quad \frac{\partial}{\partial t} \to \epsilon^2\frac{\partial}{\partial T}. \tag{2.46}$$

with the transformations equation (2.46), the linear and nonlinear operators (2.15) and (2.16) are written as

$$\mathcal{L} = \mathcal{L}_0 + \epsilon\mathcal{L}_1 + \epsilon^2\mathcal{L}_2 \cdots, \tag{2.47}$$

$$\mathcal{N} = \epsilon^2\mathcal{N}_0 + \epsilon^3\mathcal{N}_1 + \cdots, \tag{2.48}$$

substituting equations (2.47), (2.48) and (2.43) into equation (2.14), equating the $\epsilon, \epsilon^2, \epsilon^3$ coefficients on both sides, we get

$$\mathcal{L}_0 w_0 = 0, \tag{2.49}$$

$$\mathcal{L}_0 w_1 + \mathcal{L}_1 w_0 = \mathcal{N}_0, \tag{2.50}$$

$$\mathcal{L}_0 w_2 + \mathcal{L}_1 w_1 + \mathcal{L}_2 w_0 = \mathcal{N}_1, \tag{2.51}$$

where

$$\mathcal{L}_0 = -\Lambda\nabla^8 + \frac{1}{Da}\nabla^6 + Q\nabla^4\frac{\partial^2}{\partial y^2} + R_{sc}\nabla^2\nabla_h^2, \tag{2.52}$$

$$\mathcal{L}_1 = D_{xy}\mathcal{D}_Q + D_y^2\left[\left(\frac{1}{Da} - \Lambda\nabla^2\right)\nabla^6 + Q\nabla^2\frac{\partial^2}{\partial y^2}\right] + Q\nabla^4\frac{\partial^2}{\partial y^2}, \tag{2.53}$$

$$\mathcal{L}_2 =\frac{\partial}{\partial T}\Bigg[\Big(\Lambda+\frac{1}{M\phi Pr_1}+\phi\frac{\Lambda}{M}\frac{Pr_2}{Pr_1}\Big)\nabla^6-\Big(\frac{1}{Da}+\phi\frac{Pr_2}{Pr_1}\frac{1}{MD_a}\Big)\nabla^4-$$
$$Q\nabla^2\frac{\partial^2}{\partial y^2}-\frac{R_{sc}}{M}\phi\frac{Pr_2}{Pr_1}\nabla_h^2\Bigg]+\frac{\partial^2}{\partial X^2}\mathcal{D}_{\mathcal{Q}}+2D_{xy}\Bigg[-6\Lambda\nabla^4+\frac{3}{Da}\nabla^2+Q\frac{\partial^2}{\partial y^2}+R_{sc}\Bigg]+$$
$$4D_y^2D_{xy}\Big(\frac{1}{Da}-8\Lambda\nabla^2+Q\Big)+8D_xD_y^2\Big(\frac{1}{Da}-3\Lambda\nabla^2+Q\Big)+D_{xy}^2Q\nabla^2\frac{\partial^2}{\partial y^2}16D_y^4\Lambda+$$
$$4QD_y^2\frac{\partial^2}{\partial Y^2}+2Q\nabla^2D_x\frac{\partial^2}{\partial Y^2}, \tag{2.54}$$

where $D_x = \frac{\partial^2}{\partial x\partial X}$, $D_y = \frac{\partial^2}{\partial y\partial Y}$, $D_{xy} = \left(2\frac{\partial^2}{\partial x\partial X}+\frac{\partial^2}{\partial Y^2}\right)$, $\mathcal{D}_{\mathcal{Q}} = [R_{sc}\nabla^2-4\Lambda\nabla^6]$ Substituting zeroth order solution w_0 in equation (2.52), $\mathcal{L}_0w_0=0$, we get

$$R_{sc}=\frac{\delta_{sc}^2}{q_{sc}^2}\left[\delta_{sc}^4\Lambda+\frac{1}{D_a}\delta_{sc}^2+Qm_{sc}^2\right]. \tag{2.55}$$

From equation (2.50), $\mathcal{N}_0=0, \mathcal{L}_1w_0=0$ and substituting zeroth order solutions we get first order solutions,

$$\begin{aligned}
u_1 &=0,\ v_1=0,\ w_1=0,\\
\theta_1 &=-\frac{1}{2\pi M^2\delta_{sc}^2}|A|^2\sin 2\pi z,\\
H_{x_1} &=\frac{Pr_2}{Pr_1}\cdot\frac{m_{sc}}{M^2\delta_{sc}^2 l_{sc}}|A|^2\cos 2\pi z,\\
H_{y_1} &=0,\ H_{z_1}=0.
\end{aligned} \tag{2.56}$$

Taking $w_1=0$ in equation (2.51), $\mathcal{N}_1-\mathcal{L}_2w_0$ is vertical to w_0. This is ensured if the coefficient of $\sin\pi z$ in $\mathcal{N}_1-\mathcal{L}_2w_0$ is zero. By using zeroth order and first order solutions, we get the two dimensional time dependent nonlinear Landau-Ginzburg equation

$$\lambda_0\frac{\partial A}{\partial T}-\lambda_1\left(\frac{\partial}{\partial X}-\frac{i}{2q_{sc}}\frac{\partial^2}{\partial Y^2}\right)^2A-\lambda_2A+\lambda_3|A|^2A=0, \tag{2.57}$$

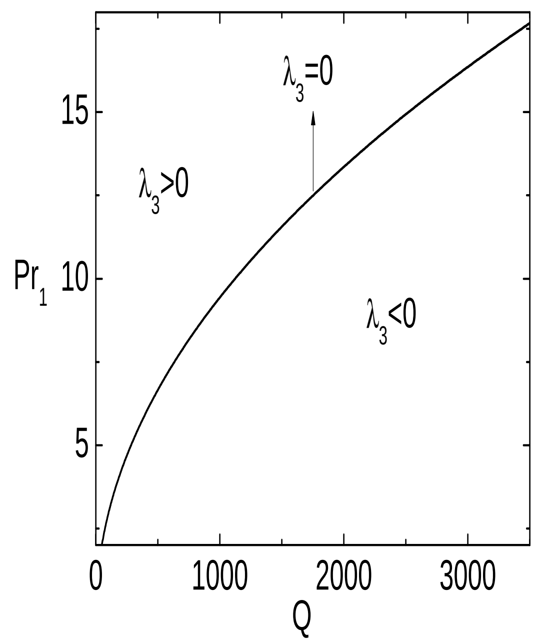

Figure 2.6: Neutral curve for the coefficient of LG equation at the onset of stationary convection. Pitchfork bifurcation is supercritical if $\lambda_3 > 0$, subcritical if $\lambda_3 < 0$ and $\lambda_3 = 0$ for the curve $Da = 1500$, $\Lambda = 0.85$, $M = 0.85$, $\phi = 0.9$ and $Pr_2 = 1.5$

where

$$\lambda_0 = \left(\Lambda + \frac{1}{M\phi Pr_1} + \phi\frac{Pr_2}{Pr_1}\frac{\Lambda}{M}\right)\delta_{sc}^6 + \left(\frac{1}{D_a} + \phi\frac{Pr_2}{Pr_1}\frac{1}{MD_a}\right)\delta_{sc}^4 + Qm_{sc}^2\delta_{sc}^2 - \frac{R_{sc}}{M}\frac{Pr_2}{Pr_1}q_{sc}^2\phi,$$
$$\lambda_1 = 4l_{sc}^2\left[6\Lambda\delta_{sc}^4 + \frac{3}{D_a}\delta_{sc}^2 + Qm_{sc}^2 - R_{sc}\right],$$
$$\lambda_2 = R_{sc}q_{sc}^2\delta_{sc}^2,$$
$$\lambda_3 = Q\frac{Pr_2^2}{Pr_1^2}\frac{\pi^2(q_{sc}^2 - \pi^2)}{M^2} + \frac{R_{sc}}{2M^2}q_{sc}^2. \tag{2.58}$$

According to Steinberg and Brand [115], if $\lambda_3 > 0$, the pitchfork bifurcation is supercritical, if $\lambda_3 < 0$, the pitchfork bifurcation is subcritical and if $\lambda_3 = 0$, then tricritical bifurcation point is attained. From the Figure 2.6, we studied pitchfork bifurcation. Dropping t and y dependence from equation (2.57), we get

$$\frac{\mathrm{d}^2A}{\mathrm{d}X^2} + \frac{\lambda_2}{\lambda_1}(1 - \frac{\lambda_3}{\lambda_2}|A|^2)A = 0, \tag{2.59}$$

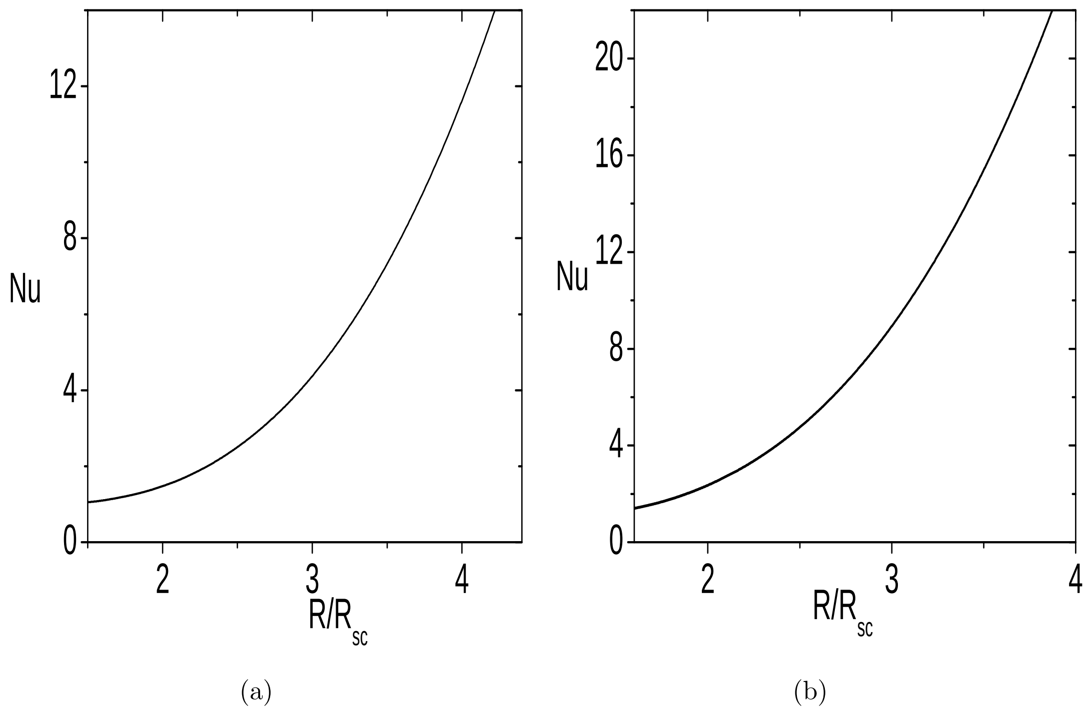

Figure 2.7: Above figure is plotted for $Da = 1500$, $\Lambda = 3$, $M = 0.85$, $\phi = 0.9$, $Pr_1 = 1.1$, $Pr_2 = 1.25$ at (a) $Q = 600, (b)$ $Q = 800$.

$$A(X) = A_1 \tanh(X/Ł_1), \tag{2.60}$$

where $A_1 = (\frac{\lambda_2}{\lambda_3})^{\frac{1}{2}}$ and $Ł_1 = (\frac{2\lambda_1}{\lambda_2})^{\frac{1}{2}}$.

Heat Transport by Convection

The maximum aptitude of A is denoted by $|A_{max}|$ which is given as

$$|A_{max}| = \left(\frac{\epsilon^2 \lambda_2}{\lambda_3}\right)^{\frac{1}{2}}. \tag{2.61}$$

Nusselt number Nu calculated in terms of amplitude as

$$Nu = \frac{\epsilon^2}{\delta_{sc}^2}|A_{max}|^2 + 1. \tag{2.62}$$

Nusselt number grows if $\frac{R}{R_{sc}} > 1$ and decays if $\frac{R}{R_{sc}} \leq 1$ convection for $Nu > 1$. Then there is convection if $Nu > 1$, conduction if $Nu \leq 1$. In Figure 2.7 Nusselt number

Nu was derived for distinct values of Q and for some fixed values of remaining parameters. It was observed that by increasing the value of Q, Nusselt number grows exponentially at unit value.

Long Wave-length Instabilities

Newell and Whitehead [77] derived envelope equations In order to study the properties of a structure with a given phase winding number δq, we write equation (2.57) in fast variables x, y, t and $A(X, Y, T) = \frac{A(x,y,t)}{\epsilon}$, as

$$\frac{\partial A_1}{\partial t} - \Big(\epsilon^2 \frac{\lambda_2}{\lambda_0} - \frac{\lambda_1}{\lambda_0}\delta q^2\Big) A_1 + 2i\delta q \frac{\lambda_1}{\lambda_0}\Big(\frac{\partial}{\partial x} - \frac{i}{2q_{sc}}\frac{\partial^2}{\partial y^2}\Big) A_1 + \\ \frac{\lambda_1}{\lambda_0}\Big(\frac{\partial}{\partial x} - \frac{i}{2q_{sc}}\frac{\partial^2}{\partial y^2}\Big)^2 A_1 - \frac{\lambda_3}{\lambda_0}|A_1|^2 A_1 = 0, \tag{2.63}$$

$$A_1 = \left[\frac{\epsilon^2\lambda_2 - \lambda_1 \delta q^2}{\lambda_3}\right]^{\frac{1}{2}}. \tag{2.64}$$

Let $\tilde{u} + i\tilde{v}$ be an infinitesimal perturbation of steady state solution A_1 given by equation (2.64). Substitute

$$A_1 = \tilde{u} + i\tilde{v} + [\left(\epsilon^2\lambda_2 - \lambda_1\delta q^2\right)\lambda_3^{-1}]^{\frac{1}{2}}, \tag{2.65}$$

into equation (2.63) and equate the real and imaginary parts, we obtain

$$\frac{\partial \tilde{u}}{\partial t} = -2\left(\epsilon^2 \frac{\lambda_2}{\lambda_0} - \frac{\lambda_1}{\lambda_0}\delta q^2\right)\tilde{u} + \frac{\lambda_1}{\lambda_0}\tilde{u} - \frac{\lambda_1}{\lambda_2}\partial_2 \frac{\partial \tilde{v}}{\partial x}, \tag{2.66a}$$

$$\frac{\partial \tilde{v}}{\partial t} = \frac{\lambda_1}{\lambda_0}\partial_2 \frac{\partial \tilde{u}}{\partial x} + \frac{\lambda_1}{\lambda_0}\partial_1 \tilde{v}. \tag{2.66b}$$

where $\partial_1 = \frac{\partial^2}{\partial x^2} + \frac{\delta q}{q_{sc}}\frac{\partial^2}{\partial y^2} - \frac{1}{4q_{sc}^2}\frac{\partial^4}{\partial y^4}$ and $\partial_2 = 2\delta q - \frac{1}{q_{sc}}\frac{\partial^2}{\partial y^2}$ We analyse equations (2.66a) and (2.66b) by using normal modes form

$$\tilde{u} = U\cos(q_x x)\cos(q_y y)e^{St}, \qquad \tilde{v} = V\sin(q_x x)\cos(q_y y)e^{St}. \tag{2.67}$$

Substituting equation (2.67) in equations (2.66a) and (2.66b) weget,

$$\Big[2(\epsilon^2\lambda_2 - \lambda_1\delta k^2) + \lambda_0 S + \chi_1\Big]U + \lambda_1\chi_2 q_x V = 0 \tag{2.68a}$$

$$\lambda_1 q_x \chi_2 U + (\chi_1 + \lambda_0 S)V = 0. \tag{2.68b}$$

Here $\chi_1 = \lambda_1\Big(q_x^2 + \frac{q_y^2\delta k}{q_{sc}} + \frac{q_y^4}{4q_{sc}^2}\Big)$ and $\chi_2 = (2\delta k + \frac{q_y^2}{q_{sc}})$. On solving equations (2.68a) and (2.68b), we get

$$S^2 + \frac{2S}{\lambda_0}\Big[2\Big(\epsilon^2\lambda_2 - \lambda_1(\delta k)^2\Big) + \chi_1\Big] + \Big[2\Big(\frac{\epsilon^2\lambda_2}{\lambda_0^2} - \frac{\lambda_1\delta k^2}{\lambda_0^2}\Big) + \chi_1\Big]\psi_1 - q_x^2\chi_2\frac{\lambda_1}{\lambda_0^2} = 0, \tag{2.69}$$

whose real roots are $(S\pm)$,

$$(S\pm) = -\frac{1}{\lambda_0^2}\left\{\Big[2\lambda_0(\epsilon^2\lambda_2 - \lambda_1\delta k q^2) + \lambda_0\chi_1\Big] \pm \Big[2\lambda_0(\epsilon^2\lambda_2 - \lambda_1\delta q^2)^2 + \lambda_1^2 q_x^2\chi_2^2\Big]^{\frac{1}{2}}\right\}. \tag{2.70}$$

The equivalent mode is stable if $S(-)$ is negative and unstable if $S(+)$ is positive. Symmetry significance helps to confine the field of $S(+)$ to $q_x \geq 0, q_y \geq 0$.

Eckhaus Instability

Putting $q_y = 0$ into equation (2.70), we get

$$S^2 + \frac{2S}{\lambda_0}\Big[2(\epsilon^2\lambda_2 - \lambda_1\delta q^2) + \lambda_1 q_x^2\Big] + \frac{\lambda_1 q_x^2}{\lambda_0^2}\Big[2(\epsilon^2\lambda_2 - 3\lambda_1\delta q^2) + q_x^2\Big] = 0, \tag{2.71}$$

The roots are real numbers and their sum is negative number and the product of roots is positive number, the pattern is stable and if the product of roots is negative number then the pattern becomes unstable.
Eckhaus instability defines $q_x^2 \leq 2\Big(3\lambda_1\delta q^2 - \epsilon^2\lambda_2\Big)$ for $|\delta q| \geq \sqrt{\frac{\epsilon^2\lambda_2}{3\lambda_1}}$ and unstable wave tends to zero when $|\delta q| \to \sqrt{\frac{\epsilon^2\lambda_2}{3\lambda_1}}$.

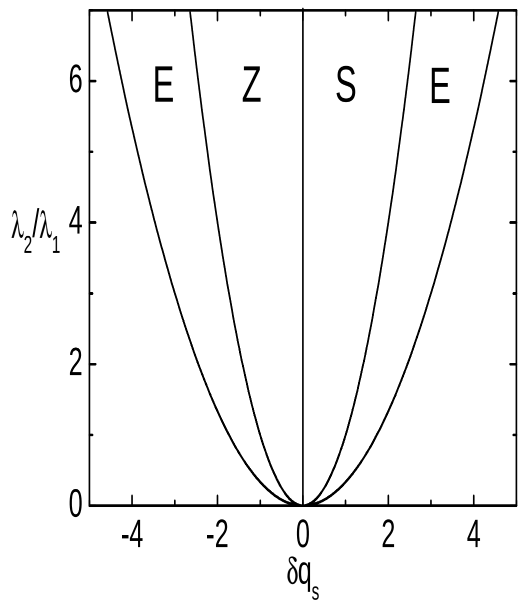

Figure 2.8: Numerically calculated secondary instability regions of Eckhaus instability (E), Zigzag instability (Z), and Stable region (S) are plotted for $Da = 1500$, $\Lambda = 2$, $M = 0.9$,$\phi = 0.9$, $Pr_1 = 1$, $Pr_2 = 2$, $Q = 10^5$.

Zigzag Instability

putting $q_x = 0$ into equation (2.71), we get

$$\lambda_0^2 S^2 + 2S(2\lambda_0\chi_{11} + \lambda_0\chi_{12}) + (2\chi_{11} + \chi_{12})\chi_{12} = 0, \tag{2.72}$$

where $\chi_{11} = \epsilon^2\lambda_2 - \lambda_1\delta q^2$ and $\chi_{12} = \lambda_1\left(\frac{q_y^2\delta q}{q_s c} + \frac{q_y^4}{4q_{sc}^2}\right)$, the two eigen conditions are unrelated and amplified when $S(-) = -2(\epsilon^2\lambda_2 - \lambda_1\delta q^2) - \frac{\lambda_1}{q_{sc}}q_y^2\delta q - \frac{\lambda_1}{4q_{sc}^2}q_y^2 < 0$ and $S(+) = -\lambda_1 q_y^2\left(\delta q + \frac{q_y^2}{4q_{sc}}\right) > 0$. These conditions define the domain of Zigzag Instability when $\delta q_s < 0$. In Figure 2.8, we observed that by increasing the Q value, the region of Eckhaus and Zigzag instability increases.

2.4.2 One dimensional amplitude equation at the onset of oscillatory convection

Consider cylindrical rolls along y-axis, so only x-dependence and z-dependence appears from $\mathcal{L}w = \mathcal{N}$. Obtained coupled one dimensional nonlinear time dependent Landau-Ginzburg type equations at the supercritical Hopf bifurcation. We define ϵ as

$$\epsilon^2 = \frac{R_o - R_{oc}}{R_{oc}} \ll 1, \tag{2.73}$$

and take

$$w_0 = \left[A_{1L}e^{i(l_{oc}x+m_{oc}y+\omega_{oc}t)} + A_{1R}e^{i(l_{oc}x+m_{oc}y-\omega_{oc}t)} + c\cdot c.\right]\sin\pi z, \tag{2.74}$$

is a solution of $\mathcal{L}w = 0$. Here A_{1L} and A_{1R} represents the amplitudes of left and right travelling wave rolls respectively and depend on slow space X and time variables $\tau,\ T$, Knobloch and Luca [57],

$$X = \epsilon x, \quad \tau = \epsilon t, \quad T = \epsilon^2 t, \tag{2.75}$$

and assume that $A_{1L} = A_{1L}(X,\tau,T),\ A_{1R} = A_{1R}(X,\tau,T)$. Differential operators can be expressed as

$$\frac{\partial}{\partial x} \to \frac{\partial}{\partial x} + \epsilon\frac{\partial}{\partial X}, \quad \frac{\partial}{\partial t} \to \frac{\partial}{\partial t} + \epsilon\frac{\partial}{\partial \tau} + \epsilon^2\frac{\partial}{\partial T}. \tag{2.76}$$

The solution of basic equations can be sought as power series in ϵ, the first approximation is given by eigenvector of the linearised problem

$$
\begin{aligned}
u_0 =& -\frac{\pi}{iq_{oc}}\left[A_{1L}e^{i(l_{oc}x+m_{oc}y+\omega_{oc}t)}+A_{1R}e^{i(l_{oc}x+m_{oc}y-\omega_{oc}t)}-c\cdot c.\right]\cos\pi z,\\
v_0 =& 0,\\
\theta_0 =& \frac{1}{M}\left[\frac{1}{e_1}A_{1L}e^{i(l_{oc}x+m_{oc}y+\omega_{oc}t)}+\frac{1}{e_1^*}A_{1R}e^{i(l_{oc}x+m_{oc}y-\omega_{oc}t)}+c\cdot c.\right]\sin\pi z,\\
H_{x_0} =& \frac{-m_{oc}\pi}{l_{oc}}\left[\frac{1}{e_2}A_{1L}e^{i(l_{oc}x+m_{oc}y+\omega_{oc}t)}+\frac{1}{e_2^*}A_{1R}e^{i(l_{oc}x+m_{oc}y-\omega_{oc}t)}+c\cdot c.\right]\cos\pi z,\\
H_{y_0} =& 0,\\
H_{z_0} =& im_{oc}\left[\frac{1}{e_2}A_{1L}e^{i(l_{oc}x+m_{oc}y+\omega_{oc}t)}+\frac{1}{e_2^*}A_{1R}e^{i(l_{oc}x+m_{oc}y-\omega_{oc}t)}-c\cdot c.\right]\sin\pi z. \qquad (2.77)
\end{aligned}
$$

where $\delta_{oc}^2=(\pi^2+q_{oc}^2)$, $e_1=(\delta_{oc}^2+i\omega_{oc})$ and $e_2=(M\delta_{oc}^2+i\omega_{oc}\phi\frac{Pr_2}{Pr_1})$, here e_1^* and e_2^* are complex conjugate of e_1 and e_2. From equations (2.49), (2.50) and (2.51)

$$
\begin{aligned}
\mathcal{L}_0 =& (\mathcal{D}_\phi\mathcal{D}_{Pr_1}-Q\frac{\partial^2}{\partial y^2})\mathcal{D}\nabla^2-\frac{R}{M}\nabla_h^2\mathcal{D}_\phi,\\
\mathcal{L}_1 =& \frac{\partial}{\partial\tau}\mathcal{F}_1+D_{xy}\mathcal{F}_2+4D_y^2\mathcal{F}_3,\\
\mathcal{L}_2 =& \frac{\partial\mathcal{F}_1}{\partial T}+\frac{\partial^2\mathcal{F}_2}{\partial X^2}+D_x^2\mathcal{F}_4+2D_x\frac{\partial}{\partial\tau}\mathcal{F}_5+\frac{\partial^2}{\partial\tau^2}\mathcal{F}_6+\frac{\partial}{\partial\tau}4D_y^2\mathcal{F}_7+4D_Y^2D_{xy}\mathcal{F}_8\\
&-Q(\nabla^2-\nabla)D_YD_{xy}+4QD_YD_y^2-16\frac{\Lambda}{M}D_y^4, \qquad (2.78)\\
\mathcal{F}_1 =& (\mathcal{D}_\phi\mathcal{D}_{Pr_1}+\phi\frac{Pr_2}{Pr_1}\mathcal{D}\mathcal{D}_{Pr_1}+\frac{1}{M^2\phi Pr_1}\mathcal{D}\mathcal{D}_\phi)\nabla^2-Q\nabla^2\frac{\partial^2}{\partial y^2}-\frac{\phi RPr_2}{MPr_1}\nabla_h^2,\\
\mathcal{F}_2 =& (\mathcal{D}\mathcal{D}_\phi-\mathcal{D}_\phi\nabla^2-M\mathcal{D}\nabla^2)\mathcal{D}_{Pr_1}-\frac{\Lambda}{M}\mathcal{D}\mathcal{D}_\phi\nabla^2+Q\nabla^2\frac{\partial^2}{\partial y^2}-Q\mathcal{D}\frac{\partial^2}{\partial y^2}-\frac{R}{M}\mathcal{D}_\phi+R\nabla_h^2,\\
\mathcal{F}_3 =& Q(\frac{\partial^2}{\partial y^2}+\nabla^2-\mathcal{D})-\frac{R}{M}+\frac{\Lambda}{M}(\mathcal{D}\nabla^2-\mathcal{D}\mathcal{D}_\phi+\mathcal{D}_\phi\nabla^2)+\mathcal{D}_{Pr_1}(\nabla^2-\mathcal{D}-\mathcal{D}_\phi),\\
\mathcal{F}_4 =& (M\nabla^2-(\mathcal{D}_\phi+M\mathcal{D}))\mathcal{D}_{Pr_1}+\Lambda\mathcal{D}\nabla^2-\frac{\Lambda}{M}\mathcal{D}\mathcal{D}_\phi+\frac{\Lambda}{M}\mathcal{D}_\phi\nabla^2+Q\frac{\partial^2}{\partial y^2}+R,\\
\mathcal{F}_5 =& \mathcal{D}_\phi\mathcal{D}_{Pr_1}-M\nabla^2\mathcal{D}_{Pr_1}-\phi\nabla^2\mathcal{D}_{Pr_1}\frac{Pr_2}{Pr_1}-(M+\phi\frac{Pr_2}{Pr_1})\mathcal{D}_{Pr_1}\nabla^2-Q\frac{\partial^2}{\partial y^2}-\\
&\left(\phi\frac{Pr_2}{Pr_1}\frac{\Lambda}{M}+\frac{1}{M\phi Pr_1}\right)\mathcal{D}\nabla^2+\frac{1}{M^2\phi Pr_1}\mathcal{D}\mathcal{D}_\phi+\phi\frac{Pr_2}{Pr_1}\mathcal{D}\mathcal{D}_{Pr_1}-\frac{\phi RPr_2}{MPr_1}-
\end{aligned}
$$

$$\mathcal{F}_6 =\phi\frac{Pr_2}{Pr_1}\mathcal{D}_{Pr_1}\nabla^2+\frac{Pr_2}{M^2Pr_1^2}\mathcal{D}\nabla^2+\frac{1}{M^2\phi Pr_1}\mathcal{D}_\phi\nabla^2,$$
$$\mathcal{F}_7 =\frac{1}{M^2\phi Pr_1}(\nabla^2-\mathcal{D}-\mathcal{D}_\phi)+\phi\frac{\Lambda}{M}\frac{Pr_2}{Pr_1}(\nabla^2-\mathcal{D})+\frac{\Lambda}{M}(1-\mathcal{D}_\phi)-\phi\mathcal{D}_{Pr_1}\frac{Pr_2}{Pr_1},$$
$$\mathcal{F}_8 =2Q+\Lambda(\mathcal{D}+\mathcal{D}^2)+M\mathcal{D}_{Pr_1}+2\mathcal{D}_{Pr_1}+\frac{\Lambda}{M}(2\mathcal{D}-\mathcal{D}^2+3\mathcal{D}_\phi-1),\ D_Y=\frac{\partial^2}{\partial Y^2}.$$

At $O(\epsilon)$, equation (2.49) gives critical Rayleigh number for the onset of oscillatory convection). At $O(\epsilon^2)$, from equation (2.50) $\mathcal{N}_0=0$ and $\mathcal{L}_1 w_0=0$ gives

$$\frac{\partial A_{1L}}{\partial\tau}-v_g\frac{\partial A_{1L}}{\partial X}=0 \quad\text{and}\quad \frac{\partial A_{1R}}{\partial\tau}-v_g\frac{\partial A_{1R}}{\partial X}=0, \tag{2.79}$$

where $v_g=(\partial\omega/\partial q)_{q=q_{oc}}$ is the group velocity and is real. We get,

$$u_1 =0,\ v_1=0,\ w_1=0,$$
$$\theta_1 =\frac{-\pi}{M^2}\left[\left(|A_{1L}|^2+|A_{1R}|^2\right)e_7+\frac{2}{e_1e_4}e_6+\frac{2}{e_1^*e_4^*}e_6^*\right]\sin 2\pi z,$$
$$H_{x_1} =\frac{2m_{oc}\pi^2}{l_{oc}}\frac{Pr_2}{Pr_1}\left[\frac{2}{e_2e_3}A_{1L}A_{1R}^*e^{2i\omega_{oc}t}+\frac{2}{e_2^*e_3^*}A_{1R}A_{1L}^*e^{-2i\omega_{oc}t}\right.$$
$$\left.+\frac{1}{4M\pi^2}\left(\frac{1}{e_2}+\frac{1}{e_2^*}\right)\left(|A_{1L}|^2+|A_{1R}|^2\right)\right]\cos 2\pi z,$$
$$H_{y_1} =0,\ H_{z_1}=0, \tag{2.80}$$

where $e_3=\left(\frac{i\omega}{M^2\phi Pr}+\frac{\Lambda}{M}\delta^2+\frac{1}{MD_a}\right)$, $e_4=(4\pi^2{+}2i\omega_{oc})$, $e_5=(4Mq_{oc}^2{+}2i\phi\omega_{oc}\frac{Pr_2}{Pr_1})$, $e_6=A_{1L}A_{1R}^*e^{2i\omega_{oc}t}$, $e_7=\frac{1}{4\pi^2}\left(\frac{1}{e_1}+\frac{1}{e_1^*}\right)$, and e_3^*, e_4^*, e_5^*, e_6^* and e_7^* are complex conjugate of e_3, e_4, e_5, e_6 and e_7 respectively. The equation (2.51) is solvable when $\mathcal{L}_0 w_0=0$, equate the coefficients of $\sin\pi z$ in $\mathcal{N}_1-\mathcal{L}_2 w_0$ to zero. We get

$$\Lambda_0\frac{\partial A_{1L}}{\partial T}+\Lambda_1\left(\frac{\partial}{\partial\tau}-v_g\frac{\partial}{\partial X}\right)A_{2L}-\Lambda_2\frac{\partial^2A_{1L}}{\partial X^2}-\Lambda_3A_{1L}$$
$$+\Lambda_4|A_{1L}|^2A_{1L}+\Lambda_5|A_{1R}|^2A_{1L}=0, \tag{2.81}$$
$$\Lambda_0\frac{\partial A_{1R}}{\partial T}+\Lambda_1\left(\frac{\partial}{\partial\tau}-v_g\frac{\partial}{\partial X}\right)A_{2R}-\Lambda_2\frac{\partial^2A_{1R}}{\partial X^2}-\Lambda_3A_{1R}$$
$$+\Lambda_4|A_{1R}|^2A_{1R}+\Lambda_5|A_{1L}|^2A_{1R}=0. \tag{2.82}$$

Where

$$
\begin{aligned}
\Lambda_0 =& \left(\frac{1}{M^2\phi Pr_1}e_1e_2 + e_2e_3 + \phi\frac{Pr_2}{Pr_1}e_1e_3 + Qm_{oc}^2\right)\delta_{oc}^2 - \frac{R_{oc}q_{oc}^2\phi Pr_2}{MPr_1},\\
\Lambda_1 =& \delta_{oc}^2\left[e_3\phi\frac{Pr_2}{Pr_1} + \frac{e_1Pr_2}{M^2Pr_1^2} + \frac{e_2}{M^2\phi Pr_1}\right],\\
\Lambda_2 =& 4l_{oc}^2\left[e_2e_3 + Me_3\delta_{oc}^2 + \Lambda e_1\delta_{oc}^2 + \frac{\Lambda}{M}e_1e_2 + Me_1e_3 + \frac{\Lambda}{M}e_2\delta_{oc}^2 + Qm_{oc}^2 - R\right],\\
\Lambda_3 =& \frac{R}{M}q_{oc}^2e_2,\\
\Lambda_4 =& Qm_{oc}^2\delta_{oc}^2e_1\frac{1}{2M}\left(\frac{1}{e_2} + \frac{1}{e_2^*}\right) - e_2\frac{R}{4M^3}q_{oc}^2\left(\frac{1}{e_1} + \frac{1}{e_1^*}\right),\\
\Lambda_5 =& Q\pi^2m_{oc}^2\delta_{oc}^2\frac{Pr_2^2}{Pr_1^2}e_1\left(\frac{1}{e_2} + \frac{1}{e_2^*}\right)\left(\frac{e_1}{e_2} + 1\right) - 2Q\pi^2m_{oc}^2\delta_{oc}^2\frac{Pr_2^2}{Pr_1^2}\frac{e_1}{e_3e_2^*}\\
&- \pi^2q_{oc}^2\frac{R}{M^3}e_2\left[\frac{2}{e_1e_d} + \frac{1}{4\pi^2}\left(\frac{1}{e_1} + \frac{1}{e_1^*}\right)\right].
\end{aligned}
\tag{2.83}
$$

Here it needs to be noted that A_{1L} and A_{1R} are of order ϵ and A_{2L} and A_{2R} are of order ϵ^2. If $\omega_{oc} = 0$ in Λ_0, Λ_1, Λ_2, Λ_3 and Λ_4, these expressions match with coefficients $\lambda_0, \lambda_1, \lambda_2$ and λ_3 of LG equation at the onset of stationary convection. From equation (2.79), we get $A_{1L}(\xi', T)$ and $A_{1R}(\eta', T)$, where $\xi' = v_g\tau + X$, $\eta' = v_g\tau - X$. Equations (2.81) and (2.82) can be written as

$$
2v_g\Lambda_1\frac{\partial A_{2L}}{\partial \eta'} = -\Lambda_0\frac{\partial A_{1L}}{\partial T} + \Lambda_2\frac{\partial A_{1L}}{\partial X^2} + \lambda_3 A_{1L} - \left(\Lambda_4|A_{1L}|^2 + \Lambda_5|A_{1R}|^2\right)A_{1L}, \tag{2.84}
$$

$$
2v_g\Lambda_1\frac{\partial A_{2R}}{\partial \eta'} = -\Lambda_0\frac{\partial A_{1R}}{\partial T} + \Lambda_2\frac{\partial A_{1R}}{\partial X^2} + \lambda_3 A_{1R} - \left(\Lambda_4|A_{1R}|^2 + \Lambda_5|A_{1L}|^2\right)A_{1R}. \tag{2.85}
$$

Let $\xi'\epsilon[0, l_1]$, $\eta'\epsilon[0, l_2]$ where l_1 and l_2 are periods of A_{1L} and A_{1R}. This condition is obtained by integrating equation (2.84) over η' and equation (2.85) over ξ', we get

$$
\Lambda_0\frac{\partial A_{1L}}{\partial T} = \Lambda_2\frac{\partial A_{1L}}{\partial X^2} + \lambda_3 A_{1L} - \left(\Lambda_4|A_{1L}|^2 + \Lambda_5|A_{1R}|^2\right)A_{1L}, \tag{2.86}
$$

$$
\Lambda_0\frac{\partial A_{1R}}{\partial T} = \Lambda_2\frac{\partial A_{1R}}{\partial X^2} + \lambda_3 A_{1R} - \left(\Lambda_4|A_{1R}|^2 + \Lambda_5|A_{1L}|^2\right)A_{1R}. \tag{2.87}
$$

Travelling wave and standing wave convection

According to Coullet [37] and Matthews [67], we studied the region of waves by dropping variable X from equations (2.86) and (2.87), we get a pair of first order differential equations

$$\frac{\mathrm{d}A_{1L}}{\mathrm{d}T} = \frac{\Lambda_3}{\Lambda_0}A_{1L} - \frac{\Lambda_4}{\Lambda_0}A_{1L}|A_{1L}|^2 - \frac{\Lambda_5}{\Lambda_0}A_{1L}|A_{1R}|^2, \tag{2.88}$$

$$\frac{\mathrm{d}A_{1R}}{\mathrm{d}T} = \frac{\Lambda_3}{\Lambda_0}A_{1R} - \frac{\Lambda_4}{\Lambda_0}A_{1R}|A_{1R}|^2 - \frac{\Lambda_5}{\Lambda_0}A_{1R}|A_{1L}|^2. \tag{2.89}$$

Put $\beta' = \frac{\Lambda_3}{\Lambda_0}$, $\gamma' = -\frac{\Lambda_4}{\Lambda_0}$ and $\delta' = -\frac{\Lambda_5}{\Lambda_0}$. Then equations (2.88) and (2.89) take the following form

$$\frac{\mathrm{d}A_{1L}}{\mathrm{d}T} = \beta' A_{1L} + \gamma' A_{1L}|A_{1L}|^2 + \delta' A_{1L}|A_{1R}|^2, \tag{2.90}$$

$$\frac{\mathrm{d}A_{1R}}{\mathrm{d}T} = \beta' A_{1R} + \gamma' A_{1R}|A_{1R}|^2 + \delta' A_{1R}|A_{1L}|^2. \tag{2.91}$$

Consider A_{1L}=$a_L e^{i\phi_L}$ and A_{1R}=$a_L e^{i\phi_R}$, where $a_L = |A_{1L}|$, $\phi_L = \tan^{-1}\left(\frac{Im(A_{1L})}{Re(A_{1L})}\right) = arg(A_{1L})$ and $a_R = |A_{1R}|$, $\phi_R = \tan^{-1}\left(\frac{Im(A_{1R})}{Re(A_{1R}}) = arg(A_{1R})\right)$, here a_L, a_R, ϕ_L and ϕ_R are functions of time T, a_L and a_R are positive functions. Substitute A_{1L}, A_{1R}, $\beta' = \beta_1 + i\beta_2$, $\gamma' = \gamma_1 + i\gamma_2$, $\delta' = \delta_1 + i\delta_2$ into equations (2.90) and (2.91) we get, $(a_L, a_R) = (-\beta_1/(\gamma_1 + \delta_1), -\beta_1/(\gamma_1 + \delta_1))$ for standing waves. $(a_L, a_R) = (a_L, 0)$ for left travelling waves and $(a_L, a_R) = (0, a_R)$ for right travelling waves. $(a_L, a_R) = (0, 0)$ for conduction state. In Figure 2.9, we studied the regions of travelling and standing waves at Hopf bifurcation. The stability regions of standing wave increased when Pr_2/Pr_1 increases.

2.5 Conclusions

In this chapter we studied linear and nonlinear stabilities of magnetoconvection in a sparsely packed porous medium over a horizontal magnetic field. We have de-

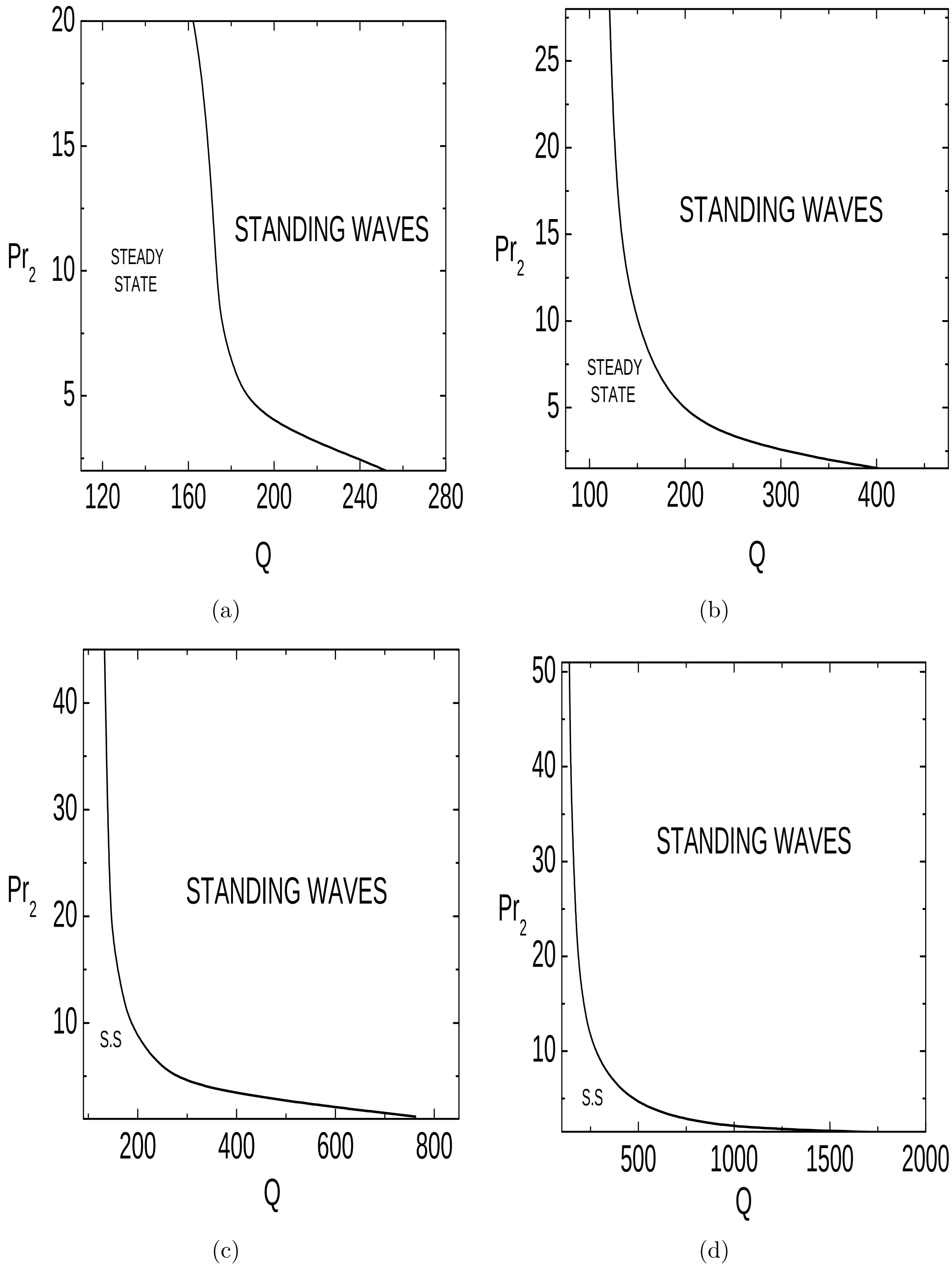

Figure 2.9: Stability regions of steady state (S.S) and standing waves $Da = 1500$, $\Lambda = 2$, $M = 0.9$, $\phi = 0.85$, $Pr_2 = 1.5$, (a)$\frac{Pr_2}{Pr_1} = 2$, (b)$\frac{Pr_2}{Pr_1} = 6$, (c)$\frac{Pr_2}{Pr_1} = 12$, (d)$\frac{Pr_2}{Pr_1} = 24$.

rived thermal Rayleigh value at the onset of stationary and oscillatory convection by assuming periodic disturbances along x-direction, y-direction and in both x-y directions, and obtained critical thermal Rayleigh values at the corresponding critical wave numbers by considering R_1 as dependent variable. We also traced marginal stability curves between thermal Rayleigh value and wave number. We found an analytical relation for stationary and oscillatory convective curves by considering R_1 as independent variable. Takens-Bogdanov bifurcation and co-dimension two bifurcation points on neutral curves were identified and are shown in figures 2.2 - 2.3. We observed the thermal and magnetic Prandtl numbers are not affected on convective stationary thermal Rayleigh value. We derived two dimensional Ginzburg Landau equation at the onset of stationary mode, explored heat transport from Nusselt number, studied long wave length aas well as Eukhaus and Zigzag instabilities. At the onset of super critical pitchfork bifurcation, we obtained two dimensional Ginzburg Landau equation which is valid only for $\lambda_3 > 0$. If $\lambda_3 = 0$ we get tricritical bifurcation point. $\lambda_3 = 0$ is a necessary condition to study heat transport for various physical parameters. Nusselt number grows exponentially if $\frac{R}{R_{sc}} > 1$ and decay if $\frac{R}{R_{sc}} \leq 1$ for $Nu > 1$. Nusselt number grows exponentially for unit value. At the onset of Hopf bifurcation, we obtained LG equations and we discussed secondary instabilities. For $\beta_1 > 0$ and $\gamma_1 < 0$ travelling and standing waves are stable and for $\beta_1 < 0$ and $\gamma_1 < 0$ travelling and standing waves are unstable (see Figure 2.9). The region of existing standing waves increases by increasing the ratio of magneto and thermal prandtl number.

Chapter 3

Instabilities of Rayleigh Benard Convection in a Sparsely Packed Porous Medium with the Effect of Rotation and Horizontal Magnetic Field

3.1 Introduction

The Hydrodynamic and Hydromagnetic stability problems have several scientific applications in astrophysics, geophysics and space sciences. These problems with the effect of rotation and externally impressed magnetic field was carried out by Chandrasekhar [35] The effects of both magnetic field and rotation prevent the onset of instability and increase the cells at marginal stability. The magnetic field affects the rate of flow velocity, mass and heat transfer of the onset of convection. In the presence of vertical magnetic field, the magnetic field leads the boundary of monotonous instability and increases the stability of the conductive state. The presence of horizontal magnetic field creates the rolls and breaks the symmetry. Busse and Pesch [31] studied the effect of horizontal magnetic field at the onset of thermal convectoin. The system is also subjected to the rotation about its vertical axis and the Buoyancy-driven flows are affected by this rotation. The presence of the rotating fluid layer is what makes the system more stable. Lyubimov et al. [63] studied the effect of rotating magnetic field convection emerge in the form of rolls.

Nield and Bejan [80] have made deep investigations on various porous medium convective problems. Detailed investigations on thermal instability of horizontal fluid layer which is heated from below through a porous medium under the influence of a uniform magnetic field were presented by Sharma and Thakur [111], Anwar et al [17], Wang et al. [130], Srivastava et al. [114], Altawallbeh et al. [5] and Harfash et al. [52]. Linear and nonlinear stability analysis onset of convection through sparsely packed porous medium with Darcy Lapwood Brinkman model was studied by Tagare [119, 120], Benerji et al. [7, 9–11] and Shivakumara et al. [112]. In this chapter, we study Rayleigh Benard convection with respect to the effect of the convection vertical axis of rotation and horizontal magnetic field in a sparsely packed porous medium. Travelling and standing waves in magneto convection in a nonporous medium was studied by Matthews et al. [67].

The basic equations and boundary conditions are discussed in section 3.2. Linear

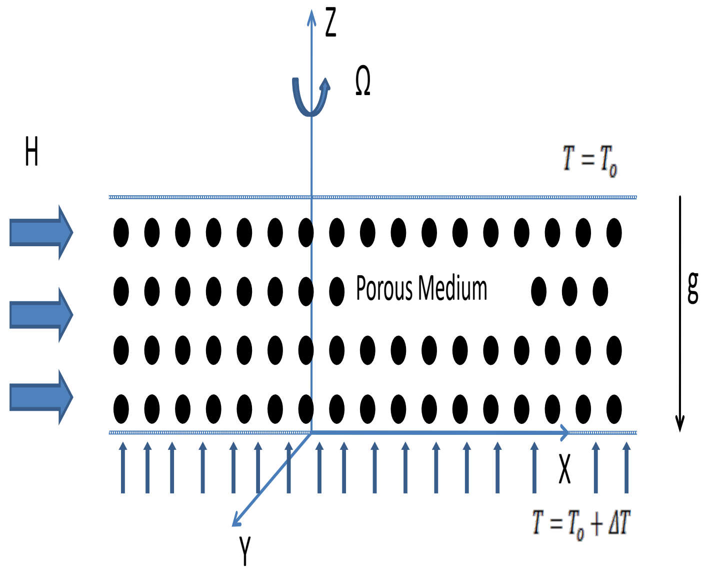

Figure 3.1: Schematic of the physical configuration

and nonlinear stability analysis of stationary and oscillatory convection are studied in section 3.3 and section 3.4 respectively. Finally, conclusions are discussed in section 3.5.

3.2 Basic Equations

We considered the thermally and electrically conducting fluid in an unbounded horizontal layer of a thinly packed porous medium with an magnetic field H_o of depth d in the horizontal x-direction and vertical angular rotation $\overline{\Omega}$. Upper and lower force free bounding surfaces of the layer heated from below is valid Bousssinesq approximation. The temperature variation across the free-free boundaries is $\Delta T'$. The flow in the thinly packed porous medium is governed by the Darcy-Lapwood-Brinkman model. The relevant basic equations of continuity, momentum, energy and magnetic induction along with Boussinesq approximation are

$$\rho = \rho_0 \left[1 - \alpha(T' - T_o')\right], \tag{3.1}$$

and

$$\nabla'.\overline{V}' = 0, \nabla'.\overline{H}' = 0, \tag{3.2}$$

$$\rho_0' \left[\frac{1}{\phi} \frac{\partial \overline{V}'}{\partial t'} + \frac{2}{\phi}(\overline{\Omega} \times \overline{V}') + \frac{1}{\phi^2}(\overline{V}'.\nabla')\overline{V}' \right] - \frac{\mu_m}{4\pi} \left[H_0 \frac{\partial \overline{H}'}{\partial y'} + (\overline{H}'.\nabla')\overline{H}' \right] =$$

$$- \nabla' \left[P' + \frac{\mu_m}{8\pi}|\overline{H}'|^2 + \frac{\mu_m}{4\pi} H_o {H_y}' - \frac{1}{2}|\overline{\Omega} \times \overline{V}'|^2 \right] + \rho' \overline{g} - \frac{\mu}{K}\overline{V}' + \mu_e \nabla'^2 \overline{V}', \tag{3.3}$$

$$M \frac{\partial T'}{\partial t'} - k \nabla'^2 T' = -(\overline{V}'.\nabla')T', \tag{3.4}$$

$$\phi \frac{\partial \overline{H}'}{\partial t} - \nabla' \times (\overline{V} \times H_0 \widehat{e_y}) = \nabla' \times (\overline{V} \times \overline{H}') + \eta \nabla'^2 \overline{H}'. \tag{3.5}$$

Where fluid density is ρ , mean fluid density is ρ_0, thermal expansion coefficient is $\alpha = -\frac{1}{\rho_0}(\frac{\partial \rho}{\partial T'})$, temperature is T', mean flow fluid velocity is $\overline{V}'$, magnetic field is $\overline{H}'$, porosity is ϕ, magnetic permeability is μ_m, angular velocity along vertical direction is $\bar{\Omega} = \Omega \widehat{e_z}$, pressure is P', acceleration due to gravity is $\overline{g}$, permeability of porous medium is K, effective fluid viscosity is μ_e, dimensionless heat capacity is M, thermal diffusivity is k and magnetic diffusivity is η. We use the following scaling

$$\begin{aligned}
x &= x'/d & u &= \frac{u'}{(k/Md)} & t &= \frac{t'}{(Md^2/k)} \\
y &= y'/d & v &= \frac{v'}{(k/Md)} & \theta &= \frac{\theta'}{\triangle T'} \\
z &= z'/d & w &= \frac{w'}{(k/Md)} & \rho &= \frac{\rho'}{\rho_0 k^2 M^{-2} d^{-2}} \\
\overline{H} &= \frac{\overline{H}'}{\kappa H_o/\eta} & R &= \frac{g\alpha \Delta T d^3}{\kappa \nu} & Pr_1 &= \frac{\nu}{\kappa} \\
Pr_2 &= \frac{\nu}{\eta} & Q &= \frac{\mu_m H_0^2 d^2}{4\pi \rho_0 \nu \eta} & Da &= \frac{\kappa}{d^2} \\
Ta &= \frac{4\Omega^2 d^4}{\nu^2}
\end{aligned} \tag{3.6}$$

[47] shows the value of $\Lambda = \frac{\mu_e}{\mu}$ varies from 0.5 to 10.9 . The dimensionless equations for magneto rotating convection in a sparsely packed porous medium due to

horizontal magnetic field with Boussinesq approximation are

$$\nabla.\overline{V} = 0, \nabla.\overline{H} = 0, \tag{3.7}$$

$$\left(\frac{1}{M^2\phi Pr_1}\frac{\partial}{\partial t} - \frac{\Lambda}{M}\nabla^2 + \frac{1}{MDa}\right)\overline{V} - \frac{Ta^{\frac{1}{2}}}{M\phi}\left(\overline{V}\times\hat{e_z}\right) - Q\frac{\partial\overline{H}}{\partial y} - R\theta\hat{e}_z = Q\frac{Pr_2}{Pr_1}(\overline{H}.\nabla)\overline{H}$$
$$- \frac{1}{M^2\phi^2 Pr_1}(\overline{V}.\nabla)\overline{V} - \nabla\left(\frac{P}{MPr_1} + \frac{Q}{2}\frac{Pr_2}{Pr_1}|\overline{H}|^2 + QH_y - \frac{TaPr_1}{8\phi}|\hat{e}_z\times\overline{V}|^2\right), \tag{3.8}$$

$$\left(\frac{\partial}{\partial t} - \nabla^2\right)\theta - \frac{w}{M} = -\frac{1}{M}\left(\overline{V}.\nabla\right)\theta, \tag{3.9}$$

$$\left(\phi\frac{Pr_2}{Pr_1}\frac{\partial}{\partial t} - M\nabla^2\right)\overline{H} - \nabla\times(\overline{V}\times\hat{e_y}) = \frac{Pr_2}{Pr_1}\left[\nabla\times\left(\overline{V}\times\overline{H}\right)\right]. \tag{3.10}$$

The curl and curl of curl of equation (3.8) are

$$\left(\frac{1}{M^2\phi Pr_1}\frac{\partial}{\partial t} - \frac{\Lambda}{M}\nabla^2 + \frac{1}{MDa}\right)(\nabla\times\overline{V}) - \frac{Ta^{\frac{1}{2}}}{M\phi}\left[\nabla\times\left(\overline{V}\times\hat{e_z}\right)\right] -$$
$$Q\left(\nabla\times\frac{\partial\overline{H}}{\partial y}\right) - R(\nabla\times\theta\hat{e}_z) = Q\frac{Pr_2}{Pr_1}\left[\nabla\times(\overline{H}.\nabla)\overline{H}\right] - \frac{1}{M^2\phi^2 Pr_1}\left[\nabla\times(\overline{V}.\nabla)\overline{V}\right]. \tag{3.11}$$

$$\left(\frac{1}{M^2\phi Pr_1}\frac{\partial}{\partial t} - \frac{\Lambda}{M}\nabla^2 + \frac{1}{MDa}\right)\left[\nabla\times(\nabla\times\overline{V})\right] - \frac{Ta^{\frac{1}{2}}}{M\phi}\left\{\nabla\times\left[\nabla\times\left(\overline{V}\times\hat{e_z}\right)\right]\right\} -$$
$$Q\left[\nabla\times\left(\nabla\times\frac{\partial\overline{H}}{\partial y}\right)\right] - R\left[\nabla\times(\nabla\times\theta\hat{e}_z)\right] = Q\frac{Pr_2}{Pr_1}\left\{\nabla\times\left[\nabla\times\left(\overline{H}.\nabla\right)\overline{H}\right]\right\} -$$
$$\frac{1}{M^2\phi^2 Pr_1}\left\{\nabla\times\left[\nabla\times(\overline{V}.\nabla)\overline{V}\right]\right\}. \tag{3.12}$$

The curl of equation (3.10) is

$$\left(\phi\frac{Pr_2}{Pr_1}\frac{\partial}{\partial t} - M\nabla^2\right)(\nabla\times\overline{H}) - \left[\nabla\times\nabla\times(\overline{V}\times\hat{e_y})\right] = \frac{Pr_2}{Pr_1}\left\{\nabla\times\left[\nabla\times\left(\overline{V}\times\overline{H}\right)\right]\right\}, \tag{3.13}$$

from equation (3.9) and z-component of equations (3.10), (3.11), (3.12) and (3.13), we obtain a single equation of the form

$$\mathcal{L}w = \mathcal{N}, \tag{3.14}$$

where

$$\mathcal{L} =\mathcal{D}_y^2\nabla^2\mathcal{D} - \frac{R}{M}\mathcal{D}_y\nabla_h^2\mathcal{D}_\phi + \frac{Ta}{M^2\phi^2}\partial_z^2\mathcal{D}^2{\mathcal{D}_\phi}^2, \tag{3.15}$$

$$\begin{aligned}\mathcal{N} =&\mathcal{D}_y\left\{-\mathcal{D}\mathcal{D}_\phi\mathcal{D}_\nabla.\overline{e}_z + Q\frac{Pr_2}{\mathrm{Pr}_1}\nabla^2\mathcal{D}\partial_y\left[\nabla\times(\overline{V}\times\overline{H})\overline{e}_z\right] - \frac{R}{M}\mathcal{D}_\phi\nabla_h^2(\overline{V}\nabla)\theta\right\} - \\ &\frac{Ta^{1/2}}{M\phi}\mathcal{D}\mathcal{D}_\phi\partial_z\left\{\mathcal{D}_\phi\mathcal{D}_\nabla\overline{e}_z + Q\frac{Pr_2}{Pr_1}\partial_y\left[\nabla\times\nabla\times(\overline{V}\times\overline{H})\overline{e}_z\right]\right\},\end{aligned} \tag{3.16}$$

where $\mathcal{D} = \left(\frac{\partial}{\partial t} - \nabla^2\right)$, $\mathcal{D}_\phi = \phi\frac{Pr_2}{Pr_1}\frac{\partial}{\partial t} - M\nabla^2$, $\mathcal{D}_{Pr_1} = \frac{1}{M^2\phi Pr_1}\frac{\partial}{\partial t} + \frac{1}{MD_a} - \frac{\Lambda}{M}\nabla^2$, $\nabla^2 = \frac{\partial^2}{\partial x^2}+\frac{\partial^2}{\partial y^2}+\frac{\partial^2}{\partial z^2}$, $\nabla_h^2 = \frac{\partial^2}{\partial x^2}+\frac{\partial^2}{\partial y^2}$, $\mathcal{D}_y = \mathcal{D}_{Pr_1}\mathcal{D}_\phi - Q\partial_y^2$, $\mathcal{D}_\nabla = -\frac{1}{M^2\phi^2Pr_1}\left[\nabla\times\nabla\times(\overline{V}\cdot\nabla)\overline{V}\right] + Q\frac{Pr_2}{Pr_1}\left[\nabla\times\nabla\times(\overline{H}\cdot\nabla)\overline{H}\right]$, $\partial_y = \frac{\partial}{\partial y}$, $\partial_z = \frac{\partial}{\partial z}$. The boundary conditions are are follows from the section 2.2.1.

3.3 Linear stability analysis

The solution of linearised system $\mathcal{L}\omega = 0$ corresponds to the formation of convection rolls. The rolls characterised by assuming periodic disturbances with period $\frac{2\pi}{l}$ along x-direction and periodic disturbances with period $\frac{2\pi}{m}$ along y-direction with growth rate p of the form

$$w = W(z)e^{i(lx+my)+pt}, \tag{3.17}$$

where $W(z) = \sin\pi z$ and $p = i\omega$. substituting w into $\mathcal{L}w = 0$, we get

$$(p+\delta^2)\delta^2\left[\left(\frac{1}{M^2\phi Pr_1}p+\frac{\Lambda}{M}\delta^2+\frac{1}{MDa}\right)\left(\phi\frac{Pr_2}{Pr_1}p+M\delta^2\right)+Qm^2\right]^2-$$
$$\frac{R}{M}q^2\left(\phi\frac{Pr_2}{Pr_1}p+M\delta^2\right)\left[\left(\frac{1}{M^2\phi Pr_1}p+\frac{\Lambda}{M}\delta^2+\frac{1}{MDa}\right)\left(\phi\frac{Pr_2}{Pr_1}p+M\delta^2\right)+Qm^2\right]+$$
$$\frac{Ta^{1/2}}{M^2\phi^2}\pi^2(p+\delta^2)\left(\phi\frac{Pr_2}{Pr_1}p+M\delta^2\right)^2=0, \tag{3.18}$$

where $q^2=l^2+m^2$ and $\delta^2=q^2+\pi^2$.

3.3.1 When Rayleigh number R is a Dependent Variable

Substitute w in equation 3.18, we get

$$R=\frac{M}{q^2}\mathcal{K}\left[\left(h_1+h_2\omega^2+h_3\omega^4+h_4\omega^6+h_5\omega^8\right)+i\omega\left(I_1+I_2\omega^2+I_3\omega^4+I_4\omega^6\right)\right], \tag{3.19}$$

where $\mathcal{K}=(F_1+F_2\omega^2)^2+\omega^2(F_3+F_4\omega^2)^{2-1}$, $h_1=F_1G_1$, $h_2=F_2G_1+F_1G_2-F_3G_4$, $h_3=F_2G_2+F_1G_3-F_4G_4-F_3G_5$, $h_4=F_2G_3-F_4G_5-F_3G_6$, $h_5=-F_4G_6$, where

$$\begin{aligned} I_1 &=F_3G_1+F_1G_4, & F_1 &=m^2Qa_2+a_2^2b_2,\\ I_2 &=F_4G_1+F_3G_2+F_2G_4+F_1G_5, & F_2 &=-2a_1a_2b_1-a_2^2b_2,\\ I_3 &=F_4G_2+F_3G_3+F_2G_5+F_1G_6, & F_3 &=m^2Qa_1+a_2^2b_1+2a_1a_2b_2,\\ I_4 &=F_4G_3+F_2G_6 & F_4 &=-a_1^2b_1, \end{aligned} \tag{3.20}$$

$$\begin{aligned} G_1 =&m^4Q^2\delta^4+2m^2Q\delta^4a_2b_2+\delta^4a_2^2b_2^2+Ta\delta^2a_2^2c_1,\\ G_2 =&-\delta^4(2m^2Qa_1b_1+4a_1a_2b_1b_2+a_2^2b_1^2+a_1^2b_2^2)-\delta^2(2m^2Qa_2b_1+\\ &2m^2Qa_1b_2+2a_2^2b_1b_2+2a_1a_2b_2^2+Taa_1^2c_1)-2Taa_1a_2c_1,\\ G_3 =&\delta^4a_1^2b_1^2+2\delta^2a_1a_2b_1^2+2\delta^2a_1^2b_1b_2, \end{aligned}$$

$$G_4 = 2\delta^4(m^2Qa_2b_1 + m^2Qa_1b_2 + a_2^2b_1b_2 + a_1a_2b_2^2) + \delta^2(m^4Q^2 + 2m^2Qa_2b_2 + a_2^2b_2^2 + 2Taa_1a_2c_1) + Taa_2^2c_1,$$

$$G_5 = -2\delta^4(a_1a_2b_1^2 + a_1^2b_1b_2) - \delta^2(2m^2Qa_1b_1 + a_2^2b_1^2 + 4a_1a_2b_1b_2 + a_1^2b_2^2) - Taa_1^2b_2^2,$$

$$G_6 = \delta^2a_1^2b_1^2, a_1 = \phi\frac{Pr_2}{Pr_1}, a_2 = M\delta^2, b_1 = \frac{1}{M^2\phi Pr_1}, b_2 = \frac{1}{M}\left(\Lambda\delta^2 + \frac{1}{Da}\right), c_1 = \frac{\pi^2}{M^2\phi^2}.$$

Stationary Convection

For stationary convection put $p = 0$ *i.e.* $\omega = 0$ in equation (3.18), we then obtain stationary Rayleigh number and it is represented as R_s,

$$R_s = \frac{\delta^2}{q^2}\left[\left(\Lambda\delta^2 + \frac{1}{Da}\right)\delta^2 + Qm^2\right] + \frac{Ta\pi^2\delta^4}{\phi^2q^2}\frac{1}{\left[\left(\Lambda\delta^2 + \frac{1}{Da}\right)\delta^2 + Qm^2\right]}, \tag{3.21}$$

Cross rolls : If there is a periodic disturbance along x-direction and no perturbation along y-direction with growth rate p, we take $m = 0$ in equation (3.21) and obtain stationary Rayleigh number for cross roll which is represented as $R_s^l(m = 0)$,

$$R_s^l(m = 0) = \frac{(l^2 + \pi^2)}{l^2}\left[\left(\Lambda(l^2 + \pi^2) + \frac{1}{Da}\right)(l^2 + \pi^2)\right] + \frac{1}{l^2}\frac{Ta\pi^2(l^2 + \pi^2)^2}{\phi^2}\frac{1}{\left[\left(\Lambda(l^2 + \pi^2) + \frac{1}{Da}\right)(l^2 + \pi^2)\right]}, \tag{3.22}$$

the critical stationary Rayleigh number for cross rolls is $R_{sc}^l(m = 0)$,

$$R_{sc}^l(m = 0) = \Lambda\frac{(l_c^2 + \pi^2)^3}{l_c^2} + \frac{Ta\pi^2}{\phi^2}\frac{1}{l_c^2}.$$

Parallel rolls : If there is no periodic disturbance along x-direction but periodic disturbance along y-direction with growth rate p, we take $l = 0$ in Equation (3.21),

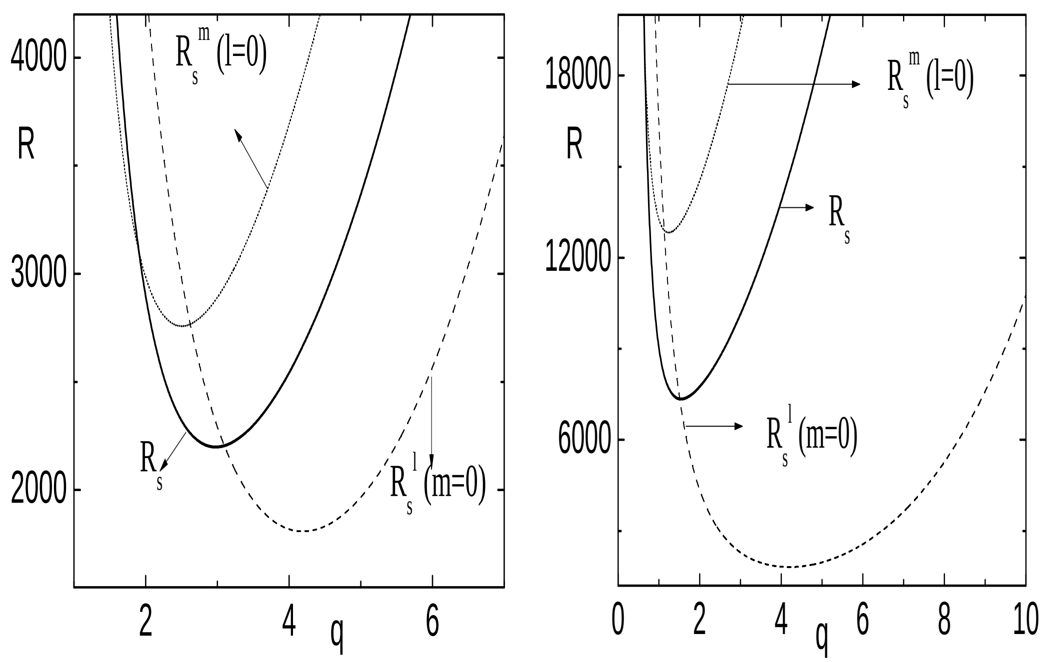

(a) (b)

Figure 3.2: Marginal stability curves of the cross, parallel and oblique rolls for $Da = 1500$, $\Lambda = 0.8$, $M = 0.9$, $\phi = 0.85$, $Pr_1 = 1.5$, $Pr_2 = 1.65$, $Ta = 10^5$, (a) $Q = 100$, (b) $Q = 1000$.

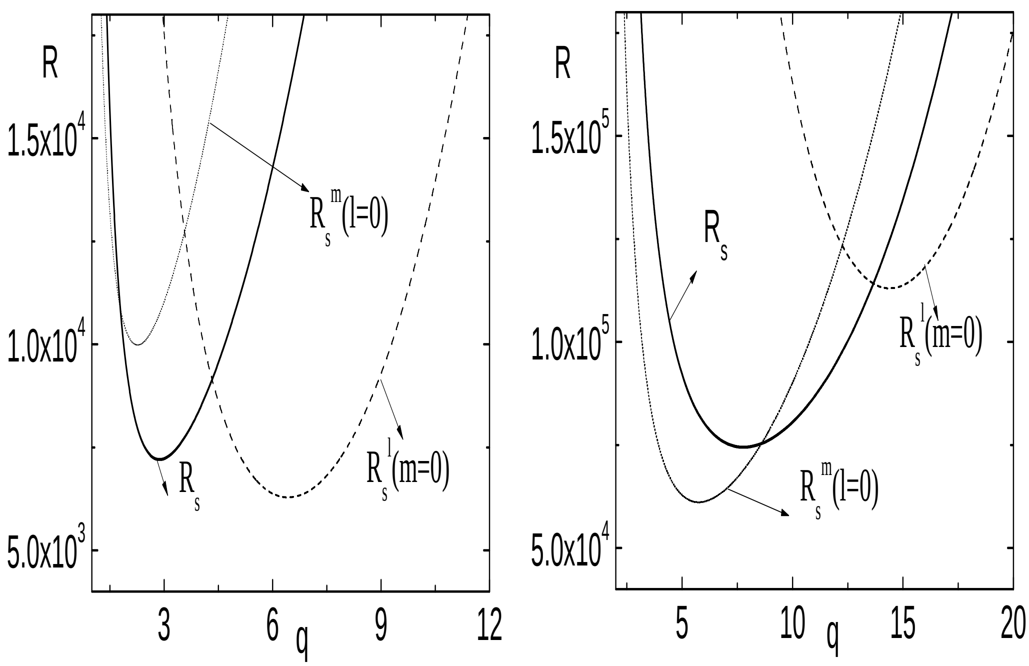

(a) (b)

Figure 3.3: Marginal stability curves of the cross, parallel and oblique rolls for $Da = 1500$, $\Lambda = 0.8$, $M = 0.9$, $\phi = 0.85$, $Pr_1 = 1.5$, $Pr_2 = 1.65$, $Q = 500$, (a) $Ta = 10^4$, (b) $Ta = 10^6$.

and get stationary Rayleigh number for parallel rolls is $R_s^m(l=0)$,

$$R_s^m(l=0) = \frac{(m^2+\pi^2)}{m^2}\left\{\left[\Lambda(m^2+\pi^2)+\frac{1}{Da}\right](m^2+\pi^2)+Qm^2\right\}+ \frac{1}{m^2}\frac{Ta\pi^2}{\phi^2}\frac{(m^2+\pi^2)^2}{\left\{\left[\Lambda(m^2+\pi^2)+\frac{1}{Da}\right](m^2+\pi^2)+Qm^2\right\}},$$

The critical stationary Rayleigh number for parallel rolls is $R_{sc}^m(l=0)$,

$$R_{sc}^m(l=0) = \frac{m_c^2+\pi^2}{m_c^2}\left[\Lambda(m_c^2+\pi^2)^2+Qm_c^2\right]+\frac{1}{m_c^2}\frac{Ta\pi^2}{\phi^2}\frac{(m_c^2+\pi^2)^2}{\left[\Lambda(m_c^2+\pi^2)^2+Qm_c^2\right]}, \tag{3.23}$$

Oblique rolls : If there is a periodic disturbance along x-direction and y-direction with growth rate p. The stationary Rayleigh number for oblique rolls is Equation(3.21). The critical stationary Rayleigh number is R_{sc} for critical wave numbers q_{sc},

$$R_{sc} = \frac{\delta_{sc}^2}{q_{sc}^2}\left[\left(\Lambda\delta_{sc}^2+\frac{1}{Da}\right)\delta_{sc}^2+Qm^2\right]+\frac{Ta\pi^2\delta_{sc}^4}{\phi^2 q_{sc}^2}\frac{1}{\left[\left(\Lambda\delta_{sc}^2+\frac{1}{Da}\right)\delta_{sc}^2+Qm^2\right]}, \tag{3.24}$$

where $q_{sc}^2 = l^2+m^2$ and $\delta_{sc}^2 = \pi^2+q_{sc}^2$. Figures 3.2 - 3.3 show the marginal curves of cross rolls $R_s^l(m=0)$, parallel rolls $R_s^m(l=0)$ and oblique rolls R_s. As shown in Figure 3.2, the critical Rayleigh number is increasing along with increasing magnetic field. In Figure 3.3, critical Rayleigh number is smaller for cross roll $R_s^m(l=0)$ than parallel roll $R_s^l(m=0)$ in the low rotation case while the opposite is true in high rotation case. The oblique critical Rayleigh number is always between the cross rolls and parallel rolls.

Oscillatory Convection

For oscillatory convection ($\omega^2>0$) and from equation (3.18), R represents imaginary number but Rayleigh number is always real, so equate imaginary part of the equation

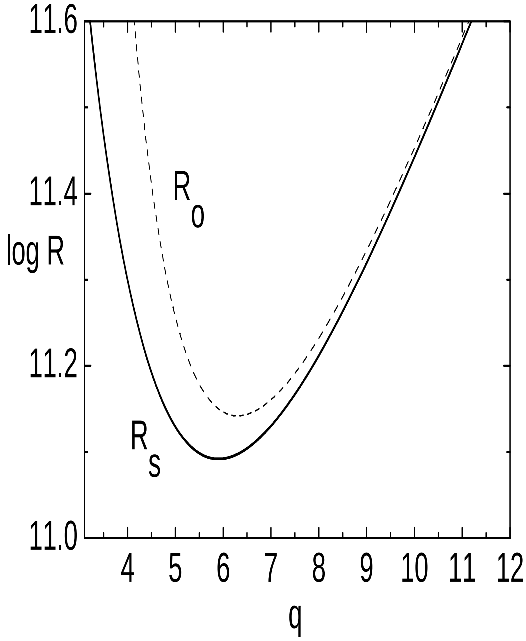

(a)

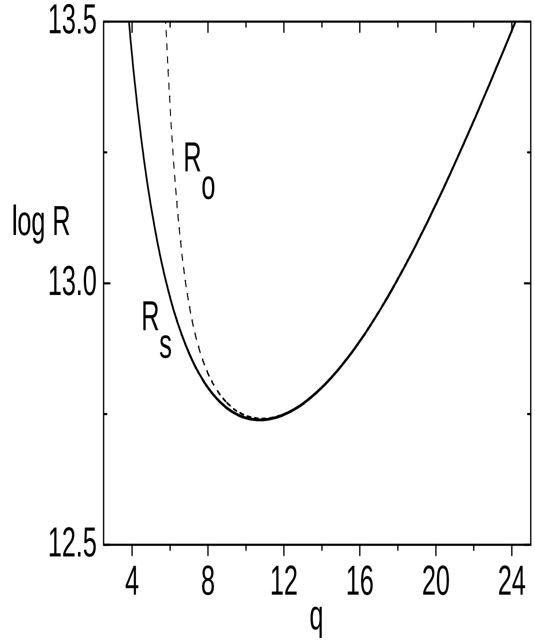

(b)

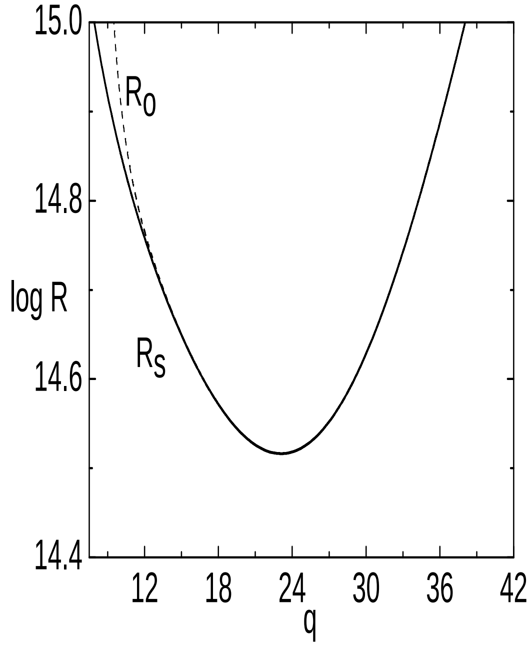

(c)

Figure 3.4: Solid lines represent stationary Rayleigh number R_s and doted lines represents oscillatory Rayleigh number R_o for $Da = 1500$, $\Lambda = 0.8$, $M = 0.9$, $\phi = 0.85$, $Pr_1 = 1.5$, $Pr_2 = 3.5$, $Q = 1200$, (a) $Ta = 10^6$, (b) $Ta = 10^7$, (c) $Ta = 10^8$.

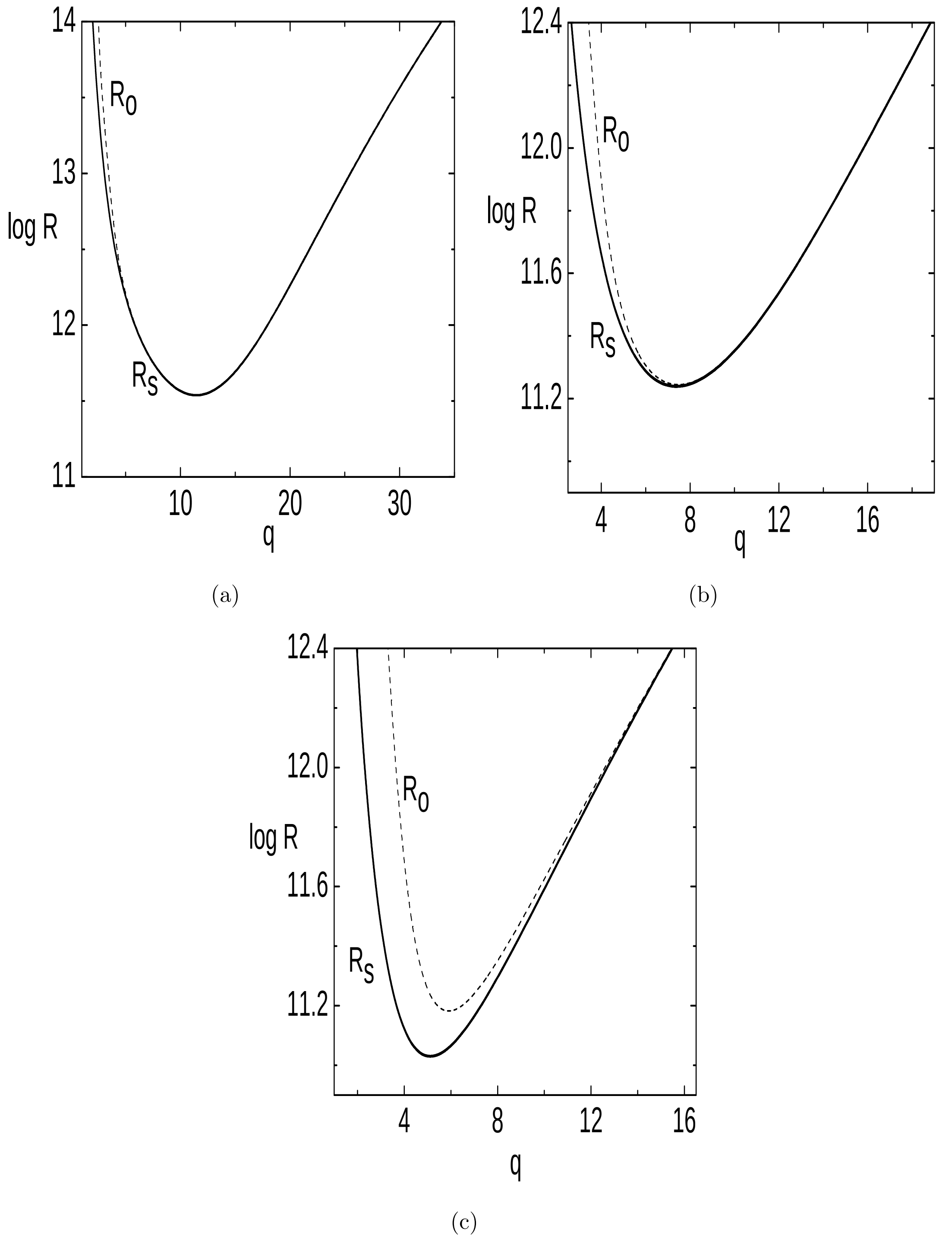

Figure 3.5: Solid lines represent Stationary convection R_s and doted lines represents Oscillatory convection R_o for $Da = 1500$, $\Lambda = 0.8$, $M = 0.9$, $\phi = 0.85$, $Pr_1 = 1.5$, $Pr_2 = 1.65$, $Ta = 6 \times 10^5$ at (a) $Q = 200$, (b) $Q = 600$, (c) $Q = 1400$.

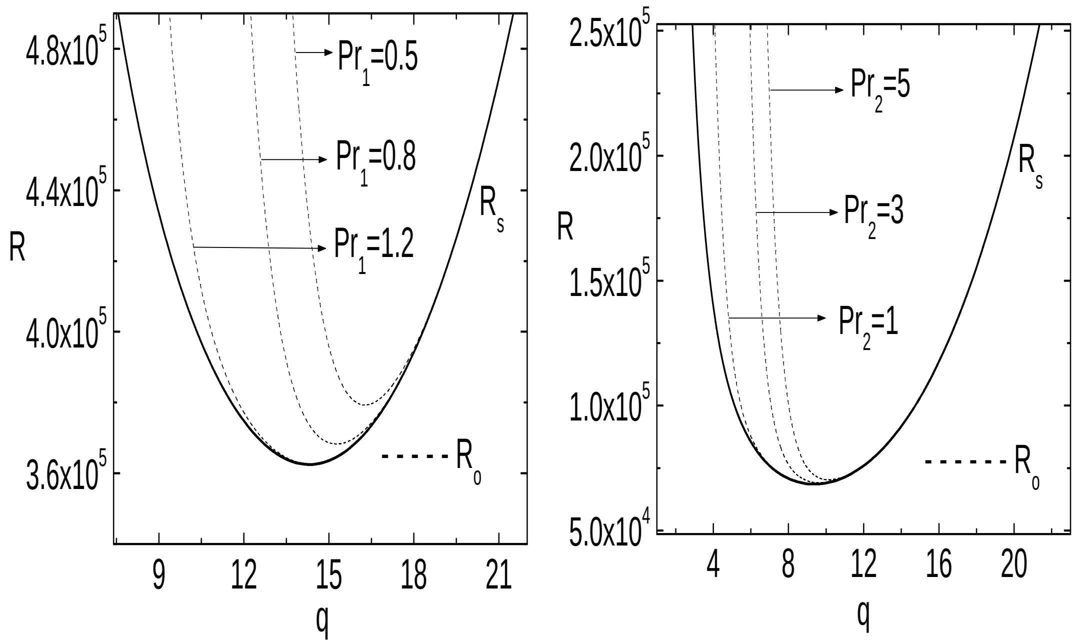

(a) (b)

Figure 3.6: Solid lines represent Stationary convection R_s and doted lines represents Oscillatory convection R_o for $Da = 1500$, $\Lambda = 0.9$, $M = 0.9$, $\phi = 0.85$, $Q = 500$, $Ta = 8 \times 10^6$, (a) $Pr_2 = 3$, (b) $Pr_1 = 0.8$.

(3.18) to zero. By solving the imaginary part, the oscillatory Rayleigh number is

$$R_o = \frac{MK_1}{q^2}\left[H_1 + H_2\omega^2 + H_3\omega^4 + H_4\omega^6 + H_5\omega^8\right], \tag{3.25}$$

$$\omega^2 = \frac{I_3^2 + I_5(I_3 + I_2) - 3I_4I_2}{I_4I_5}, \tag{3.26}$$

where $G_1 = m^4Q^2\delta^4 + 2m^2Q\Lambda\delta^8 + \Lambda^2\delta^{10} + \frac{Ta\delta^4}{Pr_1^2}$, $G_2 = \frac{2m^2Q\phi\delta^4Pr_2}{M^2\phi Pr_1} + \frac{\Lambda\delta^4Pr_2}{M^2Pr_1^2} + \frac{\delta^2Pr_2^2}{M^4Pr_1^2} + \frac{Pr_2^2}{M^2Pr_1^4} + \frac{Qm^2\delta^4}{M\phi Pr_1} - 2\delta^2m^2Q^2 + \frac{Ta\pi\delta^2Pr_2}{M\phi Pr_1} - \phi\frac{Pr_2^2}{Pr_1^2}$, $G_3 = \frac{\delta^4Pr_2^2}{M^4Pr_1^4} + \frac{\delta^2Pr_2}{M^3Pr_1^3} + \frac{2\Lambda\delta^4Pr_2^2}{M^3Pr_1^3}$,
$G_4 = \frac{Ta\pi\delta^4Pr_2}{M\phi Pr_1} + \frac{Qm^2\delta^2}{M\phi Pr_1} + 2m^2Q^2\delta^2$, $G_5 = -\phi\frac{Pr_2^2}{Pr_1^2} + \Lambda M^2\delta^6 + \frac{2m^2Q\phi\delta^4Pr_2}{M^2\phi Pr_1}$,
$G_6 = \frac{\delta^2Pr_2^2}{M^4Pr_1^4}$, $F_1 = Q\delta^2m^2 + \Lambda M^2\delta^6$, $F_2 = -\frac{2\delta^2Pr_2}{Pr_1^2}$, $F_3 = QM\delta^2m^2 + \frac{\delta^4}{\phi Pr_1}$,
$F_4 = -\phi\frac{Pr_2^2}{Pr_1^2}$, $H_1 = F_1G_1$, $H_2 = F_2G_1 + F_1G_2 - F_3G_4$, $H_3 = F_2G_2 + F_1G_3 - F_4G_4 - F_3G_5$, $H_4 = F_2G_3 - F_4G_5 - F_3G_6$, $H_5 = -F_4G_6$, $I_1 = F_3G_1 + F_1G_4$,
$I_2 = F_4G_1 + F_3G_2 + F_2G_4 + F_1G_5$, $I_3 = F_4G_2 + F_3G_3 + F_2G_5 + F_1G_6$, $I_4 = F_4G_3 + F_2G_6$,
$I_5 = [-2I_3^3 + 9I_4I_3I_2 - 27I_4^2I_1 + [4(-I_3^2 + 3I_4I_2)^3 + (-2I_3^3 + 9I_4I_3I_2 - 27I_4^2I_1)^2]^{1/2}]^{1/3}$.
In Figures 3.3 - 3.5, the neutral curves are plotted in the (q, R) - plane with the effects of Ta, Q, Pr_1 and Pr_2. The solid line represents the stationary Rayleigh number R_s while the dotted line represents the oscillatory Rayleigh number R_o. At Takens-Bogdanov bifurcation point we get $R_s(q_s) = R_o(q_o) = R_c(q_c)$ and $q_s = q_o = q_c$. At co-dimension two bifurcation point we get $R_s(q_s) = R_c(q_c)$ and $q_s \neq q_c$. The stationary Rayleigh number was not affected by thermal and magnetic prandtl numbers. There exist co-dimension two bifurcation points in Figure 3.3(b), Figure 3.4(b), at $Pr_1 = 1.2$ in Figure 3.5(a) and at $Pr_2 = 3$ in Figure 3.5(b). Over the oscillatory convection, the critical Rayleigh value increases when the thermal prandtl value decreases and the critical Rayleigh value decreases when the magnetic prandtl number increases.

3.3.2 When Rayleigh number R is an Independent Variable

The equation (3.18) represents as a fifth degree polynomial in powers of p,

$$Ap^5 + Bp^4 + Cp^3 + Dp^2 + Ep + F = 0, \tag{3.27}$$

where

$$\begin{aligned}
A =& -\delta^2 a_1^2 b_1^2,\ B = -\delta^2 a_1 b_1[2a_2b_1 + a_1(\delta^2 b_1 + 2b_2)],\\
C =& -\frac{1}{M^2\phi^2}\{M^2\delta^2\phi^2 a_2^2 b_1^2 + 2M^2\delta^2\phi^2 a_1 b_1[m^2Q + a_2(\delta^2 b_1 + 2b_2)]+\\
& a_1^2[\pi^2 Ta + M^2\delta^2\phi^2 b_2^2 + M\phi^2 b_1(-q^2R + 2M\delta^4 b_2)]\},\\
D =& -\frac{1}{M^2\phi^2}\{a_1^2(\pi^2 Ta\delta - Mq^2R\phi^2 b_2 + M^2\delta^4\phi^2 b_2^2)M^2\delta^2\phi^2 a_2 b_1[2m^2Q + a_2(\delta^2 b_1 + 2b_2)]+\\
& 2a_1[m^2M^2Q\delta^2\phi^2(\delta^2 b_1 + b_2) + a_2[\pi^2 Ta + M^2\delta^2\phi^2 b_2^2 + M\phi^2 b_1(-q^2R + 2M\delta^4 b_2)]]\},\\
E =& -\frac{1}{M^2\phi^2}\{m^4M^2Q^2\delta^2\phi^2 + 2m^2M^2Q\delta^2\phi^2 a_2(\delta^2 b_1 + b_2) + a_2^2[\pi^2 Ta+\\
& M^2\delta^2\phi^2 b_2^2 + M\phi^2 b_1(-q^2R + 2M\delta^4 b_2) + a_1[m^2MQ\phi^2(-q^2R + 2M\delta^4 b_2)+\\
& 2a_2(\pi^2 Ta\delta^2 - Mq^2R\phi^2 b_2 + M^2\delta^4\phi^2 b_2^2)]]\},\\
F =& -m^4Q^2\delta^4 + \frac{M^2Qa_2(q^2R - 2M\delta^4 b_2)}{M} + a_2^2\left(-\frac{\pi^2 Ta\delta^2}{M^2\phi^2} + \frac{q^2Rb_2}{M} - \delta^4 b_2^2\right).
\end{aligned} \tag{3.28}$$

Take $p = i\omega$ in equation (3.27), we get

$$(B\omega^4 - D\omega^2 + F) + i\omega(A\omega^4 - C\omega^2 + E) = 0, \tag{3.29}$$

from the above equation 3.29, the real and imaginary parts are $B\omega^4 - D\omega^2 + E = 0$ and $A\omega^4 - C\omega^2 + E = 0$.

stationary convection ($\omega = 0$)

At the onset of stationary convection take $\omega = 0$ in equation (3.27), we get $F = 0$.

$$q^2\left[m^2Q+\left(\Lambda\delta^2+\frac{1}{Da}\right)\delta^2\right]R=\delta^2\left[m^2Q+\left(\Lambda\delta^2+\frac{1}{Da}\right)\delta^2\right]^2+\frac{\pi^2Ta}{\phi^2}\delta^4, \quad (3.30)$$

which is same as equation (3.21). If there is a periodic disturbance along x-direction and no perturbation along y-direction with growth rate p, then which represents cross rolls in the system. If vanish the Chandrasekhar number we get

$$l^2\lambda R = \Lambda(l^2+\pi^2)^3 + \frac{Ta\pi^2}{\phi^2}, \quad (3.31)$$

differentiating equation (3.31) with respect to l, we get

$$l^2 = \sqrt{\frac{R}{3}} - \pi^2, \quad (3.32)$$

substituting l^2 in equation (3.31), we get

$$Ta_x = \frac{\Lambda\phi^2}{\pi^2}\left[R\left(\sqrt{\frac{R}{3}}-\pi^2\right)-\Lambda\sqrt[3]{\frac{R}{3}}\right] \quad (3.33)$$

If there is a periodic disturbance along y-direction and no disturbance along x-direction with growth rate p, then which represents parallel rolls. If vanish the Chandrasekhar number we get

$$m^2\lambda R = \Lambda^2(m^2+\pi^2)^3 + \frac{Ta\pi^2}{\phi^2}, \quad (3.34)$$

differentiating above equation (3.34) with respect to m, we get

$$m^2 = \sqrt{\frac{R}{3\Lambda}} - \pi^2, \quad (3.35)$$

substituting l^2 in equation (3.34), we get

$$Ta_y = \frac{\Lambda\phi^2}{\pi^2}\left[R\left(\sqrt{\frac{R}{3\Lambda}}-\pi^2\right)-\Lambda\sqrt[3]{\frac{R}{3\Lambda}}\right]. \tag{3.36}$$

The equations (3.33) and (3.36) both are same if $\Lambda = 1$. The Stationary Taylor number by considering R as an independent variable represents as Ta_s,

$$Ta_s = \frac{\phi^2}{\pi^2}\left[R\left(\sqrt{\frac{R}{3}}-\pi^2\right)-\sqrt[3]{\frac{R}{3}}\right]. \tag{3.37}$$

Oscillatory convection ($\omega^2 > 0$)

We have marginal stability if $\omega^2 = \frac{C\pm\sqrt{C^2-4AE}}{2A}$ from $A\omega^4 - C\omega^2 + E = 0$ and substitute this ω^2 in $B\omega^4 - D\omega^2 + E = 0$, $2BC^2 - 4AE - 2ADC + 4A^2E \pm (2BC \pm 2AD)\sqrt{C^2 - -4AE} = 0$ with $C^2 > 4AE$. At Takens-Bogdanov bifurcation point we get $\omega^2 = 0$, which gives $F = 0$ and $E = 0$. Eliminating R from $F = 0$ and $E = 0$ we get

$$Ta_{oc} = -\frac{M^2\delta^2\phi^2(m^2Q + a_2b_2)^2[-m^2Q\delta^2a_1 + a_2(m^2Q + a_2(\delta^2b_1 + b_2))]}{\pi^2a_2^2[m^2Q\delta^2a_1 + a_2(m^2Q + a_2(-\delta^2b_1 + b_2))]} \tag{3.38}$$

We get Takens-Bogdanov bifurcation point if $Ta > 0$. Here $Ta > 0$ if

$$Q < \frac{a_2^2(\delta^2b_1 + b_2)}{m^2(\delta^2a_1 - a_2)}. \tag{3.39}$$

On eliminating Q and Ta from $D = 0$, $E = 0$ and $F = 0$ we get codimention three bifurcation point.

3.4 Nonlinear stability analysis

3.4.1 Amplitude equation at the onset of stationary convection

According to Newell and Whitehead Multiple scale analysis [77] when small scale convection cells disturb basic flow, we assume that the solution is in the form of

$$f = \epsilon f_0 + \epsilon^2 f_1 + \epsilon^3 f_2 + \cdot, \tag{3.40}$$

where $\epsilon^2 = \frac{R - R_{sc}}{R_{sc}} << 1$ and $f = f(u, v, w, \theta, H_x, H_y, H_z)$, with the first approximation given by the eigenvectors of the linearised problem as

$$\begin{aligned}
u_0 =& \frac{i\pi}{l}\left[Ae^{i(lx+my)} - c\cdot c\cdot\right]\cos\pi z,\\
v_0 =& -\frac{i\pi Ta^{1/2}\delta^2}{\phi l\left(\lambda\delta^4 + Qm^2\right)}\left[Ae^{i(lx+my)} - c\cdot c\cdot\right]\cos\pi z,\\
w_0 =& \left[Ae^{i(lx+my)} + c\cdot c\cdot\right]\sin\pi z,\\
\theta_0 =& \frac{1}{M\delta^2}\left[Ae^{i(lx+my)} + c\cdot c\cdot\right]\sin\pi z,\\
H_{x_0} =& \frac{-m\pi}{Ml\delta^2}\left[Ae^{i(lx+my)} + c\cdot c\cdot\right]\cos\pi z,\\
H_{y_0} =& \frac{m\pi Ta^{1/2}}{M\phi l\left(\lambda\delta^4 + Qm^2\right)}\left[Ae^{i(lx+my)} + c\cdot c\cdot\right]\cos\pi z,\\
H_{z_0} =& \frac{im}{M\delta^2}\left[Ae^{i(lx+my)} - c\cdot c\cdot\right]\sin\pi z,
\end{aligned} \tag{3.41}$$

where $A = A(X, Y, T)$ is the amplitude and $c.c$ represents the complex conjugate of the amplitude. The variables $X,\ Y,\ Z$ and T are scaled as

$$X = \epsilon x, \quad Y = \epsilon^{\frac{1}{2}} y, \quad Z = z \quad T = \epsilon^2 t, \tag{3.42}$$

are suitably scattered the fast and slow unconventional variables in f. The derivative operators can be formulated as

$$\frac{\partial}{\partial x} \to \frac{\partial}{\partial x} + \epsilon \frac{\partial}{\partial X}, \quad \frac{\partial}{\partial y} \to \frac{\partial}{\partial y} + \epsilon^{\frac{1}{2}} \frac{\partial}{\partial Y}, \quad \frac{\partial}{\partial z} \to \frac{\partial}{\partial Z}, \quad \frac{\partial}{\partial t} \to \epsilon^2 \frac{\partial}{\partial T}. \tag{3.43}$$

with the transformations equation (3.43), the linear and nonlinear operators $\mathcal{L}$ and $\mathcal{N}$ are written as

$$\mathcal{L} = \mathcal{L}_0 + \epsilon \mathcal{L}_1 + \epsilon^2 \mathcal{L}_2 \cdots, \tag{3.44}$$

$$\mathcal{N} = \epsilon^2 \mathcal{N}_0 + \epsilon^3 \mathcal{N}_1 + \cdots, \tag{3.45}$$

substituting equations (3.44) and (3.45) into equation (3.14), equating the ϵ, ϵ^2 and ϵ^3 coefficients on both side.

$$\mathcal{L}_0 w_0 = 0, \tag{3.46}$$

$$\mathcal{L}_0 w_1 + \mathcal{L}_1 w_0 = \mathcal{N}_0, \tag{3.47}$$

$$\mathcal{L}_0 w_2 + \mathcal{L}_1 w_1 + \mathcal{L}_2 w_0 = \mathcal{N}_1, \tag{3.48}$$

where

$$\begin{aligned}
\mathcal{L}_0 =& -\frac{R}{Da}\nabla_h^2\nabla^4 + R\Lambda\nabla_h^2\nabla^6 - \frac{1}{Da^2}\nabla^8 + \frac{2\Lambda}{Da}\nabla^{10} - \Lambda^2\nabla^{12} - Qr\nabla_h^2\nabla^2\partial_y^2 - \\
& \frac{2Q}{Da}\nabla^6\partial_y^2 - Q^2\nabla^4\partial_y^4 - \frac{Ta}{\phi^2}\nabla^6\partial_Z^2, \\
\mathcal{L}_1 =& -4R\nabla_h^2\partial_y^2\partial_Y^2\Big(Q + \frac{1}{Da} + 3\Lambda\nabla^2\Big) - (2\partial_x\partial_X + \partial_Y^2)\nabla^2 F_1 - \nabla^2\partial_y^2\partial_Y^2 F_2 + \\
& F_3 - \partial_y^2\partial_Y^2\nabla^2 - 4Q\partial_y^4\partial_Y^2\Big[R + 2\Big(2Q + \frac{3}{Da}\Big)\nabla^2 + 12\Lambda\nabla^4\Big] - 4Q^2\partial_y^6\partial_Y^2, \\
\mathcal{L}_2 =& (2\partial_x\partial_X + \partial_Y^2)\Big[(2\partial_y\partial_Y)^2 F_4 - \partial_Y^2 F_5\Big] + (2\partial_x\partial_X + \partial_Y^2)^2 F_6 - (2\partial_y\partial_Y)^4 \\
& \Big[Q^2 + R\Lambda + \partial 1 Da^2 + \frac{2Q}{Da} + (\frac{10\Lambda}{Da} + 8Q\Lambda)\nabla^2\Big] + \partial_X^2\partial_y^2 F_7 + \partial_X^2\nabla_h^2 - \\
& (3R\Lambda\nabla^4\frac{2R}{Da}\nabla^2) + \partial_X^2\nabla^2 F_8 + \partial_T F_9 - \partial_Y^2(2\partial - Y\partial_Y)^2,
\end{aligned} \tag{3.49}$$

$$
\begin{aligned}
F_1 =& \Big(2Q^2\partial_y^4 + QR\partial_y^2\Big) + \Big(3\frac{Ta}{\phi^2}\partial_z^2 - 3R\Lambda\nabla_h^2\Big)\nabla^2 - 8Q\Lambda\partial_y^2\nabla^4 + 6\nabla^2\delta^8,\\
F_2 =& \Big(QR + 12\frac{Ta}{\phi^2}\partial_z^2\Big) + \Big(6Q^2 - 12\Lambda R\Big)\nabla^2 - 16Q\Lambda\nabla^4 + 60\nabla_h^2\nabla^6,\\
F_3 =& 2\nabla^6 Q\partial_Y^2 Q\nabla^2 - QR\nabla_h^2\partial_Y^2\Big(2\partial_x\partial_X + \partial_Y^2 + \nabla^2\Big),\\
F_4 =& -\frac{3Ta}{\phi^2}\partial_Z^2 + 4Q^2\partial_y^2 + 2QR - 3R\Lambda\nabla_h^2 + \nabla^2\Big(9R\Lambda + 24Q\Lambda\partial_y^2\Big) + \nabla^4 Q\Lambda\nabla^4 - 60\nabla^6\Lambda^2,\\
F_5 =& QR\nabla_h^2 + \nabla^2 Q(R - 4\nabla^2\partial_y^2) - 8Q\Lambda\nabla^6,\\
F_6 =& 3R\Lambda\nabla_h^2 + \nabla^4(3R\Lambda - \frac{3Ta}{\phi^2}\partial_Z^2) + \nabla^4(3R\Lambda + 12Q\Lambda\partial_y^2) - 15\Lambda^2\nabla^8 - QR\partial_y^2 Q^2\partial_y^4,\\
F_7 =& -QR\nabla_h^2 - QR\nabla^2 + 8Q\Lambda\nabla^6\\
F_8 =& -2Q\partial_y^2 - \frac{3Ta}{\phi^2}\partial_T + R\Lambda\nabla^4 - 6\Lambda^2\nabla^8,\\
F_9 =& \frac{QR\phi Pr_2}{MPr_1}\nabla_h^2\partial_y^2 + Q^2\partial_y^6 + \Big(\frac{Ta}{\phi^2} + \frac{2TaPr_2}{M\phi Pr_1}\Big)\partial_Z^2 + \frac{2R\Lambda\phi Pr_2}{Pr_1}\nabla^4 - \Big(-2Q\Lambda +\\
& \frac{2Q}{M\phi Pr_1} + \frac{2Q\Lambda\phi Pr_2}{MPr_1}\Big)\partial_y^2\nabla^6 - \frac{4\Lambda\phi Pr_2}{DaMPr_1}\nabla^8 + (\Lambda^2 + \frac{2\Lambda}{M\phi Pr_1} + \frac{2\Lambda^2\phi Pr_2}{MPr_1})\nabla^{10},\\
F_{10} =& \partial_X^2\nabla^2 F_8 + \partial_T F_9 - \partial_Y^2(2q - Y\partial_Y)^2\Big[QR + 2q^2\partial_y^2 + 4Q^2\nabla^2 - 12Q\Lambda\nabla^4\Big].
\end{aligned}
\tag{3.50}
$$

Substituting the zeroth order solution w_0 in equation $\mathcal{L}_0 w_0 = 0$, we get

$$
R_s = \frac{\delta_s^2}{q_s^2}\left[\left(\Lambda\delta_s^2 + \frac{1}{Da}\right)\delta_s^2 + Qm^2\right] + \frac{1}{q_s^2}\frac{Ta\pi^2\delta_s^4}{\phi^2}\frac{1}{\left[\left(\Lambda\delta_s^2 + \frac{1}{Da}\right)\delta_s^2 + Qm^2\right]}, \tag{3.51}
$$

from the equations (3.46) to (3.48), $\mathcal{N}_0 = 0$, $\mathcal{L}_1 w_0 = 0$ and hence $w_1 = 0$. The second order approximations which are based on the eigen vector of the problem are

$$
\begin{aligned}
u_1 =& 0, w_1 = 0,\\
v_1 =& K_1\left[A^2 e^{2i(lx+my)} - c\cdot c\cdot\right],\\
\theta_1 =& -\frac{1}{2\pi M^2\delta^2}|A|^2 sin2\pi z,
\end{aligned}
$$

$$
\begin{aligned}
H_{x_1} =& \frac{m}{2M^2\delta^2 l}|A|^2 cos 2\pi z,\\
H_{y_1} =& \frac{mK_1}{2Mq^2}\left[A^2 e^{2i(lx+my)}\cos\pi z + c\cdot c\cdot\right],\\
H_{z_1} =& 0,
\end{aligned} \tag{3.52}
$$

where $K_1 = \frac{-4i\pi^2 q^2\sqrt{Ta}\delta^2(\frac{1}{M\phi^2}+\frac{Qm^2 Pr_2}{\delta^4})}{Pr_1 M\phi l(4\Lambda Mq^4+4QM^2)(\Lambda Mq^4+QM^2)}$. Taking $w_1 = 0$ in equation (3.48), $\mathcal{N}_1 - \mathcal{L}_2 w_0$ is orthogonal to w_0. Equating the coefficient of $\sin\pi z$ in $\mathcal{N}_1 - \mathcal{L}_2 w_0$ is zero. We obtain two dimensional time dependent nonlinear Landau-Ginzburg equation

$$
\lambda_0\frac{\partial A}{\partial T} - \lambda_1\left(\frac{\partial}{\partial X} - \frac{i}{2q}\frac{\partial^2}{\partial Y^2}\right)^2 A - \lambda_2 A + \lambda_3|A|^2 A = 0, \tag{3.53}
$$

where

$$
\begin{aligned}
\lambda_0 =& \frac{\phi Pr_2 QR}{Pr_1 M}q^2 m^2 - Q^2 m^4\delta^2 + \Big(-\frac{Ta}{\phi^2}\pi^2 + \frac{2R\Lambda\phi Pr_2}{MPr_1}q^2 - \frac{2Ta\pi^2 Pr_2}{M\phi Pr_1}\Big)\delta^4 -\\
& 2Q\Lambda m^2\Big(1+\frac{\phi Pr_2}{MPr_1}\Big)\delta^6 - \Lambda^2\delta^{10},\\
\lambda_1 =& QRm^2 - Q^2m^4 + \Big(3R\Lambda q^2 - \frac{3Ta\pi^2}{\phi^2}\Big)\delta^2 + \Big(3R\Lambda - 15\Lambda^2 - 12\Lambda Qm^2\Big)\delta^4,\\
\lambda_2 =& \left(Qm^2 + \Lambda\delta^4\right)q^2,\\
\lambda_3 =& \left[\frac{Qm^2 Pr_2}{4Pr_1}\left(\frac{\delta^2}{\pi^2} - \frac{l^2}{M^2}\right) + \frac{Rq^2}{2M^2}\right]\left(Qm^2+\Lambda\delta^4\right) -\\
& \frac{Ta^{1/2}\delta^4}{\phi}\left[\frac{2\pi^2\delta^2 S_3}{M\phi^2 Pr_1} + M\delta^2 Q\left(lS_2 + \frac{m\pi S_1}{8\pi^2 M^2\delta^2}\right) + Q\frac{S_1 lmPr_2}{4M\pi Pr_1}\right],
\end{aligned} \tag{3.54}
$$

where $S_1 = \frac{2\pi^2 Ta^{1/2} mPr_2}{(Qm^2+\Lambda\delta^4)Pr_1}$, $S_2 = \frac{\pi m^2 Ta^{1/2}}{4M^2\delta^2 l(Qm^2+\Lambda\delta^4)}$ and $S_3 = \frac{4\pi^2 q^2 Ta^{1/2}\delta^2}{\phi Pr_1 l[4Qm^2+4\Lambda Mq^4]}$. From figure 3.7, if $\lambda_3 > 0$ then the pitchfork bifurcation is supercritical, if $\lambda_3 < 0$ then it is subcritical and tricritical bifurcation at $\lambda_3 = 0$. Dropping the t and y dependent terms from equation (3.53), we get

$$
\frac{\mathrm{d}^2 A}{\mathrm{d}X^2} + \frac{\lambda_2}{\lambda_1}A - \frac{\lambda_3}{\lambda_1}|A|^2 A = 0, \tag{3.55}
$$

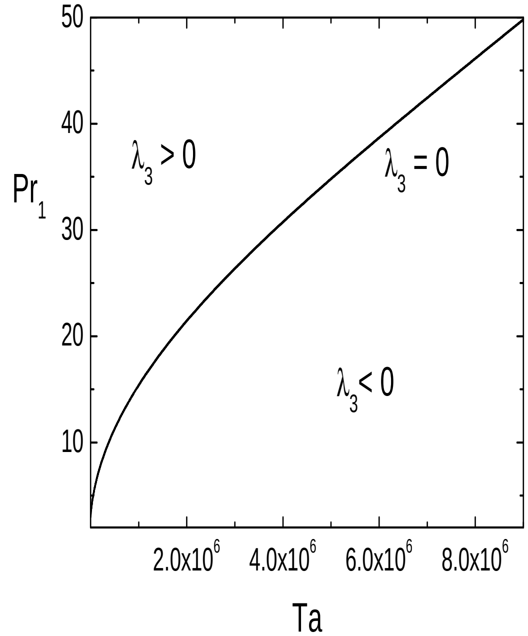

Figure 3.7: The curve λ_3 is plotted for $Da = 1500$, $\Lambda = 1.5$, $M = 0.85$, $\phi = 0.85$, $Q = 500$, $Pr_2 = 50$, $R = 68000$ and $Ta = 8 \times 10^6$. The pitchfork bifurcation is super-critical if $\lambda_3 > 0$, sub-critical if $\lambda_3 < 0$.

the solution is

$$A(X) = A_0 \tanh\left(\frac{X}{\Lambda_1}\right). \tag{3.56}$$

where

$$A_0 = \left(\frac{\lambda_2}{\lambda_3}\right)^{\frac{1}{2}} \quad \text{and} \quad \Lambda_1 = 2\left(\frac{\lambda_1}{\lambda_2}\right)^{\frac{1}{2}}. \tag{3.57}$$

Secondary Instabilities and Nusselt Number

Newell and Whitehead [77] derived envelope equations In order to study the properties of a structure with a given phase winding number δq, we write equation (3.53) in fast variables x, y, t and $A(X, Y, T) = \frac{A(x,y,t)}{\epsilon}$, as

$$\begin{aligned}&\frac{\partial A_1}{\partial t} - \Big(\epsilon^2\frac{\lambda_2}{\lambda_0} - \frac{\lambda_1}{\lambda_0}\delta q^2\Big)A_1 + 2i\delta q\frac{\lambda_1}{\lambda_0}\Big(\frac{\partial}{\partial x} - \frac{i}{2q_{sc}}\frac{\partial^2}{\partial y^2}\Big)A_1 + \\ &\frac{\lambda_1}{\lambda_0}\Big(\frac{\partial}{\partial x} - \frac{i}{2q_{sc}}\frac{\partial^2}{\partial y^2}\Big)^2 A_1 - \frac{\lambda_3}{\lambda_0}|A_1|^2A_1 = 0,\end{aligned} \tag{3.58}$$

$$A_1 = \left[\frac{\epsilon^2\lambda_2 - \lambda_1\delta q^2}{\lambda_3}\right]^{\frac{1}{2}}. \tag{3.59}$$

Let $\tilde{u} + i\tilde{v}$ be an infinitesimal perturbation of steady state solution A_1 given by equation (3.59). Substitute

$$A_1 = \tilde{u} + i\tilde{v} + [\left(\epsilon^2\lambda_2 - \lambda_1\delta q^2\right)\lambda_3^{-1}]^{\frac{1}{2}}, \tag{3.60}$$

into equation (3.58) and equate the real and imaginary parts, we obtain

$$\frac{\partial\tilde{u}}{\partial t} = -2\left(\epsilon^2\frac{\lambda_2}{\lambda_0} - \frac{\lambda_1}{\lambda_0}\delta q^2\right)\tilde{u} + \frac{\lambda_1}{\lambda_0}\tilde{u} - \frac{\lambda_1}{\lambda_2}\partial_2\frac{\partial\tilde{v}}{\partial x}, \tag{3.61a}$$

$$\frac{\partial\tilde{v}}{\partial t} = \frac{\lambda_1}{\lambda_0}\partial_2\frac{\partial\tilde{u}}{\partial x} + \frac{\lambda_1}{\lambda_0}\partial_1\tilde{v}. \tag{3.61b}$$

where $\partial_1 = \frac{\partial^2}{\partial x^2} + \frac{\delta q}{q_{sc}}\frac{\partial^2}{\partial y^2} - \frac{1}{4q_{sc}^2}\frac{\partial^4}{\partial y^4}$ and $\partial_2 = 2\delta q - \frac{1}{q_{sc}}\frac{\partial^2}{\partial y^2}$ We analyse equations (4.63a) and (4.63b) by using normal modes form

$$\tilde{u} = U\cos(q_x x)\cos(q_y y)e^{St}, \qquad \tilde{v} = V\sin(q_x x)\cos(q_y y)e^{St}. \tag{3.62}$$

Substituting equation (3.62) in equations (3.61a) and (3.61b) weget,

$$\Big[2(\epsilon^2\lambda_2 - \lambda_1\delta k^2) + \lambda_0 S + \chi_1\Big]U + \lambda_1\chi_2 q_x V = 0 \tag{3.63a}$$

$$\lambda_1 q_x\chi_2 U + (\chi_1 + \lambda_0 S)V = 0. \tag{3.63b}$$

Here $\chi_1 = \lambda_1\Big(q_x^2 + \frac{q_y^2\delta k}{q_{sc}} + \frac{q_y^4}{4q_{sc}^2}\Big)$ and $\chi_2 = (2\delta k + \frac{q_y^2}{q_{sc}})$. On solving equations (3.63a) and (3.63b), we get

$$S^2 + \frac{2S}{\lambda_0}\Big[2\Big(\epsilon^2\lambda_2 - \lambda_1(\delta k)^2\Big) + \chi_1\Big] + \Big[2\Big(\frac{\epsilon^2\lambda_2}{\lambda_0^2} - \frac{\lambda_1\delta k^2}{\lambda_0^2}\Big) + \chi_1\Big]\psi_1 - q_x^2\chi_2\frac{\lambda_1}{\lambda_0^2} = 0, \tag{3.64}$$

whose real roots are $(S\pm)$,

$$(S\pm) = -\frac{1}{\lambda_0^2}\left\{\left[2\lambda_0(\epsilon^2\lambda_2 - \lambda_1\delta kq^2) + \lambda_0\chi_1\right] \pm \left[2\lambda_0(\epsilon^2\lambda_2 - \lambda_1\delta q^2)^2 + \lambda_1^2 q_x^2\chi_2^2\right]^{\frac{1}{2}}\right\}. \tag{3.65}$$

The equivalent mode is stable if $S(-)$ is negative and unstable if $S(+)$ is positive. Symmetry significance helps to confine the field of $S(+)$ to $q_x \geq 0, q_y \geq 0$.

Eckhaus Instability

Putting $q_y = 0$ into equation (3.65), we get

$$S^2 + \frac{2S}{\lambda_0}\left[2(\epsilon^2\lambda_2 - \lambda_1\delta q^2) + \lambda_1 q_x^2\right] + \frac{\lambda_1 q_x^2}{\lambda_0^2}\left[2(\epsilon^2\lambda_2 - 3\lambda_1\delta q^2) + q_x^2\right] = 0, \tag{3.66}$$

The roots are real numbers and their sum is negative number and the product of roots is positive number, the pattern is stable and if the product of roots is negative number then the pattern becomes unstable.
Eckhaus instability defines $q_x^2 \leq 2\Big(3\lambda_1\delta q^2 - \epsilon^2\lambda_2\Big)$ for $|\delta q| \geq \sqrt{\frac{\epsilon^2\lambda_2}{3\lambda_1}}$ and unstable wave tends to zero when $|\delta q| \to \sqrt{\frac{\epsilon^2\lambda_2}{3\lambda_1}}$.

Zigzag Instability

putting $q_x = 0$ into equation (3.66), we get

$$\lambda_0^2 S^2 + 2S(2\lambda_0\chi_{11} + \lambda_0\chi_{12}) + (2\chi_{11} + \chi_{12})\chi_{12} = 0, \tag{3.67}$$

where $\chi_{11} = \epsilon^2\lambda_2 - \lambda_1\delta q^2$ and $\chi_{12} = \lambda_1\left(\frac{q_y^2\delta q}{q_s c} + \frac{q_y^4}{4q_{sc}^2}\right)$, the two eigen conditions are unrelated and amplified when $S(-) = -2(\epsilon^2\lambda_2 - \lambda_1\delta q^2) - \frac{\lambda_1}{q_{sc}}q_y^2\delta q - \frac{\lambda_1}{4q_{sc}^2}q_y^2 < 0$ and $S(+) = -\lambda_1 q_y^2\Big(\delta q + \frac{q_y^2}{4q_{sc}}\Big) > 0$. These conditions define the domain of Zigzag Instability when $\delta q_s < 0$. In figure 3.8, we have shown the Eckhaus and Zigzag instabilities known as secondary instabilities regions at fixed parameters. When

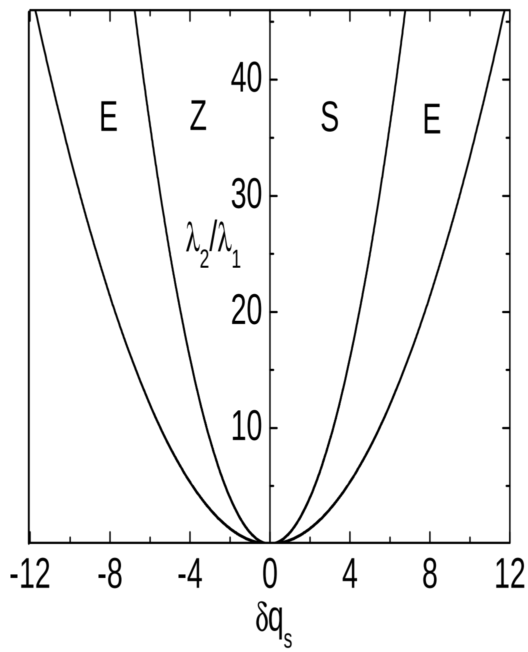

Figure 3.8: Region of secondary instabilities and stable region for $Da = 1500$, $\Lambda = 1.5$, $M = 0.9$, $\phi = 0.85$, $Pr_1 = 1.5$, $Pr_2 = 1.55$, $R = 41000$, $Q = 500$, $Ta = 1320$.

increase the magnetic field the stability regions also increases.

Nusselt Number

Heat transport by the convection, the Nusselt number studied in section 2.4.1. λ_1 and λ_2 are always positive. The Nusselt number Nu can calculated in terms of amplitude (A) as

$$Nu = 1 + \frac{\epsilon^2}{\delta^2}|A_m|^2. \tag{3.68}$$

Nusselt number grows if $\frac{R}{R_{sc}} > 1$ and decays if $\frac{R}{R_{sc}} \leq 1$ convection for $Nu > 1$. Then there is convection if $Nu > 1$, conduction if $Nu \leq 1$. Amplitude is valid for $\lambda_3 > 0$ and it is possible when $R > R_{sc}$, Thus we obtain convection for $Nu > 1$ and conduction for $Nu \leq 1$ see in Figure 3.9.

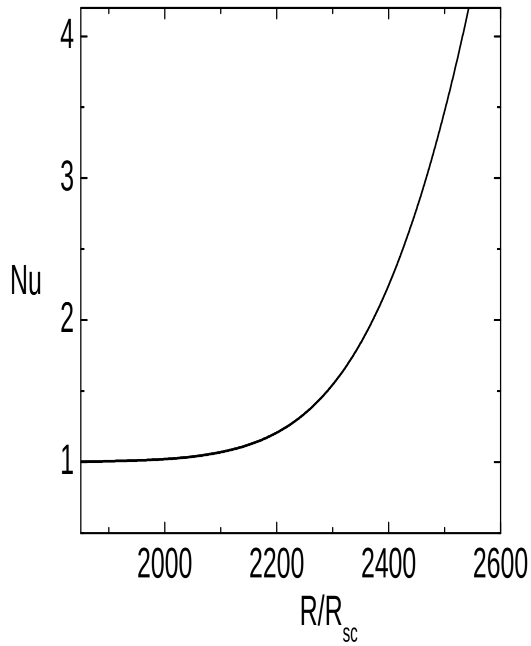

Figure 3.9: solid lines represents Stationary convection R_s and doted lines represents Oscillatory convection R_o for $Da = 1500$, $\Lambda = 1.5$, $M = 0.9$, $\phi = 0.85$, $Pr_1 = 1.5$, $Pr_2 = 1.55$, $Q = 1000$, $Ta = 10^5$, $R = 41000$.

3.4.2 Amplitude equations at the onset of oscillatory convection

We have assumed that the solution of the equation $\mathcal{L}w = 0$, which satisfies the linear system of the form

$$w_0 = \left[A_{1L}e^{i(lx+my+\omega t)} + A_{1R}e^{i(lx+my-\omega t)} + c \cdot c.\right] \sin \pi z, \tag{3.69}$$

where $A_{1L} = A_{1L}(X, \tau, T)$ and $A_{1R} = A_{1R}(X, \tau, T)$ are the amplitudes of left travelling and right travelling waves of the roll and these amplitudes depend on the following slow variables

$$X = \epsilon x, \quad Y = \epsilon^{\frac{1}{2}} y, \quad \tau = \epsilon t, \quad T = \epsilon^2 t, \tag{3.70}$$

we express the differential operators in the form of

$$\frac{\partial}{\partial x} \to \frac{\partial}{\partial x} + \epsilon \frac{\partial}{\partial X}, \quad \frac{\partial}{\partial y} \to \frac{\partial}{\partial y} + \epsilon^{\frac{1}{2}} \frac{\partial}{\partial Y}, \quad \frac{\partial}{\partial t} \to \frac{\partial}{\partial t} + \epsilon \frac{\partial}{\partial \tau} + \epsilon^2 \frac{\partial}{\partial T}. \tag{3.71}$$

We consider the solution of basic equations in the form of

$$f = \epsilon f_0 + \epsilon^2 f_1 + \epsilon^3 f_2 + \cdots, \tag{3.72}$$

where

$$\epsilon^2 = \frac{R_o - R_{oc}}{R_{oc}} \ll 1, \tag{3.73}$$

here $f = f(u, v, w, \theta, H_x, H_y, H_z)$ and the first approximation or zeroth order solutions is given by eigenvector of the linearized problem are

$$\begin{aligned}
u_0 =& \frac{i\pi}{l} \left[A_{1L} e^{i(lx+my+\omega t)} + A_{1R} e^{i(lx+my-\omega t)} - c \cdot c.\right] \cos \pi z, \\
v_0 =& \frac{iTa^{1/2}\pi}{M\phi l} \left[A_{1L} e_3 e^{i(lx+my+\omega t)} + A_{1R} e_3^* e^{i(lx+my-\omega t)} - c \cdot c.\right] \cos \pi z, \\
w_0 =& \left[A_{1L} e^{i(lx+my+\omega t)} + A_{1R} e^{i(lx+my-\omega t)} + c \cdot c.\right] \sin \pi z, \\
\theta_0 =& \frac{1}{M} \left[\frac{1}{e_1} A_{1L} e^{i(lx+my+\omega t)} + \frac{1}{e_1^*} A_{1R} e^{i(lx+my-\omega t)} + c \cdot c.\right] \sin \pi z, \\
H_{x_0} =& \frac{-m\pi}{l} \left[\frac{1}{e_2} A_{1L} e^{i(lx+my+\omega t)} + \frac{1}{e_2^*} A_{1R} e^{i(lx+my-\omega t)} + c \cdot c.\right] \cos \pi z, \\
H_{y_0} =& \frac{mTa^{1/2}\pi}{lM\phi} \left[\frac{K_1}{e_2} A_{1L} e^{i(lx+my+\omega t)} + \frac{K_2}{e_2^*} A_{1R} e^{i(lx+my-\omega t)} + c \cdot c.\right] \cos \pi z, \\
H_{z_0} =& im \left[\frac{1}{e_2} A_{1L} e^{i(lx+my+\omega t)} + \frac{1}{e_2^*} A_{1R} e^{i(lx+my-\omega t)} - c \cdot c.\right] \sin \pi z.
\end{aligned} \tag{3.74}$$

where $\delta^2 = (\pi^2 + q_{oc}^2)$, $e_1 = (\delta^2 + i\omega_)$, $e_2 = (M\delta^2 + i\omega_\phi \frac{Pr_2}{Pr_1})$ and $e_3 = \frac{e_2}{(\frac{iw}{M^2\phi Pr_1} + \frac{\Lambda\delta^2}{M})e_2 + Qm^2}$, here e_1^*, e_2^*, e_3^* are complex conjugate of e_1, e_2 and e_3. We obtain the critical Rayleigh number from the linear equation $\mathcal{L}_0 w_0 = 0$. At $O(\epsilon^2)$, $\mathcal{N}_0 = 0$ and $\mathcal{L}_1 w_0 = 0$ gives $\frac{\partial A_{1L}}{\partial \tau} - \nu_g \frac{\partial A_{1L}}{\partial X} = 0$ and $\frac{\partial A_{1L}}{\partial \tau} + \nu_g \frac{\partial A_{1L}}{\partial X} = 0$. Where $\nu_g = (\frac{\partial \omega}{\partial q})_{q=q_{sc}}$ is the group velocity and is real. Hence we obtain $u_1 = 0$. Similarly, the remaining first order solutions are

$$
\begin{aligned}
u_1 =& 0,\\
v_1 =& \frac{-i}{2le_8}\left[A_{1L}^2 e_5 e^{2i(lx+my+t\omega)} + A_{1R}^2 e_5^* e^{2i(lx+my-t\omega)} - c\cdot c\right] -\\
& \frac{i}{2l[(\frac{\Lambda q^2}{M}+\frac{1}{MDa})Mq^2+4Qm^2]}\left[A_{1L}A_{1R}e^{2i(lx+my)} - c\cdot c\right],\\
w_1 =& 0,\\
\theta_1 =& \frac{\pi}{M^2(\omega^2+\delta_{oc}^4)}\left[A_{1L}A_{1R}^*\frac{e_1^*}{e_7}e^{2it\omega} + \delta_{oc}^2(|A_{1L}|^2+|A_{1R}|^2) + c\cdot c\right]\sin 2\pi z,\\
H_{x_1} =& [(\frac{\Lambda q^2}{M}+\frac{1}{MDa})Mq^2+4Qm^2]\left[A_{1L}A_{1R}e^{2i(lx+my)} + c\cdot c\right]\cos 2\pi z +\\
& \frac{2m\pi^2 Pr_2}{l|e_2|^2 Pr_1}\left[A_{1L}A_{1R}^*\frac{e_2^*}{e_4^*}e^{2it\omega} + \frac{\delta_{oc}^2}{4\pi^2}(|A_{1L}|^2+|A_{1R}|^2) + c\cdot c\right],\\
H_{y_1} =& \frac{m}{4Mlq^2 e_6}\left[A_{1L}A_{1R}e^{2i(lx+my)} + c\cdot c\right] + \frac{2\pi\delta_{oc}^2 mPr_2}{|e_2|^2 lPr_1}(|A_{1L}|^2+|A_{1R}|^2)\sin 2\pi z +\\
& \frac{m}{2le_6e_8}\left[|A_{1L}|^2 e_5 e^{2i(lx+my+t\omega)} + |A_{1R}|^2 e_5^* z_1 e^{2i(lx+my-t\omega)} + c\cdot c\right] +\\
& \frac{4\pi^3 mPr_2}{l|e_2|^2 e_4 Pr_1}\left[A_{1L}A_{1R}^* e_2^* e^{2it\omega} - c\cdot c\right],\\
H_{z_1} =& 0,
\end{aligned}
\tag{3.75}
$$

where $e_4 = 2M\pi^2 + \phi\frac{Pr_2}{Pr_1}i\omega$, $e_5 = \frac{\Lambda}{M}\delta^2 + \frac{1}{MDa} + \frac{1}{M^2\phi Pr_1}i\omega$, $e_6 = 2Mq^2 + \phi\frac{Pr_2}{Pr_1}i\omega$, $e_7 = 2\pi^2 + i\omega$ and $e_8 = \frac{\Lambda}{4M}\delta^2 + \frac{1}{MDa} + \frac{2}{M^2\phi Pr_1}i\omega$, their corresponding complex conjugates are e_4^*, e_5^*, e_6^*, e_7^* and e_8^* respectively. Equating the coefficients of $\sin\pi z$ in $\mathcal{N}_1 - \mathcal{L}_2 w_0$ equal to zero. We get,

$$
\begin{aligned}
\Lambda_0\frac{\partial A_{1L}}{\partial T} + \Lambda_1\left(\frac{\partial}{\partial\tau} - v_g\frac{\partial}{\partial X}\right)A_{2L} - \Lambda_2\frac{\partial^2 A_{1L}}{\partial X^2} - \Lambda_3 A_{1L}&\\
+\Lambda_4|A_{1L}|^2A_{1L} + \Lambda_5|A_{1R}|^2A_{1L} = 0,&
\end{aligned}
\tag{3.76}
$$

$$
\begin{aligned}
\Lambda_0\frac{\partial A_{1R}}{\partial T} + \Lambda_1\left(\frac{\partial}{\partial\tau} - v_g\frac{\partial}{\partial X}\right)A_{2R} - \Lambda_2\frac{\partial^2 A_{1R}}{\partial X^2} - \Lambda_3 A_{1R}&\\
+\Lambda_4|A_{1R}|^2A_{1R} + \Lambda_5|A_{1L}|^2A_{1R} = 0.&
\end{aligned}
\tag{3.77}
$$

Where

$$
\begin{aligned}
\Lambda_0 =& -\frac{Ta\pi^2 e_2}{M^2\phi^2} - \frac{Rq^2 e_2^2}{M^3\phi Pr_1} + (Ta\pi^2 Pr_2 + Qm^2\delta_{oc}^2)\frac{2e_1e_2}{M^2\phi Pr_1} + Q^2m^4\delta_{oc}^2 + \\
& \frac{2\phi Q\delta_{oc}^2 m^2 Pr_2}{Pr_1}e_1e_5 + 2(Qm^2\delta_{oc}^2 - \frac{\phi\delta_{oc}^2 Pr_2}{MPr_1})e_2e_5 - \frac{\phi RQq^2m^2Pr_2}{MPr_1} + \\
& 2\delta_{oc}^2(\frac{e_1}{M^2\phi Pr_1} - \frac{\phi Pr_2 e_5}{Pr_1})e_1e_2e_5, \\
\Lambda_1 =& -\frac{\delta_{oc}^2 e_1 e_2^2}{M^4\phi^2 Pr_1^2} + \frac{2\delta_{oc}^2 e_5}{M^2\phi Pr_1}(e_4 - e_2^2) - \frac{2Ta\pi^2 e_2 Pr_2}{M^2\phi Pr_1} + \frac{2e_1\delta_{oc}^2 Pr_2}{M^2 Pr_1^2}(Qe_4 - 2e_2e_5) - \\
& \frac{Ta\phi^2 Pr_2}{M^2Pr_1^2} - \frac{2\phi\delta_{oc}^2 Pr_2}{Pr_1}(e_2e_5 - e_4)e_5 + \frac{\phi^2 Pr_2^2}{Pr_1^2}(Rq^2 - e_1e_5\delta_{oc}^2) + \frac{2Rq^2e_2Pr_2}{M^3Pr_1^2}, \\
\Lambda_2 =& -2Rq^2e_2e_5 + 2\delta_{oc}^2 e_1e_2e_5(Me_5 + \frac{\Lambda e_2}{M}) - \frac{R\Lambda q^2}{M^2}e_5^2 + (\delta_{oc}^2 + e_1)e_2^2e_5^2 + \\
& \frac{2Tae_1e_2\pi^2}{M\phi^2} + \frac{Ta\pi^2 e_5^2}{M^2\phi^2} + RQq^2e_4 - 2MQ\delta_{oc}^2 e_1e_4e_5 + Q(\frac{R}{M} - 2\delta_{oc}^2 e_5)e_2e_4 - \\
& 2Q(e_5 + \lambda\delta_{oc}^2)e_1e_2e_4 + Q^2(\delta_{oc}^2 + e_1)e_4^2, \\
\Lambda_3 =& -\frac{Qm^2q^2}{M}e_2 - \frac{q^2}{M}e_5e_2^2, \\
\Lambda_4 =& \frac{Qlm\delta_{oc}^2 t_2 Pr_2}{4Pr_1}(e_2e_5 + Qm^2)(4 + \frac{m^2}{\pi^2}) - \frac{\sqrt{Ta}Qm^2\pi^2 e_1e_2e_7Pr_2(1-i)}{2M\phi e_9 Pr_1} \\
& (\frac{1}{e_6} + \frac{e_7}{e_2^*}) + \frac{\sqrt{Ta}e_1e_2^2e_7\pi}{Me_9\phi Pr_1}(\frac{QPr_2m^2}{le_6e_2^*}i - \frac{\pi}{M^2\phi^2}) - \frac{TaQ\delta_{oc}^2 lme_1e_2e_7t_2Pr_2}{4M^2\phi^2Pr_1}, \\
\Lambda_5 =& (e_1e_5 + Qm^2)\frac{Qlm\delta_{oc}^2 Pr_2}{Pr_1}\left[\left(3 - \frac{l^2}{m^2}\right)\frac{t_2}{e_2} + e_1\left(e_{10} + \frac{t_2\delta_{oc}^2}{2\pi^2} + \frac{t_2e_2^*}{e_4^*}\right)\right] + \\
& \frac{\sqrt{Ta}e_1e_2m^2\pi^2QPr_2}{M\phi Pr_1}\left(\frac{1}{4Mq^2e_6} + \frac{1}{2e_2t_1}\right) + \frac{2\sqrt{Ta}e_1e_2^2\pi}{6M\phi Pr_1}\left(\frac{\pi}{t_1} - \frac{Qm^2Pr_2}{4lq^2e_6Pr_1}i\right) + \\
& \frac{Tae_1e_2^2Q\phi^2Pr_2}{2M^2\phi^2Pr_1}\left[l(m + \frac{1}{e_2})e_7^*e_{10} - m\left(\frac{\delta^2e_7l}{2} - \frac{e_2^8e_7^*}{e_4^*}\right)\right], \qquad (3.78)
\end{aligned}
$$

where $t_1 = (\frac{1}{MDa} + \frac{\Lambda q^2}{M})Mq^2 + 4Qm^2$, $t_2 = \frac{2m\pi^2 Pr_2}{l|e_2|^2 Pr_1}$, $e_9 = 2e_8e_6 + 4Qm^2$ and $e_{10} = \frac{-m^2\pi^2\sqrt{Ta}Pr_2^2 1\omega}{2M^2\delta_{oc}^2 l^2|e_2|^2Pr_1^2}(e_5^* - e_1)$. Where Λ_0, Λ_1, Λ_2, Λ_3, Λ_4 and Λ_5 are the complex coefficients in physical components q_{oc}, Ro, E_z, Λ, α and q_z. Here $e_1 = \delta_{oc}^2 + i\omega_{oc}$, $e_2 = \delta_{oc}^2 + \alpha q_{oc}^2 + \frac{i\omega_{oc}}{q_z}$ and $e_5 = \delta_{oc}^2 + \alpha q_{oc}^2 + Roi\omega_{oc}$.

Here $A_{2L} = \left(\frac{\partial}{\partial\tau} + \nu_g\frac{\partial}{\partial X}\right)A_{1L}$ and $A_{2R} = \left(\frac{\partial}{\partial\tau} - \nu_g\frac{\partial}{\partial X}\right)A_{1R}$. A_{1L}, A_{1R} and A_{2L}, A_{2R} are of orders ϵ and ϵ^2 respectively. From the equations $\frac{\partial A_{1L}}{\partial\tau} - \nu_g\frac{\partial A_{1L}}{\partial X} = 0$

and$\frac{\partial A_{1L}}{\partial \tau} + \nu_g \frac{\partial A_{1L}}{\partial X} = 0$ we obtain $A_{1L}(\xi', T)$ and $A_{1R}(\eta', T)$. Where $\xi' = \nu_g \tau + X$ $\eta' = \nu_g \tau - X$. Equations (3.76) and (3.77) can be written as

$$2v_g \Lambda_1 \frac{\partial A_{2L}}{\partial \eta'} = -\Lambda_0 \frac{\partial A_{1L}}{\partial T} + \Lambda_2 \frac{\partial A_{1L}}{\partial X^2} + \Lambda_3 A_{1L} - \left(\Lambda_4 |A_{1L}|^2 + \Lambda_5 |A_{1R}|^2\right) A_{1L}, \quad (3.79)$$

$$2v_g \Lambda_1 \frac{\partial A_{2R}}{\partial \eta'} = -\Lambda_0 \frac{\partial A_{1R}}{\partial T} + \Lambda_2 \frac{\partial A_{1R}}{\partial X^2} + \lambda_3 A_{1R} - \left(\Lambda_4 |A_{1R}|^2 + \Lambda_5 |A_{1L}|^2\right) A_{1R}. \quad (3.80)$$

Let $\xi' \epsilon [0, l_1]$, $\eta' \epsilon [0, l_2]$ where l_1 is the period of A_{1L} and l_2 is the period of A_{1R} . Expansion (3.72) remains asymptotic for times $t = O\left(\epsilon^{-2}\right)$ only if an appropriate solvability condition holds. This condition is derived by integrating equations (3.79) and (3.80) over η', ξ' respectively, we obtain

$$\Lambda_0 \frac{\partial A_{1L}}{\partial T} = \Lambda_2 \frac{\partial A_{1L}}{\partial X^2} + \lambda_3 A_{1L} - \left(\Lambda_4 |A_{1L}|^2 + \Lambda_5 |A_{1R}|^2\right) A_{1L}, \quad (3.81)$$

$$\Lambda_0 \frac{\partial A_{1R}}{\partial T} = \Lambda_2 \frac{\partial A_{1R}}{\partial X^2} + \lambda_3 A_{1R} - \left(\Lambda_4 |A_{1R}|^2 + \Lambda_5 |A_{1L}|^2\right) A_{1R}. \quad (3.82)$$

Equations (3.81) and (3.82) are left and right moving waves known as coupled one-dimensional LG equations.

Travelling wave and standing wave

Dropping the variable X from equations (3.81) and (3.82)

$$\frac{\mathrm{d}A_{1L}}{\mathrm{d}T} = \frac{\Lambda_3}{\Lambda_0} A_{1L} - \frac{\Lambda_4}{\Lambda_0} A_{1L} |A_{1L}|^2 - \frac{\Lambda_5}{\Lambda_0} A_{1L} |A_{1R}|^2, \quad (3.83)$$

$$\frac{\mathrm{d}A_{1R}}{\mathrm{d}T} = \frac{\Lambda_3}{\Lambda_0} A_{1R} - \frac{\Lambda_4}{\Lambda_0} A_{1R} |A_{1R}|^2 - \frac{\Lambda_5}{\Lambda_0} A_{1R} |A_{1L}|^2. \quad (3.84)$$

Put

$$\beta' = \frac{\Lambda_3}{\Lambda_0}, \quad \gamma' = -\frac{\Lambda_4}{\Lambda_0} \quad \text{and} \quad \delta' = -\frac{\Lambda_5}{\Lambda_0}.$$

Then equations (3.83) and (3.84) take the following form

$$\frac{\mathrm{d}A_{1L}}{\mathrm{d}T} = \beta' A_{1L} + \gamma' A_{1L}|A_{1L}|^2 + \delta' A_{1L}|A_{1R}|^2, \tag{3.85}$$

$$\frac{\mathrm{d}A_{1R}}{\mathrm{d}T} = \beta' A_{1R} + \gamma' A_{1R}|A_{1R}|^2 + \delta' A_{1R}|A_{1L}|^2. \tag{3.86}$$

Where

$$\begin{aligned} A_{1L} =& a_L e^{i\phi_L} & a_L =& |A_{1L}| & \phi_L =& arg(A_{1L}) \\ A_{1R} =& a_L e^{i\phi_R} & a_R =& |A_{1R}| & \phi_R =& arg(A_{1R}) \\ \beta' =& \beta_1 + i\beta_2 & \gamma' =& \gamma_1 + i\gamma_2 & \delta' =& \delta_1 + i\delta_2 \end{aligned} \tag{3.87}$$

Substituting of A_{1L},A_{1R},β', γ' and δ' in (3.85) and (3.86). we get,

$$(a_L, a_R) = \left(-\beta_1/(\gamma_1+\delta_1), -\beta_1/(\gamma_1+\delta_1)\right), \tag{3.88}$$

Substituting A_{1L}, A_{1R}, β' , γ' and δ' in (3.85) and (3.86). we get $a_L = -\beta_1/(\gamma_1+\delta_1)$ and $a_R = -\beta_1/(\gamma_1+\delta_1)$ for standing waves. $(a_L, a_R) = (a_L, 0)$ for left travelling waves and $(a_L, a_R) = (0, a_R)$ for right travelling waves. $(a_L, a_R) = (0, 0)$ for conduction state. Standing waves exist if $| A_L |^2 = | A_R |^2 = -\frac{\beta_1}{\gamma_1+\delta_1} > 0$ and supercritical if $\gamma_1 + \delta_1 < 0$. Standing waves are stable if $\beta_1 > 0, \gamma_1 < 0$ and

(i) if $\delta_1 > 0$, then $-\gamma_1 > \delta_1 > 0$,

(ii) if $\delta_1 < 0$, then $-\gamma_1 > -\delta_1 > 0$.

Travelling waves exist if $| A_L |^2 = -\frac{\beta_1}{\gamma_1} > 0$ and they are supercritical if $\gamma_1 < 0$. Travelling waves are stable if $\beta_1 > 0, \gamma_1 < 0$ and $\delta_1 < \gamma_1 < 0$. We studied onset of Hopf bifurcation of stability regions of travelling, standing wave and steady states in figure 3.10. It can be observed that, when $\frac{Pr2}{Pr1}$ increases, the standing wave stability regions decreases for fixed parameters.

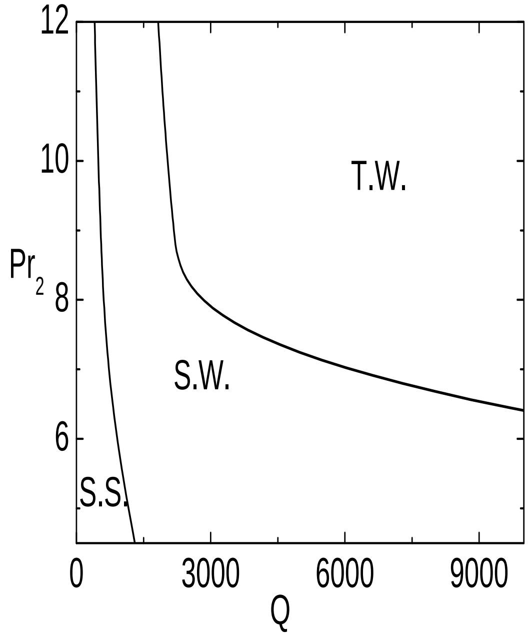

(a)

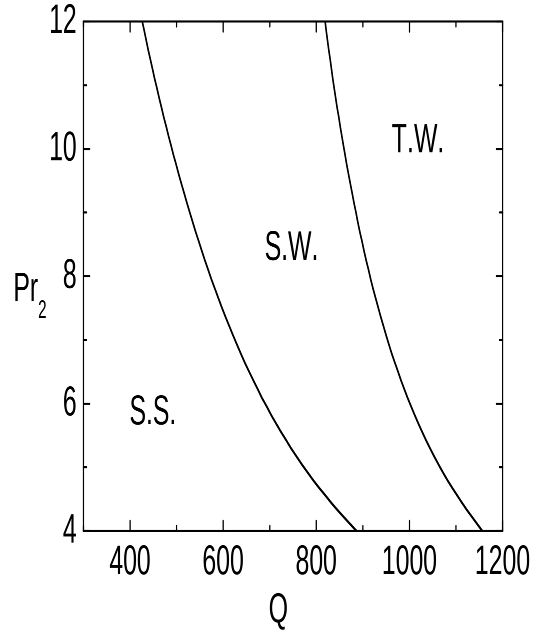

(b)

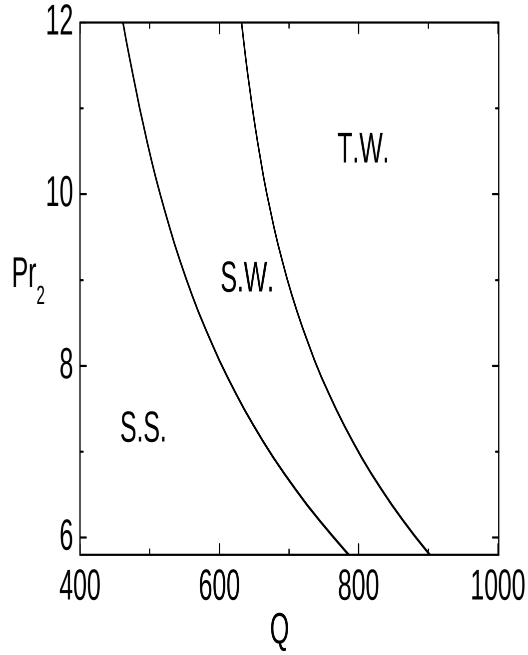

(c)

Figure 3.10: Stability regions of steady state (S.S), standing waves (S.W.) and travelling waves (T.W.) for $Da = 1500$, $\Lambda = 2$, $M = 0.9$, $\phi = 0.85$, $R = 41000$, $Ta = 10^5$, (a)$\frac{Pr_2}{Pr_1} = 6$, (b)$\frac{Pr_2}{Pr_1} = 9$, (c)$\frac{Pr_2}{Pr_1} = 12$.

3.5 Conclusions

In this chapter, linear and weakly nonlinear stabilities of horizontal magneto convection in a sparsely packed porous medium due to rotation have been discussed. Rayleigh value at the onset of stationary and oscillatory convection by assuming periodic disturbances along x-direction, y-direction and both directions was obtained. Marginal stability curves between Rayleigh value and wave number was discussed graphically. The existence of Takens-Bogdanov bifurcation and codimension of two bifurcation points on neutral curves was shown in Figures 3.3 - 3.6. The thermal and magnetic Prandtl numbers do not have an effect on convective stationary Rayleigh value. By deriving two dimensional LG equation at the onset of stationary mode, we have studied heat transport from Nusselt number and the occurrence of long wave length instabilities. Heat transport by convection through Nusselt number was discussed. Nusselt number grows exponentially if $\frac{R}{R_{sc}} > 1$ and decays if $\frac{R}{R_{sc}} \leq 1$ for $Nu > 1$. Nusselt number grows exponentially at unit value. From Figure 3.10 it can be observed that the region of existing standing waves starts decreasing by increasing the ratio of magneto and thermal prandtl number.

Chapter 4

Nonlinear Thermohaline Convection in a Sparsely Packed Porous Medium with the Effect of Horizontal Magnetic Field

4.1 Introduction

Thermohaline convection arises due to the gradient in the molecular diffusivities of salt and temperature and the density gradients is caused by temperature and solute concentration. Thermohaline convection affects the large-scale dynamics of ocean circulation and it begins when the salt gradient is high compared with the thermal gradient. Rudraiah et al. [100], Bhadauria [20], Malashetty et al. [64, 65] and Kumar [60] resesarchers studied thermohaline convection by Darcy flow model which is related to densely packed porous media. This process is mainly used in oceanography, limnology and ocean mixing. A broad study of this type of convection about porous medium was done by Nield and Bejan [80]. Malashetty [64] and Benerji Babu [7] studied thermohaline convection due to sparsely packed porous medium as well as studied linear and nonlinear stability analysis.

The onset of convection in electrically conducting fluid in the presence of magnetic field was studied by Thompson [125], Chandrasekhar [35] and Drazin [42]. The presence of vertical magnetic field leads to the boundary of monotonous instability and increases the stability of the conductive state. The presence of a horizontal magnetic field breaks the symmetry and convection in the form of rolls. In this chapter, we studied instabilities and bifurcation of the thermohaline convection due to horizontal magnetic field in porous medium. Tagare [119, 120] and Benerji [7], derived amplitude equations to study heat transport, instabilities and traveling and standing wave regions. Benerji [10] derived amplitude equations for thermohaline magneto convection in a sparsely packed porous medium.

In this chapter, we examine thermohaline horizontal magneto convection in a sparsely packed porous medium. In section 4.2, the basic dimensionless equations are derived using Boussinesq approximation. In section 4.3, we studied linear stability analysis and identified bifurcation points in neutral curves. In section 4.4, using multiple scale analysis derived two dimensional nonlinear LG equation in complex amplitude with real coefficients. We studied Nusselt number and secondary insta-

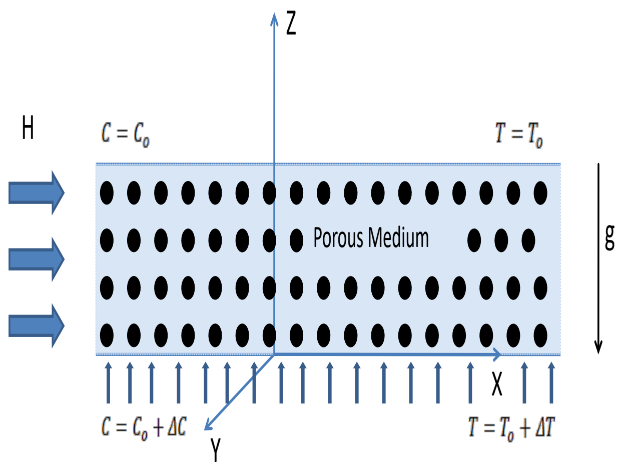

Figure 4.1: Physical Configuration

bilities. In section 4.5, we derived coupled LG equations with complex coefficients and studied the stability regions of the steady state, standing waves and travelling waves.

4.2 Basic Equations

We consider an electrically and thermally conducting infinitely extended layer of a sparsely packed isotropic porous medium of depth $'d'$ with horizontal magnetic field H_o. This layer is heated from below saturated with a solute solution of a specific concentration gradient. The temperature and salinity differences across the stress-free boundaries are denoted by $\Delta T'$ and $\Delta S'$ and the flow in sparsely packed porous medium governed by DLB model, the basic equations for which are

$$\nabla'.\overline{V}' = 0, \quad \text{and} \quad \nabla'.\overline{H}' = 0, \tag{4.1}$$

$$\frac{\rho_0'}{\phi}\left[\frac{\partial \overline{V}'}{\partial t'} + \frac{1}{\phi}(\overline{V}'.\nabla')\overline{V}'\right] - \frac{\mu_m}{4\pi}\left[\overline{H}_0'\frac{\partial \overline{H}'}{\partial y'} + (\overline{H}'.\nabla')\overline{H}'\right] =$$
$$-\nabla'\left(P' + \frac{\mu_m}{8\pi}|\overline{H}'|^2 + \frac{\mu_m}{4\pi^2}\overline{H}_0'\overline{H}_y'\right) + \rho'\overline{g} - \frac{\mu}{k}\overline{V}' + \mu_e\nabla'^2\overline{V}', \tag{4.2}$$

$$M\frac{\partial T'}{\partial t'} + (\overline{V}'.\nabla')T' = k_T\nabla'^2 T', \tag{4.3}$$

$$\phi\frac{\partial S'}{\partial t'} + (\overline{V}'.\nabla')S' = k_S\nabla'^2 S', \tag{4.4}$$

$$\phi\frac{\partial \overline{H}'}{\partial t'} - \nabla' \times (\overline{V}' \times \overline{H}'_0\hat{e_y}) = \nabla' \times (\overline{V}' \times \overline{H}') + \eta\nabla'^2\overline{H}', \tag{4.5}$$

fluid density ρ' is defined as

$$\rho' = \rho'_0\left[1 - \alpha(T' - T'_0) + \beta(S' - S'_0)\right], \tag{4.6}$$

where $\alpha = -\rho_0'^{-1}\frac{\partial\rho'}{\partial T'}$, $\beta = -\rho_0'^{-1}\frac{\partial\rho'}{\partial S'}$. Using the transformations, $x = \frac{x'}{d}$, $y = \frac{y'}{d}$, $z = \frac{z'}{d}$, $t = \frac{t'}{(Md^2/k)}$, $u = \frac{u'}{(k/Md)}$, $v = \frac{v'}{(k/Md)}$, $w = \frac{w'}{(k/Md)}$, $\theta = \frac{\theta'}{\triangle T'}$, $c = \frac{c'}{\triangle S'}$, $P = \frac{P'}{(\rho'_0 M^{-1}k^2 d^{-2})}$, $H = \frac{H'}{kH_o/\eta}$, the non dimensional governing equations are,

$$\nabla \cdot \overline{V} = 0, \quad \text{and} \quad \nabla \cdot \overline{H} = 0, \tag{4.7}$$

$$\frac{1}{M^2\phi Pr}\left[\frac{\partial\overline{V}}{\partial t} + \frac{1}{\phi}(\overline{V}\cdot\nabla)\overline{V}\right] - Q\frac{\partial\overline{H}}{\partial y} + \frac{1}{MDa}\overline{V} - Q\frac{Pr_2}{Pr_1}(\overline{H}\cdot\nabla)\overline{H} =$$
$$\frac{\Lambda}{M}\nabla^2\overline{V} - \nabla\left(\frac{P}{MPr_1} - \frac{Q}{2}\frac{Pr_2}{Pr_1}|\overline{H}|^2 + Q\overline{H}_y\right) + (R_1\theta - R_2C)\hat{e}_z, \tag{4.8}$$

$$\frac{\partial\theta}{\partial t} + \frac{1}{M}(\overline{V}.\nabla)\theta = \frac{w}{M} + \nabla^2\theta, \tag{4.9}$$

$$\frac{\phi}{L}\frac{\partial C}{\partial t} + \frac{1}{ML}(\overline{V}.\nabla)C = \frac{w}{ML} + \nabla^2 C, \tag{4.10}$$

$$\phi\frac{Pr_2}{Pr_1}\frac{\partial\overline{H}}{\partial t} - \nabla \times (\overline{V} \times \hat{e_y}) - M\nabla^2\overline{H} = \frac{Pr_2}{Pr_1}\nabla \times (\overline{V} \times \overline{H}), \tag{4.11}$$

the non dimensional numbers are $L = \frac{k_S}{k_T}$, $Da = \frac{k}{d^2}$, $R_1 = \frac{\alpha g\triangle Td^3}{\nu k_T}$, $R_2 = \frac{\alpha g\triangle Sd^3}{\gamma k_T}$, $Q = \frac{\mu_m H_o^2 d^2}{4\pi\rho_o\nu\eta}$, $Pr_1 = \frac{\nu}{k}$, $Pr_2 = \frac{\nu}{\eta}$ and $\Lambda = \frac{\mu_e}{\mu}$. The z-component of curl of equation

(4.8) is

$$\mathcal{D}_{Pr_1}(\nabla\times\overline{V})\cdot\hat{e_z}-Q\frac{\partial}{\partial y}(\nabla\times\overline{H})\cdot\hat{e_z}-R_1(\nabla\times\theta\hat{e_z})\cdot\hat{e_z}+R_2(\nabla\times C\hat{e_z})\hat{e_z}=$$
$$-\frac{1}{M^2\phi^2Pr_1}\left[\nabla\times(\overline{V}\cdot\nabla)\overline{V}\right]\cdot\hat{e_z}+Q\frac{Pr_2}{Pr_1}\left[\nabla\times(\overline{H}\cdot\nabla)\overline{H}\right]\cdot\hat{e_z}, \tag{4.12}$$

the z-component of curl of curl of (4.8) is

$$\mathcal{D}_{Pr_1}\nabla^2 w-Q\frac{\partial}{\partial y}\nabla^2 H_z-R_1\nabla_h^2\theta+R_2\nabla_h^2 C=Q\frac{Pr_2}{Pr_1}\left[\nabla\times\nabla\times(\overline{H}\cdot\nabla)\overline{H}\right]\cdot\hat{e_z}-$$
$$\frac{1}{M^2\phi^2Pr_1}\left[\nabla\times\nabla\times(\overline{V}\cdot\nabla)\overline{V}\right]\cdot\hat{e_z}, \tag{4.13}$$

the z-component of equation (4.11) is

$$\mathcal{D}_\phi H_z=\frac{\partial w}{\partial y}+\frac{Pr_2}{Pr_1}\nabla\times(\overline{V}\times\overline{H})\cdot\hat{e_z} \tag{4.14}$$

eliminating θ, C and H_z from equations (4.9), (4.10), (4.12), (4.13) and (4.14), we get the equation in the form

$$\mathcal{L}w=\mathcal{N}, \tag{4.15}$$

$$\begin{aligned}\mathcal{L}=&\mathcal{D}\mathcal{D}_\phi\mathcal{D}_L\mathcal{D}_{Pr_1}\nabla^2-Q\mathcal{D}\mathcal{D}_L\nabla^2\frac{\partial^2}{\partial y^2}-\frac{R_1}{M}\mathcal{D}_L\mathcal{D}_\phi\nabla_h^2+\frac{R_2}{ML}\mathcal{D}\mathcal{D}_\phi,\\ \mathcal{N}=&\mathcal{D}\mathcal{D}_L\mathcal{D}_\phi\left[\frac{1}{M^2\phi^2Pr_1}(\nabla\times\nabla\times(\overline{V}\cdot\nabla)\overline{V})\cdot\hat{e_z}-Q\frac{Pr_2}{Pr_1}(\nabla\times\nabla\times(\overline{H}\cdot\nabla)\overline{H})\cdot\hat{e_z}\right]\\ &\frac{R_1}{M}\mathcal{D}_\phi\mathcal{D}_L\nabla_h^2(\overline{V}\cdot\nabla)\theta+\frac{R_2}{ML}\mathcal{D}\mathcal{D}_\phi\nabla_h^2(\overline{V}\cdot\nabla)C+Q\mathcal{D}\mathcal{D}_L\frac{Pr_2}{Pr_1}\frac{\partial}{\partial y}\nabla\times(\overline{V}\times\overline{H})\cdot\hat{e_z},\end{aligned} \tag{4.16}$$

where

$$\nabla_h^2=\frac{\partial^2}{\partial x^2}+\frac{\partial^2}{\partial y^2},\qquad \nabla^2=\frac{\partial^2}{\partial x^2}+\frac{\partial^2}{\partial y^2}+\frac{\partial^2}{\partial z^2},\qquad \mathcal{D}=\frac{\partial}{\partial t}-\nabla^2,$$
$$\mathcal{D}_\phi=\phi\frac{Pr_2}{Pr_1}\frac{\partial}{\partial t}-\nabla^2,\quad \mathcal{D}_{Pr_1}=\frac{1}{M^2\phi Pr_1}\frac{\partial}{\partial t}+\frac{1}{MDa}-\frac{\Lambda}{M}\nabla^2,\quad \mathcal{D}_L=\frac{\phi}{L}\frac{\partial}{\partial t}-\nabla^2.$$

4.3 Linear Stability Analysis

The linearised system of $\mathcal{L}w = \mathcal{N}$ is $L\omega = 0$, by assuming periodic disturbances with period $\frac{2\pi}{l}$ along x-direction and periodic disturbances with period $\frac{2\pi}{m}$ along y-direction with growth rate p of the form $w = \sin \pi z e^{i(lx+my)+pt}$. We get,

$$\begin{aligned}
&\left(p+\delta^2\right)\left(\frac{\phi}{L}p+\delta^2\right)\left(\phi\frac{Pr_2}{Pr_1}p+M\delta^2\right)\left(\frac{1}{M^2\phi Pr_1}p+\frac{1}{MDa}+\frac{\Lambda}{M}\delta^2\right)\delta^2+\\
&Q\left(p+\delta^2\right)\left(\frac{\phi}{L}p+\delta^2\right)\delta^2 m^2-\frac{R_1}{M}q^2\left(\frac{\phi}{L}p+\delta^2\right)\left(\phi\frac{Pr_2}{Pr_1}p+M\delta^2\right)+\\
&\frac{R_2}{ML}q^2\left(p+\delta^2\right)\left(\phi\frac{Pr_2}{Pr_1}p+M\delta^2\right)=0,
\end{aligned} \tag{4.17}$$

where $q^2 = l^2 + m^2$ and $\delta^2 = \pi^2 + q^2$, substituting $p = i\omega$ into equation (4.15), we get

$$R_1 = \frac{M}{q^2}\mathcal{K}\left[c_0 - c_2\omega^2 + c_4\omega^4 - c_6\omega^6 + i\omega\left(c_1 - c_3\omega^2 + c_5\omega^4\right)\right], \tag{4.18}$$

here we have given different coefficient values

$$\begin{aligned}
\mathcal{K} =&(\delta^4+\frac{\phi^2}{L^2}\omega^2)^{-1}(M^2\delta^4+\phi^2\frac{Pr_2^2}{Pr_1^2}\omega^2)^{-1},\ c_0 = M\delta^8(Qm^2\delta^2+\frac{1}{Da}+\Lambda\delta^6+\frac{R_2}{L}q^2),\\
c_1 =&\Big[M(m^2Q\delta^2+\frac{\delta^4}{Da}+\Lambda\delta^6)+\frac{\delta^6}{Pr_1}(\frac{1}{\phi}-m^2Q\phi Pr_2\delta^2)+\frac{Mq^2R_2}{L^2}(L-\phi)\Big]\delta^6,\\
c_2 =&\frac{\delta^{10}}{\phi Pr_1}-\frac{q^2\delta^4\phi R_2}{L}(\frac{M}{L}+\frac{\phi}{M}\frac{Pr_2^2}{Pr_1^2})-\delta^8\phi^2M(\frac{1}{L^2}+\frac{1}{M^2}\frac{Pr_2^2}{Pr_1^2})(\frac{1}{Da}+\delta^2\Lambda)-\\
&m^2Q\delta^6\phi(\frac{M\phi}{L^2}+\frac{Pr_2}{Pr_1}),\\
c_3 =&\frac{q^2\delta^2\phi^2}{L^2M}\frac{Pr_2^2}{Pr_1^2}R_2(\phi-L)-\Big[M\delta^6\phi^2(\frac{1}{Da}+\delta^2\Lambda)-\frac{\phi\delta^8}{Pr_1}\Big](\frac{1}{M^2}\frac{Pr_2^2}{Pr_1^2}+\frac{1}{L^2})-\\
&\frac{m^2Q\delta^4\phi^2}{L^2}(M-\phi\frac{Pr_2}{Pr_1}),\\
c_4 =&\frac{\delta^4\phi^4}{L^2M}\frac{Pr_2^2}{Pr_1^2}(\frac{1}{Da}+\Lambda\delta^2)+\frac{q^2\phi^3}{L^2M}\frac{Pr_2^2}{Pr_1^2}R_2-\frac{\delta^6\phi}{Pr_1}(\frac{1}{L^2}+\frac{1}{M^2}\frac{Pr_2^2}{Pr_1^2})+\frac{m^2Q\delta^6\phi^3}{L^3}\frac{Pr_2}{Pr_1},\\
c_5 =&\frac{\delta^2\phi^4}{L^2M}\frac{Pr_2^2}{Pr_1^2}(\frac{1}{Da}+\Lambda\delta^2+\frac{\delta^2}{M\phi Pr_1}),\ c_6 = \frac{\delta^2\phi^3Pr_2^2}{L^2M^2Pr_1^3}.
\end{aligned} \tag{4.19}$$

4.3.1 Marginal stability analysis when R_1 is a dependent variable

Stationary convection:

At the onset of stationary convection take $\omega = 0$ in equation (4.18), we get

$$R_{1s} = \frac{1}{q^2}\left[\left(\frac{1}{Da} + \Lambda\delta^2\right)\delta^4 + Qm^2\delta^2 + \frac{R_2}{L}q^2\right] \tag{4.20}$$

where R_{1s} is the stationary thermal Rayleigh number. The critical stationary thermal Rayleigh number R_{1sc} for critical wave numbers l_{sc} and m_{sc} which represent the oblique rolls is

$$R_{1sc} = \frac{1}{q_{sc}^2}\left[\left(\frac{1}{Da} + \Lambda\delta_{sc}^2\right)\delta_{sc}^4 + Qm_{sc}^2\delta_{sc}^2 + \frac{R_2}{L}q_{sc}^2\right], \tag{4.21}$$

where $q_{sc}^2 = l_{sc}^2 + m_{sc}^2$ and $\delta_{sc}^2 = q_{sc}^2 + \pi^2$.

For parallel rolls, there is no periodic disturbance along x-direction and periodic disturbance along y-direction with growth rate p, take $l = 0$ in equation (4.20), we get the stationary thermal Rayleigh number for parallel rolls R_{1sm} as

$$R_{1sm} = \frac{1}{m^2}\left[\left(\frac{1}{Da} + \Lambda(m^2+\pi^2)\right)(m^2+\pi^2)^2 + Qm^2(m^2+\pi^2)^2 + \frac{R_2}{L}m^2\right]. \tag{4.22}$$

The critical Rayleigh number for parallel rolls at the critical wave number $m^2 = \frac{\pi^2}{\sqrt[3]{2}}$ is R_{1scm},

$$R_{1scm} = \sqrt[3]{2}\Lambda\pi^4(1 + \frac{1}{\sqrt[3]{2}})^3 + Q\pi^2(1 + \frac{1}{\sqrt[3]{2}}) + \frac{R_2}{L}, \tag{4.23}$$

the critical value R_{1scm} depends on Q, R_2 and L.

For cross rolls, there is no periodic disturbance along y-direction and periodic disturbance along x-direction with growth rate p, take $m = 0$ in equation (4.20), we get the stationary thermal Rayleigh number for cross rolls R_{1sl} is

$$R_{1sl} = \frac{1}{l^2}\left[\left(\frac{1}{Da} + \Lambda(l^2+\pi^2)\right)(l^2+\pi^2)^2 + \frac{R_2}{L}l^2\right]. \tag{4.24}$$

The critical Rayleigh number for cross rolls at the critical wave number $l^2 = \frac{\pi^2}{2}(\sqrt{5}-1)$ is R_{1scl},

$$R_{1scl} \approx \frac{27\pi^4}{4}\Lambda + \frac{R_2}{L}, \tag{4.25}$$

the critical value R_{1scl} depends on R_2 and L not on Q value.

Oscillatory convection

At the onset of oscillatory convection, equation (4.18) represents the imaginary but Rayleigh number is always real so equating the imaginary value of equation (4.18) to zero,

$$c_1 - c_3\omega^2 + c_5\omega^4 = 0, \tag{4.26}$$

$$\omega^2 = \frac{c_3 \pm \sqrt{c_3^2 - 4c_1c_5}}{2c_5}, \tag{4.27}$$

by substituting positive ω^2 from equation (4.27) into the real part of equation (4.18), we get the oscillatory thermal Rayleigh number R_{1o},

$$R_{1o} = \frac{M}{q^2}\mathcal{K}\left(c_0 - c_2\omega^2 + c_4\omega^4 - c_6\omega^6\right), \tag{4.28}$$

where c_0, c_2, c_4, c_6 and K are given from relation (4.19). A necessary condition for $\omega^2 > 0$ is

$$Q < \frac{\delta^6\left(\Lambda M + \frac{1}{\phi Pr_1}\right) + \frac{Mq^2R_2}{L}(1-\frac{\phi}{L})}{m^2\delta^2(\frac{\phi\delta^6 Pr_2}{Pr_1} - M)} \tag{4.29}$$

Figures 4.2 - 4.5 are marginal curves traced in (q, R_1)-plane, the solid and dotted lines represents stationary and oscillatory Rayleigh numbers respectively. We ob-

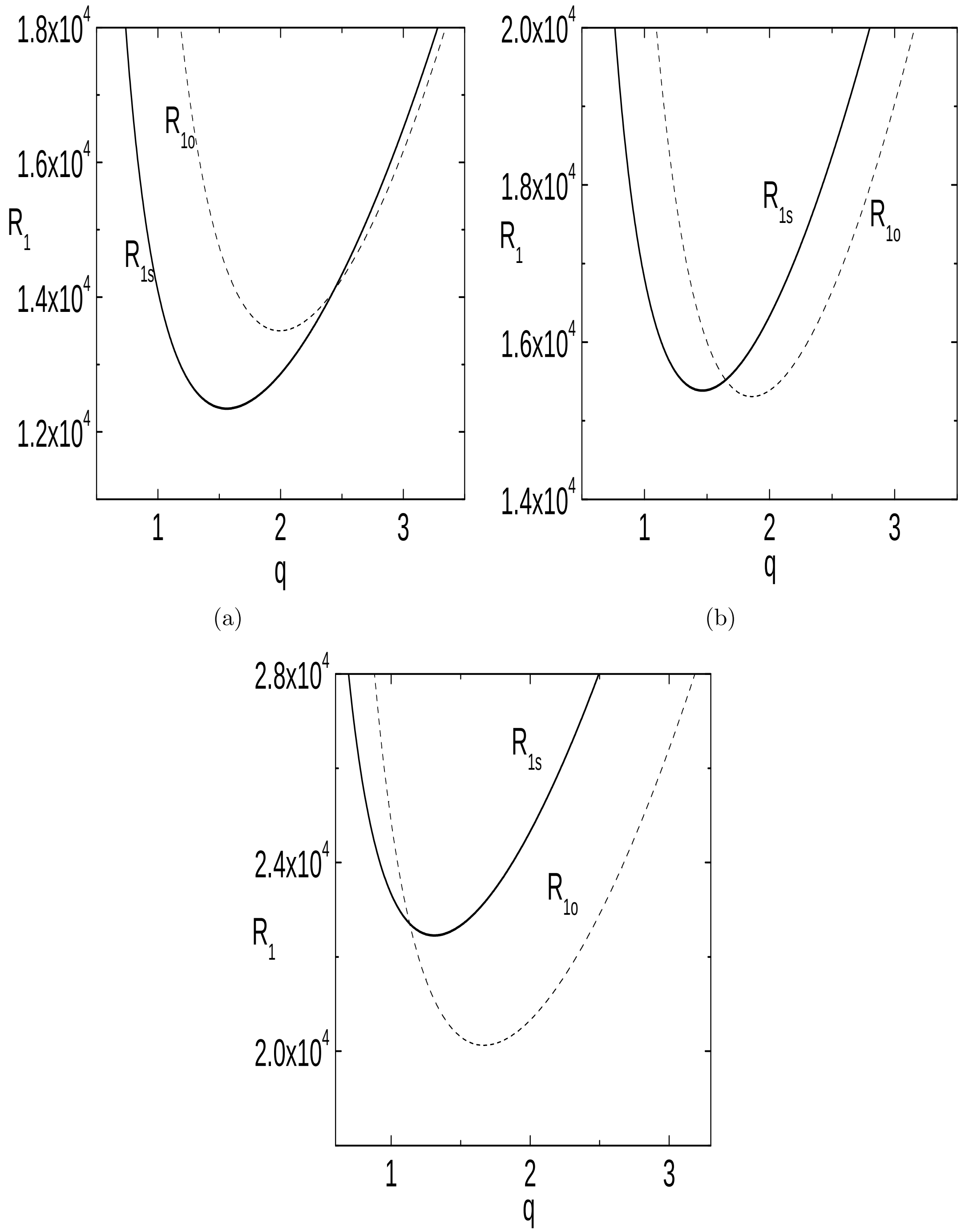

(c)

Figure 4.2: Neutral curves are plotted for $Da = 1500$, $\Lambda = 6$, $M = 0.9$, $\phi = 0.85$, $Pr_1 = 1$, $Pr_2 = 1.5$, $R_2 = 500$, $(a)Q = 1300$, $(b)Q = 1750$, $(c)Q = 3000$. Solid lines represent stationary convection R_{1s} and dotted lines represent oscillatory R_{10}

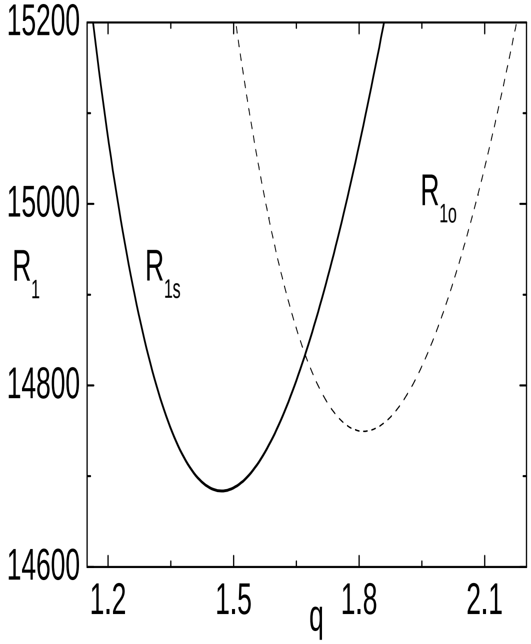

(a)

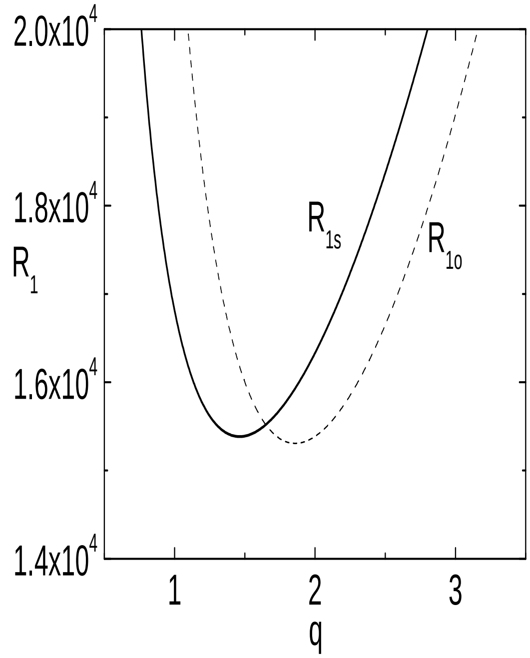

(b)

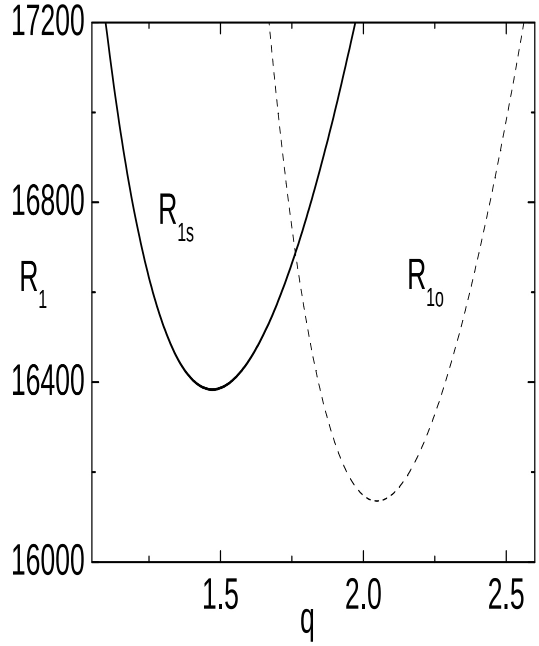

(c)

Figure 4.3: Neutral curves are plotted for $Da = 1500$, $\Lambda = 5$, $M = 0.9$, $\phi = 0.85$, $Pr_1 = 1$, $Pr_2 = 1.5$, $Q = 1750$, $(a)R_2 = 100$, $(b)R_2 = 500$, $(c)R_2 = 1800$. Solid lines represent stationary convection R_{1s} and dotted lines represent oscillatory R_{1o}

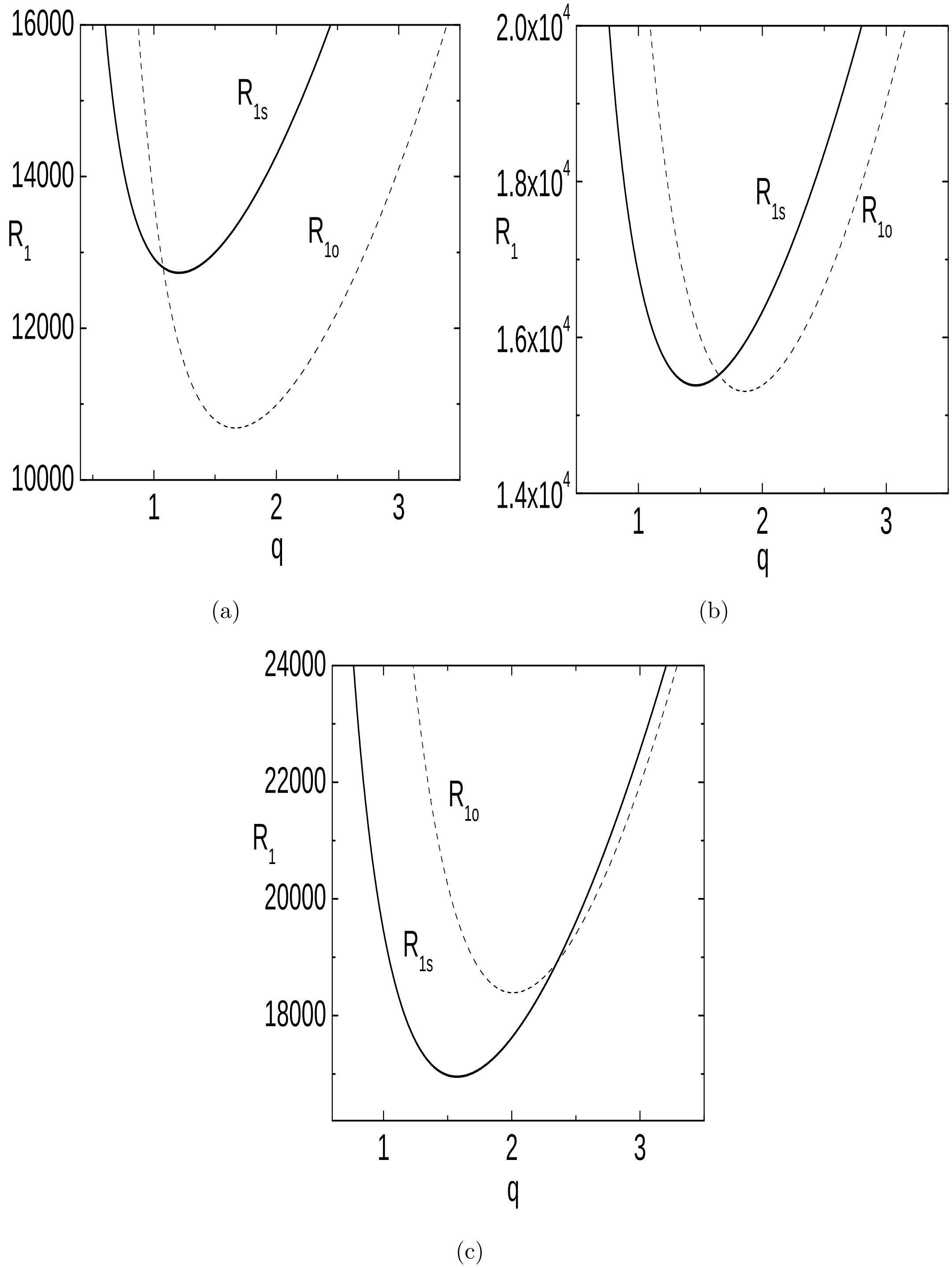

Figure 4.4: Neutral curves are plotted for $Da = 1500$, $M = 0.9$, $\phi = 0.85$, $Pr_1 = 1$, $Pr_2 = 1.5$, $Q = 1750$, $R_2 = 800$, (a) $\Lambda = 2$, (b) $\Lambda = 5$, (c) $\Lambda = 7$. Solid lines represent stationary convection R_{1s} and dotted lines represent oscillatory R_{1o}

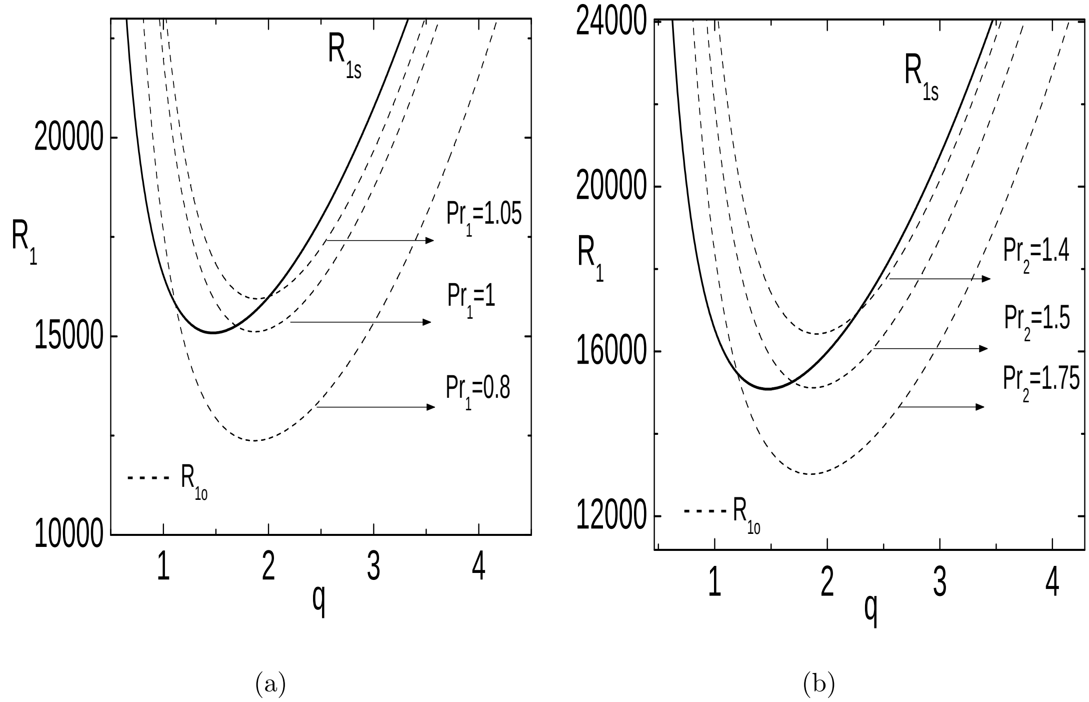

Figure 4.5: Neutral curves are plotted for $Da = 1500$, $\Lambda = 2$, $M = 0.9$, $\phi = 0.85$, $R_2 = 500$ in sub figure (a) $Pr_2 = 1.5$, vary Pr_1 values,$Pr_1 = 0.8, 1, 1.05$, in sub figure (b) $Pr_1 = 1$, vary Pr_2 values,$Pr_2 = 1.4, 1.5, 1.75$. Solid lines represent stationary convection R_{1s} and dotted lines represent oscillatory R_{10}

tained co-dimension two bifurcation points and Takens-Bogdanov bifurcations. At the co-dimension two bifurcation point we get $R_s(q_s) = R_c(q_c)$ and $q_s \neq q_c$. At Takens-Bogdanov bifurcation point $R_{10}(q_o) = R_{1s}(q_s) = R_{1c}(q_c)$ and $q_o = q_s = q_c$. The stationary Rayleigh number is not affected by thermal or magnetic prandtl numbers. In Figures 4.2(b), 4.3(b), 4.4(b), 4.5(a) at $Pr_1 = 1$ and 4.5(b) at $Pr_2 = 1.5$ there exists co-dimension two bifurcation points , while other intersection points represents Takens-Bogdanov bifurcation points. In Figure 4.5(a) co-dimension two bifurcation point moves upwards when Pr_1 increases, in Figure 4.5(b) co-dimension two bifurcation point moves downwards when Pr_2 increases.

4.3.2 Marginal stability analysis when R_1 is an independent variable

In equation (4.17) represents a fourth degree polynomial in powers of p,

$$Ap^4 + Bp^3 + Cp^2 + Dp + E = 0, \tag{4.30}$$

where

$$\begin{aligned}
A =& \frac{\delta^4 \phi Pr_2}{LM^2 Pr_1^2}, B = \frac{\delta^4 Pr_2}{M^2 Pr_1^2}(1 + \frac{\phi}{L}) + \frac{\delta^2 \phi^2 Pr_2}{LMPr_1}(\Lambda + \frac{1}{Da}) + \frac{\delta^4}{LMPr_1}, \\
C =& \frac{\phi \delta^2}{L}(m^2 Q + \frac{\delta^2}{Da}) + \frac{\delta^4 \phi Pr_2}{MPr_1}(1 + \frac{\phi}{L})(\Lambda \phi \delta^2 + \frac{1}{Da}) + \frac{\delta^6}{MPr_1}(\frac{1}{\phi} + \frac{Pr_2}{MPr_1}) + \\
& \frac{\delta^6}{L}(\Lambda \phi + \frac{1}{MPr_1}) + \frac{q^2 \phi Pr_2}{LMPr_1}(R_1 - R_1 \phi), \\
D =& q^2 \delta^2 \left[\frac{\phi Pr_2}{MPr_1}(R_1 + \frac{R_2}{L}) + \frac{1}{L}(R_1 - \phi R_1) \right] + m^2 Q \delta^4 (1 + \frac{\phi}{L}) + \frac{\delta 6}{Da}(1 + \frac{\phi}{L} + \\
& \frac{\phi Pr_2}{MPr_1}) + \delta^8 \left[\Lambda(1 + \frac{\phi}{L}) + \frac{1}{MPr_1}(\Lambda \phi Pr_2 + \frac{1}{\phi}) \right], \\
E =& \delta^4 \left[m^2 Q \delta^2 + \delta^4 (\Lambda \delta^2) + \frac{1}{Da} - q^2 (R_1 - \frac{R_2}{L})) \right].
\end{aligned} \tag{4.31}$$

Substituting $p = i\omega$ in equation (4.30), we get

$$(A\omega^4 - C\omega^2 + E) - i\omega(B\omega^2 - D) = 0, \tag{4.32}$$

the real and imigenary part of above equation (4.32) are

$$A\omega^4 - C\omega^2 + E = 0, \tag{4.33}$$

$$B\omega^2 - D = 0 \tag{4.34}$$

Stationary convection:

At the onset of stationary convection taking $\omega = 0$ in equation (4.30), we get $E = 0$,

$$m^2 Q\delta^2 + \delta^4(\Lambda\delta^2 + \frac{1}{Da}) - q^2(R_1 - \frac{R_2}{L})) = 0 \tag{4.35}$$

from equation (4.35), we get stationary thermal Rayleigh number R_{1s} is

$$R_{1s} = \frac{1}{q^2}\left[\left(\frac{1}{Da} + \Lambda\delta^2\right)\delta^4 + Qm^2\delta^2 + \frac{R_2}{L}q^2\right], \tag{4.36}$$

which is the same as equation (4.20). Differentiating equation (4.35) with respect to l^2 and m^2, we get

$$Qm^2 + \frac{1}{Da}2(l^2 + m^2 + \pi^2) + 3\Lambda(l^2 + m^2 + \pi^2)^2 - (R_1 - \frac{R_2}{L}) = 0 \tag{4.37}$$

$$Q(l^2 + 2m^2 + \pi^2) + \frac{1}{Da}2(l^2 + m^2 + \pi^2) + 3\Lambda(l^2 + m^2 + \pi^2)^2 - (R_1 - \frac{R_2}{L}) = 0, \tag{4.38}$$

solving equations (4.37) and (4.38) we get

$$\delta^2 = \left(\frac{R_1 - \frac{R_2}{L}}{3\Lambda}\right)^{1/2} \tag{4.39}$$

now substituting δ^2 from equation (4.39) in equation (4.36), we get the stationary critical Chandrasekhar number $Q = Q_{sc}$ where

$$Q_{sc} = \frac{1}{2m^2}\left[2\left(R_1 - \frac{R_2}{L}\right) - \Lambda\sqrt{R_{rb}}\left(R_1 - \frac{R_2}{L}\right)^{1/2}\right], \tag{4.40}$$

where R_{rb} is the critical thermal Rayleigh number of the Rayleigh-Benard convection, $R_{rb} = \frac{27\pi^4}{4}$. From equation (4.39),

$$q_{sc} = \left[\left(\frac{R_1 - \frac{R_2}{L}}{3\Lambda}\right)^{1/2} - \pi^2\right]^{\frac{1}{2}}, \tag{4.41}$$

we use equation (4.41) to determine the sign of E, (i.e. $E = 0, E > 0$). In figure 4.6 shows the plotted curve (R_1, Q_{sc})- plane for equation (4.40). In figure on R_1 x-axis $Q = 0$ and each solid line represents R_2 and starting from $R_1 = R_{1rb} + \frac{R_1}{L}$.

Oscillatory convection:

At the onset of oscillatory convection, from equation (4.32) $A\omega^4 - C\omega^2 + E = 0$ and $B\omega^2 - D = 0$. From equation $B\omega^2 - D = 0$, $\omega^2 = \frac{D}{B}$. Substituting $\omega^2 = \frac{D}{B}$ in equation $A\omega^4 - C\omega^2 + E = 0$, we get $AD^2 - BCD + B^2E = 0$ and the thermal Rayleigh number onset of oscillatory convection exists for a set of physical parameters corresponding to positive value of ω^2. For a large value of Da and unit values of Λ, L, the equation $AD^2 - BCD + B^2E = 0$ is expressed as

$$-Q\frac{m^2\delta^2(Pr_2 + MPr_1)}{M^3\phi Pr_1^3} + q^2(R_1O_1 - R_2O_2) - \delta^6O_3 = 0, \tag{4.42}$$

where $O_1 = \frac{\phi(MPr_1+Pr_2)(M^2Pr_1^2+Pr_2^2)}{M^5Pr_1^5}$, $O_2 = \frac{M^2Pr_1^2(MPr_1-Pr_2)+\phi^2Pr_2^3}{M^5\phi Pr_1^5}$ and $O_3 = \frac{(MPr_1+Pr_2)(MPr_1+\phi Pr_2)}{M^5\phi^2Pr_1^5}$. Comparing equations (4.35) and (4.42), and substituting in equations (4.39) and (4.40), we get the critical wave number q_{oc} and critical

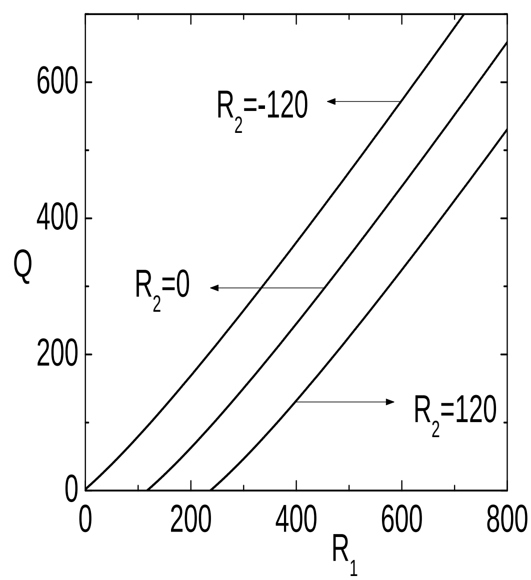

Figure 4.6: curves are plotted for R_2=-120, 0 and 120 in (R_1, Q)- plane at $Da = 1500$, $\Lambda = 0.8$, $M = 0.85$, $\phi = 0.9$, $Pr_1 = 1$, $Pr_2 = 1.25$ and $L = 1$.

Chandrasekhar number Q_{oc},

$$q_{oc} = \left[\frac{1}{\sqrt{3}}\left(R_1O_1 - R_2O_2\right)^{1/2} - \pi^2\right]^{\frac{1}{2}}, \tag{4.43}$$

$$Q_{oc} = \frac{1}{m^2}\left[2\left(R_1O_1 - R_2O_2\right) - \pi^2 3\sqrt{3}\left(R_1O_1 - R_2O_2\right)^{1/2}\right]. \tag{4.44}$$

In Figure 4.7, if $w^2 > 0$ the get codimension two bifurcation point.It moves upward when Pr_1 increases and it moves downwards when Pr_2 decreases.

4.4 Nonlinear stability analysis

4.4.1 LG equation at the onset of stationary convection

According to Newell and Whitehead [77] multiple scale analysis , small scale convection cells disturb the vital flow. If the scale range is $O(\epsilon)$ then the the collaboration of the cell with itself forces a second harmonic and a standard state of rectification of range $O(\epsilon^2)$ and these in turn impel an $O(\epsilon^3)$ rectification to the structural module

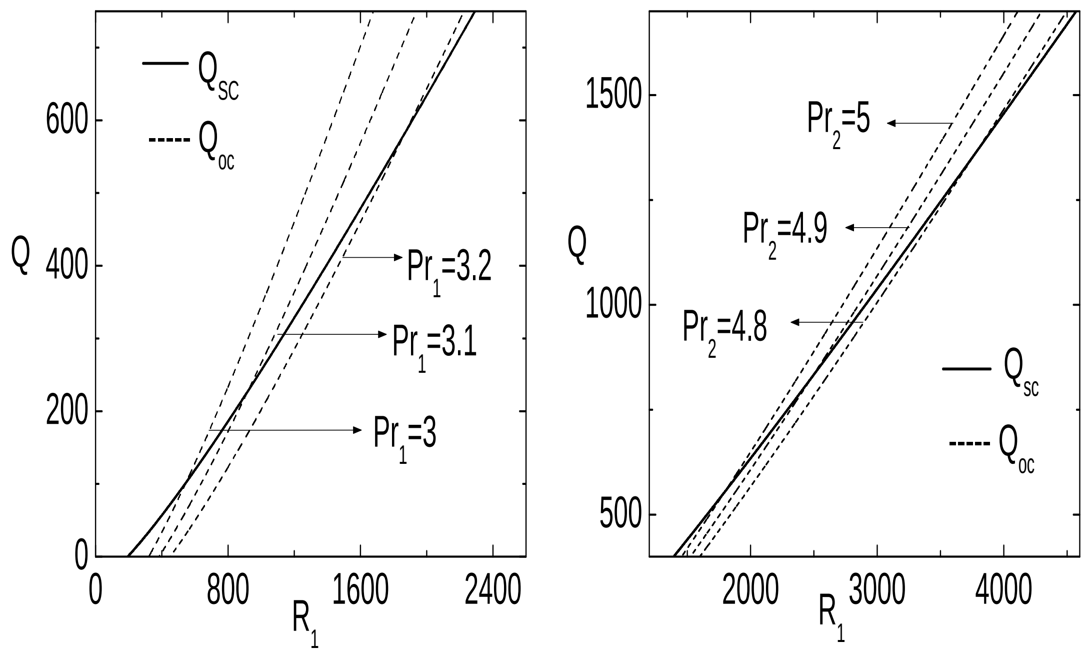

(a) (b)

Figure 4.7: Solid curve represent stationary critical Chandrasekhar number (Q_{sc}) and dotted curves represents the oscillatory critical Chandrasekhar number at $Da = 1500$, $\Lambda = 0.6$, $M = 0.85$, $L = 1$, $\phi = 0.85$ (a) Pr_1=3, 3.1, 3.2 and $Pr_2 = 4.2$ (b) $Pr_1 = 3.3$ and $Pr_2 = 4.8$, 4.9, 5.

of the imposed roll. Let us assume the solution of equations (4.7)-(4.11) in series ϵ form

$$f(u, v, w, \theta, C, H_x, H_y, H_z) = f = \epsilon f_0 + \epsilon^2 f_1 + \epsilon^3 f_2 + \cdots . \tag{4.45}$$

The first order calculations of the linearised problem given by approximation are given by the eigenvectors

$$\begin{aligned}
u_0 =& \frac{i\pi}{l_{sc}} \left[Ae^{i(l_{sc}x+m_{sc}y)} - c \cdot c\cdot\right] \cos \pi z,\ v_0 = 0,\\
w_0 =& \left[Ae^{i(l_{sc}x+m_{sc}y)} z + c \cdot c\cdot\right] \sin \pi,\\
\theta_0 =& \frac{1}{M\delta_{sc}^2} \left[Ae^{i(l_{sc}x+m_{sc}y)} + c \cdot c\cdot\right] \sin \pi z,\\
C_0 =& \frac{1}{ML\delta_{sc}^2} \left[Ae^{i(l_{sc}x+m_{sc}y)} + c \cdot c\cdot\right] \sin \pi z,\\
H_{x_0} =& \frac{-\pi m_{sc}}{Ml_{sc}\delta_{sc}^2} \left[Ae^{i(l_{sc}x+m_{sc}y)} + c \cdot c\cdot\right] \cos \pi z, H_{y_0} = 0,\\
H_{z_0} =& \frac{im_{sc}}{M\delta_{sc}^2} \left[Ae^{i(l_{sc}x+m_{sc}y)} - c \cdot c\cdot\right] \sin \pi z,
\end{aligned} \tag{4.46}$$

here $A = A(X, Y, T)$ is the complex scale varying on gradual variables X, Y and T while complex conjugates are represented as c.c. The analytical mode for the linear problem at $R_{1s} = R_{1sc}$ is $e^{iqx} \sin \pi z$. The variables x, y, z and t are scaled by

$$X = \epsilon x, \quad Y = \epsilon^{\frac{1}{2}} y, \quad Z = z \quad \text{and} \quad T = \epsilon^2 t, \tag{4.47}$$

are suitably scattered for the fast and slow unconventional variables in f. The derivative operators can be formulated as

$$\frac{\partial}{\partial x} \to \frac{\partial}{\partial x} + \epsilon \frac{\partial}{\partial X}, \quad \frac{\partial}{\partial y} \to \frac{\partial}{\partial y} + \epsilon^{\frac{1}{2}} \frac{\partial}{\partial Y}, \quad \frac{\partial}{\partial z} \to \frac{\partial}{\partial Z}, \quad \frac{\partial}{\partial t} \to \epsilon^2 \frac{\partial}{\partial T}. \tag{4.48}$$

Based on the transformations equation (4.48), the linear and nonlinear operators $\mathcal{L}$ and $\mathcal{N}$ are written as

$$\mathcal{L} = \mathcal{L}_0 + \epsilon \mathcal{L}_1 + \epsilon^2 \mathcal{L}_2 \cdots , \tag{4.49}$$

$$\mathcal{N} = \epsilon^2\mathcal{N}_0 + \epsilon^3\mathcal{N}_1 + \cdots, \tag{4.50}$$

substituting equations (4.49), (4.50) and (4.45) into equation (4.15), and equating the $\epsilon, \epsilon^2, \epsilon^3$ coefficients on both sides, we obtain

$$\mathcal{L}_0 w_0 = 0, \tag{4.51}$$

$$\mathcal{L}_0 w_1 + \mathcal{L}_1 w_0 = \mathcal{N}_0, \tag{4.52}$$

$$\mathcal{L}_0 w_2 + \mathcal{L}_1 w_1 + \mathcal{L}_2 w_0 = \mathcal{N}_1, \tag{4.53}$$

where

$$\begin{aligned}
\mathcal{L}_0 =& -\nabla^6\left(Q\frac{\partial^2}{\partial y^2} + \frac{1}{Da}\nabla^2 - \Lambda\nabla^4\right) - \nabla^4\nabla_h^2 R_{12},\\
\mathcal{L}_1 =& \left[\nabla^2(-3Q\partial_y^2 - \nabla^2(\frac{6}{Da} + 3Q) + 10\Lambda\nabla^4) - R_{12}(\nabla_h^2 + 2\nabla^2)\right] a_3^2 - \\
& R_{12}a_2\nabla^2(a_5 + 2\nabla_h^2) + a_2\nabla^4(-3Q\partial_y^2 - \frac{4}{Da}\nabla^2 + 5\Lambda\nabla^4) - Qc_2\nabla^6,\\
\mathcal{L}_2 =& (1 + \frac{\phi}{L})(Q\partial_y^2 + \frac{\nabla^2}{Da} - \Lambda\nabla^4)\nabla^2 + R_{12}(\frac{1}{L} + \frac{\phi Pr_2}{MPr_1})\nabla_2^2\nabla^2 - \\
& \left[\frac{\nabla^2}{\phi} + \phi Pr_2(\frac{1}{Da} - \Lambda\nabla^2)\right]\frac{\nabla^6}{M\phi Pr_1} + a_2^2\nabla^2[-3Q\partial_y^2 - 2R_{12}] - \\
& 3Qa_2\nabla^4\partial_y^2 - a_2^2\nabla_h^2 R_{12} + a_2a_3^3p_1 + a_2^2p_2 - 3a_2a_3^2p_3,
\end{aligned} \tag{4.54}$$

where $a_1 = \frac{\partial^2}{\partial X^2}$, $a_2 = \frac{\partial^2}{\partial x \partial X}$, $a_3 = 2\frac{\partial^2}{\partial y \partial Y}$, $R_{12} = \left(R_1 - \frac{R_2}{L}\right)$, $p_1 = -6(Q + \frac{2}{Da})\nabla^2 - 3R_{12} + 30\Lambda\nabla^4 - 3Q\partial_y^2$, $p_2 = \nabla^2(-3Q\partial_y^2 - \frac{6\nabla^2}{Da} + 10\Lambda\nabla^4) - R_{12}(\nabla_h^2 + 2\nabla^2)$, $p_3 = -2(Q+\frac{2}{Da})\nabla^2 + 10\Lambda\nabla^4 - Q\partial_y^2 - R_{12}$ Substituting zeroth order solution w_0 in equation (4.54) $\mathcal{L}_0 w_0 = 0$, we get

$$R_{sc} = \frac{\delta_{sc}^2}{q_{sc}^2}\left[\delta_{sc}^4\Lambda + \frac{1}{D_a}\delta_{sc}^2 + Qm_{sc}^2\right]. \tag{4.55}$$

In equation (4.52), $\mathcal{N}_0 = 0, \mathcal{L}_1 w_0 = 0$ and hence

$$
\begin{aligned}
u_1 =& 0, v_1 = 0, w_1 = 0,\\
\theta_1 =& -\frac{1}{2\pi M^2 \delta_{sc}^2}|A|^2 \sin 2\pi z,\\
C_1 =& -\frac{1}{2M^2 L^2 \delta_{sc}^2}|A|^2 \sin 2\pi z,\\
H_{x_1} =& \frac{1}{M^2\delta^2}\frac{m}{l}\frac{Pr_2}{Pr_1}|A|^2 \cos 2\pi z,\\
H_{y_1} =& 0, H_{z_1} = 0.
\end{aligned} \tag{4.56}
$$

Taking $w_1 = 0$ in equation (4.53), $\mathcal{N}_1 - \mathcal{L}_2 w_0$ is vertical to w_0. This is ensured if the coefficient of $\sin \pi z$ in $\mathcal{N}_1 - \mathcal{L}_2 w_0$ is zero. We get 2-D time dependent nonlinear LG equation as follows

$$
\lambda_0 \frac{\partial A}{\partial T} - \lambda_1 \left(\frac{\partial}{\partial X} - \frac{i}{2q_{sc}} \frac{\partial^2}{\partial Y^2} \right)^2 A - \lambda_2 A + \lambda_3 |A|^2 A = 0, \tag{4.57}
$$

where

$$
\begin{aligned}
\lambda_0 =& \delta^4(1+\frac{\phi}{L})\left[-Qm^2 - \frac{\delta^2}{Da} - \Lambda\delta^4\right] + q^2\delta^2\left[\frac{R_2}{2}(1+\phi\frac{Pr_2}{Pr_1}) + \phi R_1(\frac{1}{L}+\frac{Pr_2}{Pr_1})\right] -\\
& \frac{\delta^6}{MPr_1}\left[\phi Pr_2(\frac{1}{Da}+\Lambda\delta^2) + \frac{\delta^2}{\phi}\right],\\
\lambda_1 =& -\delta^2(Qm^2 + \frac{6\delta^2}{Da} + 10\delta^4) + R_{12}(q^2+\delta^2),\\
\lambda_2 =& q^2\delta^4 R_1,\\
\lambda_3 =& -Q\frac{m^2\delta^2}{2M^2}(\frac{Pr_2}{Pr_1})^2(-3\pi^2 + l^2) - \frac{\delta^2 q^2}{2M^2}(R_1 - \frac{R_2}{2ML^3}) + \frac{Qm^2\delta^4}{2M^2}(\frac{Pr_2}{Pr_1})^2.
\end{aligned} \tag{4.58}
$$

According to Steinberg and Brand [115], from the Fig. 4.10, if $\lambda_3 > 0$ the pitchfork bifurcation is supercritical, if $\lambda_3 < 0$ subcritical and if $\lambda_3 = 0$, then tricritical bifurcation point.

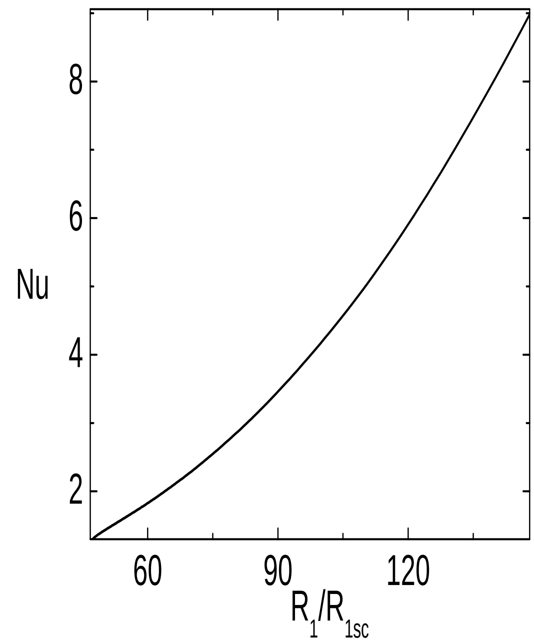

Figure 4.8: The figure is plotted for Q=600, Da=1500, $\Lambda = 3$, M=0.85, $Pr_1 = 1$, $Pr_2 = 1.25$ and $\phi = 0.9$, R/R_{sc} increases then Nu increases.

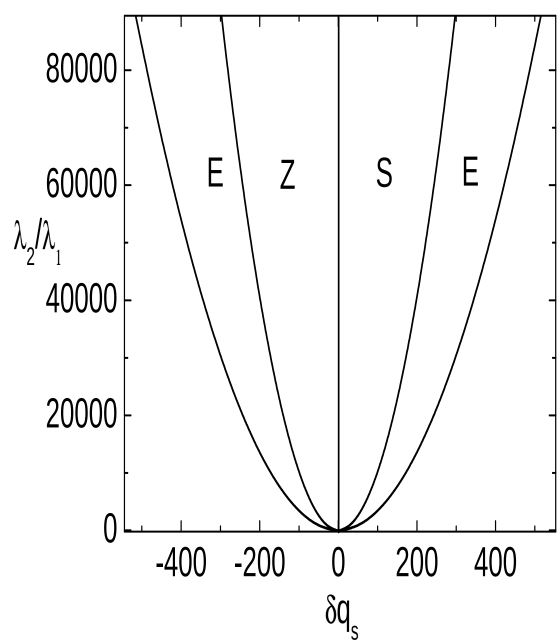

Figure 4.9: Numerically calculated secondary instability regions of Eckhaus instability (E), Zigzqg instability (Z), and Stable region (S) are plotted for $Da = 1500$, $\Lambda = 2$, $M = 0.9$, $\phi = 0.9$, $Pr_1 = 1$, $Pr_2 = 2$, $Q = 10^5$.

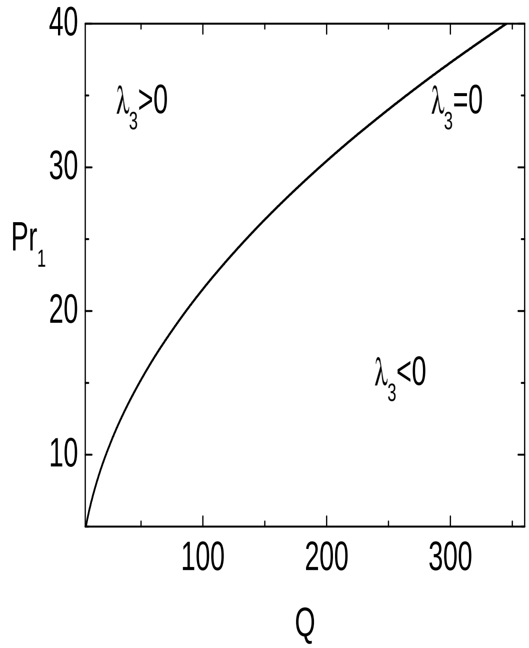

Figure 4.10: λ_3 is nonlinear coefficient of LG equation at the onset of stationary convection. The pitchfork bifurcation is supercritical if $\lambda_3 > 0$, subcritical if $\lambda_3 < 0$ and $\lambda_3 = 0$ for the curve Da=1500, $\Lambda = 0.85$, $\phi = 0.9$, $R_2 = 500$ and $Pr_2 = 1.5$

Nusselt Number

Heat transport by the convection, the Nusselt number studied in section 2.4.1. λ_1 and λ_2 are always positive. The Nusselt number Nu can calculated in terms of amplitude (A) as

$$Nu = 1 + \frac{\epsilon^2}{\delta_{sc}^2}|A_{max}|^2. \tag{4.59}$$

Nusselt number grows if $\frac{R}{R_{sc}} > 1$ and decays if $\frac{R}{R_{sc}} \leq 1$ convection for $Nu > 1$. Then there is convection if $Nu > 1$, conduction if $Nu \leq 1$. Amplitude is valid for $\lambda_3 > 0$ and it is possible when $R > R_{sc}$, Thus we obtain convection for $Nu > 1$ and conduction for $Nu \leq 1$ see in Figure 4.8.It is observed that by increasing the value of Q, Nusselt number grows exponentially at unit value.

Secondary Instabilities

Newell and Whitehead [77] derived envelope equations In order to study the properties of a structure with a given phase winding number δq, we write equation (4.57) in fast variables x, y, t and $A(X,Y,T) = \frac{A(x,y,t)}{\epsilon}$, as

$$\frac{\partial A_1}{\partial t} - \Big(\epsilon^2 \frac{\lambda_2}{\lambda_0} - \frac{\lambda_1}{\lambda_0}\delta q^2\Big) A_1 + 2i\delta q \frac{\lambda_1}{\lambda_0}\Big(\frac{\partial}{\partial x} - \frac{i}{2q_{sc}}\frac{\partial^2}{\partial y^2}\Big) A_1 + \frac{\lambda_1}{\lambda_0}\Big(\frac{\partial}{\partial x} - \frac{i}{2q_{sc}}\frac{\partial^2}{\partial y^2}\Big)^2 A_1 - \frac{\lambda_3}{\lambda_0}|A_1|^2 A_1 = 0, \tag{4.60}$$

$$A_1 = \left[\frac{\epsilon^2 \lambda_2 - \lambda_1 \delta q^2}{\lambda_3}\right]^{\frac{1}{2}}. \tag{4.61}$$

Let $\tilde{u} + i\tilde{v}$ be an infinitesimal perturbation of steady state solution A_1 given by equation (4.61). Substitute

$$A_1 = \tilde{u} + i\tilde{v} + [\big(\epsilon^2 \lambda_2 - \lambda_1 \delta q^2\big)\, \lambda_3^{-1}]^{\frac{1}{2}}, \tag{4.62}$$

into equation (4.60) and equate the real and imaginary parts, we obtain

$$\frac{\partial \tilde{u}}{\partial t} = -\,2\left(\epsilon^2 \frac{\lambda_2}{\lambda_0} - \frac{\lambda_1}{\lambda_0}\delta q^2\right)\tilde{u} + \frac{\lambda_1}{\lambda_0}\tilde{u} - \frac{\lambda_1}{\lambda_2}\partial_2 \frac{\partial \tilde{v}}{\partial x}, \tag{4.63a}$$

$$\frac{\partial \tilde{v}}{\partial t} = \frac{\lambda_1}{\lambda_0}\partial_2 \frac{\partial \tilde{u}}{\partial x} + \frac{\lambda_1}{\lambda_0}\partial_1 \tilde{v}. \tag{4.63b}$$

where $\partial_1 = \frac{\partial^2}{\partial x^2} + \frac{\delta q}{q_{sc}}\frac{\partial^2}{\partial y^2} - \frac{1}{4q_{sc}^2}\frac{\partial^4}{\partial y^4}$ and $\partial_2 = 2\delta q - \frac{1}{q_{sc}}\frac{\partial^2}{\partial y^2}$ We analyse equations (4.63a) and (4.63b) by using normal modes form

$$\tilde{u} = U\cos(q_x x)\cos(q_y y)e^{St}, \qquad \tilde{v} = V\sin(q_x x)\cos(q_y y)e^{St}. \tag{4.64}$$

Substituting equation (4.64) in equations (4.63a) and (4.63b) weget,

$$\Big[2(\epsilon^2\lambda_2 - \lambda_1\delta k^2) + \lambda_0 S + \chi_1\Big]U + \lambda_1\chi_2 q_x V = 0 \tag{4.65a}$$

$$\lambda_1 q_x \chi_2 U + (\chi_1 + \lambda_0 S)V = 0. \tag{4.65b}$$

Here $\chi_1 = \lambda_1\Big(q_x^2 + \frac{q_y^2\delta k}{q_{sc}} + \frac{q_y^4}{4q_{sc}^2}\Big)$ and $\chi_2 = (2\delta k + \frac{q_y^2}{q_{sc}})$. On solving equations (4.65a) and (4.65b), we get

$$S^2 + \frac{2S}{\lambda_0}\Big[2\Big(\epsilon^2\lambda_2 - \lambda_1(\delta k)^2\Big) + \chi_1\Big] + \Big[2\Big(\frac{\epsilon^2\lambda_2}{\lambda_0^2} - \frac{\lambda_1\delta k^2}{\lambda_0^2}\Big) + \chi_1\Big]\psi_1 - q_x^2\chi_2\frac{\lambda_1}{\lambda_0^2} = 0, \tag{4.66}$$

whose real roots are $(S\pm)$,

$$(S\pm) = -\frac{1}{\lambda_0^2}\left\{\Big[2\lambda_0(\epsilon^2\lambda_2 - \lambda_1\delta kq^2) + \lambda_0\chi_1\Big] \pm \Big[2\lambda_0(\epsilon^2\lambda_2 - \lambda_1\delta q^2)^2 + \lambda_1^2 q_x^2\chi_2^2\Big]^{\frac{1}{2}}\right\}. \tag{4.67}$$

The equivalent mode is stable if $S(-)$ is negative and unstable if $S(+)$ is positive. Symmetry significance helps to confine the field of $S(+)$ to $q_x \geq 0, q_y \geq 0$.

Eckhaus Instability

Putting $q_y = 0$ into equation (4.67), we get

$$S^2 + \frac{2S}{\lambda_0}\Big[2(\epsilon^2\lambda_2 - \lambda_1\delta q^2) + \lambda_1 q_x^2\Big] + \frac{\lambda_1 q_x^2}{\lambda_0^2}\Big[2(\epsilon^2\lambda_2 - 3\lambda_1\delta q^2) + q_x^2\Big] = 0, \tag{4.68}$$

The roots are real numbers and their sum is negative number and the product of roots is positive number, the pattern is stable and if the product of roots is negative number then the pattern becomes unstable.
Eckhaus instability defines $q_x^2 \leq 2\Big(3\lambda_1\delta q^2 - \epsilon^2\lambda_2\Big)$ for $|\delta q| \geq \sqrt{\frac{\epsilon^2\lambda_2}{3\lambda_1}}$ and unstable wave tends to zero when $|\delta q| \to \sqrt{\frac{\epsilon^2\lambda_2}{3\lambda_1}}$.

Zigzag Instability

putting $q_x = 0$ into equation (4.68), we get

$$\lambda_0^2 S^2 + 2S(2\lambda_0\chi_{11} + \lambda_0\chi_{12}) + (2\chi_{11} + \chi_{12})\chi_{12} = 0, \tag{4.69}$$

where $\chi_{11} = \epsilon^2\lambda_2 - \lambda_1\delta q^2$ and $\chi_{12} = \lambda_1\left(\frac{q_y^2\delta q}{q_s c} + \frac{q_y^4}{4q_{sc}^2}\right)$, the two eigen conditions are unrelated and amplified when $S(-) = -2(\epsilon^2\lambda_2 - \lambda_1\delta q^2) - \frac{\lambda_1}{q_{sc}}q_y^2\delta q - \frac{\lambda_1}{4q_{sc}^2}q_y^2 < 0$ and $S(+) = -\lambda_1 q_y^2\Big(\delta q + \frac{q_y^2}{4q_{sc}}\Big) > 0$. These conditions define the domain of Zigzag Instability when $\delta q_s < 0$. In Figure 4.9, we have shown the secondary instability regions like Eckhaus instability and Zigzag instability regions and fixed parameters, we observed this by increasing Q value, the region of Eckhaus and Zigzag instability increases.

4.4.2 LG equations at the onset of Oscillatory Convection

When cylindrical rolls along y-axis are considered only x-dependence and z-dependence appears from $\mathcal{L}w = \mathcal{N}$. Based on this we coupled one dimensional nonlinear time dependent LG type equations at the supercritical Hopf bifurcation. We establish ϵ as

$$\epsilon^2 = \frac{R_o - R_{oc}}{R_{oc}} \ll 1, \tag{4.70}$$

and take

$$w_0 = \left[A_{1L}e^{i(l_{oc}x + m_{oc}y + \omega_{oc}t)} + A_{1R}e^{i(l_{oc}x + m_{oc}y - \omega_{oc}t)} + c\cdot c.\right]\sin\pi z,$$

is a solution of $\mathcal{L}w = 0$. Here A_{1L} and A_{1R} represents the amplitude of left and right travelling wave for the rolls respectively and this depends on slow space X and time variables $\tau,\ T$, Knobloch and Luca [57],

$$X = \epsilon x, \quad \tau = \epsilon t, \quad T = \epsilon^2 t, \tag{4.71}$$

we assume that $A_{1L} = A_{1L}(X, \tau, T)$, $A_{1R} = A_{1R}(X, \tau, T)$. The differential operators can be expressed as

$$\frac{\partial}{\partial x} \rightarrow \frac{\partial}{\partial x} + \epsilon\frac{\partial}{\partial X}, \quad \frac{\partial}{\partial t} \rightarrow \frac{\partial}{\partial t} + \epsilon\frac{\partial}{\partial \tau} + \epsilon^2\frac{\partial}{\partial T}. \tag{4.72}$$

The solution of basic equations can be sought as power series in ϵ, the first approximation is given by eigenvector of the linearised problem

$$\begin{aligned}
u_0 =& -\frac{i\pi}{l_{oc}}\left[A_{1L}e^{i(l_{oc}x+m_{oc}y+\omega_{oc}t)} + A_{1R}e^{i(l_{oc}x+m_{oc}y-\omega_{oc}t)} - c\cdot c.\right]\cos\pi z,\\
v_0 =& 0,\\
w_0 =& \left[A_{1L}e^{i(l_{oc}x+m_{oc}y+\omega_{oc}t)} + A_{1R}e^{i(l_{oc}x+m_{oc}y-\omega_{oc}t)} + c\cdot c.\right]\sin\pi z\\
\theta_0 =& \frac{1}{M}\left[\frac{A_{1L}}{e_1}e^{i(l_{oc}x+m_{oc}y+\omega_{oc}t)} + \frac{A_{1R}}{e_1^*}e^{i(l_{oc}x+m_{oc}y-\omega_{oc}t)} + c\cdot c.\right]\sin\pi z,\\
C_0 =& \frac{1}{ML}\left[\frac{A_{1L}}{e_2}e^{i(l_{oc}x+m_{oc}y+\omega_{oc}t)} + \frac{A_{1R}}{e_2^*}e^{i(l_{oc}x+m_{oc}y-\omega_{oc}t)} + c\cdot c.\right]\sin\pi z,\\
H_{x_0} =& -\frac{m_{oc}\pi}{l_{oc}}\left[\frac{A_{1L}}{e_3}e^{i(l_{oc}x+m_{oc}y+\omega_{oc}t)} + \frac{A_{1R}}{e_3^*}e^{i(l_{oc}x+m_{oc}y-\omega_{oc}t)} + c\cdot c.\right]\cos\pi z,\\
H_{y_0} =& 0,\\
H_{z_0} =& im_{oc}\left[\frac{A_{1L}}{e_3}e^{i(l_{oc}x+m_{oc}y+\omega_{oc}t)} + \frac{A_{1R}}{e_3^*}e^{i(l_{oc}x+m_{oc}y-\omega_{oc}t)} - c\cdot c.\right]\sin\pi z.
\end{aligned} \tag{4.73}$$

where $\delta_{oc}^2 = (\pi^2 + q_{oc}^2)$, $e_1 = (\delta_{oc}^2 + i\omega_{oc})$ and $e_2 = (\delta_{oc}^2 + i\omega_{oc}\frac{\phi}{L}, e_3 = M\delta^2 + i\omega\phi\frac{Pr_2}{Pr_1})$, here e_1^*, e_2^* and e_3^* are complex conjugate of e_1, e_2 and e_3 respectively.. From equations (4.51), (4.52) and (4.53). At $O(\epsilon)$, the equation (4.51) gives critical Rayleigh number for the onset of oscillatory convection), at $O(\epsilon^2)$, from equation (4.52) $\mathcal{N}_0 = 0$ and $\mathcal{L}_1 w_0 = 0$ gives

$$\frac{\partial A_{1L}}{\partial \tau} - v_g\frac{\partial A_{1L}}{\partial X} = 0 \quad \text{and} \quad \frac{\partial A_{1R}}{\partial \tau} - v_g\frac{\partial A_{1R}}{\partial X} = 0, \tag{4.74}$$

where $v_g = (\partial\omega/\partial q)_{q=q_{oc}}$ is the group velocity and is real. We get,

$$\begin{aligned}
u_1 =&0,\ v_1 = 0,\ w_1 = 0,\\
\theta_1 =& -\frac{1}{M^2}\left[\frac{(|A_{1L}|^2+|A_{1R}|^2)}{e_1}+\frac{\pi A_{1L}A_{1R}^*}{e_1e_4}e^{2it\omega}+c\cdot c.\right]\sin 2\pi z,\\
C_1 =& -\frac{\pi}{M^2L^2}\left[\frac{(|A_{1L}|^2+|A_{1R}|^2)}{e_2}+\frac{A_{1L}A_{1R}^*}{e_2e_5}e^{2it\omega}+c\cdot c.\right]\sin 2\pi z,\\
H_{x_1} =& \frac{2m_{oc}\pi^2}{l_{oc}}\frac{Pr_2}{Pr_1}\left[\frac{(|A_{1L}|^2+|A_{1R}|^2)}{e_3}+\frac{A_{1L}A_{1R}^*}{e_3e_6}e^{2it\omega}+c\cdot c.\right]\cos 2\pi z,\\
H_{y_1} =& 0, H_{z_1}=0, \qquad (4.75)
\end{aligned}$$

by using zeroth and first order solutions, the coefficients of $\sin\pi z$ in $\mathcal{N}_1 - \mathcal{L}_2 w_0$ are equal to zero. We get

$$\Lambda_0\frac{\partial A_{1L}}{\partial T}+\Lambda_1\left(\frac{\partial}{\partial\tau}-v_g\frac{\partial}{\partial X}\right)A_{2L}-\Lambda_2\frac{\partial^2 A_{1L}}{\partial X^2}-\Lambda_3 A_{1L}$$
$$+\Lambda_4|A_{1L}|^2A_{1L}+\Lambda_5|A_{1R}|^2A_{1L}=0, \qquad (4.76)$$
$$\Lambda_0\frac{\partial A_{1R}}{\partial T}+\Lambda_1\left(\frac{\partial}{\partial\tau}-v_g\frac{\partial}{\partial X}\right)A_{2R}-\Lambda_2\frac{\partial^2 A_{1R}}{\partial X^2}-\Lambda_3 A_{1R}$$
$$+\Lambda_4|A_{1R}|^2A_{1R}+\Lambda_5|A_{1L}|^2A_{1R}=0, \qquad (4.77)$$

where

$$\begin{aligned}
\Lambda_0 =& \Big[\delta^4(1+\frac{\phi}{L})(m^2Q+\frac{\delta^2}{Da}+\Lambda\delta^2)-(\phi R_1-R_2)\frac{q^2\delta^2}{L}-\frac{q^2\delta^2\phi R_{12}Pr_2}{MPr_1}-\\
&\frac{3\delta^4\omega^2Pr_2}{M^2Pr_1^2}(1+\frac{\phi}{L})+\frac{\delta^2\phi Pr_2}{MPr_1}(\frac{1}{+}Da+\Lambda\delta^2)(\delta^4-\frac{3\phi^2\omega^2}{L})+\frac{\delta^4}{MPr_1}\\
&(\frac{\delta^4}{\phi}-\frac{3\omega^2}{L})\Big]+i\Big[\frac{2\delta^6\omega}{L}(\Lambda\phi+\frac{1}{MPr_1})+\frac{2\delta^6\omega}{MPr_1}(\frac{1}{\phi}+\frac{Pr_2}{MPr_1})+\frac{2\delta^2\phi\omega}{L}\\
&(m^2Q+\frac{\delta^2}{Da})+\frac{2\delta^4\phi\omega Pr_2}{MPr_1}(\frac{1}{Da}+\Lambda\delta^2)(1+\frac{\phi}{L})-\frac{4\delta^2\phi\omega^3Pr_2}{LM^2Pr_1^2}\Big],
\end{aligned}$$

$$\Lambda_1 =\Big[\frac{q^2\phi Pr_2}{LMPr_1}(R_2-\phi R_1)+\frac{\delta 6}{MPr_1}(\frac{1}{L}+\frac{1}{\phi}+\frac{Pr_2}{Pr_1})+\frac{\delta^2\phi}{L}(m^2Q-\frac{6\omega^2Pr_2}{M^2Pr_1^2})+$$
$$\delta^4\phi(\frac{1}{Da}+\delta^2\Lambda)(\frac{1}{L}+\frac{Pr_2}{Pr_1}+\frac{\phi Pr_2}{LMPr_1})\Big]+i\Big[\frac{3\delta^2\phi^2\omega Pr_2}{LMPr_1}(\frac{1}{Da}+\delta^2\Lambda)+$$
$$\frac{3\delta^2\omega}{MPr_1}(\frac{1}{L}+\frac{Pr_2}{MPr_1}+\frac{\phi Pr_2}{LMPr_1})\Big],$$
$$\Lambda_2 =\Big[\frac{\delta^2\phi\omega^2Pr_2}{MPr_1}(1+\frac{\phi}{L})(\frac{2}{Da}+3\Lambda\delta^2)+\frac{3\delta^4\omega^2}{MPr_1}(\frac{1}{L}+\frac{1}{\phi}+\frac{Pr_2}{MPr_1})-$$
$$(\frac{\omega^2}{MPr_1}+\phi R_1-R_2)+\delta^2(R_1-\frac{R_2}{L})(2Qq^2+\delta^2)+\frac{\phi\omega^2}{L}(m^2Q+\frac{2\delta^2}{Da})+$$
$$\delta^4(3m^2Q+\frac{4\delta^2}{Da}+5\Lambda\delta^4-\frac{3\omega^2\Lambda\delta^4}{L})\Big]+i\Big[\frac{\phi^2\omega^3Pr_2}{LMPr_1}(\frac{1}{Da}+2\delta^2)-$$
$$2\omega\delta^2(1+\frac{\phi}{L})(m^2Q-\frac{\omega^2Pr_2}{M^2Pr_1^2})-4\delta^6\omega(\frac{\Lambda\phi}{L}+\frac{1}{M\phi Pr_1}+\frac{\Lambda\phi Pr_2}{MPr_1})+$$
$$\delta^2\omega(\frac{2\omega 62}{LMPr_1}-\frac{3\delta^2\phi}{DaL}-4\delta^4\Lambda)+\phi\omega R_1(q^2+\delta^2)(\frac{1}{L}+\frac{Pr_2}{MPr_1})+$$
$$\omega(1+\frac{\phi Pr_2}{MPr_1})(\frac{(q^2+\delta^2)R_2}{L}+\frac{3\delta^4}{Da}),$$
$$\Lambda_3 =q^2(\delta^4-\frac{\phi^2\omega^2Pr_2}{LMPr_1})+iq^2\delta^2\phi\omega(\frac{1}{L}+\frac{Pr_2}{MPr_1}),$$
$$\Lambda_4 =-\frac{QPr_2}{4M\pi^2Pr_1}e_1e_2e_3\left[\frac{s_1}{e_3}(\frac{1}{e_6})+(\frac{s_1}{2}+s_2)(\frac{1}{e_3^3}+\frac{1}{|e_3|^2})\right]+\frac{R_1q^2}{4M^3}e_2e_3(\frac{1}{e_1}+\frac{1}{e_1^*})-$$
$$\frac{R_2q^2}{4M^3L^3}e_1e_3(\frac{1}{e_2}+\frac{1}{e_2^*})-\frac{Qm^2\delta^2}{4M}(\frac{Pr_2}{Pr_1})^2e_1e_2(\frac{1}{e_3}+\frac{1}{e_3^*}),$$
$$\Lambda_5 =-\frac{QPr_2}{Pr_1}e_1e_2e_3\left\{\frac{1}{4M\pi^2}\Big[\frac{s_1}{e_3}(\frac{1}{e_3}+\frac{1}{e_3^*})+(s_1+s_2)(\frac{1}{e_3^2}+\frac{1}{|e_3|^2})\Big]+\frac{1}{|e_3|^2e_6}(\frac{3s_1}{2}+s_2)\right\}+$$
$$\frac{R_1q^2}{M}e_2e_3\Big[\frac{1}{4M^2}(\frac{1}{e_1}+\frac{1}{e_1^*})+\frac{\pi^2}{M^2e_1e_4}\Big]-\frac{R_2q^2}{ML}e_1e_3\Big[\frac{1}{4M^2L^2}(\frac{1}{e_2}+\frac{1}{e_2^*})+\frac{\pi^2}{M^2L^2e_2e_5}\Big]-$$
$$\frac{Q\delta^2Pr_2}{Pr_1}e_1e_2\Big[\frac{m^2Pr_2}{4MPr_1}(\frac{1}{e_3}+\frac{1}{e_3^*})+\frac{m^2\pi^2Pr_2}{Pr_1e_3e_6}\Big] \tag{4.78}$$

$$e_1 =i\omega+\delta^2, \qquad e_4 =i\omega+2\pi^2, \qquad s_1 =-2m^2\pi^4\frac{Pr_2}{Pr_1},$$
$$e_2 =\frac{\phi}{L}\omega+\delta^2, \qquad e_5 =\frac{\phi}{L}i\omega+2\pi^2, \qquad s_2 =-l^2m^2\pi^2\frac{Pr_2}{Pr_1},$$
$$e_3 =\phi\frac{Pr_2}{Pr_1}i\omega+\delta^2, \qquad e_6 =\phi\frac{Pr_2}{Pr_1}i\omega+2M\pi^2.$$

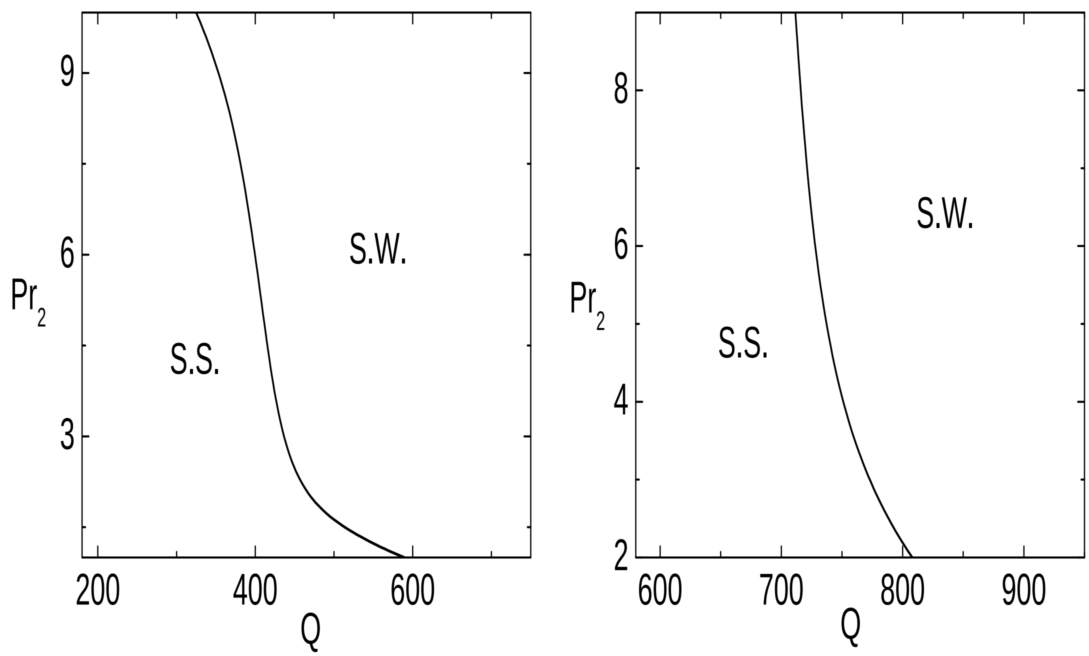

Figure 4.11: Stability regions of steady state (S.S) and standing waves $Da = 1500$, $\Lambda = 2$, $M = 0.9$, $\phi = 0.85$, (a)$\frac{Pr_2}{Pr_1} = 3$, (b)$\frac{Pr_2}{Pr_1} = 6$

Solving equations (4.76) and (4.77) by taking $\xi' = \nu_g\tau + X$ and $\eta' = \nu_g\tau - X$, we get

$$2v_g\Lambda_1\frac{\partial A_{2L}}{\partial\eta'} = -\Lambda_0\frac{\partial A_{1L}}{\partial T} + \Lambda_2\frac{\partial A_{1L}}{\partial X^2} + \Lambda_3 A_{1L} - \left(\Lambda_4|A_{1L}|^2 + \Lambda_5|A_{1R}|^2\right)A_{1L}, \quad (4.79)$$

$$2v_g\Lambda_1\frac{\partial A_{2R}}{\partial\eta'} = -\Lambda_0\frac{\partial A_{1R}}{\partial T} + \Lambda_2\frac{\partial A_{1R}}{\partial X^2} + \lambda_3 A_{1R} - \left(\Lambda_4|A_{1R}|^2 + \Lambda_5|A_{1L}|^2\right)A_{1R}. \quad (4.80)$$

This integrating equations (5.69) and (5.70) over η' and ξ' respectively, we get

$$\Lambda_0\frac{\partial A_{1L}}{\partial T} = \Lambda_2\frac{\partial A_{1L}}{\partial X^2} + \lambda_3 A_{1L} - \left(\Lambda_4|A_{1L}|^2 + \Lambda_5|A_{1R}|^2\right)A_{1L}, \quad (4.81)$$

$$\Lambda_0\frac{\partial A_{1R}}{\partial T} = \Lambda_2\frac{\partial A_{1R}}{\partial X^2} + \lambda_3 A_{1R} - \left(\Lambda_4|A_{1R}|^2 + \Lambda_5|A_{1L}|^2\right)A_{1R}. \quad (4.82)$$

Equations (4.81) and (4.82) are left and right moving waves known as coupled one-dimensional LG equations.

Travelling wave and standing wave

Dropping the variable X from equations (4.81) and (4.82)

$$\frac{dA_{1L}}{dT} = \frac{\Lambda_3}{\Lambda_0}A_{1L} - \frac{\Lambda_4}{\Lambda_0}A_{1L}|A_{1L}|^2 - \frac{\Lambda_5}{\Lambda_0}A_{1L}|A_{1R}|^2, \quad (4.83)$$

$$\frac{dA_{1R}}{dT} = \frac{\Lambda_3}{\Lambda_0}A_{1R} - \frac{\Lambda_4}{\Lambda_0}A_{1R}|A_{1R}|^2 - \frac{\Lambda_5}{\Lambda_0}A_{1R}|A_{1L}|^2. \quad (4.84)$$

Put

$$\beta' = \frac{\Lambda_3}{\Lambda_0}, \quad \gamma' = -\frac{\Lambda_4}{\Lambda_0} \quad \text{and} \quad \delta' = -\frac{\Lambda_5}{\Lambda_0}.$$

Then equations (4.83) and (4.84) take the following form

$$\frac{dA_{1L}}{dT} = \beta' A_{1L} + \gamma' A_{1L}|A_{1L}|^2 + \delta' A_{1L}|A_{1R}|^2, \quad (4.85)$$

$$\frac{dA_{1R}}{dT} = \beta' A_{1R} + \gamma' A_{1R}|A_{1R}|^2 + \delta' A_{1R}|A_{1L}|^2. \quad (4.86)$$

Where

$$\begin{aligned} A_{1L} &= a_L e^{i\phi_L} & a_L &= |A_{1L}| & \phi_L &= arg(A_{1L}) \\ A_{1R} &= a_L e^{i\phi_R} & a_R &= |A_{1R}| & \phi_R &= arg(A_{1R}) \\ \beta' &= \beta_1 + i\beta_2 & \gamma' &= \gamma_1 + i\gamma_2 & \delta' &= \delta_1 + i\delta_2 \end{aligned} \quad (4.87)$$

Substituting of A_{1L},A_{1R},β', γ' and δ' in (4.85) and (4.86). we get,

$$(a_L, a_R) = (-\beta_1/(\gamma_1 + \delta_1), -\beta_1/(\gamma_1 + \delta_1)), \quad (4.88)$$

Substituting A_{1L}, A_{1R}, β' , γ' and δ' in (4.85) and (4.86). we get $a_L = -\beta_1/(\gamma_1+\delta_1)$ and $a_R = -\beta_1/(\gamma_1+\delta_1)$ for standing waves. $(a_L, a_R) = (a_L, 0)$ for left travelling waves and $(a_L, a_R) = (0, a_R)$ for right travelling waves. $(a_L, a_R) = (0, 0)$ for conduction state. Standing waves exist if $| A_L |^2 = | A_R |^2 = -\frac{\beta_1}{\gamma_1+\delta_1} > 0$ and supercritical if

$\gamma_1 + \delta_1 < 0$. Standing waves are stable if $\beta_1 > 0, \gamma_1 < 0$ and

(i) if $\delta_1 > 0$, then $-\gamma_1 > \delta_1 > 0$,

(ii) if $\delta_1 < 0$, then $-\gamma_1 > -\delta_1 > 0$.

Travelling waves exist if $\mid A_L \mid^2 = -\frac{\beta_1}{\gamma_1} > 0$ and they are supercritical if $\gamma_1 < 0$. Travelling waves are stable if $\beta_1 > 0, \gamma_1 < 0$ and $\delta_1 < \gamma_1 < 0$. We studied onset of Hopf bifurcation of stability regions of travelling, standing wave and steady states in figure 4.11. It can be observed that the stability regions of standing waves increases when Pr_2/Pr_1 increases for fixed parameters and fixed Pr_1.

4.5 Conclusions

This chapter studied linear and weakly nonlinear stabilities of thermohaline convection in a sparsely packed porous medium over horizontal magnetic field. Derived thermal Rayleigh value at the onset of stationary and oscillatory convection by assuming periodic disturbances along x-direction, y-direction and both directions, obtained critical thermal Rayleigh values at the corresponding critical wave numbers by considering R_1 as dependent variable. The chapter also traced marginal stability curves between thermal Rayleigh value and wave number. An analytical relation was found for stationary oscillatory convective curves in by considering R_1 as an independent variable. Takens-Bogdanov bifurcation and co-dimension two bifurcation points were identified and shown in neutral curves Figs 4.2 -4.5. We observed that thermal and magnetic Prandtl numbers are not affected on convective stationary thermal Rayleigh value. Two dimensional LG equation was derived at onset of stationary mode, studied heat transport from Nusselt number was explored and long wave length Eukhaus and Zigzag instabilities. At the onset of super critical pitchfork bifurcation we obtained two dimensional LG equation which is valid only for $\lambda_3 > 0$. If $\lambda_3 = 0$ we get tricritical bifurcation point. $\lambda_3 = 0$ is a necessary condition to study heat transport for various physical parameters. Nusselt number grows exponentially if $\frac{R}{R_{sc}} > 1$ and decay if $\frac{R}{R_{sc}} \leq 1$ for $Nu > 1$. Nusselt number grows exponentially at unit value. At the onset of Hopf bifurcation, we obtained one dimensional nonlinear coupled LG equations by using multiple scale analysis and studied secondary instabilities. For $\beta_1 > 0$ and $\gamma_1 < 0$, travelling and standing waves are stable and for $\beta_1 < 0$ and $\gamma_1 < 0$ travelling and standing waves are unstable (see Fig. 4.11). From the ratio Pr_2/Pr_1, first we getting steady state and it is replaced by standing waves, and travelling waves are unstable.

The region of existing standing waves increases by increasing the ratio of magneto and thermal prandtl number.

Chapter 5

Nonlinear Thermohaline Convection in a Sparsely Packed Porous Medium with the Effect of Rotation

5.1 Introduction

Thermohaline convection is a double diffusive convection, density gradients are caused by temperature and solute concentration. Nield and Bejan [79] have made exhaustive investigation on various porous mediums for convective problems. Darcy and Brinkman equation are for fluid flow through porous medium. In case of significant macroscopic and shear inertial effects, DLB equation is adequate enough to describe the fluid flow in a porous medium. Thermohaline convection in a porous medium was first studied by Nield [78], Poulikakos [88], Sunil et al. [117], Tagare et al. [120] and Benerji et al. [9]. Thermohaline convection in porous media has many applications in atmospheric science, astrophysics, earth's mantle convection, oceanic and continental crust, seawater flow, solidification of binary alloys.

The effect of rotation in thermohaline convection has important implications for mixing of light alloys at the earth's outer core, mixing of different masses of water in oceans and mixing of Helium with Hydrogen in stellar core. This chapter studies the thermohaline convection in rotating fluid with a constant angular velocity about the vertical axis between horizontal stress free boundaries and in a sparsely packed porous medium. Pearlstein [86], Chakrabarti et al. [32] and Tagare et al. [121] studied the effect of instabilities of thermohaline convection on rotation.

Normal mode is used to understand linear stability analysis. Two dimensional Ginzburg Landau equation was derived and the transport of heat by convection was investigated in addition to the occurrence of secondary instabilities. The system of one dimensional Ginzburg Landau equations are derived and obtained the stability regions of steady state, standing and travelling waves.

5.2 Basic Equations

Consider an infinitely horizontal fluid sparsely packed porous medium rotating with an angular velocity Ω about z-axis of depth d. This layer is heated from below and

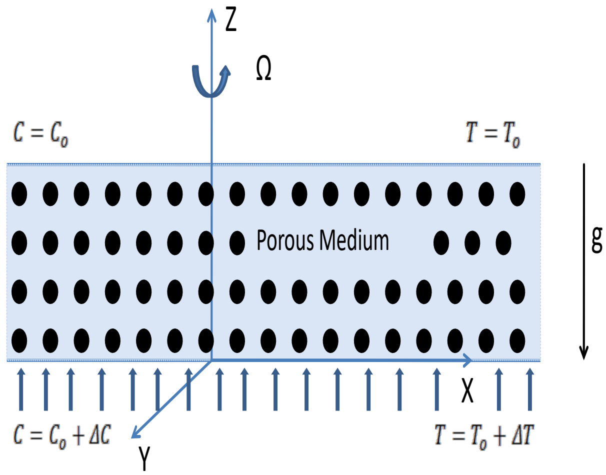

Figure 5.1: Physical Configuration

saturated with a solute solution of a specific concentration gradient. The salinity and temperature differences across the stress-free boundaries are $\Delta S'$ and $\Delta T'$. Darcy-lapwood-Brinkman model was used to study sparsely packed porous medium. The governing equations, the equation of continuity, Darcy-Lapwood -Brinkman model for momentum equation, energy equation and solute concentration over Boussinesq approximation have been included to understand the phenomenon of rotation in a fluid that is sparely packed and rotating with a fixed angular velocity are

$$\nabla'.\overline{V}' = 0, \tag{5.1}$$

$$\rho_0' \left[\frac{1}{\phi}\frac{\partial \overline{V}'}{\partial t'} + \overline{\Omega} \times (\overline{\Omega} \times \overline{V}') + \frac{2}{\phi}(\overline{\Omega} \times \overline{V}') + \frac{1}{\phi^2}(\overline{V}'.\nabla')\overline{V}' \right] =$$

$$\mu_e \nabla'^2 \overline{V}' - \nabla' p' + \rho' \overline{g} - \frac{\mu}{\kappa}\overline{V}', \tag{5.2}$$

$$M\frac{\partial T'}{\partial t'} + (\overline{V}'.\nabla')T' = \kappa_T \nabla'^2 T', \tag{5.3}$$

$$\phi\frac{\partial S'}{\partial t'} + (\overline{V}'.\nabla')S' = \kappa_S \nabla'^2 S'. \tag{5.4}$$

Fluid density ρ' is defined as

$$\rho' = \rho_0' \left[1 - \beta_s(S' - S_b') - \alpha_t(T' - T_b')\right], \tag{5.5}$$

where thermal expansion coefficient $\alpha_t = -\rho_0'^{-1}(\frac{\partial \rho'}{\partial T'})$, solutal expansion coefficient $\beta_s = -\rho_0'^{-1}(\frac{\partial \rho'}{\partial S'})$, mean flow velocity is $\overline{V}'$, pressure is P', porosity is ϕ, acceleration due to gravity is g, temperature is T', κ_T is thermal diffusivity, S' is saline concentration, M is dimensionless heat capacity, κ_S saline diffusivity, κ is the permeability of the porous medium and μ is fluid viscosity. The conduction state is characterized by $\overline{V}' = 0$, $T_s' = T_b' - (\frac{\triangle T'}{d})\overline{z}'$ and $S_s' = S_b' - (\frac{\triangle S'}{d})\overline{z}'$. Now the temperature and concentration perturbations can be written as $\theta' = T' - T_s'$ and $C' = S' - S_s'$. We use the scaling $x = \frac{x'}{d}$, $y = \frac{y'}{d}$, $z = \frac{z'}{d}$, $t = \frac{t'}{(Md^2/k)}$, $u = \frac{u'}{(k/Md)}$, $v = \frac{v'}{(k/Md)}$, $w = \frac{w'}{(k/Md)}$, $\theta = \frac{\theta'}{\triangle T'}$, $C = \frac{c'}{\triangle S'}$, $p = \frac{p'}{(\rho_0' M^{-1} k^2 d^{-2})}$,Thermal Prandtl number $Pr = \frac{\nu}{\kappa_T}$, Lewis number $L = \frac{\kappa_S}{\kappa_T}$, Darcy number $Da = \frac{\kappa}{d^2}$, Thermal Rayleigh number $R_1 = \frac{\alpha g \triangle T d^3}{\nu k_T}$, Salinity Rayleigh number $R_2 = \frac{\alpha g \triangle S d^3}{\nu k_S}$, Taylor number $Ta = \frac{4\Omega^2 d^4}{\nu^2}$. The basic non dimensionless equations are

$$\nabla \cdot \overline{V} = 0, \tag{5.6}$$

$$\frac{1}{M^2 \phi Pr}\left[\frac{1}{\phi}(\overline{V}\cdot\nabla)\overline{V} + \frac{\partial \overline{V}}{\partial t}\right] - (R_1\theta - R_2 C)\hat{e}_z + \frac{1}{MDa}\overline{V} = \\ -\nabla\left(\frac{P}{MPr} - \frac{TaPr}{8M\phi^2}|\hat{e}_z \times \overline{V}|^2\right) + \frac{Ta^{\frac{1}{2}}}{\phi}(\overline{V}\times\hat{e}_z) + \frac{\Lambda}{M}\nabla^2\overline{V}, \tag{5.7}$$

$$\left(\frac{\partial}{\partial t} - \nabla^2\right)\theta + \frac{1}{M}(\overline{V}\cdot\nabla)\theta = \frac{\omega}{M}, \tag{5.8}$$

$$\frac{\phi}{L}\frac{\partial C}{\partial t} + \frac{1}{ML}(\overline{V}\cdot\nabla)C = \frac{\omega}{ML} + \nabla^2 C. \tag{5.9}$$

The curl of equation (5.7) is

$$\Big[\frac{1}{M^2\phi Pr}\frac{\partial}{\partial t} + \frac{1}{MDa} - \frac{\Lambda}{M}\nabla^2\Big](\nabla\times\overline{V}) - \frac{Ta^{1/2}}{\phi}\nabla\times(\overline{V}\times\hat{e}_z) - \nabla\times(R_1\theta\hat{e}_z) \\ + \nabla\times(R_2 C\hat{e}_z) = -\frac{1}{M^2\phi^2 Pr}\nabla\times(\overline{V}.\nabla)\overline{V}. \tag{5.10}$$

The curl of equation (5.10) is

$$\Big[\frac{1}{M^2\phi Pr}\frac{\partial}{\partial t}+\frac{1}{MDa}-\frac{\Lambda}{M}\nabla^2\Big](\nabla\times\nabla\times\overline{V})-\frac{Ta^{1/2}}{\phi}\nabla\times\nabla\times(\overline{V}\times\hat{e}_z)$$
$$-\nabla\times\nabla\times(R_1\theta\hat{e}_z)+\nabla\times\nabla\times(R_2C\hat{e}_z)=-\frac{1}{M^2\phi^2 Pr}\nabla\times\nabla\times(\overline{V}.\nabla)\overline{V}. \tag{5.11}$$

Now taking z-component of equations (5.10) and (5.11)

$$\Big[\frac{1}{M^2\phi Pr}\frac{\partial}{\partial t}+\frac{1}{MDa}-\frac{\Lambda}{M}\nabla^2\Big]w_z-\frac{Ta^{1/2}}{\phi}\frac{\partial w}{\partial z}=-\frac{1}{M^2\phi^2 Pr}\Big[\nabla\times(\overline{V}.\nabla)\overline{V}\Big].\hat{e}_z, \tag{5.12}$$

$$\Big[\frac{1}{M^2\phi Pr}\frac{\partial}{\partial t}+\frac{1}{MDa}-\frac{\Lambda}{M}\nabla^2\Big]\nabla^2 w-\frac{Ta^{1/2}}{\phi}\frac{\partial w_z}{\partial z}-R_1\nabla_h^2\theta+R_2\nabla_h^2 C=$$
$$-\frac{1}{M^2\phi^2 Pr}\Big[\nabla\times\nabla\times(\overline{V}.\nabla)\overline{V}\Big].\hat{e}_z. \tag{5.13}$$

Where $\nabla\times\overline{V}=\overline{W}=(w_x,w_y,w_z)$ and $\nabla_h^2=\frac{\partial^2}{\partial x^2}+\frac{\partial^2}{\partial y^2}$. By eliminating w_z, θ, C from equations (5.8), (5.9), (5.12) and equation (5.13), we get

$$\mathcal{L}w=\mathcal{N}, \tag{5.14}$$

where

$$\mathcal{L}=\mathcal{D}\mathcal{D}_\phi\Big(\mathcal{D}_{Pr}^2\nabla^2+\frac{Ta}{\phi^2}\partial_z^2\Big)-\frac{1}{M}\mathcal{D}_{Pr}\nabla_h^2(R_1\mathcal{D}_\phi-\frac{R_2}{M}\mathcal{D}), \tag{5.15}$$

$$\mathcal{N}=\frac{1}{M^2\phi^2 Pr}\mathcal{D}\mathcal{D}_\phi\mathcal{D}_{Pr}\Big\{\nabla\times\big[(\overline{V}.\nabla)\overline{W}-(\overline{W}.\nabla)\overline{V}\big]\Big\}.\hat{e}_z+\frac{Ta^{\frac{1}{2}}}{M^2\phi^3 Pr}\mathcal{D}\mathcal{D}_\phi$$
$$\Big[(\overline{V}\nabla)w_z-(\overline{W}.\nabla)w\Big]-\frac{1}{M}\mathcal{D}_{Pr}\nabla_h^2(\overline{V}.\nabla)(R_1\mathcal{D}_\phi\theta-\frac{R_2}{M}\mathcal{D}C), \tag{5.16}$$

where $\mathcal{D}=(\frac{\partial}{\partial t}-\nabla^2)$, $\mathcal{D}_\phi=(\frac{\phi}{L}\frac{\partial}{\partial t}-\nabla^2)$, $\mathcal{D}_{Pr}=(\frac{1}{M^2\phi Pr}\frac{\partial}{\partial t}+\frac{1}{MDa}-\frac{\Lambda}{M}\nabla^2)$, and $\partial_z=\frac{\partial}{\partial z}$. The boundary conditions are follows from the section 2.2.1.

5.3 Linear Stability Analysis

The linearised system $\mathcal{L}w = \mathcal{N}$ is $\mathcal{L}\omega = 0$, by assuming periodic disturbances with a period $\frac{2\pi}{q}$ along x-direction at a growth rate p of the form $w = W(z)e^{iqx+pt}$ and we obtain

$$\begin{aligned}&\Bigg[\left(\frac{1}{M^2\phi Pr}p + \frac{1}{MDa} + \frac{\Lambda}{M}q^2 - \frac{\Lambda}{M}D^2\right)^2\left(\frac{\phi}{L}p + q^2 - D^2\right)(p+q^2-D^2)(D^2-q^2)\\&+\frac{R_1}{M}\left(\frac{1}{M^2\phi Pr}p + \frac{1}{MDa} + \frac{\Lambda}{M}q^2 - \frac{\Lambda}{M}D^2\right)\left(\frac{\phi}{L}p + q^2 - D^2\right)(D^2-q^2)q^2\\&-\frac{R_2}{ML}\left(\frac{1}{M^2\phi Pr}p + \frac{1}{MDa} + \frac{\Lambda}{M}q^2 - \frac{\Lambda}{M}D^2\right)(p+q^2-D^2)q^2\\&+\frac{Ta}{\phi^2}\left(\frac{\phi}{L}p + q^2 - D^2\right)(p+q^2-D^2)D^2\Bigg]W(z) = 0, \qquad (5.17)\end{aligned}$$

put $W(z) = \sin\pi z$ and growth rate $p = i\omega$ in to equation (5.17), we get

$$\begin{aligned}R_1 = &\left[\frac{\Lambda_a\delta^4}{q^2} - \frac{\delta^2\omega^2}{M_1q^2} + \frac{TaM^2\pi^2}{\phi^2q^2}\frac{\Lambda_a^2\delta^2 + \frac{\omega^2}{M_1}}{\Lambda_a^2 + \frac{\omega^2}{M_1^2}} + \frac{R_2}{L}\frac{\delta^4 + \frac{\phi}{L}\omega^2}{\delta^4 + \frac{\phi^2}{L^2}\omega^2}\right]+\\&i\omega\frac{1}{D_1}\Bigg[A_1\omega^4 + B_1\omega^2 + C_1\Bigg], \qquad (5.18)\end{aligned}$$

where

$$A_1 = \frac{\phi^2\delta^2}{M_1^2L^2q^2}\left(\Lambda_a + \frac{\delta^2}{M_1}\right), \qquad (5.19)$$

$$B_1 = \left(\Lambda_a + \frac{\delta^2}{M_1}\right)\left[\frac{\delta^6}{M_1^2q^2} + \frac{\Lambda_a^2\phi^2\delta^2}{L^2q^2}\right] + \left(\Lambda_a - \frac{\delta^2}{M_1}\right)\frac{TaM^2\pi^2\delta^4}{L^2q^2} + \frac{R_2\delta^2}{M_1^2L}\left(1 - \frac{\phi}{L}\right), \qquad (5.20)$$

$$C_1 = \frac{\delta^6}{q^2}\left(\Lambda_a + \frac{\delta^2}{M_1}\right)\Lambda_a^2 + \frac{TaM^2\pi^2}{\phi^2q^2}\left(\Lambda_a - \frac{\delta^2}{M_1}\right)\delta^4 + \frac{R_2\Lambda_a^2\delta^2}{L}\left(1 - \frac{\phi}{L}\right), \qquad (5.21)$$

$$D_1 = \left[\Lambda_a^2 + \omega^2\frac{1}{M_1^2}\right]\left[\delta^4 + \frac{\phi^2}{L^2}\omega^2\right], \qquad (5.22)$$

where $\Lambda_a = \frac{1}{Da} + \Lambda\delta^2$ and $M_1 = M\phi Pr$.

5.3.1 Rayleigh Number R_1 is a Dependent Variable

Stationary Convection:

The onset of stationary convection take $\omega = 0$ in to equation (5.18) leads to,

$$R_{1s} = \Lambda_a \frac{\delta^4}{q^2} + \frac{TaM^2\pi^2\delta^2}{\Lambda_a\phi^2 q^2} + \frac{R_2}{L}, \tag{5.23}$$

where R_{1s} represents the stationary convection of Rayleigh number R_1. Differentiating equation (5.23) with respect to q and equating it to zero, we get

$$\begin{gathered} 2\Lambda^3 s^5 + \left(\frac{5}{Da} - 3\Lambda\pi^2\right)\Lambda^2 s^4 + 4\frac{\Lambda}{Da}\left(\frac{1}{Da} - 2\Lambda\pi^2\right)s^3 + \\ \left(\frac{1}{Da^3} - \frac{7\Lambda\pi^2}{Da^2} + \frac{TaM^2\pi^2}{\Lambda\phi^2}(\frac{1}{Da} - \Lambda\pi^2)\right)s^2 - \left(\frac{2TaM^2\pi^4}{\Lambda\phi^2 Da} + \frac{2\pi^2}{Da^3}\right)s + \\ \frac{TaM^2\pi^2\pi^4}{\Lambda\phi^2 Da} = 0 \end{gathered} \tag{5.24}$$

and $s = \delta^2 = q^2 + \pi^2$. From equation (5.24), the critical wave number $q = q_{sc},\ \delta = \delta_{sc}$ and critical Rayleigh number is R_{1sc},

$$R_{1sc} = \Lambda_{asc}\frac{\delta_{sc}^4}{q_{sc}^2} + \frac{TaM^2\pi^2\delta_{sc}^2}{\phi^2 q_{sc}^2\Lambda_{as}} + \frac{R_2}{L}, \tag{5.25}$$

where $\Lambda_{asc} = \frac{1}{Da} + \Lambda\delta_{sc}^2$. For large value of Da, equations (5.24) and (5.25) are

$$2(\frac{q}{\pi})^6 + 3(\frac{q}{\pi})^4 = 1 + \frac{TaM^2}{\Lambda^2\phi^2\pi^4} \tag{5.26}$$

$$R_{1sc} = \frac{\Lambda\delta_{sc}^6}{q_{sc}^2} + \frac{TaM^2\pi^2}{\Lambda\phi^2 q_{sc}^2} + \frac{R_2}{L} \tag{5.27}$$

Eliminating Ta from equations (5.26) and (5.27) we get

$$R_{1sc} = 3\delta_{sc}^4 + \frac{R_2}{L} \tag{5.28}$$

Oscillatory Convection:

The thermal Rayleigh number R_1 is a real number and equating imaginary part of equation (5.18) to zero, we obtain$A_1\omega^4 + B_1\omega^2 + C_1 = 0$. From these

$$\omega^2 = \frac{-B_1 + \sqrt{B_1^2 - 4A_1C_1}}{2A_1},$$

Where A_1, B_1 and C_1 are from the equations (5.19), (5.20) and (5.21). The value A_1 is always positive.According to Descarte's rule the quadratic equation has two positive roots because of $B_1 < 0$ and $C_1 > 0$ when $\frac{L}{\phi} < \Lambda M\phi Pr < 1$. By substituting ω^2 in real part of R_1 in equation (5.18), we get oscillatory thermal Rayleigh number R_{1o},

$$R_{1o} = \frac{\Lambda_a\delta^4}{q^2} - \frac{\delta^2\omega^2}{M_1q^2} + \frac{TaM^2\pi^2}{\phi^2q^2}\frac{\Lambda_a^2\delta^2 + \frac{\omega^2}{M_1}}{\Lambda_a^2 + \frac{\omega^2}{M_1^2}} + \frac{R_2}{L}\frac{\delta^4 + \frac{\phi}{L}\omega^2}{\delta^4 + \frac{\phi^2}{L^2}\omega^2} \tag{5.29}$$

Takens-Bogdanov bifurcation points arises,

$$R_{1s}(q_s) = R_{1o}(q_o) = R_{1c}(q_c) \tag{5.30}$$

when

$$q_s = q_o = q_c \tag{5.31}$$

Co-dimension two bifurcation points arises,

$$R_{1sc}(q_{sc}) = R_{1oc}(q_{oc}) \tag{5.32}$$

when

$$q_{sc} \neq q_{oc}. \tag{5.33}$$

In Figures 5.2 - 5.4, solid and dotted marginal curves represent the thermal stationary and oscillatory Rayleigh numbers respectively. Stationary thermal Rayleigh number is independent of Prandtl number Pr. There is variation of Rayleigh number with wave number for different values of physical parameters viz. Ta, R_2 and Pr.

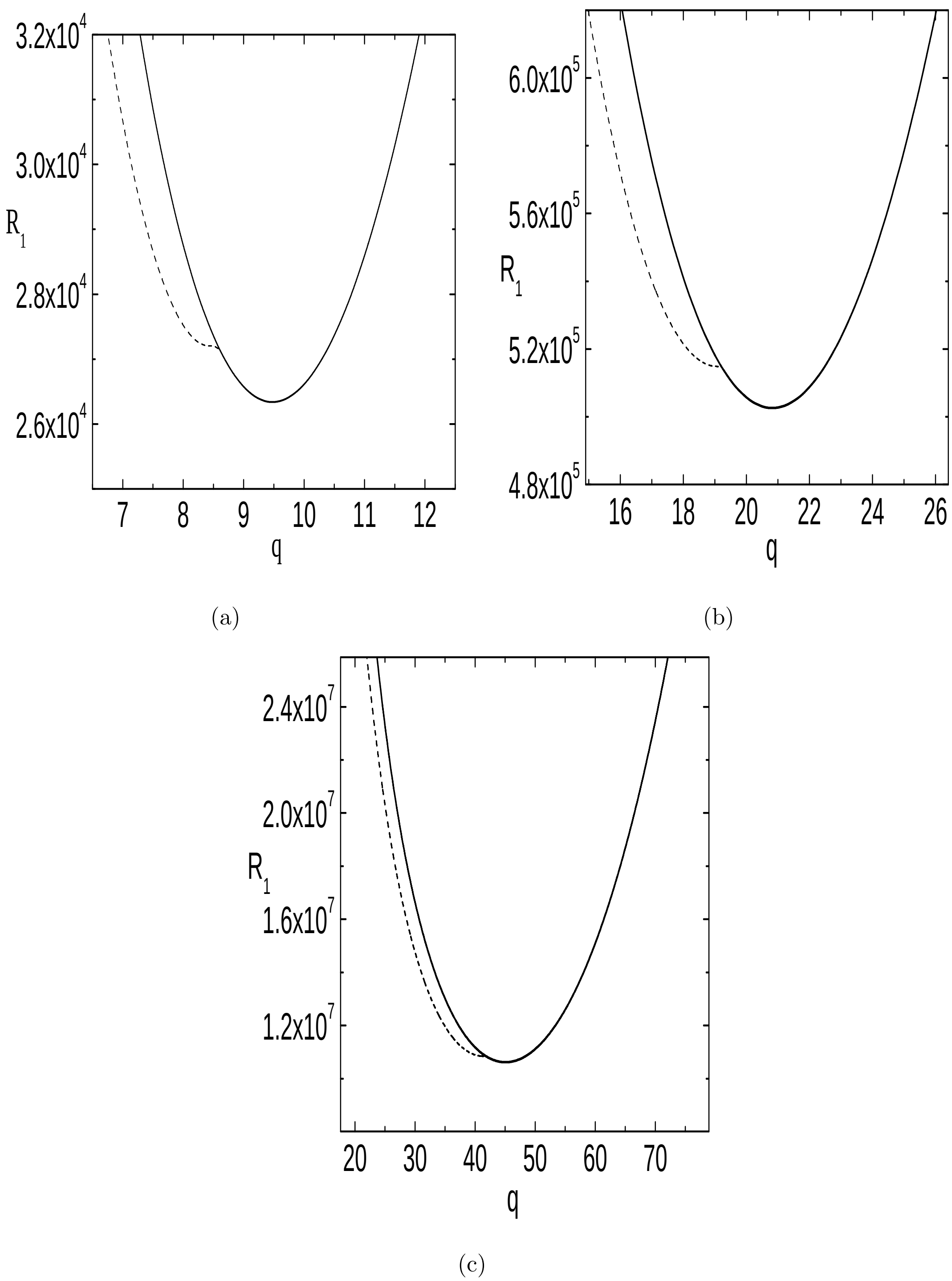

Figure 5.2: The neutral curves in (q, R_1) plane for $Da = 1500, \Lambda = 0.85,\ M = 1,$ $\phi = 0.9,\ Pr = 0.5,\ R_2 = 0.5,\ L = 0.1$, $(a) Ta = 10^5$, $(b) Ta = 10^7$, $(c) Ta = 10^9$.

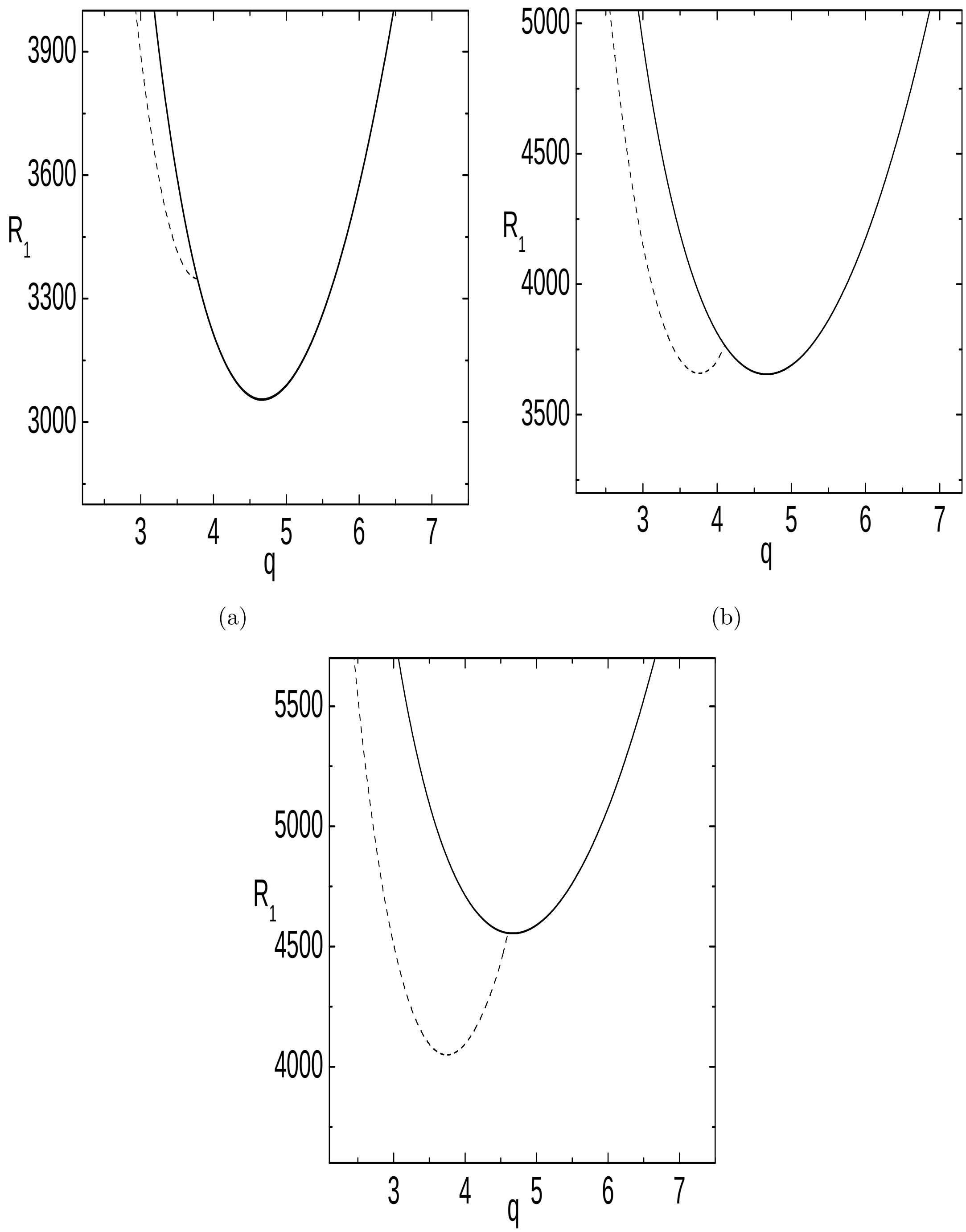

(a) (b)

(c)

Figure 5.3: The neutral curves in (q, R_1) plane for $Da = 1500$, $\Lambda = 0.85$, $M = 1$, $\phi = 0.9$, $Pr = 0.5, Ta = 2000 and\ L = 0.1$ at (a) $R_2 = 50$, (b) $R_2 = 110$, (c) $R_2 = 200$.

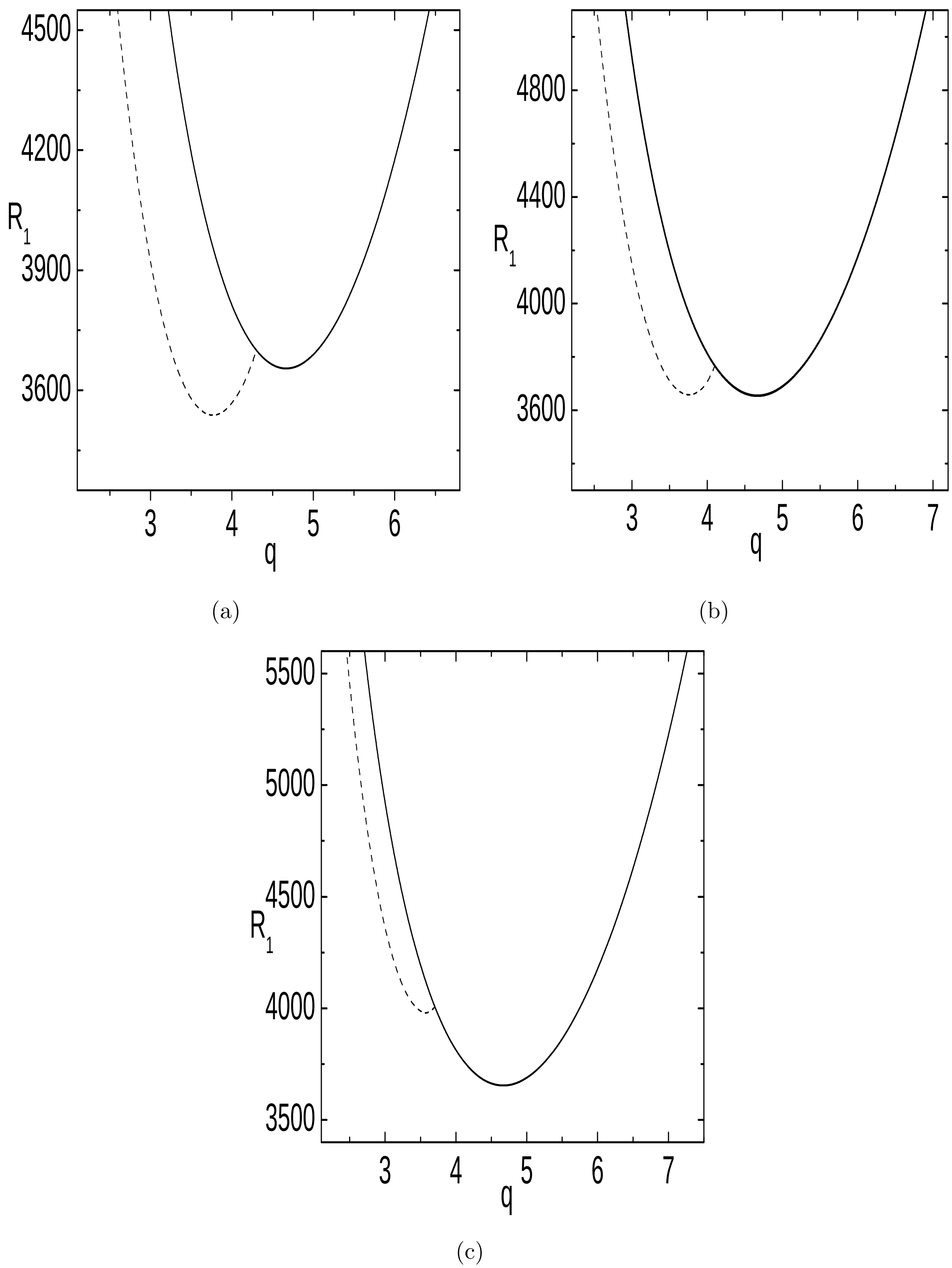

Figure 5.4: The neutral curves in (q, R_1) plane for for $Da = 1500, \Lambda = 0.85,\ M = 1,\ \phi = 0.9, Ta = 2000,\ R_2 = -0.5$ and $L = 0.1$ at $(a)\ Pr = 0.25$, $(b)\ Pr = 0.5$, $(c)\ Pr = 0.75$.

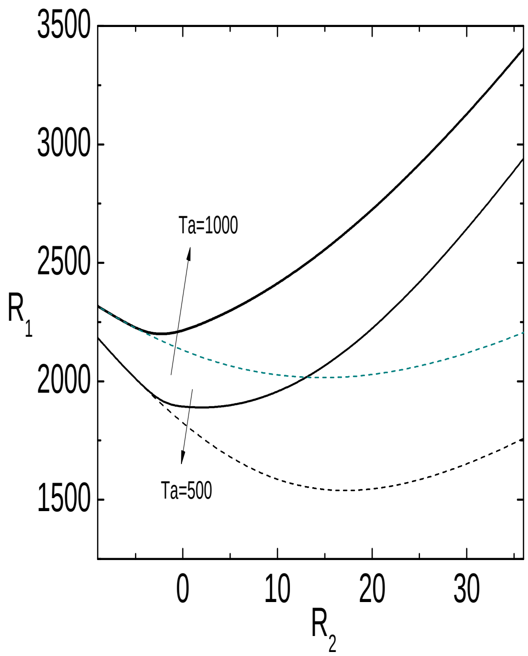

(a)

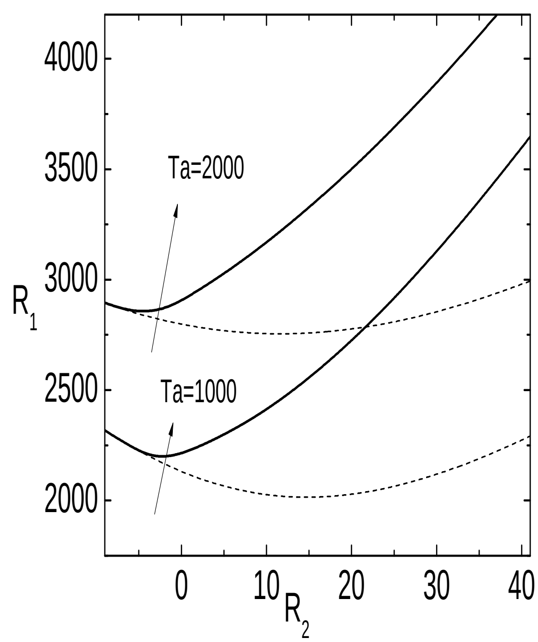

(b)

Figure 5.5: Solid and dotted lines represents for stationary and oscillatory Rayleigh number plotted in (R_1, R_2) plane for $Da = 1500$, $\Lambda = 0.85$, $M = 1$, $\phi = 0.9$, $Pr = 0.5$ and $L = 0.1$ at $Ta = 500,\ 1000,\ 2000$.

In Figure 5.2 the Ta value of rotation is increased while other parameters remain constant. Thus, Rayleigh value increased along with parallel rolls. In Figures 5.3 and 5.4, salinity Rayleigh R_2 value and Pr increased respectively, we also observed increases in Rayleigh value along with wave number. Takens-Bogdanov and co-dimention two bifurcation points were identified on neutral curves. In Figures 5.3(b) and 5.4(b), co-dimension two bifurcation point exists. Figure 5.5 is plotted in $(R_2,\ R_1)$ plane, the region of Salinity Rayleigh value R_2 verses thermal Rayleigh value R_1 over stationary and oscillatory waves increased from internal forces over the rotating field. The intersection point of a solid line and dotted line appears at corresponding to the bifurcation point associated with a TakensBogdanov bifurcation point.

5.3.2 Rayleigh number R_1 is an independent variable

Putting $W = \sin \pi z$ and $p = i\omega$ into equation(5.17), we get

$$\left(\omega^4 - C\omega^2 + E\right) + i\omega\left(B\omega^2 - D\right) = 0 \tag{5.34}$$

where

$$\begin{aligned}
B =& \frac{2MPr\phi}{Da} + \delta^2\Big(1 + \frac{L}{\phi} + 2MPr\Lambda\phi\Big),\\
C =& 2MPr\delta^4\Lambda(L+\phi) + M^2Pr^2 + \delta^4 + \lambda^2\phi^2 + \frac{M^2Pr^2\phi^2}{Da^2} + 2M^2Pr^2\phi^2\delta^2\Lambda\Big)\\
&+ \frac{1}{Da}\Big(2MPr(L+\phi)\delta^2 + \frac{1}{\delta^2}\Big(M^4\pi^2Pr^2Ta + MPrq^2(R_1\phi + R_2)\Big),\\
D =& \frac{MPr\delta^2}{Da^2\delta^2\phi}\Big[MPr\delta^2\phi^2(L+\phi) + 2Da\delta^4\phi(L + LMPr\Lambda\phi + MPr\Lambda\phi^2) +\\
& Da^2\Big(LM^3\pi^2PrTa + M^3\pi^2PrTa\phi + 2L\delta^6\Lambda\phi + LMPr\delta^6\Lambda^2\phi^2\Big)\Big]\\
E =& \frac{M^2Pr^2}{Da^2\phi}\Big[Da^2LM^2\pi^2Ta\delta^2 + L\delta^4\phi^2(1+Da\delta^2\Lambda)^2 - Daq^2\phi^2(1+Da\delta^2\Lambda)(R_1 - R_2)\Big].
\end{aligned} \tag{5.35}$$

Stationary Convection

Putting $\omega = 0$ into equation (5.34), we get $E_2 = 0$ and written as

$$\Big(R_1 - \frac{R_2}{L}\Big)q^2 = \frac{M^2\delta^2}{\frac{1}{Da} + \Lambda\delta^2}\left(\frac{\Lambda^2}{M^2}\delta^6 + \frac{2\Lambda}{DaM^2}\delta^4 + \frac{1}{Da^2M^2}\delta^2 + \frac{Ta\pi^2}{\phi^2}\right). \quad (5.36)$$

The critical stationary Taylor number derived Rayleigh number R_1 as an independent variable,Kloosterziel [56]. For finding Taylor number, differentiate equation (5.36) with respect to q^2 , we get

$$R_1 - \frac{R_2}{L} = -\frac{\Lambda}{M^2\Big(\frac{1}{DaM^2} + \frac{\Lambda}{M^2}q^2\Big)^2}\left(\frac{\Lambda^2}{M^2}q^8 + \frac{2\Lambda}{DaM^2}q^6 + \frac{1}{Da^2M^2}q^4 + \frac{Ta\pi^2}{\phi^2}q^2\right) + \frac{1}{\Big(\frac{1}{DaM^2} + \frac{\Lambda}{M^2}q^2\Big)}\left(4\frac{\Lambda^2}{M^2}q^6 + \frac{6\Lambda}{DaM^2}q^4 + \frac{2}{Da^2M^2}q^2 + \frac{Ta\pi^2}{\phi^2}\right), \quad (5.37)$$

eliminating R_1 and R_2 from (5.36) and (5.37), we get

$$2\Lambda^3\delta^{10} + \left(\frac{5}{Da} - 3\Lambda\pi^2\right)\Lambda^2\delta^8 + 4\frac{\Lambda}{Da}\left(\frac{1}{Da} - 2\Lambda\pi^2\right)\delta^6 + \left(\frac{1}{Da^3} - \frac{7\Lambda\pi^2}{Da^2} + \frac{TaM^2\pi^2}{\Lambda\phi^2}(\frac{1}{Da} - \Lambda\pi^2)\right)\delta^4 - \left(\frac{2TaM^2\pi^4}{\Lambda\phi^2 Da} + \frac{2\pi^2}{Da^3}\right)\delta^2 + \frac{TaM^2\pi^2\pi^4}{\Lambda\phi^2 Da} = 0, \quad (5.38)$$

equations (5.24) and (5.38) are same. For large value of Da the equation (5.37) is

$$q^2 = \left(\frac{R_1 - \frac{R_2}{L}}{3\Lambda}\right)^{\frac{1}{2}} - \pi^2, \quad (5.39)$$

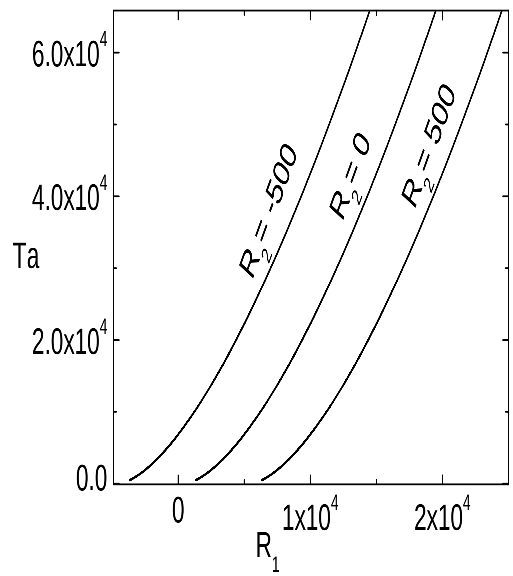

Figure 5.6: The lines are plotted for $R_2 = -500, 0, 500$ at $Da = 1500,\ \Lambda = 0.85,\ M = 1,\ \phi = 0.9,\ Pr = 0.5,\ Ta = 500,\ L = 0.1.$

for large Da, substituting q^2 from equation (5.39) in equation (5.36), we get critical Taylor number $Ta = Ta_{sc}$. where

$$Ta_{sc} = \frac{\phi^2}{\pi^2}\Bigg\{\left(R_1 - \frac{R_2}{L}\right)\left[\Lambda\frac{\left(\frac{R_1-\frac{R_2}{L}}{3\Lambda}\right)^{\frac{1}{2}} - \pi^2}{M^2}\right]\left[1 - \frac{\pi^2}{\left(\frac{R_1-\frac{R_2}{L}}{3\Lambda}\right)^{\frac{1}{2}} - \pi^2}\right] - \frac{\Lambda^2}{M^2}\left[\left(\frac{R_1 - \frac{R_2}{L}}{3\Lambda}\right)^{\frac{1}{2}} - \pi^2\right]^3\Bigg\}, \tag{5.40}$$

In Figure 5.6, the figure plotted in (R_1, Ta) region for $E = 0$, the right hand side region $E > 0$ is stable and the left hand side region $E < 0$ is unstable.

Oscillatory Convection

From equation (5.34), equate imaginary part to zero

$$\omega^2 = \frac{D}{B},$$

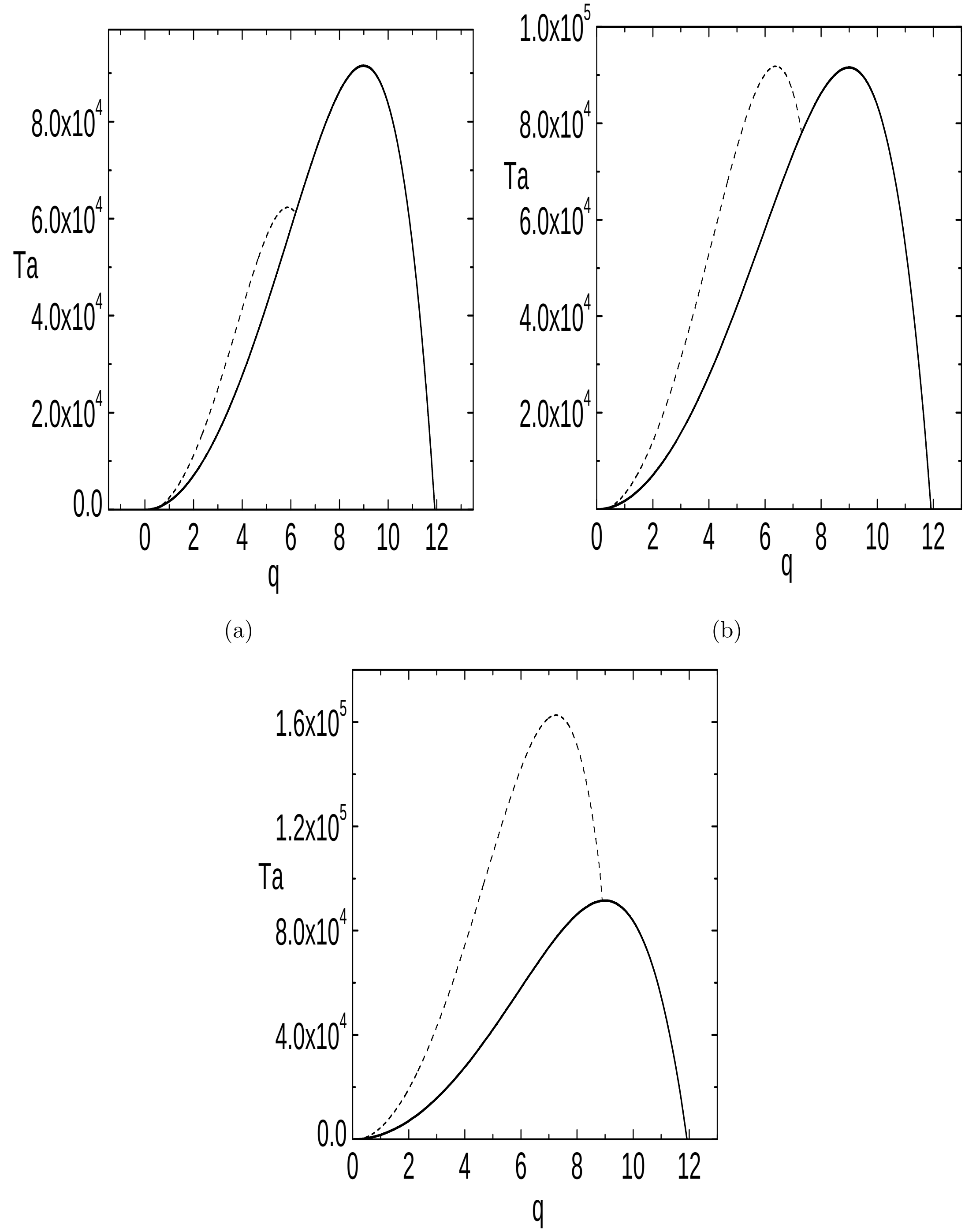

(a) (b) (c)

Figure 5.7: Solid and dotted lines are represent the Taylor number for stationary and oscillatory convection. $Da = 1500$, $\Lambda = 0.85$, $M = 0.9$, $\phi = 0.9$, $R_1 = 1000$, $R_2 = -1000$, $L = 0.05$, (a) $Pr = 0.2$, (b) $Pr = 0.255$, (c) $Pr = 0.355$.

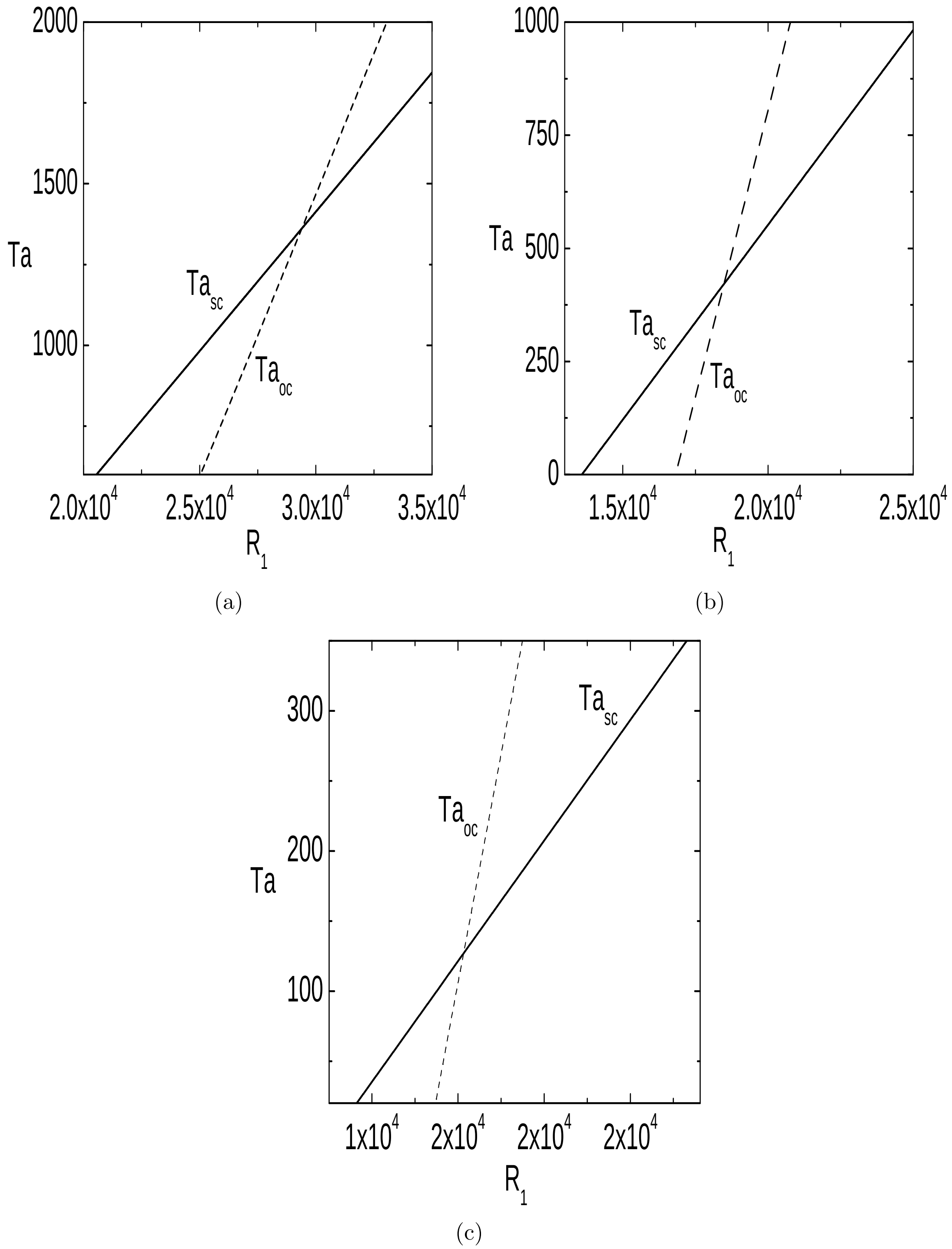

Figure 5.8: Marginal stability curves for Taylor number Ta(Solid lines represents stationary convection (Ta_{sc}) and dotted lines represents oscillatory convection (Ta_{oc})) $Da = 1500, \Lambda = 0.85,\ M = 0.9, \phi = 0.9,\ L = 0.4,\ R_2 = 5000$, (a) $Pr = 0.1$, (b) $Pr = 0.2$, (c) $Pr = 0.3$.

substitute ω^2 only in the real part of equation (5.34) and equate it to zero, to get

$$D^2 - BCD + B^2E = 0 \tag{5.41}$$

The oscillatory Taylor number is not in terms of R_1, R_2 like equation (5.40) at $\omega^2 > 0$. Eliminating Ta from $D = 0$ and $E = 0$, we get

$$q^6 + 3\pi^2 q^4 + \left[3\pi^4 + \frac{R_2}{2}\left(\frac{1}{\Lambda L} - M\phi^2 Pr\right) - \frac{R_1}{2}\left(\frac{1}{\Lambda} - M\phi Pr\Lambda\right)\right] q^2 + \pi^6 = 0. \tag{5.42}$$

If the roots of above equation (5.42) are positive we get Takens-Bogdanov bifurcation points, which is represented in Figure 5.7. Solid and dotted lines represent the Taylor number for stationary and oscillatory convection. Figure 5.7 shows primary and secondary instabilities and Figure 5.8 represented in (R_1, Ta) plane, where co-dimension two bifurcation point decreases at the intersection of stationary and oscillatory of Rayleigh and Taylor marginal curves because of variation in prandtl value.

5.4 Nonlinear Stability Analysis

5.4.1 Derivation of nonlinear two-dimensional Landau Ginzburg equation near onset of stationary convection

According to Newell and Whitehead Multiple scale analysis [77], small scale convection cells disturbed vital flow. If the scale range is $O(\epsilon)$, then the collaboration of the cell with itself forces a second harmonic and a standard state of rectification of range $O(\epsilon^2)$ and these in turn impel an $O(\epsilon^3)$ rectification to the structural module of the imposed roll. Let us assume the solution of equations (5.6) - (5.9) take the form form

$$f = f(u, v, w, \theta, C) = \epsilon f_0 + \epsilon^2 f_1 + \epsilon^3 f_2 + \cdots , \tag{5.43}$$

where

$$\epsilon^2 = \frac{R_1 - R_{1sc}}{R_{1sc}} << 1,$$

The first order calculations of the linearised problem are given by the eigenvectors,

$$\begin{aligned}
u_0 =& \frac{i\pi}{q}\Big[A.e^{iqx} - \cos\pi z - c.c\Big],\\
v_0 =& -\frac{i\pi Ta^{\frac{1}{2}}}{q\phi(\frac{1}{Da} + \frac{\Lambda}{M}\delta^2)}\Big[A.e^{iqx} - \cos\pi z - c.c\Big],\\
w_0 =& \Big[A.e^{iqx}\sin\pi z + c.c\Big]\\
C_0 =& \frac{1}{ML\delta^2}\Big[A.e^{iqx} - \sin\pi z + c.c\Big],\\
\theta_0 =& \frac{1}{M\delta^2}\Big[A.e^{iqx} - \sin\pi z + c.c\Big],
\end{aligned} \tag{5.44}$$

where $A = A(X, Y, T)$ is the complex scale varying on the gradual variables X, Y and T with complex conjugate represented as c.c. The analytical mode for the linear problem at $R_{1s} = R_{1sc}$ is $e^{iqx}\sin\pi z$. The variables x, y, z and t are scaled by

$$X = \epsilon x, \quad Y = \epsilon^{\frac{1}{2}} y, \quad Z = z, \quad T = \epsilon^2 t,$$

are suitably scattered as fast and slow unconventional variables in f. The derivative operators can be formulated as

$$\frac{\partial}{\partial x} \to \epsilon\frac{\partial}{\partial X} + \frac{\partial}{\partial x}, \quad \frac{\partial}{\partial y} \to \epsilon^{\frac{1}{2}}\frac{\partial}{\partial Y}, \quad \frac{\partial}{\partial z} \to \frac{\partial}{\partial Z}, \quad and \quad \frac{\partial}{\partial t} \to \epsilon^2\frac{\partial}{\partial T}. \tag{5.45}$$

By using the transformations equation (5.45), the linear and nonlinear operators of equation(5.14) can be written as

$$\mathcal{L} = \mathcal{L}_0 + \epsilon\mathcal{L}_1 + \epsilon^2\mathcal{L}_2 \cdots, \tag{5.46}$$

$$\mathcal{N} = \mathcal{N}_0 + \epsilon\mathcal{N}_1 + \epsilon^2\mathcal{N}_2 \cdots, \tag{5.47}$$

Substituting the zeroth order solution w_0 in to $\mathcal{L}_0 w_0 = 0$, we get

$$\frac{\Lambda^2}{M^2}\delta^8 + \frac{2\Lambda}{DaM^2}\delta^6 + \frac{1}{Da^2M^2}\delta^4 + \frac{Ta\pi^2}{\phi^2}\delta^2 - \frac{q^2}{M^2}\Big(R_1 - \frac{R_2}{L}\Big)\Big(\frac{1}{Da} + \Lambda\delta^2\Big) = 0, \quad (5.48)$$

from the equation $\mathcal{L}_0 w_1 + \mathcal{L}_1 w_0 = \mathcal{N}_0$, $\mathcal{N}_0 = 0$ and $\mathcal{L}_1 w_0 = 0$.

$$\begin{aligned}
u_1 =& 0, w_1 = 0,\\
v_1 =& -\frac{iM\pi^2 Ta^{\frac{1}{2}}}{q\phi\Big(\frac{1}{Da} + 4\Lambda q^2\Big)\Big(\frac{1}{Da} + 4\delta^2\Big)}\Big[A^2 e^{2iqx} - c.c\Big],\\
C_1 =& -\frac{1}{2M^2L^2\delta^2\pi}|A|^2 \sin 2\pi z,\\
\theta_1 =& -\frac{1}{2M^2\delta^2\pi}|A|^2 \sin 2\pi z,
\end{aligned} \quad (5.49)$$

taking $w_1 = 0$ in equation (5.46), $\mathcal{N}_1 - \mathcal{L}_2 w_0$ is vertical to w_0 and the coefficient of $\sin \pi z$ in $\mathcal{N}_1 - \mathcal{L}_2 w_0$ is vanishes. We get

$$\lambda_0 \frac{\partial A}{\partial T} - \lambda_1 \left(\frac{\partial}{\partial X} - \frac{i}{2q}\frac{\partial^2}{\partial Y^2}\right)^2 - \lambda_2 A + \lambda_3 |A|^2 A = 0, \quad (5.50)$$

where

$$\begin{aligned}
\lambda_0 =& \delta^8\Big(\frac{\Lambda^2}{M^2} + \frac{2\Lambda}{M^3Pr\phi} + \frac{\Lambda^2\phi}{LM^2}\Big) + \delta^6\Big(\frac{2\Lambda}{DaM^2} + \frac{2}{DaM^3Pr\phi} + \frac{2\Lambda\phi}{DaLM^2}\Big) +\\
& \delta^4\Big(\frac{1}{Da^2M^2}\Big) + \delta^2 q^2 \frac{R_2}{LM^2}\Big(\frac{\Lambda}{M} + \frac{1}{M\phi Pr}\Big) - \delta^2 q^2 \frac{R_1}{M^2}\Big(\frac{1}{M\phi Pr} + \frac{\Lambda\phi}{L}\Big) +\\
& \delta^2\pi^2\frac{Ta}{\phi}\Big(\frac{1}{\phi} + \frac{1}{L}\Big) + \frac{q^2}{DaLM^2}\Big(R_2 - R_1\phi\Big),\\
\lambda_1 =& \frac{10\Lambda^2}{M^2}\delta^6 + \frac{12\Lambda}{DaM^2}\delta^4 + \frac{3}{Da^2M^2}\delta^2 + \frac{Ta}{\phi^2}\pi^2 - \Big(R_1 - \frac{R_2}{L}\Big)\Big(\frac{5}{4}\frac{1}{DaM^2} + \frac{5}{2}\frac{\Lambda}{M^2}\delta^2\Big),\\
\lambda_2 =& \frac{R_1}{DaM^2}\delta^2 q^2 + \frac{\Lambda R_1}{M^2}\delta^4 q^2,\\
\lambda_3 =& \frac{q^2}{2M^4}\Big(R_1 - \frac{R_2}{L^3}\Big)\Big(\frac{1}{Da} + \Lambda\delta^2\Big) - \frac{2\pi^4 Ta\delta^4}{M^2\phi^4 Pr^2\Big(\frac{1}{MDa} + 4\frac{\Lambda}{M}q^2\Big)\Big(\frac{1}{MDa} + \frac{4}{M}\delta^2\Big)}.
\end{aligned} \quad (5.51)$$

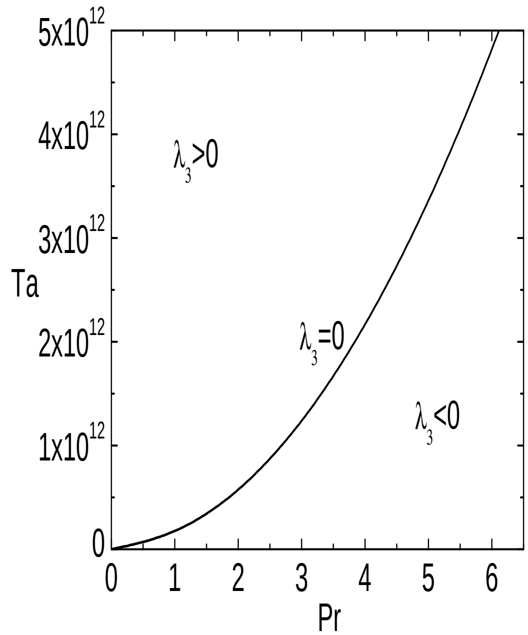

Figure 5.9: The bifurcation is supercritical if $\lambda_3 > 0$ and subcritical if $\lambda_3 < 0$, $\lambda_3 = 0$ gives critical bifurcation point. $Da = 1500, \Lambda = 0.85,\ M = 1,\ \phi = 0.9,\ Pr = 0.5,\ L = 0.8,\ R_1 = 50000,\ R_2 = 100.$

By using multiple scaling and $A(x, y, t) = \frac{A(X,Y,T)}{\epsilon}$, equation (5.50) can be written as a time dependent nonlinear two-dimensional L-G (Landau-Ginzburg) equation in fast variables as

$$\lambda_0 \frac{\partial A}{\partial t} - \lambda_1 \Big(\frac{\partial}{\partial x} - \frac{i}{2q} \frac{\partial^2}{\partial y^2} \Big)^2 A - \epsilon^2 \lambda_2 A + \lambda_3 |A|^2 A = 0, \tag{5.52}$$

which describes slow extensional scale ϵx vertical to the rolls and the variation of slow time scale $\epsilon^2 t$. If $R_2 < R_{2c}$ then λ_0 is positive and if $R_2 > R_{2c}$ then λ_0 is negative. λ_1 is positive when independent of R_1, R_2 and L. λ_2 is always positive. The ratio $\frac{\lambda_0}{\lambda_2}$ is growth rate amplitude and $\frac{\lambda_1}{\lambda_2}$ is curvature of the marginal stability curve. Forward, backward and tricritical bifurcations occur when $\lambda_3 > 0$, $\lambda_3 < 0$ and $\lambda_3 = 0$ respectively in Figure 5.9. Neglecting the y, t-dependence terms from equation (5.52), we get

$$\frac{\mathrm{d}^2A}{\mathrm{d}X^2} + \frac{\epsilon^2\lambda_2}{\lambda_1}(1 - \frac{\lambda_3}{\epsilon^2\lambda_2}|A|^2)A = 0. \tag{5.53}$$

$$A(X) = A_0 \tanh(\frac{X}{\Lambda_0}),$$

where

$$A_0 = \left(\epsilon^2\frac{\lambda_2}{\lambda_3}\right)^{\frac{1}{2}} \quad \text{and} \quad \Lambda_0 = \left(\frac{2\lambda_1}{\epsilon^2\lambda_2}\right)^{\frac{1}{2}}.$$

Heat Transport by Convection

If $|\frac{X}{\Lambda_0}| \leq 1$ then $|A|$ reaches maximum value. The maximum amplitude of A is $|A_{max}|$,

$$|A_{max}| = \left(\frac{\epsilon^2\lambda_2}{\lambda_3}\right)^{\frac{1}{2}}, \tag{5.54}$$

Heat transfer in field is Nusselt number Nu,

$$Nu = 1 + \frac{\epsilon^2}{\delta_{sc}^2}|A_{max}|^2. \tag{5.55}$$

In Figure 5.10, Nusselt number increases if $\frac{R_1}{R_{1sc}} > 1$ and decays if $\frac{R_1}{R_{1sc}} \leq 1$ convection for $Nu > 1$. Then there is convection if $Nu > 1$, conduction if $Nu \leq 1$. Nusselt number increases by increasing Ta value.

In Figure 5.11, we observed by increasing the Ta value, the region of Eckhaus and Zigzag instability increases.

5.4.2 Derivation of coupled LG equation at the onset of oscillatory convection

Consider cylindrical rolls along y-axis, so only x-dependence and z-dependence appears from $\mathcal{L}w = \mathcal{N}$. Based on this we obtained coupled LG equations at the supercritical Hopf bifurcation. We establish ϵ as

$$\epsilon^2 = \frac{R_o - R_{oc}}{R_{oc}} \ll 1. \tag{5.56}$$

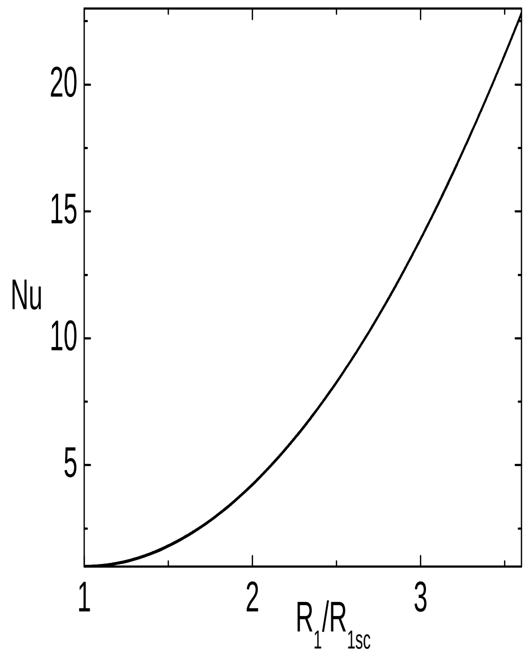

Figure 5.10: Nu grows exponentially for $Da = 1500$, $\Lambda = 0.85$, $M = 1$, $\phi = 0.9$, $L = 0.1$, $R_2 = 100$ and $Ta = 10^5$

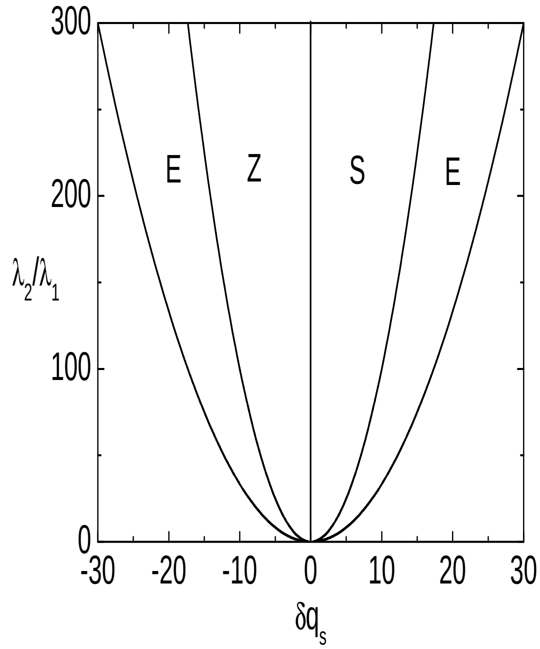

Figure 5.11: Regions of Eckhaus instability (E), zigzag instability (Z) and stable region (S) are plotted for $\phi = 0.9$, $Pr = 0.5$, $Da = 1500$, $\Lambda = 0.85$, $R_2 = 100$, L=0.1, M=0.9, (a) $Ta = 10^5$.

take

$$w_0 = \left[A_{1L}e^{i(\omega_{oc}t+q_{oc}x)} + A_{1R}e^{i(\omega_{oc}t-q_{oc}x)} + c.c\right]\sin\pi z,$$

where A_{1L} and A_{1R} represents left and right travelling amplitude of the rolls respectively and depends on varibles X, τ and T from Knobloch and Luca [57],

$$X = \epsilon x, \quad \tau = \epsilon t, \quad T = \epsilon^2 t, \tag{5.57}$$

the derivative operators are expressed as

$$\frac{\partial}{\partial x} \to \frac{\partial}{\partial x} + \epsilon\frac{\partial}{\partial X}, \quad \frac{\partial}{\partial t} \to \frac{\partial}{\partial t} + \epsilon\frac{\partial}{\partial \tau} + \epsilon^2\frac{\partial}{\partial T}. \tag{5.58}$$

The power series solution becomes

$$f = \epsilon f_0 + \epsilon^2 f_1 + \epsilon^3 f_2 + \cdots, \tag{5.59}$$

in ϵ term. The first approximation of the linearized problem is then

$$\begin{aligned}
u_0 =& \frac{i\pi}{q}\left[A_{1L}e^{i(\omega_{oc}t+q_{oc}x)} - A_{1R}e^{i(\omega_{oc}t-q_{oc}x)} - c.c\right]\cos\pi z,\\
v_0 =& -\frac{i\pi Ta^{\frac{1}{2}}}{q\phi}\frac{1}{\frac{1}{Da}+\frac{\Lambda}{M}\delta_{oc}^2}\left[A_{1L}e^{i(\omega_{oc}t+q_{oc}x)} - A_{1R}e^{i(\omega_{oc}t-q_{oc}x)} - c.c\right]\cos\pi z,\\
w_0 =& \left[A_{1L}e^{i(\omega_{oc}t+q_{oc}x)} + A_{1R}e^{i(\omega_{oc}t-q_{oc}x)} + c.c\right]\sin\pi z,\\
C_0 =& \frac{1}{ML}\frac{1}{\delta_{oc}^2 + i\omega_{oc}^2\frac{\phi}{L}}\left[A_{1L}e^{i(\omega_{oc}t+q_{oc}x)} + A_{1R}e^{i(\omega_{oc}t-q_{oc}x)} + c.c\right]\sin\pi z,\\
\theta_0 =& \frac{1}{M}\frac{1}{\delta_{oc}^2 + i\omega_{oc}}\left[A_{1L}e^{i(\omega_{oc}t+q_{oc}x)} + A_{1R}e^{i(\omega_{oc}t-q_{oc}x)} + c.c\right]\sin\pi z,
\end{aligned} \tag{5.60}$$

where $\delta_{oc}^2 = (q_{oc}^2 + \pi^2)$. By substituting equations (5.58) and equation (5.59) in to equation (5.14) and equating the coefficients of ϵ, ϵ^2, ϵ^3 to zero, we get

$$\begin{aligned}\mathcal{L}_0 w_0 =&0,\\ \mathcal{L}_1 w_0 + \mathcal{L}_0 w_1 =&\mathcal{N}_0,\\ \mathcal{L}_2 w_0 + \mathcal{L}_1 w_1 + \mathcal{L}_0 w_2 =&\mathcal{N}_1,\end{aligned} \tag{5.61}$$

we get critical Rayleigh number from the linear equation $\mathcal{L}_0 w_0 = 0$. At $O(\epsilon^2)$, $\mathcal{N}_0 = 0$ and $\mathcal{L}_1 w_0 = 0$ gives $\frac{\partial A_{1L}}{\partial \tau} - \nu_g \frac{\partial A_{1L}}{\partial X} = 0$ and $\frac{\partial A_{1L}}{\partial \tau} + \nu_g \frac{\partial A_{1L}}{\partial X} = 0$. Where $\nu_g = (\frac{\partial \omega}{\partial q})_{q=q_{sc}}$ and get

$$\Big[\frac{1}{M^2\phi Pr}\frac{\partial}{\partial t} + \frac{1}{MDa} - \frac{\Lambda}{M}\nabla^2\Big] w_{z_1} = \frac{Ta^{1/2}}{\phi}\frac{\partial w_1}{\partial z} - \frac{1}{M^2\phi^2 Pr}\Big[\nabla \times (\overline{V_0}.\nabla)\overline{V_0}\Big].\hat{e}_z, \tag{5.62}$$

$$\Big(\frac{\partial}{\partial t} - \nabla^2\Big)\theta_1 = \frac{\omega_1}{M} - \frac{1}{M}(\overline{V_0}.\nabla)\theta_0, \tag{5.63}$$

$$\Big(\frac{\phi}{L}\frac{\partial}{\partial t} - \nabla^2\Big)C_1 = \frac{\omega_1}{ML} - \frac{1}{ML}(\overline{V_0}.\nabla)C_0. \tag{5.64}$$

By using zeroth order solutions we get

$$\begin{aligned}
u_1 =&0,\ \ w_1 = 0,\\
v_1 =& -\frac{Ta^{\frac{1}{2}\pi^2}}{q_{oc}\phi}\Bigg[\frac{2q_{oc}A_{1L}^2 e^{2i(\omega_{oc}t+q_{oc}x)} + 2qA_{1R}^2 e^{2i(\omega_{oc}t-q_{oc}x)}}{\Big(\frac{1}{MDa} + \frac{\Lambda}{M}\delta^2 + i\omega_{oc}\frac{1}{M^2\phi Pr}\Big)\Big(\frac{1}{MDa} + \frac{\Lambda}{M}\delta^2 + i\omega_{oc}\frac{1}{M^2\phi Pr}\Big)}\\
&+ \frac{4qA_{1L}^* A_{1R} e^{-2iq_{oc}x}}{(\frac{1}{MDa} + \frac{\Lambda}{M}4q_{oc}^2)(\frac{1}{MDa} + \frac{\Lambda}{M}\delta^2 + i\omega_{oc}\frac{1}{M^2\phi Pr})} - c.c\Bigg],\\
C_1 =& -\frac{\pi}{M^2L^2}\Bigg[\frac{|A_{1L}|^2 + |A_{1R}|^2}{4\pi^2(\delta_{oc}^2 + \frac{\phi}{L}i\omega_{oc})} + \frac{A_{1L}A_{1R}e^{2i\omega_{oc}t}}{(2\pi^2 + i\omega_{oc}\frac{\phi}{L})(\delta_{oc}^2 + i\omega_{oc}\frac{\phi}{L})} + c.c\Bigg]\sin 2\pi z,\\
\theta_1 =& -\frac{\pi}{M^2}\Bigg[\frac{|A_{1L}|^2 + |A_{1R}|^2}{4\pi^2(\delta_{oc}^2 + i\omega_{oc})} + \frac{A_{1L}A_{1R}e^{2i\omega_{oc}t}}{(2\pi^2 + i\omega_{oc})(\delta_{oc}^2 + i\omega_{oc})} + c.c\Bigg]\sin 2\pi z.
\end{aligned} \tag{5.65}$$

Equation (5.61) is solvable when $\mathcal{L}_0 w_0 = 0$, coefficients of $\sin \pi z$ in $\mathcal{N}_1 - \mathcal{L}_2 w_0$ are equal to zero, we get

$$\Lambda_0 \frac{\partial A_{1L}}{\partial T} + \Lambda_1 \left(\frac{\partial}{\partial \tau} - v_g \frac{\partial}{\partial X} \right) A_{2L} - \Lambda_2 \frac{\partial^2 A_{1L}}{\partial X^2} - \Lambda_3 A_{1L} + \Lambda_4 |A_{1L}|^2 A_{1L} + \Lambda_5 |A_{1R}|^2 A_{1L} = 0 \tag{5.66}$$

$$\Lambda_0 \frac{\partial A_{1R}}{\partial T} + \Lambda_1 \left(\frac{\partial}{\partial \tau} - v_g \frac{\partial}{\partial X} \right) A_{2R} - \Lambda_2 \frac{\partial^2 A_{1R}}{\partial X^2} - \Lambda_3 A_{1R} + \Lambda_4 |A_{1R}|^2 A_{1R} + \Lambda_5 |A_{1L}|^2 A_{1R} = 0. \tag{5.67}$$

$$\begin{aligned}
\Lambda_0 =& (e_2 + \frac{\phi}{L} e_1)\delta^2 e_3^2 + \frac{Ta\pi^2}{\phi^2}(\frac{\phi}{L} e_1 + e_2) + \frac{2e_1 e_2 e_3^2 \delta^2}{M^2 \phi Pr} - \frac{q^2}{M^3 \phi Pr}(e_2 R_1 - e_1 \frac{R_2}{L}) - \\
& \frac{q^2 e_3}{LM}(\phi R_1 - R_2), \\
\Lambda_1 =& \Big(\frac{e_1 e_2}{M^4 Pr^2 \phi^2} + \frac{2e_1 e_3}{LM^2 Pr} + \frac{2e_2 e_3}{M^2 \phi Pr} + \frac{\phi}{L} e_3^2 \Big) \delta^2 + \frac{Ta}{\phi L}\pi^2 + \frac{R_1}{M} \Big(\frac{e_2}{M^2 \phi Pr} + \\
& \frac{\phi e_3}{L} - \frac{q^2}{LM^2 Pr} \Big) - \frac{R_2}{LM} \Big(\frac{e_1}{M^2 \phi Pr} + e_3 - \frac{q^2}{M^2 \phi Pr} \Big), \\
\Lambda_2 =& 4q^2 \Bigg[- \frac{2\lambda}{M} e_1 e_2 e_3 + (e_1 + e_2) e_3^2 + \frac{\lambda^2}{M^2} e_1 e_2 \delta^2 + \frac{2\lambda}{M} e_1 e_3 \delta^2 - \frac{\lambda R_1}{M}(e_2 + q^2) - \\
& \frac{e_3}{M}(R_1 - \frac{R_2}{L}) + \frac{\lambda R_2}{LM^2}(e_1 + q^2) \Bigg], \\
\Lambda_3 =& \frac{R_1}{M} q^2 e_2 e_3, \\
\Lambda_4 =& \frac{4iTa\phi^2 q}{M^2 \phi^4 Pr} \frac{e_1 e_2}{e_3 e_4} + \frac{R_1 q^2}{4M^2} \frac{e_2 e_3}{e_1} - \frac{R_2 \phi q^2}{4M^3 L^3} \frac{e_1 e_3}{e_2}, \\
\Lambda_5 =& \frac{8iTa\phi^4 q}{M^2 \phi^4 Pr} \frac{e_1 e_2}{e_3 e_4} + \frac{R_1 q^2 \phi^2}{M^2} \frac{e_2 e_3}{e_1 e_5} - \frac{R_2 \phi q^2}{4M^3 L^3} \frac{e_1 e_3}{e_2}.
\end{aligned} \tag{5.68}$$

Where

$$e_1 = \delta^2 + i\omega,\ e_2 = \delta^2 + i\omega\frac{\phi}{L} \qquad A_{2L} = \Big(\frac{\partial}{\partial\tau} + \nu_g\frac{\partial}{\partial X}\Big)A_{1L}$$
$$e_3 = \frac{1}{MDa} + \frac{\Lambda}{M}q^2 + \frac{1}{M^2\phi Pr}i\omega \qquad A_{2R} = \Big(\frac{\partial}{\partial\tau} - \nu_g\frac{\partial}{\partial X}\Big)A_{1R}$$
$$e_4 = \frac{1}{MDa} + \frac{\Lambda}{M}4q^2 + \frac{1}{M^2\phi Pr}i\omega \qquad e_5 = 2\pi^2 + i\omega$$

Solving equations (5.66) and (5.67) by taking $\xi' = \nu_g\tau + X$ and $\eta' = \nu_g\tau - X$, we get

$$2v_g\Lambda_1\frac{\partial A_{2L}}{\partial\eta'} = -\Lambda_0\frac{\partial A_{1L}}{\partial T} + \Lambda_2\frac{\partial A_{1L}}{\partial X^2} + \Lambda_3 A_{1L} - \left(\Lambda_4|A_{1L}|^2 + \Lambda_5|A_{1R}|^2\right)A_{1L}, \quad (5.69)$$
$$2v_g\Lambda_1\frac{\partial A_{2R}}{\partial\eta'} = -\Lambda_0\frac{\partial A_{1R}}{\partial T} + \Lambda_2\frac{\partial A_{1R}}{\partial X^2} + \lambda_3 A_{1R} - \left(\Lambda_4|A_{1R}|^2 + \Lambda_5|A_{1L}|^2\right)A_{1R}. \quad (5.70)$$

This integrating equations (5.69) and (5.70) over η' and ξ' respectively, we get

$$\Lambda_0\frac{\partial A_{1L}}{\partial T} = \Lambda_2\frac{\partial A_{1L}}{\partial X^2} + \lambda_3 A_{1L} - \left(\Lambda_4|A_{1L}|^2 + \Lambda_5|A_{1R}|^2\right)A_{1L}, \quad (5.71)$$

$$\Lambda_0\frac{\partial A_{1R}}{\partial T} = \Lambda_2\frac{\partial A_{1R}}{\partial X^2} + \lambda_3 A_{1R} - \left(\Lambda_4|A_{1R}|^2 + \Lambda_5|A_{1L}|^2\right)A_{1R}. \quad (5.72)$$

Equations (5.71) and (5.72) are left and right moving waves known as coupled one-dimensional LG equations.

Travelling Waves and Standing Waves

Knobloch [57] and Coullet [37] studied regions of travelling standing waves, on magneto convection which Matthews [67] derived. Dropping variable X from equations (5.71) and (5.72), we get

$$\frac{\mathrm{d}A_{1L}}{\mathrm{d}T} = \frac{\Lambda_3}{\Lambda_0}A_{1L} - \frac{\Lambda_4}{\Lambda_0}A_{1L}|A_{1L}|^2 - \frac{\Lambda_5}{\Lambda_0}A_{1L}|A_{1R}|^2, \quad (5.73)$$

$$\frac{\mathrm{d}A_{1R}}{\mathrm{d}T} = \frac{\Lambda_3}{\Lambda_0}A_{1R} - \frac{\Lambda_4}{\Lambda_0}A_{1R}|A_{1R}|^2 - \frac{\Lambda_5}{\Lambda_0}A_{1R}|A_{1L}|^2. \tag{5.74}$$

Put

$$\beta' = \frac{\Lambda_3}{\Lambda_0}, \quad \gamma' = -\frac{\Lambda_4}{\Lambda_0} \quad \text{and} \quad \delta' = -\frac{\Lambda_5}{\Lambda_0}.$$

Then equations (5.73) and (5.74) take the following form

$$\frac{\mathrm{d}A_{1L}}{\mathrm{d}T} = \beta' A_{1L} + \gamma' A_{1L}|A_{1L}|^2 + \delta' A_{1L}|A_{1R}|^2, \tag{5.75}$$

$$\frac{\mathrm{d}A_{1R}}{\mathrm{d}T} = \beta' A_{1R} + \gamma' A_{1R}|A_{1R}|^2 + \delta' A_{1R}|A_{1L}|^2. \tag{5.76}$$

Where

$$\begin{aligned} A_{1L} =& a_L e^{i\phi_L} & a_L =& |A_{1L}| & \phi_L =& arg(A_{1L}) = \tan^{-1}\left(\frac{Im(A_{1L})}{Re(A_{1L})}\right) \\ A_{1R} =& a_L e^{i\phi_R} & a_R =& |A_{1R}| & \phi_R =& arg(A_{1R}) = \tan^{-1}\left(\frac{Im(A_{1R})}{Re(A_{1R}})\right) \\ \beta' =& \beta_1 + i\beta_2 & \gamma' =& \gamma_1 + i\gamma_2 & \delta' =& \delta_1 + i\delta_2 \end{aligned} \tag{5.77}$$

Substituting of A_{1L},A_{1R},β', γ' and δ' in (5.75) and (5.76). we get,

$$(a_L, a_R) = \left(-\beta_1/(\gamma_1 + \delta_1), -\beta_1/(\gamma_1 + \delta_1)\right), \tag{5.78}$$

for standing waves. $(a_L, a_R) = (a_L, 0)$ for left travelling waves and $(a_L, a_R) = (0, a_R)$ for right travelling waves. $(a_L, a_R) = (0, 0)$ for conduction state. In Fig. 5.12, We have observed that the stability regions of standing waves and travelling waves increase when Pr increases.

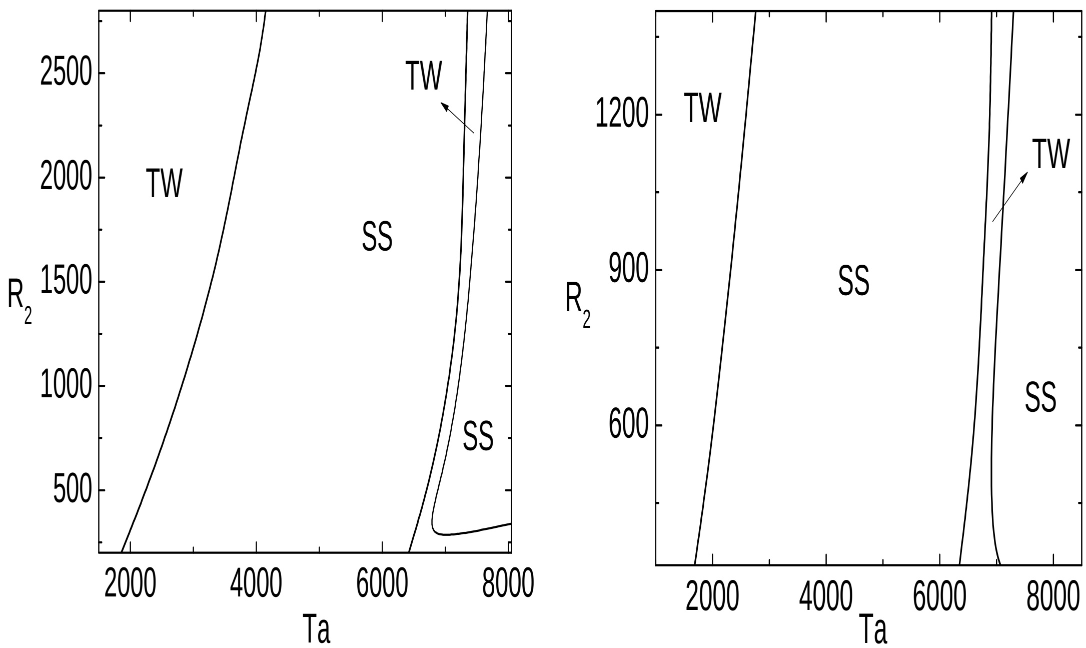

(a) (b)

Figure 5.12: Stability regions of steady state (SS), standing waves (SW), travelling waves(TW) are plotted at the onset of oscillatory convection for ϕ = 0.9, Da=1500, $\Lambda = 0.85$, M=1, L=0.1, (a) Pr=1.1, (b) Pr=1.

5.5 Conclusions

In linear stability analysis, we traced marginal stability curves in (q, R_1) plane at different parameters. Prandtl number does not affect convective stationary Rayleigh value. We also identified Takens-Bogdanov and co-dimension two bifurcation points on neutral curves. The region of salinity Rayleigh value R_2 verses thermal Rayleigh value R_1 over convective stationary and oscillatory grew by increased internal forces over rotating field. Two dimensional L-G equation at onset of stationary mode was derived and we studied heat transport from Nusselt number, and also long wave length baased on Eukhaus and Zigzag instabilities. Nusselt number grows exponentially if $\frac{R_1}{R_{1sc}} > 1$ and decays if $\frac{R_1}{R_{1sc}} \leq 1$ for $Nu > 1$. Nusselt number grows exponentially at unit value. We derived two nonlinear LG equations and observed stability regions for travelling and standing waves for fixed physical and porous parameters. Here the region of standing waves are unstable, region of travelling waves exits along with the steady state.

Chapter 6

Nonlinear Thermohaline Convection in a Sparsely Packed Porous Medium with the Effect of Rotation and Horizontal Magnetic Field

6.1 Introduction

Thermohaline convection is a double diffusive convection. Nield and Bejan [79] studied double diffusive convection in a horizontal layer of a saturated porous medium by linear perturbation analysis and observed cellular flow pattern induced by solute effects, thermal effects and both solute and thermal effects. Benerji Babu et al. [9] studied stability of thermohaline convection using Darcy-Lapwood-Brinman model with Boussinesq approximation between stress free boundaries. Thermohaline convection over a porous medium is applicable in several scientific and industrial applications such as atmospheric pollution, food processing, lakes and underground water and materials processing.

The study of thermohaline convection in a porous medium with the effects of magnetic field and rotation has importance in many fields, such as investigation of magnectic field and rotation of the earth in geothermal areas, study of core of earth in geophysics and study of manufacturing materials in industries. The magnetic field affects the rate of flow of velocity as well as rate of heat and mass transfer. The presence of a vertical magnetic field leads the boundary of monotonous instability and increases the stability of the conductive state. The presence of a horizontal magnetic field breaks the symmetry and form rolls with axes parallel to them. Chakrabarti et al. [32] studied the effect of rotation on thermohaline convection in a horizontal layer of a saturated porous medium. Infinitesimal disturbances in the form of rolls leads to marginal state of convection may be oscillatory depending on the magnitude of the rotation and solute Rayleigh parameters. Thermohaline convection over rotating fluids was studied by Tagare et al. [120, 121] who observed feasible subcritical instabilities. Malashetty [64] studied double diffusive convection in a rotating porous layer using a thermal non-equilibrium model. Thermohaline convection rotating system in a sparsely packed porous medium is one of the reason for minimizing of different phases of alloying elements like Sulphur, Iron in earth's outer core and Helium and Hydrogen in stellar core. The effects of horizontal magnetic field and

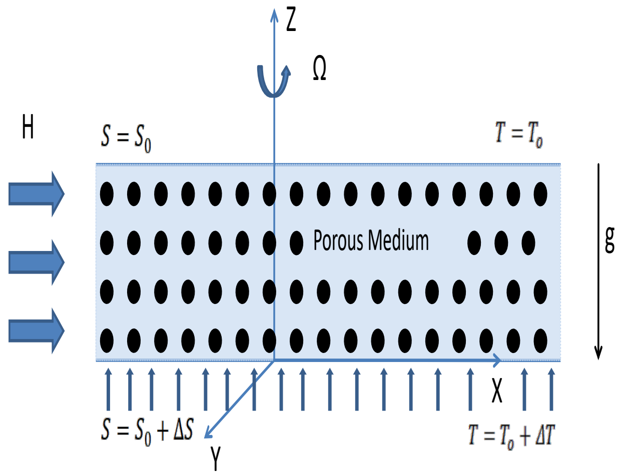

Figure 6.1: Physical Configuration

rotation of thermohaline convection through porous medium was studied by Sharma et al. [110], Sunil et al. [117], Kumar [60] and Abdullah et al. [2].

6.2 Basic Equations

Considere an horizontal layer of fluid with sparsely packed porous medium, rotating with angular velocity $\hat{\Omega}$ about z-axis and horizontal magnetic field along y-axis between parallel stress free boundaries $z = 0$ and $z = d$. This layer is heated from below and saturated with a solution of a specific concentration gradient. The temperature and salinity differences across the stress-free boundaries are denoted by $\Delta T'$ and $\Delta S'$. Darcy-lapwood-Brinkman model is used for the study of sparsely packed porous medium. In Boussinesq approximation, the dimensioned governing equations, equation of continuity, Darcy-Lapwood -Brinkman model to the momentum equation, energy equation, equation of magnetic induction and solute concentration are

$$\nabla.\overline{V} = 0,\ \nabla.\overline{H} = 0 \tag{6.1}$$

$$\left(\frac{1}{M^2\phi Pr_1}\frac{\partial}{\partial t} - \frac{\Lambda}{M}\nabla^2 + \frac{1}{MDa}\right)\overline{V} - \frac{Ta^{\frac{1}{2}}}{M\phi}\left(\overline{V}\times\widehat{e_z}\right) - Q\frac{\partial\overline{H}}{\partial y} -$$
$$(R_1\theta - R_2C)\hat{e}_z - Q\frac{Pr_2}{Pr_1}(\overline{H}.\nabla)\overline{H} - \frac{1}{M^2\phi^2 Pr_1}(\overline{V}.\nabla)\overline{V} =$$
$$-\nabla\left(\frac{P}{MPr_1} + \frac{Q}{2}\frac{Pr_2}{Pr_1}|\overline{H}|^2 + QH_y - \frac{TaPr_1}{8\phi}|\hat{e}_z\times\overline{V}|^2\right), \tag{6.2}$$

$$\left(\frac{\partial}{\partial t} - \nabla^2\right)\theta - \frac{w}{M} = -\frac{1}{M}\left(\overline{V}.\nabla\right)\theta, \tag{6.3}$$

$$\left(\phi\frac{Pr_2}{Pr_1}\frac{\partial}{\partial t} - M\nabla^2\right)\overline{H} - \nabla\times(\overline{V}\times\hat{e_y}) = \frac{Pr_2}{Pr_1}\left[\nabla\times\left(\overline{V}\times\overline{H}\right)\right]. \tag{6.4}$$

$$\frac{\phi}{L}\frac{\partial C}{\partial t} + \frac{1}{ML}(\overline{v}\cdot\nabla)C = \frac{w}{ML} + \nabla^2 C \tag{6.5}$$

Thermal Prandtl number $Pr_1 = \frac{\nu}{\kappa}$, Magnetic Prandtl number $Pr_2 = \frac{\nu}{\eta}$ Lewis number $L = \frac{\kappa_S}{\kappa_T}$, Darcy number $Da = \frac{K}{d^2}$, Thermal Rayleigh number $R_1 = \frac{\alpha g\triangle T d^3}{\nu k_T}$, Salinity Rayleigh number $R_2 = \frac{\alpha g\triangle S d^3}{\nu k_S}$, Taylor number $Ta = \frac{4\Omega^2 d^4}{\nu^2}$, velocity $\overline{V}(u,v,w)$, magnetic field $\overline{H}(H_x,\ H_y,\ H_z)$, dimensionless heat capacity is M, chandrasekhar number Q, presser P, temperature θ, and $\Lambda = \frac{Pr_2}{Pr_1}$ which varies from 0.5 to 10.9 from Givler and Altobelli [47] and concentration C. The curl of equation (6.2) is

$$\left(\frac{1}{M^2\phi Pr_1}\frac{\partial}{\partial t} - \frac{\Lambda}{M}\nabla^2 + \frac{1}{MDa}\right)(\nabla\times\overline{V}) - \frac{Ta^{\frac{1}{2}}}{M\phi}\left[\nabla\times\left(\overline{V}\times\widehat{e_z}\right)\right] - Q\left(\nabla\times\frac{\partial\overline{H}}{\partial y}\right) +$$
$$\nabla\times(R_1\theta - R_2C)\hat{e}_z = Q\frac{Pr_2}{Pr_1}\left[\nabla\times(\overline{H}.\nabla)\overline{H}\right] - \frac{1}{M^2\phi^2 Pr_1}\left[\nabla\times(\overline{V}.\nabla)\overline{V}\right]. \tag{6.6}$$

The curl of equation (6.6) is

$$\left(\frac{1}{M^2\phi Pr_1}\frac{\partial}{\partial t} - \frac{\Lambda}{M}\nabla^2 + \frac{1}{MDa}\right)\left[\nabla\times(\nabla\times\overline{V})\right] - \frac{Ta^{\frac{1}{2}}}{M\phi}\left\{\nabla\times\left[\nabla\times\left(\overline{V}\times\widehat{e_z}\right)\right]\right\} -$$
$$Q\left[\nabla\times\left(\nabla\times\frac{\partial\overline{H}}{\partial y}\right)\right] + \nabla\times\nabla\times(R_1\theta - R_2C)\hat{e}_z = Q\frac{Pr_2}{Pr_1}\left\{\nabla\times\left[\nabla\times\left(\overline{H}.\nabla\right)\overline{H}\right]\right\} -$$
$$\frac{1}{M^2\phi^2 Pr_1}\left\{\nabla\times\left[\nabla\times(\overline{V}.\nabla)\overline{V}\right]\right\}. \tag{6.7}$$

The curl of equation (6.4) is

$$\left(\phi\frac{Pr_2}{Pr_1}\frac{\partial}{\partial t} - M\nabla^2\right)(\nabla\times\overline{H}) - \left[\nabla\times\nabla\times(\overline{V}\times\hat{e_y})\right] = \frac{Pr_2}{Pr_1}\left\{\nabla\times\left[\nabla\times\left(\overline{V}\times\overline{H}\right)\right]\right\}. \tag{6.8}$$

By using equations (6.3) and (6.5) and z-component of equations (6.4), (6.6), (6.7) and (6.8) we write the equation in the form

$$\mathcal{L}w = \mathcal{N}, \tag{6.9}$$

where

$$\mathcal{L} = \left(\mathcal{D}_Q\mathcal{D}_{Pr_1} - Q\partial_y^2\right)\left(\mathcal{D}\mathcal{D}_\phi\mathcal{D}_{Pr_1}\mathcal{D}_y^2\nabla^2 - Q\mathcal{D}\mathcal{D}_\phi\nabla_h^2 - \frac{R_1}{M}\mathcal{D}_\phi\mathcal{D}_Q\nabla_h^2 + \frac{R_2}{M}\mathcal{D}_\phi\mathcal{D}_Q\nabla_h^2\right) + \frac{Ta}{M^2\phi^2}\partial_z^2\mathcal{D}^2{\mathcal{D}_\phi}^2, \tag{6.10}$$

$$\mathcal{N} = \left(\mathcal{D}_Q\mathcal{D}_{Pr_1} - Q\partial_y^2\right)N_3 - \frac{Ta^{1/2}}{M^2\phi^2}\mathcal{D}\mathcal{D}_\phi\mathcal{D}_Q^2\partial_z^2\left\{\mathcal{D}_QN_1 + Q\partial_y\frac{Pr_2}{Pr_1}[\nabla\times\nabla\times(\overline{V}\times\overline{H})]\cdot e_z\right\}, \tag{6.11}$$

where

$$\begin{aligned}
N_1 =& -\frac{1}{M^2\phi^2 Pr_1}[\nabla\times(\overline{V}\cdot\nabla)\overline{V}]\cdot e_z + Q\frac{Pr_2}{Pr_1}[\nabla\times(\overline{H}\cdot\nabla)\overline{H}]\cdot e_z\\
N_2 =& \frac{1}{M^2\phi^2 Pr_1}[\nabla\times\nabla\times(\overline{V}\cdot\nabla)\overline{V}]\cdot e_z + Q\frac{Pr_2}{Pr_1}[\nabla\times\nabla\times(\overline{H}\cdot\nabla)\overline{H}]\cdot e_z\\
N_3 =& \mathcal{D}\mathcal{D}_\phi\mathcal{D}_Q N_2 + \mathcal{D}\mathcal{D}_\phi Q\nabla^2\partial_y\{\mathcal{D}_Q N_1 + Q\partial_y\frac{Pr_2}{Pr_1}[\nabla\times\nabla\times(\overline{V}\times\overline{H})]\cdot e_z\}
\end{aligned}$$

$$\begin{aligned}
\mathcal{D} =& \frac{\partial}{\partial t} - \nabla^2,\ \partial_y = \frac{\partial}{\partial y} & \nabla_h^2 =& \frac{\partial^2}{\partial x^2} + \frac{\partial^2}{\partial y^2},\\
\mathcal{D}_\phi =& \frac{\phi}{L}\frac{\partial}{\partial t} - \nabla^2,\ \partial_z = \frac{\partial}{\partial z} & \nabla^2 =& \frac{\partial^2}{\partial x^2} + \frac{\partial^2}{\partial y^2} + \frac{\partial^2}{\partial z^2},\\
\mathcal{D}_{Pr_1} =& \frac{1}{M^2\phi Pr_1}\frac{\partial}{\partial t} + \frac{1}{MDa} - \frac{\Lambda}{M}\nabla^2, & \mathcal{D}_Q =& \phi\frac{Pr_2}{Pr_1}\frac{\partial}{\partial t} - M\nabla^2
\end{aligned}$$

6.3 Linear Stability Analysis

Analysing the disturbances into normal modes, assume the perturbation quantity

$$w = W(z)e^{i(lx+my)+pt},$$

where l, and m are horizontal wave numbers of the harmonic disturbance, $q^2 = l^2 + m^2$ and p is the growth rate. The boundary conditions appropriate for the problem are

$$w = \frac{\partial^2 w}{\partial z^2} = \frac{\partial^4 w}{\partial z^4} = 0,$$

the proper solution of equation $\mathcal{L}w = 0$ characterizing the lowest mode is

$$W(z) = \sin \pi z$$

and $p = i\omega$. For linear stability analysis substitute $w = \sin \pi z e^{i(lx+my)+i\omega t}$ in $L\omega = 0$. We get the thermal Rayleigh number R_1,

$$\begin{aligned} R_1 =& \frac{M}{q^2}\Bigg[\left(i\omega + \delta^2\right)\left(\frac{1}{M^2\phi Pr_1} i\omega + \frac{1}{MDa} - \frac{\Lambda}{M}\nabla^2\right)\delta^2 + \frac{R_2}{L}\frac{i\omega + \delta^2}{\frac{\phi}{L}i\omega + \delta^2}q^2 + \\ & \frac{Ta}{M^2\phi^2}\frac{\left(i\omega + \delta^2\right)\left(\phi\frac{Pr_2}{Pr_1}i\omega + M\delta^2\right)}{\left(\frac{1}{M^2\phi Pr_1}i\omega + \frac{1}{MDa} - \frac{\Lambda}{M}\nabla^2\right)\left(\frac{\phi}{L}i\omega + \delta^2\right) + Qm^2} + Q\frac{\left(i\omega + \delta^2\right)\delta^2 m^2}{\phi\frac{Pr_2}{Pr_1}i\omega + M\delta^2}\Bigg] \end{aligned} \tag{6.12}$$

6.3.1 Stationary Convection

For the onset of stationary convection we set $\omega = 0$ into (6.12), we get the stationary thermal Rayleigh number R_{1s} as

$$R_{1s} = \left(\frac{1}{MDa} + \frac{\Lambda}{M}\delta^2\right)\frac{\delta^4}{q^2} + \frac{R_2}{L} + \frac{Q\delta^2 m^2}{q^2} + \frac{Ta}{\phi^2 q^2}\frac{\delta^4}{\left(\frac{1}{MDa} + \frac{\Lambda}{M}\delta^2\right)\delta^2 + Qm^2}. \tag{6.13}$$

The stationary thermal Rayleigh number R_{1s} is independent of thermal and magnetic Prandtl numbers Pr_1 and Pr_2 respectively. The critical thermal Rayleigh number R_{1sc} at stationary wave numbers l_s and m_s is

$$R_{1sc} = \frac{1}{q_s^2}\left[\left(\frac{1}{MDa} + \frac{\Lambda}{M}\delta_s^2\right)\delta_s^4 + \frac{R_2}{L}q_s^2 + Q\delta_s^2 m_s^2 + \frac{Ta}{\phi^2}\frac{\delta_s^4}{\left(\frac{1}{MDa} + \frac{\Lambda}{M}\delta_s^2\right)\delta_s^2 + Qm_s^2}\right]. \tag{6.14}$$

cross rolls: If there is a periodic disturbance along x-direction and no perturbation along y-direction, with growth rate p, take $m = 0$ in equation (6.12). For cross rolls the thermal Rayleigh number is $R_{1s}^l\ (m = 0)$ is,

$$R_{1s}^l\ (m = 0) = \frac{(l^2 + \pi^2)^3\Lambda}{l^2} + \frac{TaM}{\Lambda\phi^2 l^2} + \frac{R_2}{L}, \tag{6.15}$$

parallel rolls: If there is a periodic disturbance along y-direction and no perturbation along x-direction with growth rate p, take $l = 0$ in equation (6.12). For cross rolls the thermal Rayleigh number is $R_{1s}^m\ (l = 0)$ is,

$$R_{1s}^m\ (l = 0) = \frac{\Lambda(m^2 + \pi^2)^3}{m^2} + Q(m^2 + \pi^2) + \frac{R_2}{L} + \frac{Ta(m^2 + \pi^2)^2}{\phi^2 m^2[\Lambda/M(m^2 + \pi^2)^2 + Qm^2]}. \tag{6.16}$$

From equations (6.12), (6.15) and (6.16), independent of $Q,\ Ta,\ R_2$, $\Lambda = M = 1$ and high permeability

$$R_1 = R_{1s} = R_{1s}^l\ (m = 0) = R_{1s}^m\ (l = 0) = \frac{(\pi^2 + a^2)^3}{a^2}, \tag{6.17}$$

which is equal to Rayleigh number for stress free boundaries. The critical Rayleigh number for the onset of instability is $\frac{27}{4}\pi^4$ at a critical wave number $a = \frac{\pi}{\sqrt{2}}$.

6.3.2 Oscillatory Convection

The thermal Rayleigh number R_1 is a real number and so equating the imaginary part of equation (6.12) to zero, we get oscillatory convection for positive value of ω^2 which is placed in the real part of equation (6.12). We get the oscillatory thermal Rayleigh number R_{10}.

$$R_{1o} = \delta^2\left(-c\omega^2 + d\delta^2\right) + e\left(b\omega^2 + M\delta^4\right) + f\left(d\omega^2 + \delta^4\right) + \frac{Ta}{M^2\phi^2 K_1}K_2, \qquad (6.18)$$

$$\omega^2 = \frac{I_1}{I_2} + I_3 + \frac{1}{2}\sqrt{I_4}, \qquad (6.19)$$

where $a = \frac{\phi}{L},\ b = Q\frac{Pr_2}{Pr_1},\ c = \frac{1}{M^2\phi Pr_1},\ d = \frac{\Lambda}{M}\delta^2 + \frac{1}{MDa},\ e = \frac{Q\delta^2 m^2}{b^2\omega^2+M^2\delta^4},$
$f = \frac{R_2 q^2}{ML(a^2\omega^2+\delta^4)},\ g = \frac{Ta}{M^2\phi^2 K_1},\ I_1 = aa^4b^2c^2ML(d + c\delta^2)\phi,\ I_2 = a^2M[b^2LTa(adb + bc\delta^2 - acb\delta^2 - acM\delta^2) + LM^2\delta^2(-2ab^2cm^2Q(d + c\delta^2) + 2b^2c^2\delta^4(d + c\delta^2) + a^2b^2b^3 + c(b^2d^2 + am^2(-L + M)Q)\delta^2 + c^2dM^2\delta^4 + c^3M^2\delta^6)\phi^2 + (-1 + a)b^2c^2M\delta^2\phi^2R_2],$
$I_3 = \sqrt{\frac{I_1^2}{4I_2^2} - K_3}, I_4 = \frac{I_2^2}{2I_1^2} - \frac{4}{3I_1},\ I_5 = Md^2[L(a^4d^2M^2\delta^2) + m^2(M - b)Q + dM^2\delta^2 + cM^2\delta^4 + 2cm^2M^2Q\delta^2(d + c\delta^2) - m^2Q(M\delta^2(d + c\delta^2))(-2acm^2Q\delta^4 + c^2\delta^8 + a^2(m^4Q^2 + 2dm^2Q\delta^2 + 2\delta^6))],\ I_6 = 3I_1 - \frac{I_2}{4I_1} + 3I_2 + \frac{K_2}{K_1^3+K_2^2},$
$K_1 = a^2c62\omega^4 + (c^2\delta^4 - 2acm^2Q)\omega^2 + m^4Q^2 + 2dm^2Q\delta^4 + a^2d^2,\ K_2 = abc\omega^4 + bm^2Q + d[(-1 + a)b + Ma + c\delta^4(b + M - aM)\omega^2 + m^2MQ\delta^6],\ K_3 = \frac{I_5}{I_6}.$

Figures 6.2 - 6.4 illustrate the stationary and oscillatory marginal curves at different values for physical parameters viz. Chandrashakar number Q, Taylor number Ta, thermal Prandtl number Pr_1 and magnetic Prandtl number Pr_2. At Takens-Bogdanov bifurcation point

$$R_{1s}(q_s) = R_{1o}(q_o) = R_{1c}(q_c), \qquad (6.20)$$

and $q_s = q_o = q_c$. At co-dimension two bifurcation points arises,

$$R_{1sc}(q) = R_{1oc}(q) \qquad (6.21)$$

and $q_{sc} \neq q_{oc}$. In Figures 6.2 and Figure 6.3, critical stationary and oscillatory critical thermal Rayleigh values are equal in the middle sub-figure. This represents a codimension two bifurcation point. In Figures 6.2 and Figure 6.3 other sub-graph intersection points are represented in Takens-Bogdanov bifurcation point. The Rayleigh values are increases by increasing Q, Ta, Pr_1 and Pr_2. In Figure 6.4 (a) the Takens-Bogdanov bifurcation point moves upward when Pr_1 increases and in Figure 6.4 (b) the Takens-Bogdanov bifurcation point moves downward when Pr_2 increases. At $Pr_1 = 0.65$ and $Pr_2 = 2.65$ there exists a co-dimension two bifurcation point. In Figures 6.5- 6.6, the marginal curve $l = 0$ represents for cross rolls and $m = 0$ represents for parallel rolls. In Figure 6.5 critical Rayleigh number is smaller for the cross roll ($l = 0$) than for the parallel roll at low magnetic field, critical Rayleigh number is smaller for the parallel roll ($m = 0$) than for the cross roll for a high magnetic field. In Figure 6.6, the critical Rayleigh number is smaller for the parallel roll ($m = 0$) than for the cross roll ($l = 0$) a weak magnetic field and the critical Rayleigh number for crross rolls ($l = 0$) is smaller than parallel rolls ($m = 0$).

6.4 Nonlinear Analysis

6.4.1 Amplitude equation at the onset of Hopf Bifurcation

According to Newell and Whitehead [77] multiple scale analysis , small scale convection cells disturb the vital flow. If the scale range is $O(\epsilon)$ then the collaboration of the cell with itself forces a second harmonic and a standard state of rectification of range $O(\epsilon^2)$ and these in turn impel an $O(\epsilon^3)$ rectification to the structural module of the imposed roll. Let us assume that the solution of equations (6.1) - (6.5)take the form given below

$$f = f(u, v, w, \theta, H_x, H_y, H_z, C) = \epsilon f_0 + \epsilon^2 f_1 + \epsilon^3 f_2 + \cdots , \qquad (6.22)$$

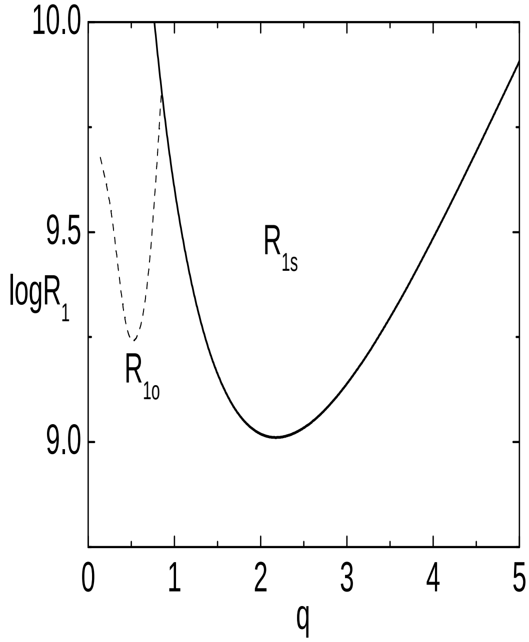

(a)

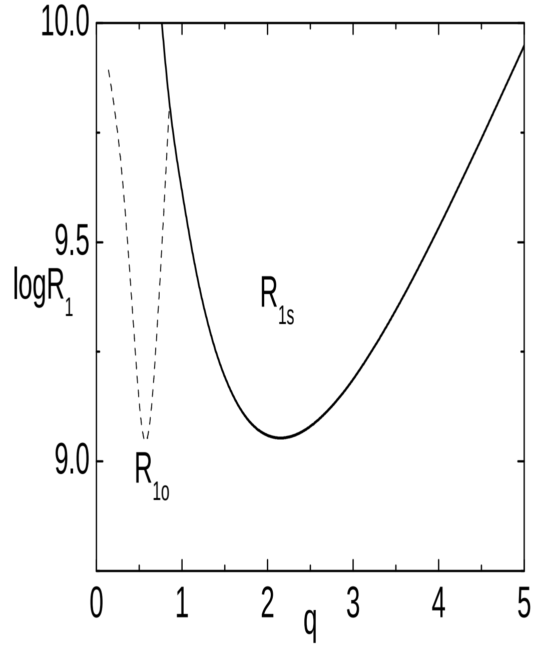

(b)

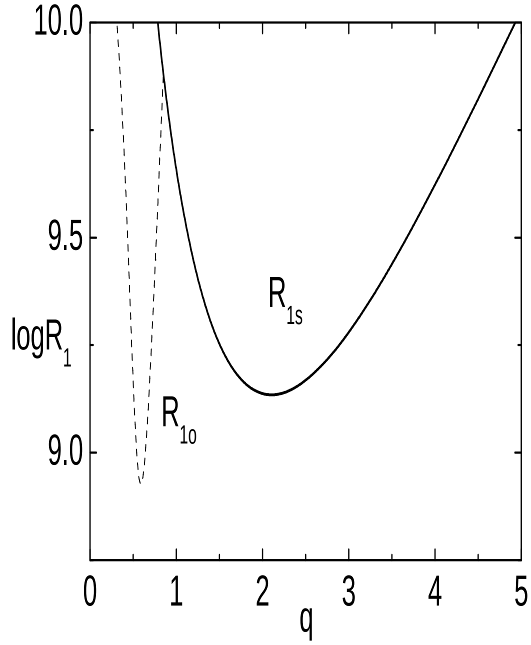

(c)

Figure 6.2: Marginal stability curves of R_{1s} and R_{1o} for $Da = 1500$, $\Lambda = 10.5$, $M = 0.85$, $\phi = 0.9$, $Pr_1 = 1$, $Pr_2 = 5$, $Ta = 2000$, (a) $Q = 100$, (b) $Q = 150$, (c) $Q = 250$.

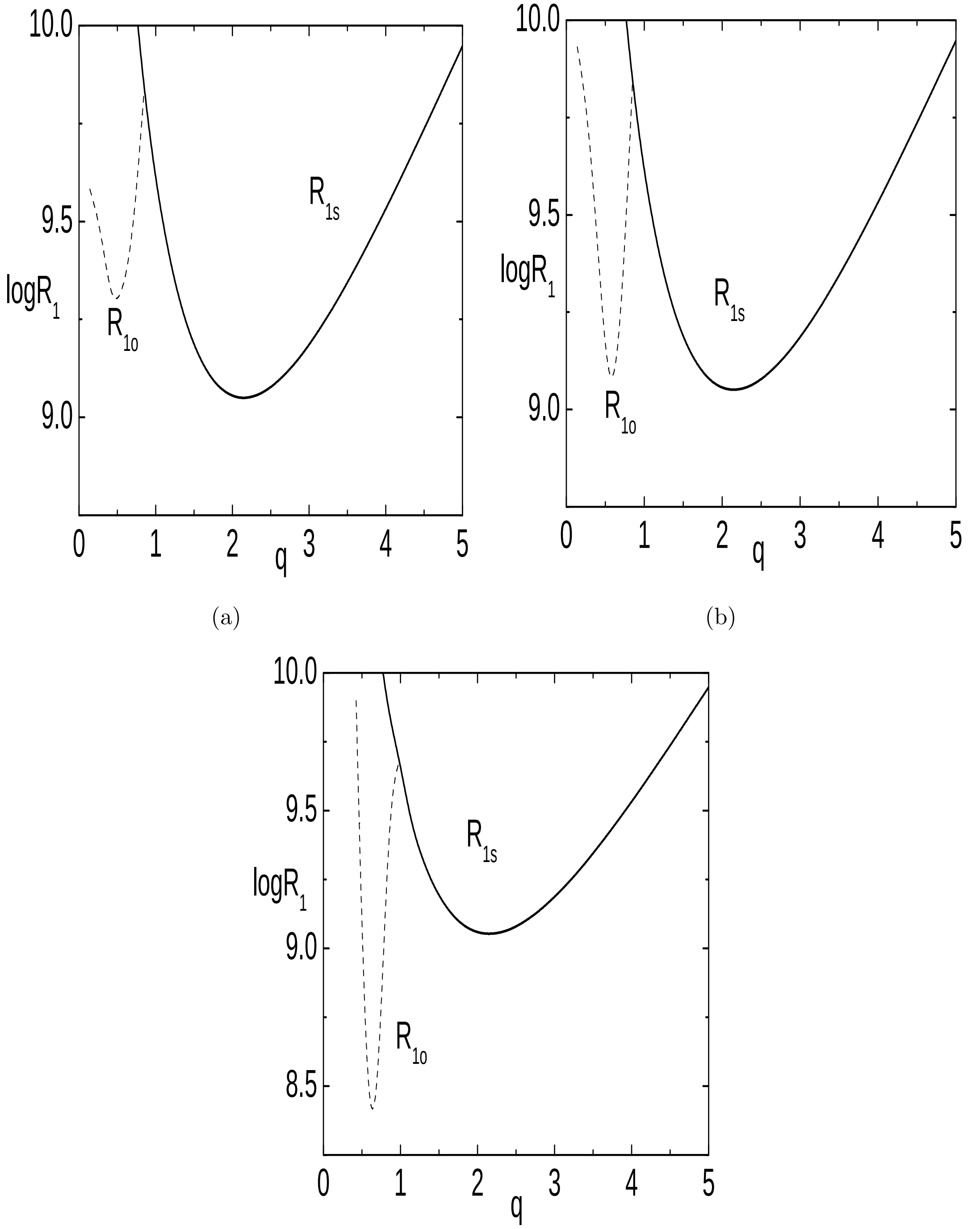

(a) (b)

(c)

Figure 6.3: Marginal stability curves of R_{1s} and R_{1o} for $Da = 1500$, $\Lambda = 10.5$, $M = 0.85$, $\phi = 0.9$, $Pr_1 = 1$, $Pr_2 = 5$, $Q = 150$, (a) $Ta = 500$, (b) $Ta = 1000$, (c) $Ta = 2000$.

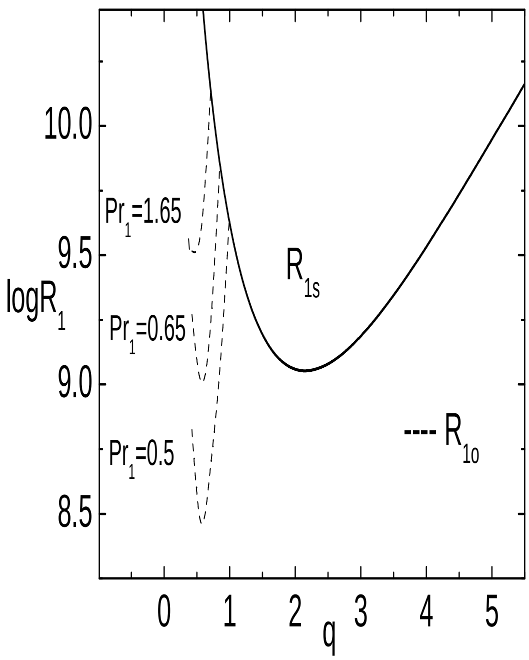

(a)

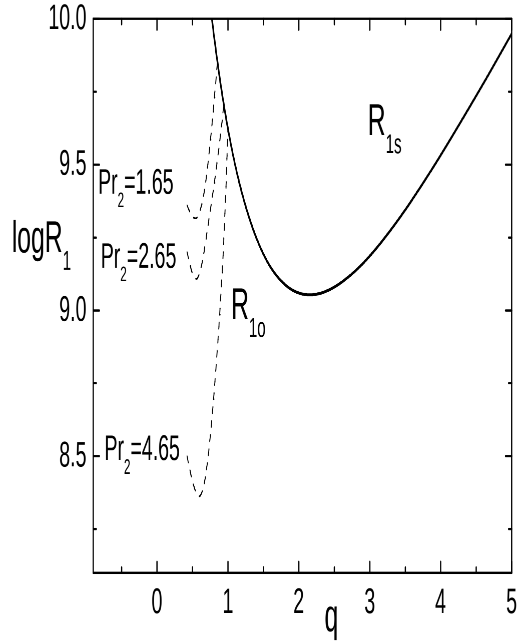

(b)

Figure 6.4: Marginal stability curves of R_{1s} and R_{1o} for $Da = 1500$, $\Lambda = 10.5$, $M = 0.85$, $\phi = 0.9$, $Pr_1 = 1$, $Pr_2 = 5$, $Ta = 1000$, $Q = 150$ (a) $Pr_2 = 2.65$ and (b) $Pr_1 = 0.65$

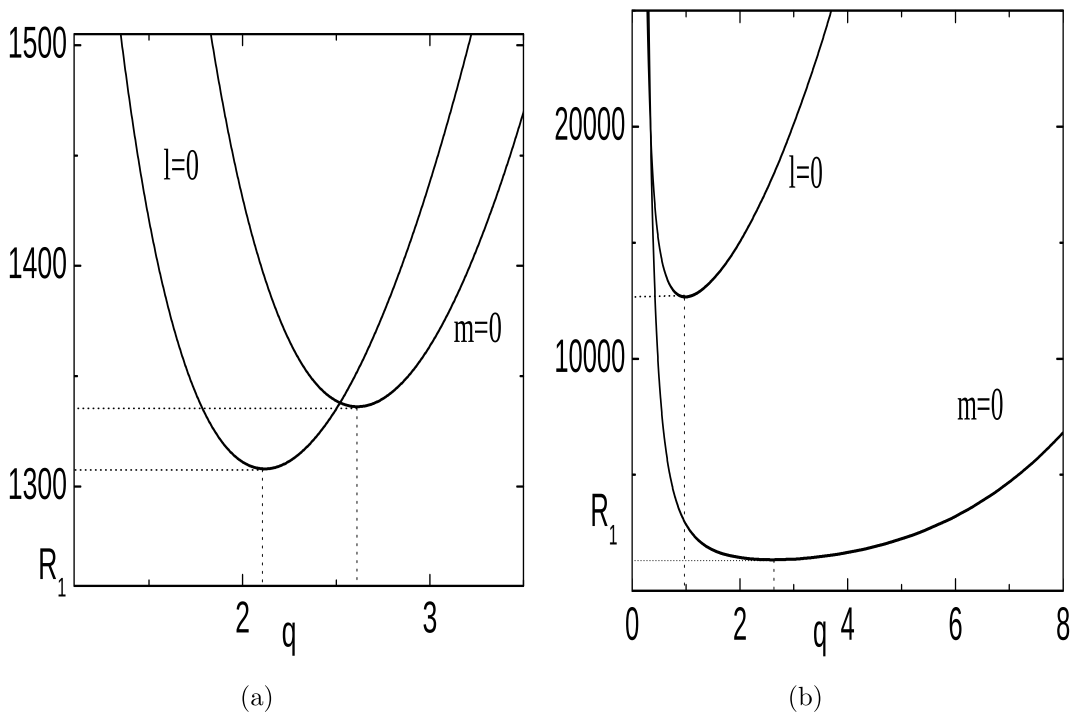

Figure 6.5: The marginal thermal Rayleigh number R_1, for steady parallel rolls ($m = 0$) and cross rolls ($l = 0$) at $Da = 1500$, $\Lambda = 10.5$, $M = 0.85$, $\phi = 0.9$, $Pr_1 = 1$, $Pr_2 = 5$, $Ta = 1000$, (a) $Q = 150$, (b) $Q = 1000$.

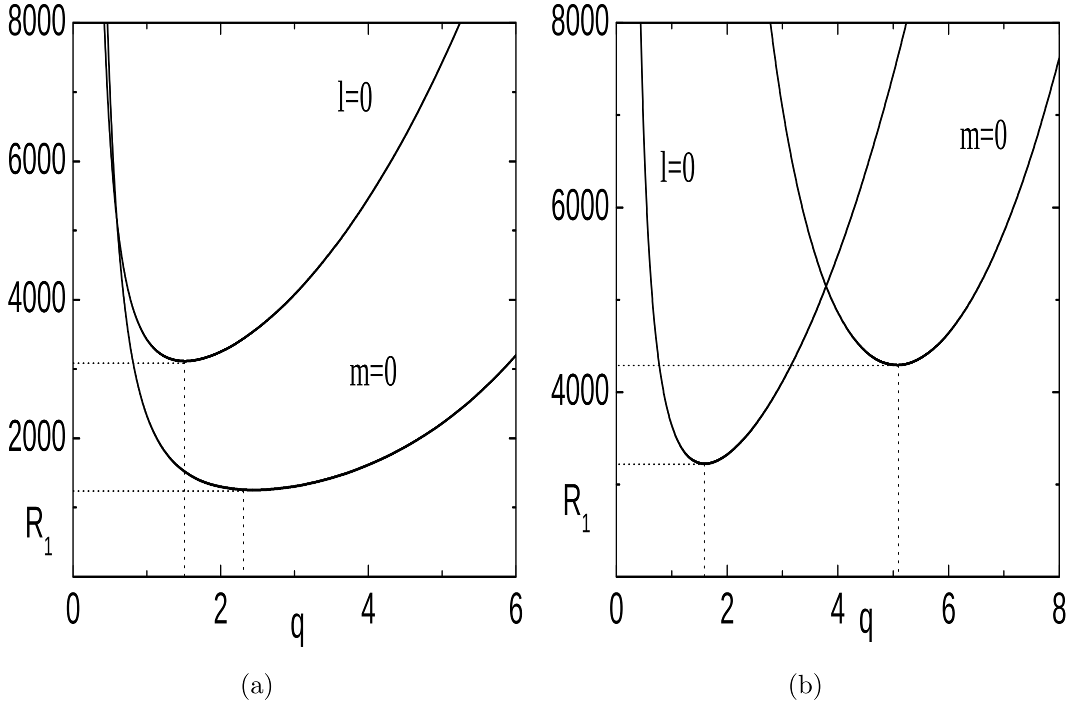

Figure 6.6: The marginal thermal Rayleigh number R_1, for steady parallel rolls $(m = 0)$ and cross rolls $(l = 0)$ at $Da = 1500$, $\Lambda = 10.5$, $M = 0.85$, $\phi = 0.9$, $Pr_1 = 1$, $Pr_2 = 5$, $Q = 150$, (a) $Ta = 500$, (b) $Ta = 50000$.

where

$$\epsilon^2 = \frac{R_1 - R_{1sc}}{R_{1sc}} << 1,$$

The first order calculations of the linearised problem given by approximation is given by the eigenvectors

$$\begin{aligned}
u_0 =& \frac{i\pi}{l}\left[Ae^{i(lx+my)} - c\cdot c\cdot\right]\cos\pi z,\\
v_0 =& -\frac{i\pi Ta^{1/2}\delta^2}{\phi l(\delta^4 + Qm^2)}\left[Ae^{i(lx+my)} - c\cdot c\cdot\right]\cos\pi z,\\
w_0 =& \left[Ae^{i(lx+my)}z + c\cdot c\cdot\right]\sin\pi,\\
\theta_0 =& \frac{1}{M\delta^2}\left[Ae^{i(lx+my)} + c\cdot c\cdot\right]\sin\pi z,\\
H_{x_0} =& \frac{-\pi m}{Ml\delta^2}\left[Ae^{i(lx+my)} + c\cdot c\cdot\right]\cos\pi z,\\
H_{y_0} =& \frac{m\pi Ta^{1/2}\delta^2}{M\phi l(\delta^4 + Qm^2)},\left[Ae^{i(lx+my)} + c\cdot c\cdot\right]\cos\pi z,\\
H_{z_0} =& \frac{im}{M\delta^2}\left[Ae^{i(lx+my)} - c\cdot c\cdot\right]\sin\pi z,\\
C_0 =& \frac{1}{ML\delta^2}\left[Ae^{i(lx+my)} + c\cdot c\cdot\right]\sin\pi z,
\end{aligned} \tag{6.23}$$

where $A = A(X, Y, T)$ is the complex scale vary on the gradual variables X, Y and T and $c.c$ represents the complex conjugate. The independent variables x, y, z and t are scaled by introducing multiple scales

$$X = \epsilon x, \quad Y = \epsilon^{\frac{1}{2}}y, \quad Z = z, \quad T = \epsilon^2 t,$$

are suitably scattered at the fast and slow unconventional variables in f. The linear and nonlinear operators $\mathcal{L}$ and $\mathcal{N}$ are written as

$$\mathcal{L} = \mathcal{L}_0 + \epsilon\mathcal{L}_1 + \epsilon^2\mathcal{L}_2\cdots, \tag{6.24}$$

$$\mathcal{N} = \epsilon^2\mathcal{N}_0 + \epsilon^3\mathcal{N}_1 + \cdots, \tag{6.25}$$

substituting equations $\mathcal{L}$, $\mathcal{N}$ and w in $\mathcal{L}w = \mathcal{N}$ and equating ϵ, ϵ^2 and ϵ^3 coefficients on both side, we obtain

$$\mathcal{L}_0 w_0 = 0, \tag{6.26}$$

$$\mathcal{L}_0 w_1 + \mathcal{L}_1 w_0 = \mathcal{N}_0, \tag{6.27}$$

$$\mathcal{L}_0 w_2 + \mathcal{L}_1 w_1 + \mathcal{L}_2 w_0 = \mathcal{N}_1, \tag{6.28}$$

The second order calculations of the linearised problem given by approximation are given by the eigenvectors

$$\begin{aligned}
u_1 =& 0, w_1 = 0, \\
v_1 =& S_1 \left[A^2 e^{2i(l_{sc}x + m_{sc}y)} - c \cdot c \cdot \right], \\
\theta_1 =& -\frac{1}{2\pi M^2 \delta^2} |A|^2 sin 2\pi z, \\
H_{x_1} =& \frac{m}{2M^2 \delta^2 l} |A|^2 cos 2\pi z \\
H_{y_1} =& \frac{m\mathcal{K}_1}{2Mq^2} \left[A^2 e^{2i(l_{sc}x + m_{sc}y)} \cos \pi z + c \cdot c \cdot \right], \\
H_{z_1} =& 0, \\
C_1 =& -\frac{1}{2M^2 L^2 \delta^2} |A|^2 sin 2\pi z,
\end{aligned} \tag{6.29}$$

taking $w_1 = 0$ in equation (6.24), $\mathcal{N}_1 - \mathcal{L}_2 w_0$ is vertical to w_0 and coefficient of $\sin \pi z$ in $\mathcal{N}_1 - \mathcal{L}_2 w_0$ vanishes. We get

$$\lambda_0 \frac{\partial A}{\partial T} - \lambda_1 \left(\frac{\partial}{\partial X} - \frac{i}{2q} \frac{\partial^2}{\partial Y^2} \right)^2 A - \left(\lambda_2 + \lambda_3 |A|^2 \right) A = 0, \tag{6.30}$$

where

$$\lambda_0 =(Q+\phi\delta^4)\frac{2\phi Pr_2\delta^8}{MPr_1}+(R_1-\frac{R_2}{L})\frac{\phi q^2\delta^2 Pr_2}{MPr_1}+(1+\frac{\phi}{L})(Q^2m^2+Ta\pi^2\delta^4+\Lambda^2\delta^8)\delta^4-$$
$$2Q\delta^8m^2(\Lambda+\frac{1}{M\phi Pr_1})+(R_1Q-R_2)(Qm^2-\Lambda\delta^4)\frac{q^2\delta^2}{L}-2qR_2Ta\delta^4\frac{Pr_2}{Pr_1},$$
$$\lambda_1 =m^2Q\delta^2(3m^2Q+20\delta^4)+(R_1-R_2L)[m^2Q(3q^2+2\pi^2)+2\delta^4(5q^2+2\pi^2)]+$$
$$21\delta^10\Lambda^2+\frac{6\pi^2\delta^4Ta}{\phi^2} \quad ,$$
$$\lambda_2 =R_1\Lambda q^2\delta^8+QR_1q^2\delta^4m^2,$$
$$\lambda_3 =(\Lambda\delta^4+Qm^2)\left[(R_1-\frac{R_2\pi}{2ML^3})\frac{\delta^2q^2}{2M^2}-Q\frac{Qm^2Pr_2}{4M^2Pr_1}(1+\delta^2(l^2+m^2))\right]-\frac{Ta^{1/2}\pi Q\delta^8Pr_2}{\phi Pr_1}$$
$$\left(\frac{m^2\pi\pi Ta^{1/2}}{2M^3\delta^2l\phi(\Lambda\delta^4+Qm^2)}+\frac{lmS_2}{4\pi M^2\delta^2}\right)+\frac{Ta\pi^2m^2\delta^6QPr_2}{4M^2\phi^2Pr_1} \tag{6.31}$$

By using multiple scaling and $A(x,y,t)=\frac{A(X,Y,T)}{\epsilon}$, equation (6.30) can be written as a nonlinear two-dimensional time dependent LG equation in fast variables as

$$\lambda_0\frac{\partial A}{\partial t}-\lambda_1\Big(\frac{\partial}{\partial x}-\frac{i}{2q}\frac{\partial^2}{\partial y^2}\Big)^2A-\left(\epsilon^2\lambda_2+\lambda_3|A|^2\right)A=0, \tag{6.32}$$

which describes slow extensional scale ϵx vertical to the rolls and the variation of the slow time scale $\epsilon^2 t$. Independent of y and t terms from equation (6.32), we get

$$\frac{\mathrm{d}^2A}{\mathrm{d}X^2}+\frac{\epsilon^2\lambda_2}{\lambda_1}(1-\frac{\lambda_3}{\epsilon^2\lambda_2}|A|^2)A=0. \tag{6.33}$$

$$A(X)=A_0\tanh\left(\frac{X}{\Lambda_0}\right),$$

where

$$A_0=\left(\epsilon^2\frac{\lambda_2}{\lambda_3}\right)^{\frac{1}{2}} \quad \text{and} \quad \Lambda_0=\left(\frac{2\lambda_1}{\epsilon^2\lambda_2}\right)^{\frac{1}{2}}.$$

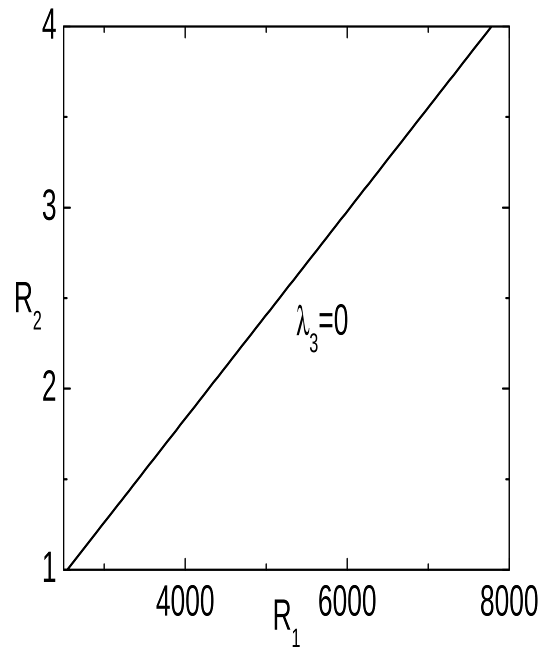

Figure 6.7: The curve $\lambda_3 = 0$ gives critical bifurcation point for $Da = 1500$, $\Lambda = 10.5$, $M = 0.85$, $\phi = 0.9$, $Pr_1 = 1$, $Pr_2 = 5$, $Ta = 1000$ and $Q = 150$. The salinity Rayleigh number increases by increasing the thermal Rayleigh number

Heat Transport by Convection

If $|\frac{X}{\Lambda_0}| \leq 1$ then $|A|$ reaches maximum value. The maximum amplitude of A is $|A_{max}|$,

$$|A_{max}| = \left(\frac{\epsilon^2 \lambda_2}{\lambda_3}\right)^{\frac{1}{2}}, \tag{6.34}$$

Heat transfer in field is Nusselt number Nu,

$$Nu = 1 + \frac{\epsilon^2}{\delta^2}|A_{max}|^2. \tag{6.35}$$

From Figure 6.8, Nusselt number Nu increases while thermal Rayleigh number R_1 also increases. In Figure 6.9, regions of Eckhaus (E), zigzag (Z) and stable (S) regions are plotted.

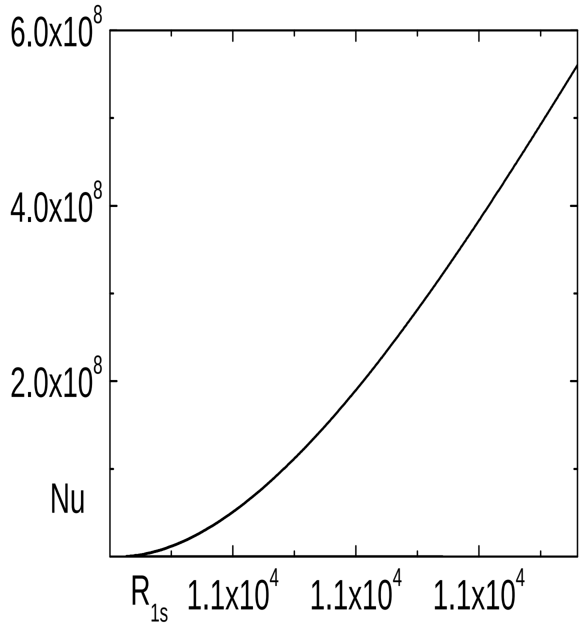

Figure 6.8: Graph is plotted in (Nu, R_{1s}) plane for $Da = 1500$, $\Lambda = 10.5$, $M = 0.85$, $\phi = 0.9$, $Pr_1 = 1$, $Pr_2 = 5$, $Q = 150$ and $Ta = 500$.

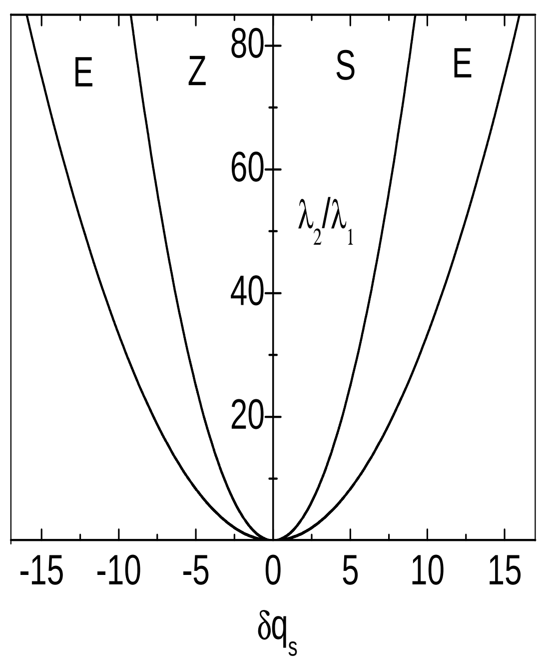

Figure 6.9: Regions of Eckhaus instability (E), zigzag instability (Z)and stable region (S) are plotted for $Da = 1500$, $\Lambda = 10.5$, $M = 0.85$, $\phi = 0.9$, $Q = 150$, $Ta = 1000$, $Pr_1 = 1$, $Pr_2 = 5$.

6.4.2 Amplitude equation at the onset of Pitchfork Bifurcation

Consider cylindrical rolls along y-axis, so that only x-dependence and z-dependence appears from $\mathcal{L}w = \mathcal{N}$. Coupled time dependent nonlinear Landau-Ginzburg type equations were obtained at the supercritical Hopf bifurcation. We establish ϵ as

$$\epsilon^2 = \frac{R_o - R}{R} \ll 1. \tag{6.36}$$

Take

$$w_0 = \Big[A_{1L}e^{i(lx+my+\omega t)} + A_{1R}e^{i(lx+my-\omega t)} + c.c\Big]\sin\pi z,$$

which is a solution of $\mathcal{L}w = 0$. Here A_{1L} and A_{1R} represent the amplitude of left and right travelling wave the rolls respectively and depends on slow space X and time variables $\tau,\ T$, Knobloch and Luca [57],

$$X = \epsilon x, \quad \tau = \epsilon t, \quad T = \epsilon^2 t. \tag{6.37}$$

The derivative operators are expressed as

$$\frac{\partial}{\partial x} \to \frac{\partial}{\partial x} + \epsilon\frac{\partial}{\partial X}, \quad \frac{\partial}{\partial t} \to \frac{\partial}{\partial t} + \epsilon\frac{\partial}{\partial \tau} + \epsilon^2\frac{\partial}{\partial T}. \tag{6.38}$$

The power series solution is

$$f = \epsilon f_0 + \epsilon^2 f_1 + \epsilon^3 f_2 + \cdots, \tag{6.39}$$

in ϵ term. The first order approximation of the linearized problem is then

$$
\begin{aligned}
u_0 =& -\frac{\pi m}{l}\big[A_{1L}e^{i(lx+my+\omega t)} + A_{1R}e^{i(lx+my-\omega t)} - c.c\big]\cos\pi z,\\
v_0 =& -\frac{i\pi Ta^{\frac{1}{2}}}{M\phi l}\big[k_1A_{1L}e^{i(lx+my+\omega t)} - k_1^cA_{1R}e^{i(lx+my-\omega t)} - c.c\big]\cos\pi z,\\
w_0 =& \big[A_{1L}e^{i(lx+my+\omega t)} + A_{1R}e^{i(lx+my-\omega t)} + c.c\big]\sin\pi z,\\
\theta_0 =& \frac{1}{M}\big[\frac{A_{1L}}{b1}e^{i(lx+my+\omega t)} + \frac{A_{1R}}{b1^c}e^{i(lx+my-\omega t)} + c.c\big]\sin\pi z,\\
C_0 =& \frac{1}{ML}\big[\frac{A_{1L}}{c1}e^{i(lx+my+\omega t)} + \frac{A_{1R}}{c1^c}e^{i(lx+my-\omega t)} + c.c\big]\sin\pi z,\\
H_{x_0} =& -\frac{\pi m}{l}\big[\frac{A_{1L}}{d1}e^{i(lx+my+\omega t)} + \frac{A_{1R}}{d1^c}e^{i(lx+my-\omega t)} + c.c\big]\cos\pi z,\\
H_{y_0} =& \frac{Ta^{1/2}\pi m}{M\phi l}\big[\frac{k_1A_{1L}}{d1}e^{i(lx+my+\omega t)} + \frac{k_2A_{1R}}{d1^c}e^{i(lx+my-\omega t)} + c.c\big]\cos\pi z,\\
H_{z_0} =& -im\big[\frac{A_{1L}}{d1}e^{i(lx+my+\omega t)} + \frac{A_{1R}}{d1^c}e^{i(lx+my-\omega t)} - c.c\big]\sin\pi z. \qquad (6.40)
\end{aligned}
$$

The second order calculations of the problem given by approximation are given by the eigen vectors

$$
\begin{aligned}
u_1 =& 0,\\
v_1 =& \frac{i}{2ls_1}\big[(A_{1L}^2 + A_{1R}^2)e^{2i(lx+my+\omega t)} + A_{1L}A_{1R}e^{2i(lx+my)} - c.c\big],\\
w_1 =& 0,\\
\theta_1 =& -\frac{1}{M^2}\left[\frac{|A_{1L}|^2 + |A_{1R}|^2}{4\pi b} + \frac{\pi A_{1L}A_{1R}^c}{b1^pb1}e^{2i\omega t} + c.c\right]\sin 2\pi z,\\
C_1 =& -\frac{\pi}{M^2L^2}\left[\frac{|A_{1L}|^2 + |A_{1R}|^2}{4\pi^2c1} + \frac{A_{1L}A_{1R}e^{2i\omega t}}{c1^cc1^p} + c.c\right]\sin 2\pi z,\\
H_{x_1} =& \frac{2m\pi^2Pr_2}{lPr_1}\left[\frac{|A_{1L}|^2 + |A_{1R}|^2}{4M\pi^2d1} + \frac{A_{1L}A_{1R}^c}{d1^pd1} + c.c\right]\cos 2\pi z,\\
H_{y_1} =& \frac{2m\pi\delta^2Pr_2}{lPr_1}\Big[|A_{1L}|^2 + |A_{1R}|^2 + A_{1L}A_{1R}e^{2i(lx+my)} + \frac{A_{1L}A_{1R}^c}{e1^pd1} + c.c\Big]\cos 2\pi z,\\
H_{z_1} =& 0, \qquad (6.41)
\end{aligned}
$$

where $b1 = \delta^2 + i\omega,\ c1 = \delta^2 + \frac{\phi}{L} i\omega,\ d1 = M\delta^2 + \phi \frac{Pr_2}{Pr_1} i\omega,\ e1 = M\delta^2 + \phi \frac{Pr_2}{Pr_1} i\omega,\ b1^p = 2\pi^2 + i\omega,\ c1^p = 2\pi^2 + \frac{\phi}{L} i\omega,\ d1^p = 2M\pi^2 + \phi \frac{Pr_2}{Pr_1} i\omega,\ e1^p = 2M\pi^2 + \phi \frac{Pr_2}{Pr_1} i\omega$ and $b1^c,\ c1^c,\ d1^c$ are complements of $b1,\ c1,\ d1$ respectively. Equation (6.28) is solvable when $\mathcal{L}_0 w_0 = 0$ and equate the coefficients of $\sin \pi z$ in $\mathcal{N}_1 - \mathcal{L}_2 w_0$ zero, we get

$$\Lambda_0 \frac{\partial A_{1L}}{\partial T} + \Lambda_1 \left(\frac{\partial}{\partial \tau} - v_g \frac{\partial}{\partial X} \right) A_{2L} - \Lambda_2 \frac{\partial^2 A_{1L}}{\partial X^2} - \Lambda_3 A_{1L} + \Lambda_4 |A_{1L}|^2 A_{1L} + \Lambda_5 |A_{1R}|^2 A_{1L} = 0 \tag{6.42}$$

$$\Lambda_0 \frac{\partial A_{1R}}{\partial T} + \Lambda_1 \left(\frac{\partial}{\partial \tau} - v_g \frac{\partial}{\partial X} \right) A_{2R} - \Lambda_2 \frac{\partial^2 A_{1R}}{\partial X^2} - \Lambda_3 A_{1R} + \Lambda_4 |A_{1R}|^2 A_{1R} + \Lambda_5 |A_{1L}|^2 A_{1R} = 0. \tag{6.43}$$

Solve equations (6.42) and (6.43) by taking $\xi' = \nu_g \tau + X$ and $\eta' = \nu_g \tau - X$, we get

$$2v_g \Lambda_1 \frac{\partial A_{2L}}{\partial \eta'} = -\Lambda_0 \frac{\partial A_{1L}}{\partial T} + \Lambda_2 \frac{\partial A_{1L}}{\partial X^2} + \Lambda_3 A_{1L} - \left(\Lambda_4 |A_{1L}|^2 + \Lambda_5 |A_{1R}|^2 \right) A_{1L}, \tag{6.44}$$

$$2v_g \Lambda_1 \frac{\partial A_{2R}}{\partial \eta'} = -\Lambda_0 \frac{\partial A_{1R}}{\partial T} + \Lambda_2 \frac{\partial A_{1R}}{\partial X^2} + \lambda_3 A_{1R} - \left(\Lambda_4 |A_{1R}|^2 + \Lambda_5 |A_{1L}|^2 \right) A_{1R}. \tag{6.45}$$

This is obtained on integrating equations (6.44) and (6.45) over η' and ξ' respectively by which, we get

$$\Lambda_0 \frac{\partial A_{1L}}{\partial T} = \Lambda_2 \frac{\partial A_{1L}}{\partial X^2} + \lambda_3 A_{1L} - \left(\Lambda_4 |A_{1L}|^2 + \Lambda_5 |A_{1R}|^2 \right) A_{1L}, \tag{6.46}$$

$$\Lambda_0 \frac{\partial A_{1R}}{\partial T} = \Lambda_2 \frac{\partial A_{1R}}{\partial X^2} + \lambda_3 A_{1R} - \left(\Lambda_4 |A_{1R}|^2 + \Lambda_5 |A_{1L}|^2 \right) A_{1R}. \tag{6.47}$$

Equations (6.46) and (6.47) are left and right moving amplitude waves known as coupled one dimensional LG equations.

Travelling Waves and Standing Waves

Coullet [37] and Knobloch [57] studied regions of travelling standing waves, on magneto convection which Matthews [67] derived. On dropping slow variable X from equations (6.46) and (6.47), we get

$$\frac{dA_{1L}}{dT} = \frac{\Lambda_3}{\Lambda_0}A_{1L} - \frac{\Lambda_4}{\Lambda_0}A_{1L}|A_{1L}|^2 - \frac{\Lambda_5}{\Lambda_0}A_{1L}|A_{1R}|^2, \tag{6.48}$$

$$\frac{dA_{1R}}{dT} = \frac{\Lambda_3}{\Lambda_0}A_{1R} - \frac{\Lambda_4}{\Lambda_0}A_{1R}|A_{1R}|^2 - \frac{\Lambda_5}{\Lambda_0}A_{1R}|A_{1L}|^2. \tag{6.49}$$

Put

$$\beta' = \frac{\Lambda_3}{\Lambda_0}, \quad \gamma' = -\frac{\Lambda_4}{\Lambda_0} \quad \text{and} \quad \delta' = -\frac{\Lambda_5}{\Lambda_0}.$$

Then equations (6.48) and (6.49) take the following form

$$\frac{dA_{1L}}{dT} = \beta' A_{1L} + \gamma' A_{1L}|A_{1L}|^2 + \delta' A_{1L}|A_{1R}|^2, \tag{6.50}$$

$$\frac{dA_{1R}}{dT} = \beta' A_{1R} + \gamma' A_{1R}|A_{1R}|^2 + \delta' A_{1R}|A_{1L}|^2. \tag{6.51}$$

Where

$$\begin{aligned} A_{1L} &= a_L e^{i\phi_L} & a_L &= |A_{1L}| & \phi_L &= arg(A_{1L}) = \tan^{-1}\left(\frac{Im(A_{1L})}{Re(A_{1L})}\right) \\ A_{1R} &= a_L e^{i\phi_R} & a_R &= |A_{1R}| & \phi_R &= arg(A_{1R}) = \tan^{-1}\left(\frac{Im(A_{1R})}{Re(A_{1R}})\right) \\ \beta' &= \beta_1 + i\beta_2 & \gamma' &= \gamma_1 + i\gamma_2 & \delta' &= \delta_1 + i\delta_2 \end{aligned} \tag{6.52}$$

Substituting A_{1L},A_{1R},β', γ' and δ' in (6.50) and (6.51). we get $a_L = -\beta_1/(\gamma_1 + \delta_1)$ and $a_R = -\beta_1/(\gamma_1+\delta_1)$ for standing waves. $(a_L, a_R) = (a_L, 0)$ for left travelling waves and $(a_L, a_R) = (0, a_R)$ for right travelling waves. $(a_L, a_R) = (0, 0)$ for conduction state. In Figure 6.10, we study the stability of regions of travelling and standing waves. The stability regions of standing waves and travelling waves increase when the ratio of thermal and magnetic prandtl number increases.

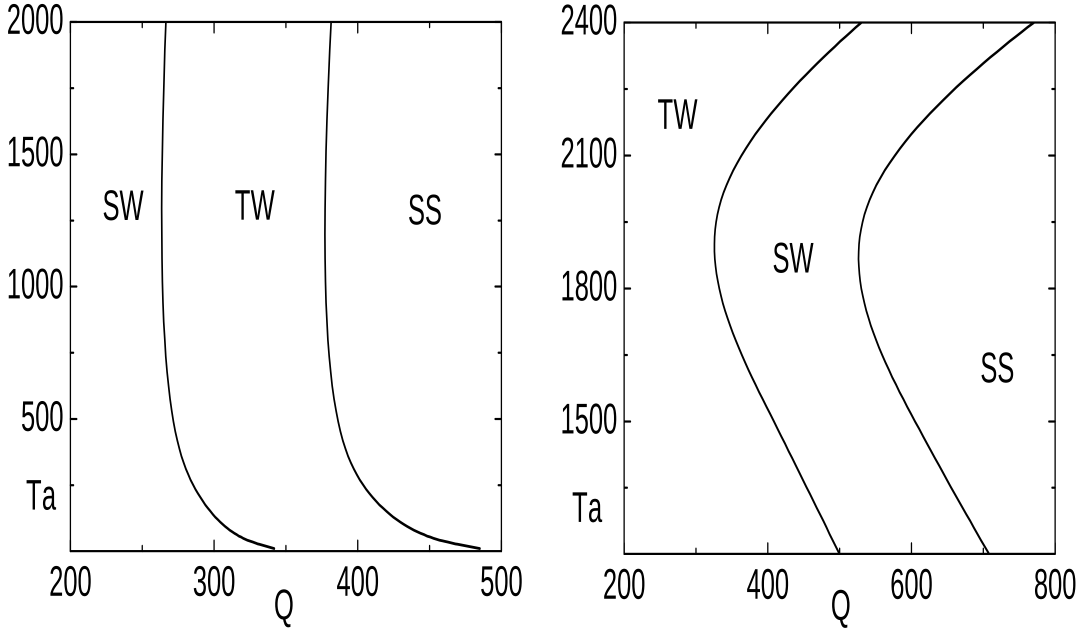

(a) (b)

Figure 6.10: Diagram illustrates the stability regions of steady state, standing and travelling waves for $Da = 1500$, $\Lambda = 5.85$, $M = 0.9$, $\phi = 0.09$ at (a) $Pr_2/Pr_1 = 6$, (b) $Pr_2/Pr_1 = 12$.

6.5 Conclusions

By using stress free boundary conditions, an analytic expressions has been found in linear convective stability analysis. In the linear model for equation $\mathcal{L}w = 0$, at the onset of convection we identified rolls emerge region. The corresponding marginal stability curves were also traced. Thermal and magnetic Prandtl numbers do not affect on convective stationary thermal Rayleigh value. Identified Takens-Bogdanov and co-dimension two bifurcation points on neutral curves were identified. The region of salinity Rayleigh value R_2 verses thermal Rayleigh value R_1 over convective stationary and oscillatory increased by increasing internal forces over a rotating field. Two dimensional LG equation was derived at the onset of stationary mode, heat transport from Nusselt number and long wave length wave based on Eukhaus and Zigzag instabilities were also studied. Nusselt number grows exponentially if thermal Rayleigh value increases. We derived two nonlinear L-G equations and observed stability regions for travelling and standing wave for fixed physical and porous parameters.

Chapter 7

Conclusions and Scope of Future Work

Conclusions

In this dissertation, we have taken model Rayleigh-Benard convection (which is example of single diffusive system), magnetoconvection, convection in rotating fluid and thermohaline convection (which are examples of double diffusive system), thermohaline magnetoconvection (which is an example of triple diffusive system) in a sparsely packed porous medium. Throughout this dissertation we have used stress-free boundary conditions. Even though stress-free boundary conditions cannot be achieved in laboratory, we can use it since they allow simple trigonometric eigenfunctions. Our goal is to identify the region of parameter values, for which rolls emerge at the onset of convection. In Chapter 2, we studied the stability of finite amplitude Rayleigh-Benard convection in a sparsely packed porous medium due to horizontal magnetic field, which is an example of double diffusive problem, where problems of both stationary convection and oscillatory convection are exists. By performing weakly nonlinear analysis, we derived a nonlinear time dependent two dimensional Landau-Ginzburg equation at supercritical Pitchfork bifurcation and showed the existence of Eckhaus and Zigzag instabilities and also studied Nusselt number contribution. We derived couple one dimensional Landau Ginzburg equation and computed stability regions of standing waves and travelling waves. In Chapter 3, we investigated the Rayleigh-Benard convection in a sparsely packed porous medium with the effect of rotation and horizontal magnetic field. This is an example of triple diffusive convection. We observed for increasing the ratio of thermal and magnetic prandtl number the instability regions are increased. In Chapter 4, we studied linear and nonlinear instabilities of thermohaline convection in a sparsely packed porous medium with the effect of horizontal magnetic field. We first identified steady state and it is replaced by standing waves, and travelling waves are unstable. In Chapter 5, we studied instabilities of thermohaline convection in a sparsely packed porous medium with the effect of rotation. The region of standing waves unstable. In Chapter 6, we investigated instabilities of thermohaline convection in a sparsely packed porous medium with the effect of rotation and magnetic field. The region of standing and travelling waves exits along with the steady state. Chapter 4 to Chapter 6 are examples of multiple diffusive systems. In double, triple and multiple diffusive systems, both stationary convection and oscillatory convection exist. Chapter 2 to Chapter 5, we have studied the linear stability analysis were analysed by taking thermal Rayleigh number R as a dependent variable and then by taking Rayleigh number R as an independent variable. By using multiple scale analysis we derived a nonlinear two-dimensional Landau-Ginzburg equation in complex amplitude $A(X, Y, T)$ with real coefficients near a supercritical Pitchfork bifurcation. We have also shown the occurrence of secondary instabilities like Eckhaus and Zigzag instabilities and we also studied Nusselt number contribution at the onset of stationary convection from Landau-Ginzburg equation. We obtained the general pattern near the onset of oscillatory convection at a supercritical Hopf bifurcation. We derived coupled nonlinear one-dimensional Landau-Ginzburg equations and studied the condition for occurrence of instability for both travelling and standing waves.

Scope of Future Work

In future we wish to investigate linear and nonlinear models along with the effect of different external fields with anisotropy in convective instabilities in a sparsely packed porous medium. We also want to explore the occurrence of Kuppers-Lortz instability and skew-varicose instability with realistic boundary conditions.

Bibliography

[1] A Abdullah. Thermosolutal convection in a nonlinear magnetic fluid. *Revue G. rale de Thermique*, 39(2):273–284, 2000.

[2] A Abdullah and Sahar Z Alkazmi. Thermohaline convection in a porous medium in the presence of magnetic field and rotation. *Development and Applications of Oceanic Engineering*, 3:32–38, 2014.

[3] S Alchaar, P Vasseur, and E Bilgen. Effects of a magnetic field on the onset of convection in a porous medium. *Heat and Mass Transfer*, 30(4):259–267, 1995.

[4] S Alchaar, P Vasseur, and E Bilgen. Hydromagnetic natural convection in a tilted rectangular porous enclosure. *Numerical Heat Transfer, Part A: Applications*, 27(1):107–127, 1995.

[5] AA Altawallbeh, NH Saeid, and Ishak Hashim. Magnetic field effect on natural convection in a porous cavity heating from below and salting from side. *Advances in Mechanical Engineering*, 5:179–183, 2013.

[6] J. M. Aurnou and P. L. Olson. Experiments on rayleigh–benard convection, magnetoconvection and rotating magnetoconvection in liquid gallium. *Journal of Fluid Mechanics*, 430:283–307, 2001.

[7] A Benerji Babu, Ragoju Ravi, and SG Tagare. Nonlinear magnetoconvection in a sparsely packed porous medium. *International Journal of Geophysics*, 2011:1–17, 2011.

[8] A Benerji Babu, Ragoju Ravi, and SG Tagare. Nonlinear rotating convection in a sparsely packed porous medium. *Communications in Nonlinear Science and Numerical Simulation*, 17(12):5042–5063, 2012.

[9] A Benerji Babu, Ragoju Ravi, and SG Tagare. Nonlinear rotating convection in a sparsely packed porous medium. *Communications in Nonlinear Science and Numerical Simulation*, 17(12):5042–5063, 2012.

[10] A Benerji Babu, Ragoju Ravi, and SG Tagare. Nonlinear thermohaline magnetoconvection in a sparsely packed porous medium. *Journal of Porous Media*, 17(1), 2014.

[11] A Benerji Babu, G Shiva Kumar Reddy, and SG Tagare. Nonlinear magneto convection due to horizontal magnetic field and vertical axis of rotation due to thermal and compositional buoyancy. *Results in Physics*, 12:2078–2090, 2019.

[12] Renu Bajaj and S. K. Malik. Convective instability and pattern formation in magnetic fluids. *Journal of Mathematical Analysis and Applications*, 207(1):172–191, 1997.

[13] Renu Bajaj and S. K. Malik. Rayleighbenard convection and pattern formation in magnetohydrodynamics. *Journal of plasma physics*, 60(3):529–539, 1998.

[14] Mihir B Banerjee, J.R Gupta, and S.P Katyal. A characterization theorem in magnetothermohaline convection. *Journal of Mathematical Analysis and Applications*, 144(1):141–146, 1989.

[15] Arnab Basak, Rohit Raveendran, and Krishna Kumar. Rayleigh-bénard convection with uniform vertical magnetic field. *Physical Review E*, 90(3):1–9, 2014.

[16] James L Beck. Convection in a box of porous material saturated with fluid. *The Physics of Fluids*, 15(8):1377–1383, 1972.

[17] O Anwar Beg, Harmindar S Takhar, and Ajay Kumar Singh. Multiparameter perturbation analysis of unsteady oscillatory magnetoconvection in porous media with heat source effects. *International journal of fluid mechanics research*, 32(6):635–661, 2005.

[18] Henry Benard. Cellular vortices in a liquid layer. *Rev. Gen. Sci. Pure Appl.*, 11:1261–1271, 1900.

[19] B. S. Bhadauria, Palle Kiran, and and. Weak nonlinear double diffusive magneto-convection in a newtonian liquid under gravity modulation. *Journal of Applied Fluid Mechanics*, 8(4):735–746, 2015.

[20] BS Bhadauria. Double diffusive convection in a porous medium with modulated temperature on the boundaries. *Transport in porous media*, 70(2):191, 2007.

[21] B.S. Bhadauria and Atul K. Srivastava. Magneto-double diffusive convection in an electrically conducting-fluid-saturated porous medium with temperature modulation of the boundaries. *International Journal of Heat and Mass Transfer*, 53(11-12):2530–2538, 2010.

[22] PK Bhatia and JM Steiner. Thermal instability in a viscoelastic fluid layer in hydromagnetics. *Journal of Mathematical Analysis and Applications*, 41(2):271–283, 1973.

[23] Dambaru Bhatta, Mallikarjunaiah S Muddamallappa, and Daniel N Riahi. On perturbation and marginal stability analysis of magneto-convection in active mushy layer. *Transport in porous media*, 82(2):385–399, 2010.

[24] W Bian, P Vasseur, and E Bilgen. Effect of an external magnetic field on buoyancy-driven flow in a shallow porous cavity. *Numerical Heat Transfer, Part A Applications*, 29(6):625–638, 1996.

[25] W Bian, P Vasseur, E Bilgen, and F Meng. Effect of an electromagnetic field on natural convection in an inclined porous layer. *International journal of heat and fluid flow*, 17(1):36–44, 1996.

[26] Sharon E Borglin, George J Moridis, and Curtis M Oldenburg. Experimental studies of the flow of ferrofluid in porous media. *Transport in Porous Media*, 41(1):61–80, 2000.

[27] Jeffrey C Buell and Ivan Catton. Effect of rotation on the stability of a bounded cylindrical layer of fluid heated from below. *The Physics of Fluids*, 26(4):892–896, 1983.

[28] FH Busse. Nonlinear interaction of magnetic field and convection. *Journal of Fluid Mechanics*, 71(1):193–206, 1975.

[29] FH Busse and RM Clever. Instabilities of convection rolls in a fluid of moderate prandtl number. *Journal of Fluid Mechanics*, 91(2):319–335, 1979.

[30] FH Busse and KE Heikes. Convection in a rotating layer: a simple case of turbulence. *Science*, 208(4440):173–175, 1980.

[31] FH Busse and W Pesch. Thermal convection in a twisted horizontal magnetic field. *Geophysical and Astrophysical Fluid Dynamics*, 100(2):139–150, 2006.

[32] A Chakrabarti and AS Gupta. Nonlinear thermohaline convection in a rotating porous medium. *Mechanics Research Communications*, 8(1):9–22, 1981.

[33] P Chand, A Mahajan, and P Sharma. Effect of rotation on double-diffusive convection in a magnetized ferrofluid with internal angular momentum. *Journal of Applied Fluid Mechanics*, 4(4), 2011.

[34] S Chandrasekhar. The instability of a layer of fluid heated below and subject to the simultaneous action of a magnetic field and rotation. il. *Proceedings of the Royal Society of London. Series A. Mathematical and Physical Sciences*, 237(1211):476–484, 1956.

[35] S Chandrasekhar. Hydromagnetic and hydrodynamic stability. *Clarendon, Oxford*, 1961.

[36] RM Clever and FH Busse. Nonlinear oscillatory convection in the presence of a vertical magnetic field. *Journal of Fluid Mechanics*, 201:507–523, 1989.

[37] P Coullet, S Fauve, and E Tirapegui. Large scale instability of nonlinear standing waves. *Journal de Physique Lettres*, 46(17):787–791, 1985.

[38] Henry Philibert Gaspard Darcy. The public fountains of the city of dijon. exhibition and application of principles to follow and forms to be used in matters of water supply, etc. *V. Dalamont*, 1856.

[39] Robert P Davies Jones and Peter A Gilman. Convection in a rotating annulus uniformly heated from below. *Journal of Fluid Mechanics*, 46(1):65–81, 1971.

[40] Thomas Desaive, Marcel Hennenberg, and Pierre C Dauby. Thermodynamic stability of a ferrofluid in a porous rotating layer. *Mechanics and Industry*, 5(5):621625, 2004.

[41] Joginder Singh Dhiman. Some characterization theorems in rotatory magneto thermohaline convection. *Proceedings of the Indian Academy of Sciences-Mathematical Sciences*, 105(4):461–469, 1995.

[42] Philip G Drazin and William Hill Reid. *Hydrodynamic stability*. Cambridge university press, 2004.

[43] IA Eltayeb. Hydromagnetic convection in a rapidly rotating fluid layer. *Proceedings of the Royal Society of London. A. Mathematical and Physical Sciences*, 326(1565):229–254, 1972.

[44] J. Friedrich, Y.S. Lee, B. Fischer, C. Kupfer, D. Vizman, and G. Mller. Experimental and numerical study of rayleigh-benard convection affected by a rotating magnetic field. *Physics of Fluids*, 11(4):853–861, 1999.

[45] Manojit Ghosh and Pinaki Pal. Zero prandtl-number rotating magnetoconvection. *Physics of Fluids*, 29(12):124105, 2017.

[46] RC Givler and SA Altobelli. A determination of the effective viscosity for the brinkman–forchheimer flow model. *Journal of Fluid Mechanics*, 258:355–370, 1994.

[47] RC Givler and SA Altobelli. A determination of the effective viscosity for the brinkman–forchheimer flow model. *Journal of Fluid Mechanics*, 258:355–370, 1994.

[48] Kanefusa Gotoh and Michio Yamada. Thermal convection in a horizontal layer of magnetic fluids. *Journal of the Physical Society of Japan*, 51(9):3042–3048, 1982.

[49] J. R. Gupta, S. K. Sood, and U. D. Bhardwaj. On rayleigh-benard convection with rotation and magnetic field. *ZAMP Zeitschrift for angewandte Mathematik und Physik*, 35(2):252–256, 1984.

[50] JR Gupta, SK Sood, and RG Shandil. A semi-circle theorem in thermohaline convection with rotation and magnetic field. *Indian J. pure appl. Math*, 14(1):115428, 1983.

[51] A. J. Harfash. Magnetic effect on instability and nonlinear stability of double-diffusive convection in a reacting fluid. *Continuum Mechanics and Thermodynamics*, 25(1):89–106, 2012.

[52] AJ Harfash. Structural stability for convection models in a reacting porous medium with magnetic field effect. *Ricerche di Matematica*, 63(1):1–13, 2014.

[53] CW Horton and FT Rogers Jr. Convection currents in a porous medium. *Journal of Applied Physics*, 16(6):367–370, 1945.

[54] K Jirlow. Experimental investigation of the inhibition of convection by a magnetic field. *Tellus*, 8(2):252–253, 1956.

[55] Daniel D Joseph. *Stability of fluid motions I*, volume 27. Springer Science & Business Media, 2013.

[56] RC Kloosterziel and GF Carnevale. Closed-form linear stability conditions for magneto-convection. *Journal of Fluid Mechanics*, 490:333–344, 2003.

[57] E Knobloch and J De Luca. Amplitude equations for travelling wave convection. *Nonlinearity*, 3(4):975, 1990.

[58] Edgar Knobloch. Rotating convection: recent developments. *International journal of engineering science*, 36(12-14):1421–1450, 1998.

[59] Hans Jorg Kull. Theory of the rayleigh-taylor instability. *Physics reports*, 206(5):197–325, 1991.

[60] Pardeep Kumar. Thermosolutal magneto-rotatory convection in couple-stress fluid through porous medium. 2012:45–52, 2012.

[61] ER Lapwood. Convection of a fluid in a porous medium. *Mathematical Proceedings of the Cambridge Philosophical Society*, 44(4):508–521, 1948.

[62] Dietrich Lortz. A stability criterion for steady finite amplitude convection with an external magnetic field. *Journal of Fluid Mechanics*, 23(01):113, 1965.

[63] DV Lyubimov, TP Lyubimova, and ES Sadilov. Effect of a rotating magnetic field on convection in a horizontal fluid layer. *Fluid Dynamics*, 43(2):169–175, 2008.

[64] MS Malashetty, Ioan Pop, and Rajashekhar Heera. Linear and nonlinear double diffusive convection in a rotating sparsely packed porous layer using a thermal non-equilibrium model. *Continuum Mechanics and Thermodynamics*, 21(4):317, 2009.

[65] MS Malashetty, Mahantesh Swamy, and Rajashekhar Heera. Double diffusive convection in a porous layer using a thermal non-equilibrium model. *International Journal of Thermal Sciences*, 47(9):1131–1147, 2008.

[66] W. V. R. Malkus and G. Veronis. Finite amplitude cellular convection. *Journal of Fluid Mechanics*, 4(3):225–260, 1958.

[67] PC Matthews and AM Rucklidge. Travelling and standing waves in magnetoconvection. *Proceedings of the Royal Society of London. Series A: Mathematical and Physical Sciences*, 441(1913):649–658, 1993.

[68] Hari Mohan. On modified thermohaline magnetoconvection-a characterization theorem. *Journal of Applied Sciences*, 12(2):186–190, 2012.

[69] G. Mulone and S. Rionero. On the nonlinear stability of the magnetic benard problem with rotation. *ZAMM - Journal of Applied Mathematics and Mechanics / Zeitschrift fr Angewandte Mathematik und Mechanik*, 73(1):35–45, 1993.

[70] G. Mulone and B. Straughan. An operative method to obtain necessary and sufficient stability conditions for double diffusive convection in porous media. *ZAMM*, 86(7):507–520, 2006.

[71] B. T. Murray and C. F. Chen. Double-diffusive convection in a porous medium. *Journal of Fluid Mechanics*, 201(-1):147, 1989.

[72] V.Dakshina Murty, Christopher L. Clay, Michael P. Camden, and Estelle R. Anselmo. A numerical study of the stability of thermohaline convection in a

rectangular box containing a porous medium. *International Communications in Heat and Mass Transfer*, 21(2):261–269, 1994.

[73] Jude L. Musuuza, Florin A. Radu, and Sabine Attinger. Predicting predominant thermal convection in thermohaline flows in saturated porous media. *Advances in Water Resources*, 49:23–36, 2012.

[74] Y Nakagawa. An experiment on the inhibition of thermal convection by a magnetic field. *Nature*, 175(4453):417–419, 1955.

[75] Y Nakagawa. Experiments on the inhibition of thermal convection by a magnetic field. *Proceedings of the Royal Society of London. Series A. Mathematical and Physical Sciences*, 240(1220):108–113, 1957.

[76] M. Narayana, S.N. Gaikwad, P. Sibanda, and R.B. Malge. Double diffusive magneto-convection in viscoelastic fluids. *International Journal of Heat and Mass Transfer*, 67:194–201, 2013.

[77] Alan C Newell and John A Whitehead. Finite bandwidth, finite amplitude convection. *Journal of Fluid Mechanics*, 38(2):279–303, 1969.

[78] DA Nield. Onset of thermohaline convection in a porous medium. *Water Resources Research*, 4(3):553–560, 1968.

[79] DA Nield and Adrian Bejan. Mechanics of fluid flow through a porous medium. *Convection in Porous Media*, pages 1–29, 2013.

[80] Donald A Nield, Adrian Bejan, et al. *Convection in porous media*, volume 3. Springer, 2006.

[81] Curtis M. Oldenburg and Karsten Pruess. Plume separation by transient thermohaline convection in porous media. *Geophysical Research Letters*, 26(19):2997–3000, 1999.

[82] Enok Palm, Jan Erik Weber, and Oddmund Kvernvold. On steady convection in a porous medium. *Journal of Fluid Mechanics*, 54(1):153–161, 1972.

[83] C. Parthiban and Prabhamani R. Patil. Effect of inclined gradients on thermohaline convection in porous medium. *Wrme- und Stoffbertragung*, 29(5):291–297, 1994.

[84] Prabhamani R Patil and N Rudraiah. Stability of hydromagnetic thermoconvective flow through porous medium. *Journal of Applied Mechanics*, 40(4):879–884, 1973.

[85] Prabhamani R. Patil and G. Vaidyanathan. Effect of variable viscosity on thermohaline convection in a porous medium. *Journal of Hydrology*, 57(1-2):147–161, 1982.

[86] Arne J Pearlstein. Effect of rotation on the stability of a doubly diffusive fluid layer. *Journal of Fluid Mechanics*, 103:389–412, 1981.

[87] Olga Podvigina. Stability of rolls in rotating magnetoconvection in a layer with no-slip electrically insulating horizontal boundaries. *Physical Review E*, 81(5), 2010.

[88] Dimos Poulikakos. Double diffusive convection in a horizontal sparcely packed porous layer. *International Communications in Heat and Mass Transfer*, 13(5):587–598, 1986.

[89] Jyoti Prakash and Sanjay Kumar Gupta. On nonexistence of oscillatory motions in magnetothermohaline convection in porous medium. *Journal of Porous Media*, 19(7):567–581, 2016.

[90] MRE Proctor and NO Weiss. Magnetoconvection. *Reports on Progress in Physics*, 45(11):1317, 1982.

[91] Lord Rayleigh. Lix. on convection currents in a horizontal layer of fluid, when the higher temperature is on the under side. *The London, Edinburgh, and Dublin Philosophical Magazine and Journal of Science*, 32(192):529–546, 1916.

[92] DAS Rees. Thermal boundary layer instabilities in porous media: a critical review. *Transport phenomena in porous media*, pages 233–259, 1998.

[93] DAS Rees. The stability of darcy–bénard convection. *Handbook of porous media*, pages 521–588, 2000.

[94] FT Rogers Jr and HL Morrison. Convection currents in porous media. iii. extended theory of the critical gradient. *Journal of Applied Physics*, 21(11):1177–1180, 1950.

[95] FT Rogers Jr, LE Schilberg, and HL Morrison. Convection currents in porous media. iv. remarks on the theory. *Journal of Applied Physics*, 22(12):1476–1479, 1951.

[96] Hillel Rubin. Effect of nonlinear stabilizing salinity profiles on thermal convection in a porous medium layer. *Water Resources Research*, 9(1):211–221, 1973.

[97] Hillel Rubin. Effect of solute dispersion on thermal convection in a porous medium layer. *Water Resources Research*, 9(4):968–974, 1973.

[98] N Rudraiah. Linear and non-linear magnetoconvection in a porous medium. *Proceedings of the Indian Academy of Sciences-Mathematical Sciences*, 93(2-3):117–135, 1984.

[99] N Rudraiah. Double-diffusive magnetoconvection. *Pramana*, 27(1-2):233–266, 1986.

[100] N Rudraiah, P Kn Srimani, and R Friedrich. Finite amplitude convection in a two-component fluid saturated porous layer. *International Journal of Heat and Mass Transfer*, 25(5):715–722, 1982.

[101] S Saravanan and H Yamaguchi. Onset of centrifugal convection in a magnetic-fluid-saturated porous medium. *Physics of Fluids*, 17(8):084105, 2005.

[102] R Sekar, D Murugan, and K Raju. Stability analysis of thermohaline convection in ferromagnetic fluid in densely packed porous medium with soret effect. *World journal of engineering*, 10(5):439–448, 2013.

[103] R Sekar and K Raju. Effect of soret and temperature dependent viscosity on thermohaline convection in a ferrofluid saturating a porous medium. *International Journal of Applied Mechanics and Engineering*, 19(2):321–336, 2014.

[104] R Sekar and K Raju. Stability analysis of soret effect on thermophaline convection in dusty ferrofluid saturating a darcy porous medium. *Global Journal of Mathematical Analysis*, 3(1):37–48, 2015.

[105] R Sekar, A Ramanathan, and G Vaidyanathan. Effect of rotation on ferro thermohaline convection saturating a porous medium. *Indian Journal of Engineering and Materials Sciences*, 5(445–452), 1998.

[106] R Sekar and G Vaidyanathan. Convective instability of a magnetized ferrofluid in a rotating porous medium. *International journal of engineering science*, 31(8):1139–1150, 1993.

[107] R Sekar, G Vaidyanathan, and A Ramanathan. The ferroconvection in fluids saturating a rotating densely packed porous medium. *International journal of engineering science*, 31(2):241–250, 1993.

[108] Subha Sengupta and Anadi Shankar Gupta. Thermohaline convection with finite amplitude in a rotating fluid. *Zeitschrift für angewandte Mathematik und Physik ZAMP*, 22(5):906–914, 1971.

[109] R. C. Sharma and K. N. Sharma. Magneto-thermohaline convection through porous medium. *Acta Physica Academiae Scientiarum Hungaricae*, 48(2-3):269–279, 1980.

[110] RC Sharma and Veena Kumari. Effect of magnetic field and rotation on thermosolutal convection in porous medium. *Japan journal of industrial and applied mathematics*, 9(1):79–90, 1992.

[111] RC Sharma and KD Thakur. On couple-stress fluid heated from below in porous medium in hydromagnetics. *Czechoslovak Journal of Physics*, 50(6):753–758, 2000.

[112] IS Shivakumara, AL Mamatha, and M Ravisha. Linear and weakly nonlinear magnetoconvection in a porous medium with a thermal nonequilibrium model. *Afrika Matematika*, 27(7-8):1111–1137, 2016.

[113] Mahinder Singh and Pardeep Kumar. Magneto and rotatory thermosolutal convection in couple-stress fluid in porous medium. *Journal of porous media*, 14(7):637–648, 2011.

[114] Atul K Srivastava, Beer S Bhadauria, and Jogendra Kumar. Magnetoconvection in an anisotropic porous layer using thermal nonequilibrium model. *Special Topics & Reviews in Porous Media: An International Journal*, 2(1):1–10, 2011.

[115] Victor Steinberg and Helmut R Brand. Crossover from critical to tricritical behavior in a nonequilibrium system: The convective instability in a binary fluid mixture. *Physical Review A*, 30(6):3366, 1984.

[116] Sunil, Divya, and R C Sharma. Effect of rotation on ferromagnetic fluid heated and soluted from below saturating a porous medium. *Journal of Geophysics and Engineering*, 1(2):116–127, 2004.

[117] Sunil, Divya, and R. C. Sharma. The effect of magnetic field dependent viscosity on thermosolutal convection in a ferromagnetic fluid saturating a porous medium. *Transport in Porous Media*, 60(3):251–274, 2005.

[118] SG Tagare. Nonlinear stationary magnetoconvection in a rotating fluid. *Journal of plasma physics*, 58(3):395–408, 1997.

[119] SG Tagare, A Benerji Babu, and Y Rameshwar. Rayleigh–benard convection in rotating fluids. *International Journal of Heat and Mass Transfer*, 51(5-6):1168–1178, 2008.

[120] SG Tagare, MV Ramana Murthy, and Y Rameshwar. Nonlinear thermohaline convection in rotating fluids. *International journal of heat and mass transfer*, 50(15-16):3122–3140, 2007.

[121] SG Tagare, Y Rameshwar, A Benerji Babu, and J Brestensky. Rotating compositional and thermal convection in earths outer core. *Contributions to Geophysics and Geodesy*, 36(2):87–113, 2006.

[122] John H Thomas and Nigel O Weiss. The theory of sunspots. *Sunspots: theory and Observations*, pages 3–59, 1992.

[123] SD Thompson. Magnetoconvection in an inclined magnetic field: linear and weakly non-linear models. *Monthly Notices of the Royal Astronomical Society*, 360(4):1290–1304, 2005.

[124] WB Thompson. Cxliii. thermal convection in a magnetic field. *The London, Edinburgh, and Dublin Philosophical Magazine and Journal of Science*, 42(335):1417–1432, 1951.

[125] WB Thompson. Cxliii. thermal convection in a magnetic field. *The London, Edinburgh, and Dublin Philosophical Magazine and Journal of Science*, 42(335):1417–1432, 1951.

[126] Ulrich and Muller. Rayleigh–benard convection in liquid metal layers under the influence of a horizontal magnetic field. *Journal of Fluid Mechanics*, 453(2002):345–369, 2002.

[127] Hirdesh Varshney and Mirza Faisal Baig. Rotating magneto-convection: Influence of vertical magnetic field. *Journal of Turbulence*, 9(33):1–20, 2008.

[128] M. P. Volz and K. Mazuruk. An experimental study of the influence of a rotating magnetic field on rayleigh–benard convection. *Journal of Fluid Mechanics*, 444, 2001.

[129] M.P. Volz and K. Mazuruk. Thermoconvective instability in a rotating magnetic field. *International Journal of Heat and Mass Transfer*, 42(6):1037–1045, 1999.

[130] QW Wang, Ming Zeng, ZP Huang, G Wang, and H Ozoe. Numerical investigation of natural convection in an inclined enclosure filled with porous medium under magnetic field. *International journal of heat and mass transfer*, 50(17-18):3684–3689, 2007.

[131] Nigel Oscar Weiss and MRE Proctor. *Magnetoconvection*. Cambridge University Press, 2014.

[132] R A Wooding. Rayleigh instability of a thermal boundary layer in flow through a porous medium. *Journal of fluid mechanics*, 9(2):183–192, 1960.

[133] R A Wooding. Convection in a saturated porous medium at large rayleigh number or peclet number. *Journal of Fluid Mechanics*, 15(4):527–544, 1963.

[134] RA Wooding. Steady state free thermal convection of liquid in a saturated permeable medium. *Journal of Fluid Mechanics*, 2(3):273–285, 1957.